The Mechanisms of Wear of the Video Head

LINDA ANN REEVES

Doctor of Philosophy

THE UNIVERSITY OF ASTON IN BIRMINGHAM

September 1990

THE UNIVERSITY OF ASTON IN BIRMINGHAM

The Mechanisms of Wear of the Video Head

Linda Ann Reeves
Doctor of Philosophy

September 1990

Thesis Summary

This thesis examines the mechanisms of wear occurring to the video head and their effect on signal reproduction. In particular it examines the wear occurring to manganese-zinc ferrite heads in sliding contact with iron oxide media.

A literature survey is presented, which covers magnetic recording technologies, focussing on video recording. Existing work on wear of magnetic heads is also examined, and gaps in the theoretical account of wear mechanisms presented in the literature are identified.

Pilot research was carried out on the signal degradation and wear associated with a number of commercial video tapes, containing a range of head cleaning agents. From this research, the main body of the research was identified. A number of methods of wear measurement were examined for use in this project. Knoop diamond indentation was chosen because experimentation showed it to be capable of measuring wear occurring in situ. This technique was then used to examine the wear associated with different levels of Al_2O_3 and Cr_2O_3 head cleaning agents.

The results of the research indicated that, whilst wear of the video head increases linearly with increasing HCA content, signal degradation does not vary significantly. The most significant differences in wear and signal reproduction were observed between the two HCAs. The signal degradation of heads worn with tape samples containing Al_2O_3 HCA was found to be lower than heads worn with tapes containing Cr_2O_3 HCA.

The results also indicated that the wear to the head is an abrasive process characterised by ploughing of the ferrite surface and chipping of the edges of the head gap. Both phenomena appear to be caused by poor dispersion of both iron oxide and head cleaning particles, which create isolated asperities on the tape surface.

Key words: Video, Magnetic Media, Magnetic Recording, Tribology, Wear.

Acknowledgements

My thanks are principally due to Dr. John Sullivan, my academic supervisor, whose guidance throughout has been greatly appreciated.

I am grateful to 3M Company, Swansea, for partly funding the project and for supplying all the samples and equipment. In particular, I would like to thank Mr.Peter Roderick for his guidance and Mr. John Minopoli for his help and support.

I am grateful to Mr. Roger Howell of the Metallurgy Department, Aston University, for his instruction in the use of the Electron Microscopes.

The writing up of the thesis took place in the main whilst I was employed as a research officer in the School of Materials Science, at the University of Bath. I am grateful to all my colleagues in the School for providing an excellent environment for writing.

Finally, I am indebted to Dr. Tom Ormerod, who spent many hours correcting and clarifying my writing, and to my parents who offered support throughout.

Contents

Page no.

Chapter 1: Literature Survey

Chapter 2: Equipment and Experimental Methods

Chapter 3: Presentation of Results

Chapter 4: Discussion

Chapter 5: Conclusions and Future Work

Tables

Page no.

Figures

Chapter 1:

Literature survey

1.0 Introduction

Two main priorities for research into the improvement of magnetic recording and reproduction may be identified; first, to increase the amount of recorded material which can be packed on to the tape or disc (packing density); and, second to maintain the continual quality of the reproduction. Improvements in both aspects are continually sought after through advances in both media and recorder technology. However, the technology has reached a stage where the main barrier to further improvement is the tribological properties of the head and media. Until the interaction between the media and head of a particular magnetic recording system is fully understood, further improvements in either head or media technology will not be realised. From an examination of the literature, it appears that the head-media interaction is not clearly understood, especially in the case of video recording, where the head and media are in contact and wear is unavoidable. In this situation wear must be carefully controlled and the resulting wear surface must be able to provide a similar performance to that of the unworn surface. There is increasing concern that the worn surface does not provide the desired properties and makes a significant contribution towards the degradation of the signal reproduced by the recorder.

In this thesis research is reported which was undertaken to clarify the mechanisms of wear occuring to the video head, in particular in the case of a single crystal Mn-Zn ferrite head in sliding contact with iron oxide media. The work is concerned with isolating the problematic features of wear, that is, those contributing towards the degradation of performance of the head. In the study of wear to the video head the head cleaning agent (HCA) is examined in detail. The HCA is a particle added to the magnetic coating to increase the abrasivity and durability of the tape. Thus it has an important effect on wear to the head. In view of this it is surprising that no literature was found which examines the HCA or its effect on wear. Thus a number of experiments were undertaken to examine this effect.

The thesis begins with a literature survey which examines previous work on magnetic recording, concentrating on video recording. The survey also examines theories of friction and wear which are relevant to this thesis. In chapter two, the methods used in the project experiments are described, beginning with a pilot project which investigated problematic features of wear. From this initial work the main research programme was established which included the development of a suitable method of head wear measurement. Using this method, an investigation of the effects of varying the level and type of HCA was undertaken. Examination of the heads before and after wear was also carried out using several surface analysis techniques, which enabled detailed study of the wear occuring to the video head. The results of these experiments are reported in chapter 3. In chapter 4 the results are discussed, and wear mechanisms are defined which occur to the head when in sliding contact with iron oxide media. Wear mechanisms with and without the inclusion of an HCA in the magnetic coating are considered. In chapter 5 a number of conclusions are drawn and suggestions for future research are made.

In this chapter the general theories behind magnetic recording are explained. Since this project concentrates specifically on video recording, the construction of the magnetic media and head is described for this particular application. The specific operation of the video recording system is also dealt with in some detail. In the project, a method of measurement of wear to the magnetic head was required. Hence, a survey of previous methods of head wear measurement was carried out, and is reported in section 1.6. Next, the general principles of friction and wear are outlined, the friction and wear of polymers, filled polymers and ceramics are also described. Finally a review of the recent literature on wear occuring due to head-media interaction is given. The focus of this project, and therefore of the literature survey, is on wear occuring to the head.

1.1 General Magnetic Recording Theory

Magnetic recording is the process by which an electrical signal is converted, via a transducer, into an equivalent magnetic pattern on a passing magnetic medium (1,2,3,4,5). The magnetic head of the recorder is the transducer in this process and takes the form of a ring core split by a narrow gap. The gap creates two pole pieces, which are both wound with copper wire through which the electrical signal travels. The changing electrical signal induces a corresponding magnetic field within the core, and the stray flux field formed across the gap, as shown in Figure 1.1, creates the recording field. As the magnetic medium is passed through the field at the gap it is left with a representation of the original electrical signal in the form of remanent magnetic flux, as shown in Figure 1.2. By definition, the remanence is the flux density remaining in the magnetic material after the magnetising field has been removed. The quality of the recording is dependent upon the linearity between the field at the recording gap and the remanent magnetization (6).

The playback process is basically the reverse of the recording process; the head material is highly permeable, so that the magnetic flux of a passing magnetic medium creates a corresponding magnetic field within the core. The field induces a voltage in the copper windings which is representative of the original electrical signal recorded. The relative permeability, μ_r, of a magnetic material is defined as the ratio between the flux density (B) induced in the material and the flux density which would be induced in air by the same applied field. In the case of video recording, each video head acts as both a read and write transducer. In order to obtain high quality recording and playback the surface of the head and the surface of the medium must be in close proximity during the recording and playback operations. This is necessary, because in order to obtain maximum efficiency, the tape is required to pass through the flux field as close as possible to the head. Separation of the tape from the head at any point will produce losses in signal. One example of head-tape separation, which can be seen clearly in the case of video recording,

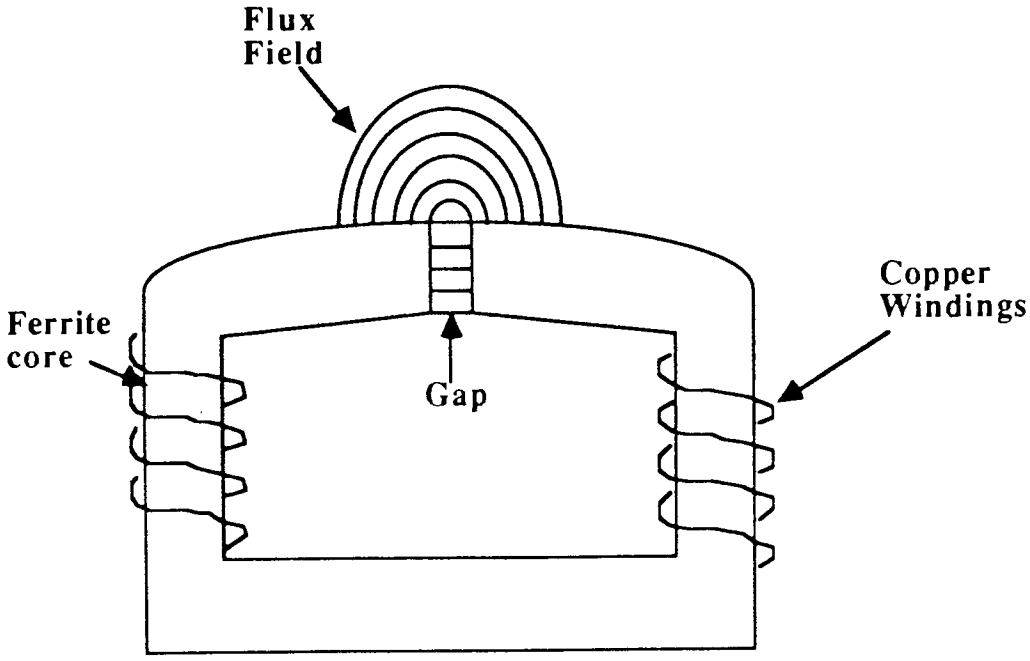

Figure 1.1: Recording field formed across the gap of the video head

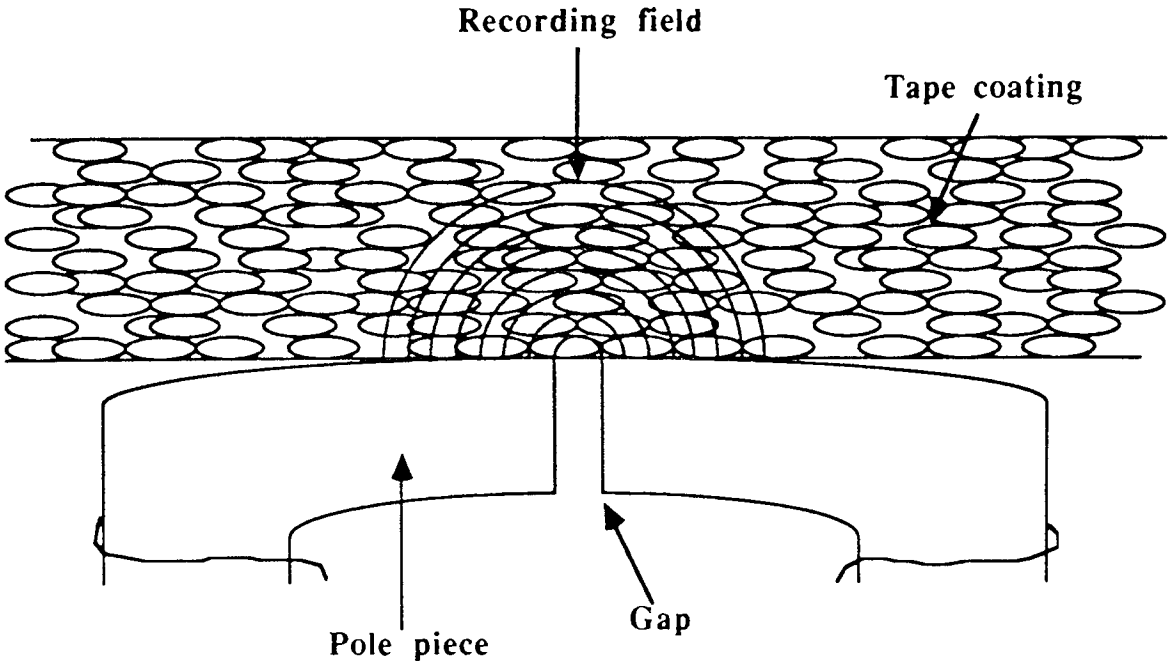

Figure 1.2: Penetration of the magnetic field into the tape coating during the recording process.

is the drop-out. Here the tape is separated from the head momentarily by dust or debris and the resulting loss in signal is seen as a white flash on the television screen (7). To maintain close contact, both surfaces must be as smooth and uniform as possible, and must retain these characteristics with continual use. The losses caused by head tape separation are mostly short wavelengths. The wavelength (λ) is determined by the tape speed (v) and the signal frequency (f) as follows:

$$\lambda = v/f \tag{1.1}$$

To encourage contact in all forms of magnetic recording, a combination of smooth contoured head, pressure pads and tension of the tape is used. If an air film is created between the two surfaces short wavelength losses result. However, in some systems the separation may be desirable to reduce wear. Video recording is unique in that the head and media are in contact. Separation of the surfaces by contamination, debris or surface films in video and any other recording system will create further losses in short wavelength recording. The spacing loss in dB is related to the head-tape separation (d) by the following formula due to Wallace (8), where λ is the wavelength of the recorded signal:

$$\textit{spacing loss} = 54.6\, d/\lambda \quad \text{dB} \tag{1.2}$$

From the formula it is apparent that the short wavelength sensitivity is reduced with spacing loss.

The origin of spacing loss is illustrated in Figure 1.3. Head-tape spacing induced by debris or surface film results in the magnetization of only a portion of the tape. The spacing has a greater effect on short wavelengths because the emergent flux spreads out further for longer wavelengths as shown in Figure 1.4. Hence, to obtain the same distance from the surface for two very different wavelengths, the percentage increase in the length of the flux path for the shorter wavelength would be much greater (1).

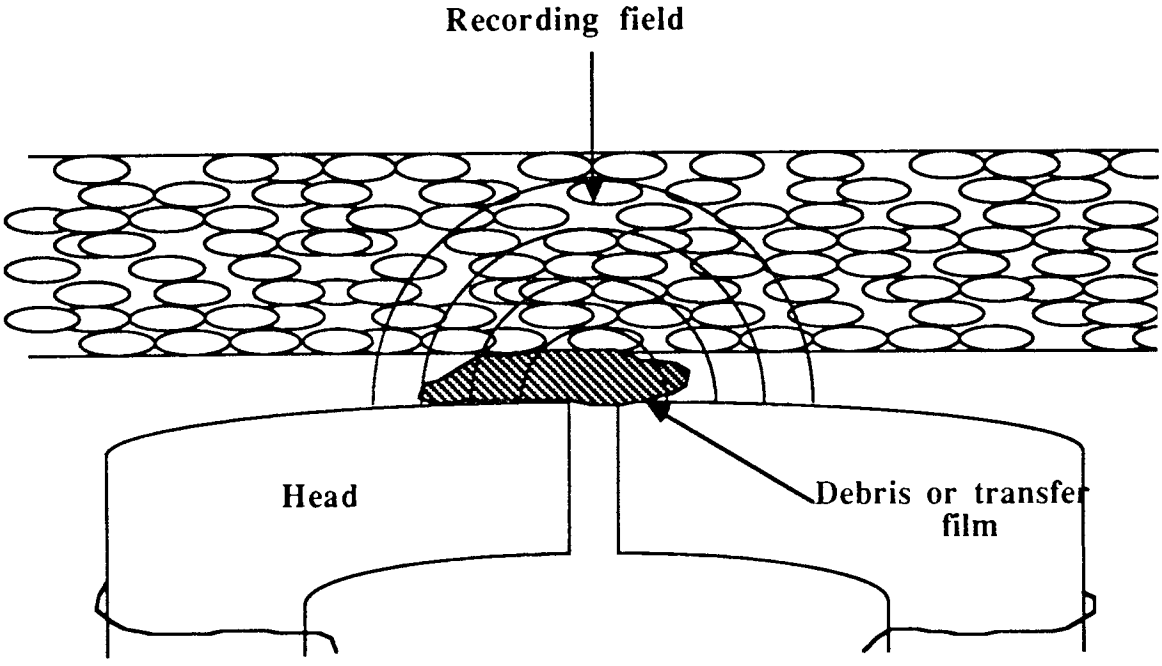

Figure 1.3: Head-tape spacing due to debris or the build-up of a polymer film on the head.

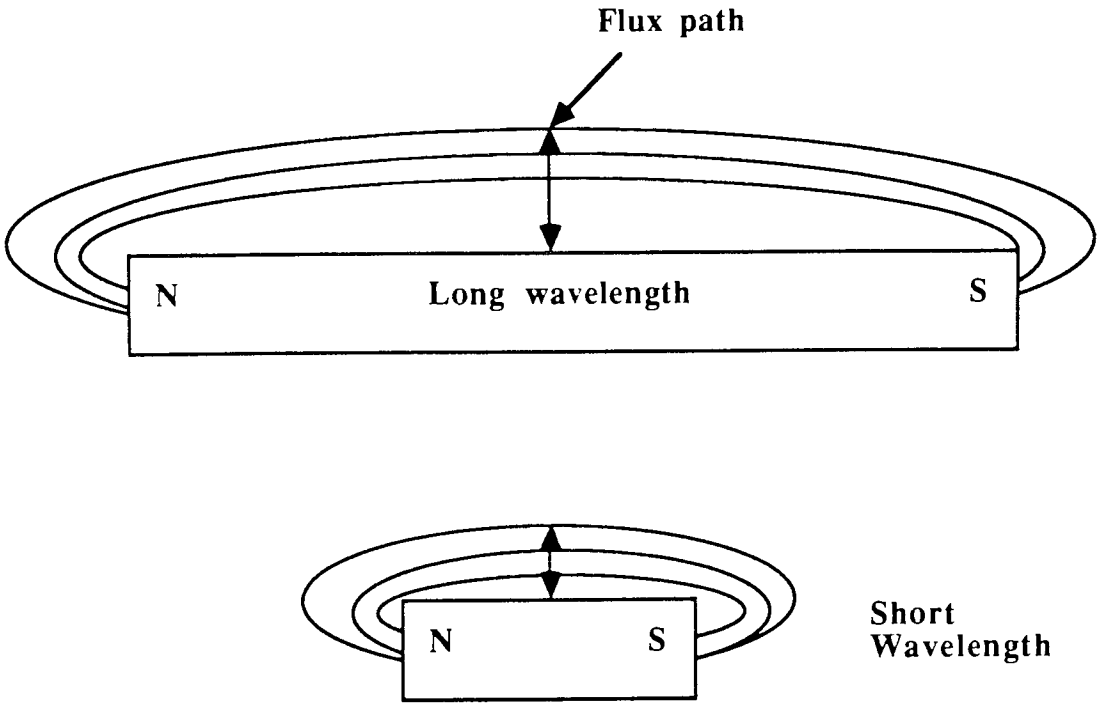

Figure 1.4: Emergent flux for two bar magnets illustrating the difference in flux path for long and short wavelengths.

For a magnetic tape to retain the remanent flux, an extremely high coercivity is required by the magnetic particles of the tape coating. The coercivity is defined as the field strength required to reduce the remanence of a magnetic material. Magnetic materials exhibiting high coercivity and high remanence are termed hard magnets (9). The magnetization and demagnetization of a magnetic material is best described by plotting the flux density (B) against the magnetic field strength (H). Figure 1.5a shows the B-H curve for a typical hard magnetic material used in the production of magnetic media. Assuming the material is initially demagnetized, a magnetization curve, shown as a-b-c on the figure, can be traced as the flux density increases with the applied magnetic field. In the centre of the curve from a to b there is a rapid increase in flux, and then at high values of H the curve levels off as the material reaches saturation (B_{sat}). The slope of the initial magnetization curve is equal to the permeability of the material (μ_r). The permeability attains a maximum value in the range a-b and then decreases to a value of 1 at saturation for high H fields.

When the magnetizing field is removed the flux density does not return to zero. A residual or remanent flux (B_{rs}) remains in the material, and in the case of a hard magnetic material B_{rs} is high, as shown in Figure 1.5a. In order to reduce the flux to zero the field direction must be reversed. The field strength required to bring the flux density to zero, $-H_c$, is the coercive force of the material. If the field continues to increase in this direction, the flux will saturate in the negative direction giving $-B_{sat}$. Removal of this field will leave a remanence $-B_{rs}$. Reversing the current once more will bring the flux back to zero, the field strength required to achieve this being the coercive force $+H_c$. The steepness of the curve going from one direction of magnetization to the opposite direction indicates the ability of the material to record. The curve is highly symmetrical about the origin.

The B-H curve or hysterisis loop of a hard magnetic material is a broad curve with high values of coercivity and remanence. These are qualities which are required by the

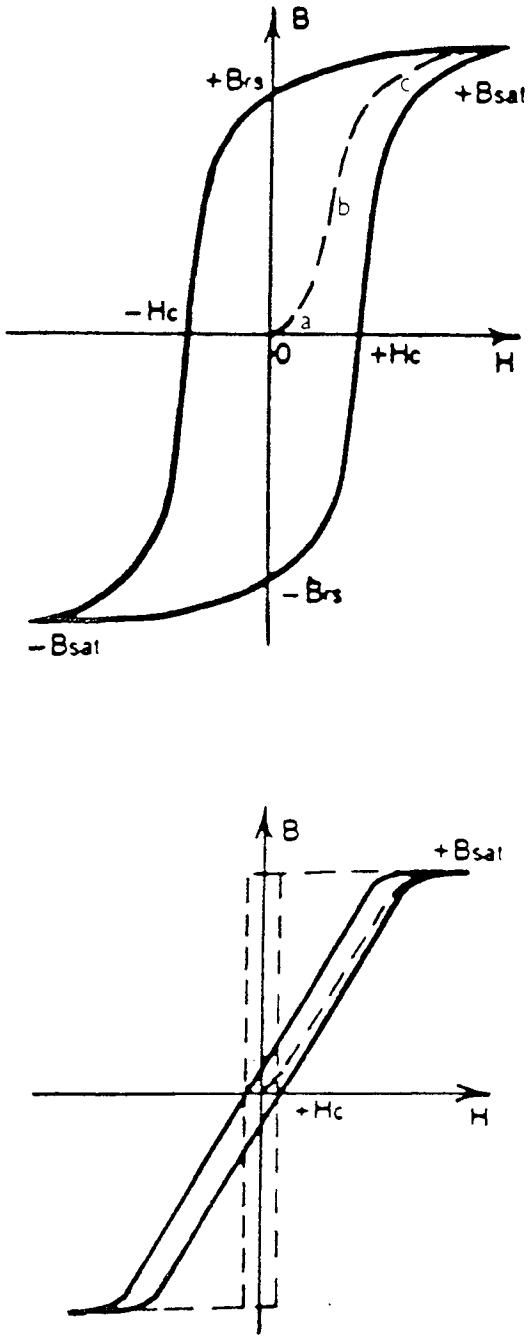

Figure 1.5: Hysterisis curves showing the magnetization and demagnetization characteristics of a) a hard magnetic material and b) a soft magnetic material.

coating of a magnetic tape. The ideal material would produce a square hysterisis loop in which the remanence was equal to the maximum flux reached. Thus the squareness of the loop (Squareness= Brs/Bsat) is an important parameter often used to indicate the recording properties of the materials used for magnetic coatings (10).

In the case of the magnetic head, the material chosen must be highly permeable; only a small magnetic flux is needed to saturate the ring core. The core is not required to retain the flux, and must be able to change magnetization quickly with changing signal field. Hence, a low coercivity and remanence are required. The materials used for the magnetic head are soft magnetic materials. The hysterisis loop for a soft magnetic material in the form of a closed ring core is shown in Figure 1.5b using a dotted line. The loop is long and thin and shows the low coercivity but high remanent magnetization. The second loop (the solid line) shows the response of a ring core of a soft magnetic material with the addition of an air gap. The addition of the air gap causes the hysterisis loop to shear over resulting in a very low remanence. The recording is also more linear; the abrupt change in flux exhibited by the closed core could cause serious amplitude distortions, with the air gap the change in flux is not so sharp. The only disadvantage of the gap is a slight reduction in permeability of the core.

1.2 The video medium

The first true magnetic tape recorder was introduced in 1935 by AEG (Allgemeine Elekrizitats Gesellschaft) (11). The magnetic medium used was a coating of carbonyl iron on either paper or cellulose acetate. After the second world war, gamma iron oxide was used and this remains the principle material used in magnetic recording today (3,12,13). Early tapes used spherical particles of naturally occuring iron oxide or even Magnetite. The iron oxide particle has since been greatly improved in terms of size and shape, and is now an acicular gamma iron oxide of approximately 0.2μm by 0.02μm with improved coercivity and stability. The particles are produced in an acicular form in order to improve

coercivity by reducing demagnetization effects (4). Each magnetic particle creates an internal field opposing the magnetization direction, which gives rise to its magnetization. The shorter the particle in the direction of magnetization the greater the demagnetization. Hence, coercivity is improved by creating long thin magnetic particles. These have the added advantage that they can be oriented along the direction of magnetization to maximise remanent magnetization. The magnetization is retained along the particles main axis.

Recorder electronics have improved steadily over the last 30 years, demanding improvements in the magnetic media such as higher coercivities, higher packing density and surface smoothness. The demand for higher coercivity has led to further modification of the iron oxide particle and also the development of alternative particles. Chromium dioxide offers an alternative magnetic particle with superior coercivity (14,15). The resulting tape product has a higher remanent magnetization, not only because the saturation magnetization is higher with this particle, but also because the particle is easier to orient. Another advantage of chromium dioxide is its inherent head cleaning properties. The particle is harder than iron oxide, which improves not only the durability of the tape but also the head wear characteristics.

In order to compete with the chromium dioxide product the performance of iron oxide media has been improved in terms of coercivity. This was achieved by the addition of cobalt atoms to the surface of the oxide particles (10,16). The resulting compound is close to Cobalt ferrite $CoFe_2O_4$ in composition and is termed cobalt doped gamma iron oxide. The interaction between the cobalt ions and the iron oxide structure provides additional resistance to the switching of magnetization direction and thus increases the coercivity (17,18). Although the production of chromium dioxide tape is expensive compared with iron oxide, both are still used in consumer video tape.

The magnetic tape is a layered structure consisting of a base film, usually Polyethylene terephalate (PET) of a thickness between 12μm and 38μm, onto which the

magnetic slurry is coated. The magnetic layer (thickness 2-5 μm) consists of the magnetic particles, termed the pigment, held in position using a polymeric binder system, together with wetting agents (dispersants), stabilizers, fungicides and lubricants. An optional head cleaning agent may also be present, depending on the hardness of the magnetic particle used (19,20).

The other side of the base film is often coated with an anti-static back coat (thickness of 1.0 μm to 1.5 μm). A non conducting surface, such as the polymer base of magnetic media, in sliding contact with another surface, such as the guides and rollers of the tape drive, would tend to result in a transfer of charge and the build up of static. An increase in the electrostatic charge on the polymer would result in an increase in the frictional force between the tape and all parts of the tape drive. Thus there is a need for a conducting coating in order to avoid these problems associated with static build up. The coating usually has the same formulation as the top coat, but with carbon black replacing the magnetic pigment. This back coat was first introduced on consumer half-inch video tape by 3M plc in 1977 (21). It was used to improve the winding characteristics of the tape, and by reducing static charge it also reduced the number of dropouts caused by the accumulation of air borne debris attracted by static. A dropout occurs during play when the tape is momentarily separated from the head by a particle of debris. The phenomenon is characterised by a white flash on the screen (7).

1.2.1 The Binder System

The binder system is present to support the magnetic particles and adhere the coating to the base film. The system is required to be rigid for support, but also flexible enough to allow the tape to conform to the head and maintain close contact. Hence the binder is most often a copolymer, for example, a polyester urethane which encorporates two phases to provide the properties required. The copolymer has both a soft flexible elastic phase and a hard crystalline phase to provide a rigid supporting medium (22). The structures of the polyester and polyurethane units of the binder are shown in Figure 1.6a. The ester

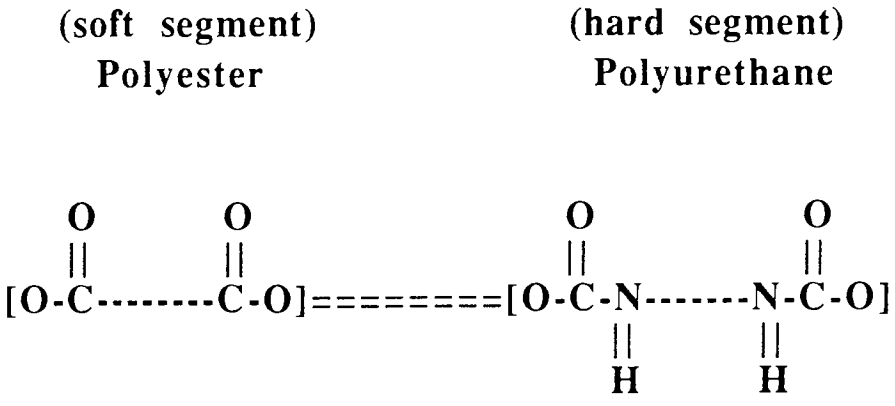

Figure 1.6a: Typical binder system used in video media, consisting of both 'hard' and 'soft' polymer segments.

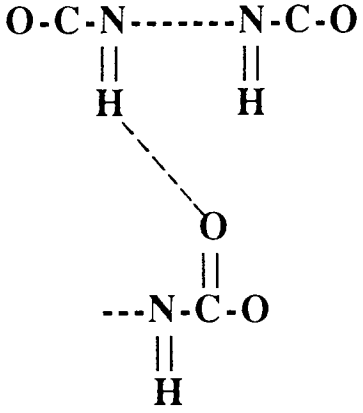

Figure 1.6b: Hydrogen bonding between polyurethane segments to form the crystalline hard binder phase.

provides the soft phase and determines the low temperature and elastomeric properties of the system. The properties can be controlled by the length of the polymer chain which is terminated by alcohol end groups. The urethane segments interact with one another forming strong hydrogen bonds, as shown in Figure 1.6b. The result of their interactions is a crystalline phase with higher thermal stability. This phase dictates the chemical and mechanical behaviour of the binder system. Thus the binder consists of crystalline domains of polyurethane surrounded by the amorphous soft polyester phase.

A plasticiser is also added to provide further flexibility to the binder. The action of the plasticiser is to force apart the chains of the amorphous phase allowing them to slip over one another. The ratio of hard to soft binder varies between manufacturers from 50%:50% to 70%:30% (hard:soft). In general, a higher percentage of binder in the hard phase will increase the head wear. A strong interaction between the binder system and the magnetic particles is required for the following reasons; to maintain the separation of the individual particles within the system; to reinforce the mechanical properties of the binder and to hold the particles to the substrate. These are difficult to achieve with present day particle loadings of over 70% by weight. An even dispersion of the particles in the medium could not be achieved purely by using the interaction of the binder system, since the particles are magnetic and would tend to agglomerate. Hence, a wetting agent or dispersant must be added to break up the agglomerated magnetic pigment (2).

1.2.2 The Lubricant

A lubricant is added to lower the coefficient of friction. In the absence of a lubricant, the resulting friction between the tape and all parts of the tape drive would produce thermal effects and lead to the rapid deterioration of the tape. Head wear decreases by a factor of ten when the tape has been lubricated (23). A lubricant which accumulates on the surface of the tape would also be undesirable since this would create a head-to-tape separation. This type of lubricant may also transfer to the tape and collect in layers thereby increasing

the separation effect and the resulting signal degradation. The lubricant is therefore at present a constituent part of the binder system. Incorporation of the lubricant into the bulk of the magnetic coating has the advantage that, as the tape wears, new layers of lubricant are exposed which keep the surface continually lubricated (23,24).

The majority of lubricant compounds are incompatible with most binder systems. Therefore, the lubricant spontaneously migrates to the surface of the tape and wets the surface by spreading out into depressions and over asperities (25). This action provides the required lubrication. However, the lubricant also has a tendency to migrate towards the binder-substrate boundary, where an excess would interfere with the binding of the magnetic coating to the substrate. The amount of lubricant in the binder has to provide a balance between the friction and wear properties and the mechanical integrity and stability of the system. The migration of the bulk lubricant cannot be controlled with any precision with the result that the coating formed on the surface is not necessarily uniform. The ideal lubricant would be a thin (100Å to 1000Å) surface lubricant which was effective, durable and, most importantly, would not be removed with repeated use. A lubricant with these properties would not transfer to the head (25). There has recently been research into topical lubricants which are present only on the surface and could represent the ideal method of lubrication (25,26).

The timing of the addition of the lubricant is also critical as it may interfere with the polymerization of the binder resin. The compounds used are usually fatty acids such as butylstearate or butylmyristate. Desirable properties of a lubricant compound are as follows; inertness, that is the lubricant must not interact specifically with the binder system or with metals, glasses or plastics below 100°C to avoid damage to all parts of the tape drive; low surface tension, since the lubricant is required to spread out spontaneously and wet the tape surface; thermal and oxidative stability, non-flammability and non-adherence to dirt or debris.

1.2.3 The Head Cleaning Agent (HCA)

Under the high tape-to-head speeds used in video recording, the head and media are kept in contact under a high normal pressure. Under these conditions wear to both head and media is unavoidable. The results of the wear are first, the production of debris, and second, a change in the contouring and state of the original head surface. The latter may include the transfer of polymeric material from the tape, which builds up on the head in the form of a film and will result in spacing losses (23). Hence, a certain amount of head wear is necessary to control the build up of debris in the gap area and also to remove 'dead layers' caused by either the build up of polymeric material or damage to the surface of the head. However, a high level of head wear is undesirable as this would reduce the life of the head to an unacceptable level.

A good contact between head and media is maintained by an optimum level of head wear. The abrasivity of a tape is set by the manufacturer, and the level of head wear produced by several brands varies enormously. Few if any studies have investigated the optimum level of wear.

In the case of chromium dioxide tapes, the magnetic particle is relatively hard, so the resulting tape has an inbuilt head cleaning action. The wear rate for a chromium dioxide tape may result in a short head life and high replacement costs. This is not usually a problem for the domestic user but is significant for commercial duplicators. Head wear can be reduced by the addition of a softer magnetic pigment such as zinc oxide. In the case of iron oxide, the particle is relatively soft. To avoid the build up of debris and deposited layers a head cleaning agent is often added to increase the abrasivity of the resulting tape. The addition of a harder particle also improves the durability and lifetime of the tape. Compounds added to the coating for this purpose are usually oxides such as Al_2O_3, Ce_2O_3, CrO_2, or TiO_2 (14). The head cleaning agent is usually added in small amounts to the coating, typically from 2% to 6% by weight relative to the magnetic

particle. Again few if any studies have investigated the effects of the head cleaning agent on head-media wear.

1.3 Longitudinal and perpendicular recording media

The magnetic media so far described fall into the category of particulate longitudinal media. The media are termed longitudinal because the particles are oriented to a high degree, such that their easy direction of magnetization is in the plane of the base film. The resulting media are mostly insensitive to vertical field components and are fully dependent on the longitudinal magnetic fields. Over the last decade, research, particularly in Japan, has centred on the development of perpendicular or vertical magnetic media (27,28), in which the magnetization is normal to the plane of the base film. The main interest in this form of media is its potential to yield a higher recording density than conventional longitudinal media. To date, significant differences in the performance of perpendicular media have yet to be proved (29,30). Perpendicular media usually take the form of thin metallic film deposited onto a plastic base such that elongated columns are formed (31,32). The material is often a cobalt-nickel or cobalt-chromium alloy. Problems with the metallic film media include wear, friction and corrosion (30,33). The latter can be controlled using a lubricant. However, a surface lubricant must be used for this application, which is not as effective for long term protection as the bulk lubricant used in particulate media.

In order to obtain the advantages of perpendicular magnetization without the disadvantages of metallic thin film media, research has been performed into the production of media using Barium ferrite $Ba.Fe_{12}O_{18}$ in a conventional binder system (34). Barium ferrite is plate-like in structure, exhibits high uniaxial crystalline anisotropy, has a single domain character, and can support a high degree of perpendicular magnetization. The platelets can be fabricated in very small sizes with a high degree of shape and size uniformity. The resulting medium exhibits, amongst other good magnetic

properties, better short wavelength response than any other particulate media and very low demagnetization losses. The disadvantages of the material include overwriting problems which may have to be countered by lowering the coercivity. Also, the barium ferrite is difficult to disperse which creates problems in obtaining a sufficiently smooth surface. Without a smooth surface the short wavelength recording properties of the medium cannot be realized (30,35,36)

1.4 The Video Head

Figure 1.7 shows a photomicrograph of a video head taken at a magnification of X44. A length of the ferrite core either side of the gap provides the sliding surface. The width of the gap is set using two glass infils. This width also dictates the width of the recorded track on the tape. The length of the gap determines the minimum wavelength and the overall size of the head dictates the wavelength of the recorded signal. The two main formulations of ferrite used in the production of video heads are Ni-Zn and Mn-Zn ferrite. The ferrites are a class of ceramic magnetic materials based on the naturally occuring Iron oxide, magnetite Fe_3O_4. They exhibit chemical stability, mechanical hardness and superior magnetic properties at high frequencies (37,38,39). One of the main advantages of ferrites is the fact that they are non-conducting. The original magnetic heads were manufactured from a stack of thin laminations in order to avoid eddy current losses at high frequencies. The use of non-conducting ferrites eliminates these losses. The ferrite used in the construction of magnetic heads usually takes one of three forms. The first is the single crystal; a majority of video heads are cut from single crystals. The other two forms are polycrystalline for which grains of ferrite are pressed together to form the head material (40,41).

In the single crystal form, the head is cut from a single crystal of Mn-Zn ferrite. The crystal is cut such that the planes which exhibit the greatest hardness and hence the best wear characteristics coincide with the sliding surface in contact with the tape. Figure

Figure 1.7: Scanning electron photomicrograph of the video head

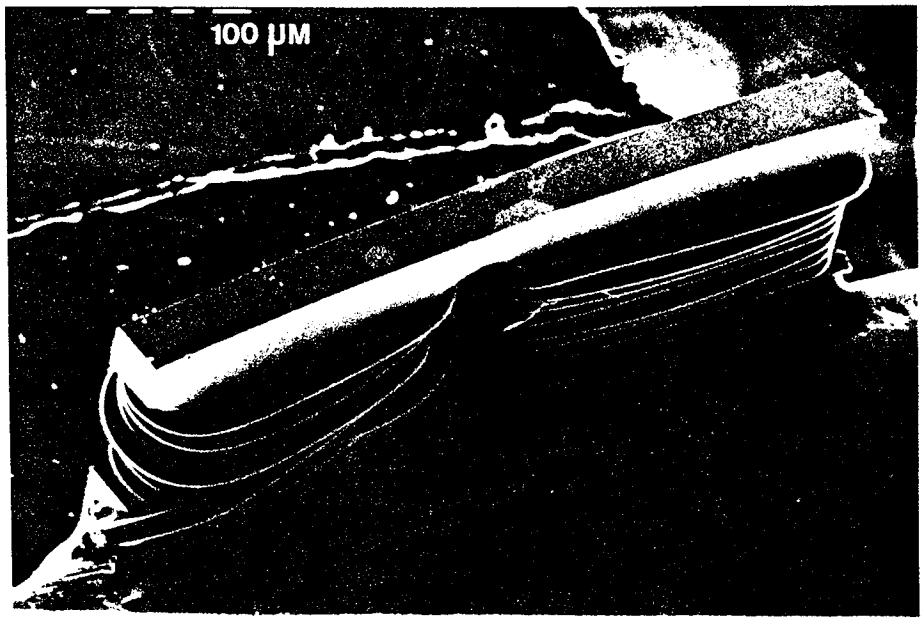
100 µM

1.8 shows the Mn-Zn crystal and the oriented planes. The {110} plane in the <100> direction exhibits the greatest hardness. The head is oriented with its {110} surface nearly parallel to the sliding direction. The orientation is performed to an accuracy of 1%. The resultant head has a high density with a mechanically strong gap (38,42,43). Two polycrystalline forms are possible depending on whether the grains are oriented or not before pressing. Recently hot-press sintered polycrystalline ferrites have been developed which provide a more homogeneous structure than the single crystal (42,44). The polycrystalline material has high density, low porosity and high strength, so long as the microstructure is controlled. The wear resistance of these materials can be improved by orientation. Grain oriented ferrites have been developed with either or both the <111> and the <110> grain axes oriented. The orientation is achieved at the powder stage, the powder being prepared so that it has a shape anisotropy. For example, the <111> axis hexagonal platelets of a Fe_2O_3 are used together with thin stripe shaped γ MnOOH. The compacting process then orients the powder and produces a highly dense body approaching 100% orientation. The orientation increases the output of the head by 10dB compared with the standard polycrystalline material and by 3dB when compared with the single crystal.

The head is produced so that the optimum wear characteristics of the material coincide with the sliding surface. The surface is also contoured so that the maximum point of head-tape contact, and consequently the maximum wear, occurs at the gap. The sliding surface is curved away from the gap in both the sliding direction and perpendicular to the sliding direction so that the gap is at the peak of the sliding surface (40).

1.5 Video Recording

Video recording differs from other forms of magnetic recording in two ways; first, by the use of frequency modulated (FM) recording; and second, by the use of rotary head technology.

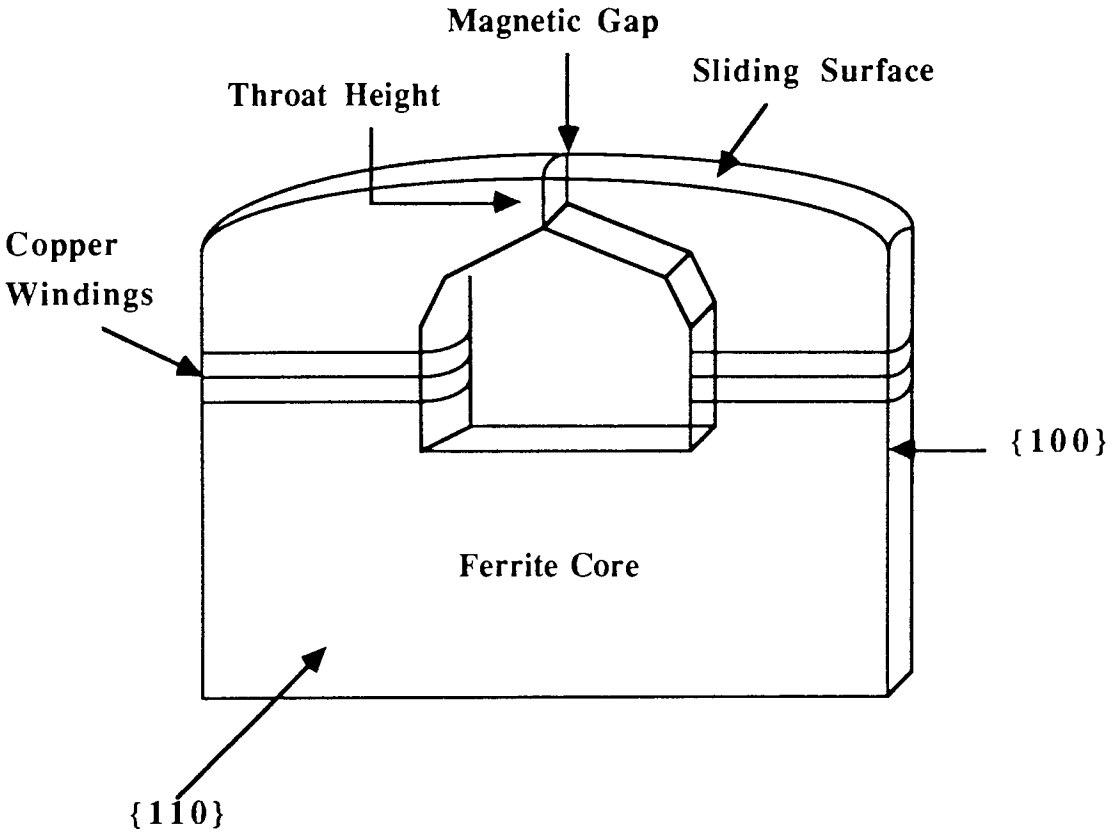

Figure 1.8: Single crystal Mn-Zn ferrite video head showing the orientation of the crystal planes to obtain low wear of the sliding surface.

FM recording: Generally the linearity of the recording is one of the most important factors in magnetic recording. However, there are two types of magnetic recording which do not rely on linearity, namely digital and FM recording. For both types, the recorded information does not depend on the shape or amplitude of the wave itself but on the timing of the zero crossing points of the signal. The signal to be recorded is passed through an oscillator or frequency modulator. This produces an output signal which varies in frequency corresponding to the input signal voltage. This signal is then recorded on the tape (1,2,4). Figure 1.9a shows the input signal to the modulator and Figure 1.9b shows the modulator output and its relationship with the input signal.

In playback mode the frequencies are demodulated, and a signal identical to the original input signal is produced. As the information is contained in the frequency, the amplitude does not affect the recording quality, assuming the signal to noise ratio is sufficiently low. One advantage of this system is that it is immune to fluctuations in the amplitude of the wave form. Another advantage, especially in video recording, is the reduction in the ratio of highest to lowest frequency. This would otherwise be a problem in video recording, where the highest frequencies recorded are typically 2MHz for domestic machines and 5MHz for professional duplicators, both very high when compared with audio recording. The ratio of high to low frequencies recorded is limited by the size of the head. The gap length and the length of the head determine the shortest and longest wavelengths recorded respectively, and hence, the maximum and minimum recorded frequencies.

Rotary head technology: the use of FM recording reduces the frequency ratio and enables the recording of a larger frequency span. However, the limits imposed on recording by the size of the read write head mean that even with the use of FM recording the head-to-tape speed must be high compared with audio recording. The tape speeds required to record the high frequencies would not be possible or economical over long periods of operation with a fixed head machine, even with a submicron gap length. Using a

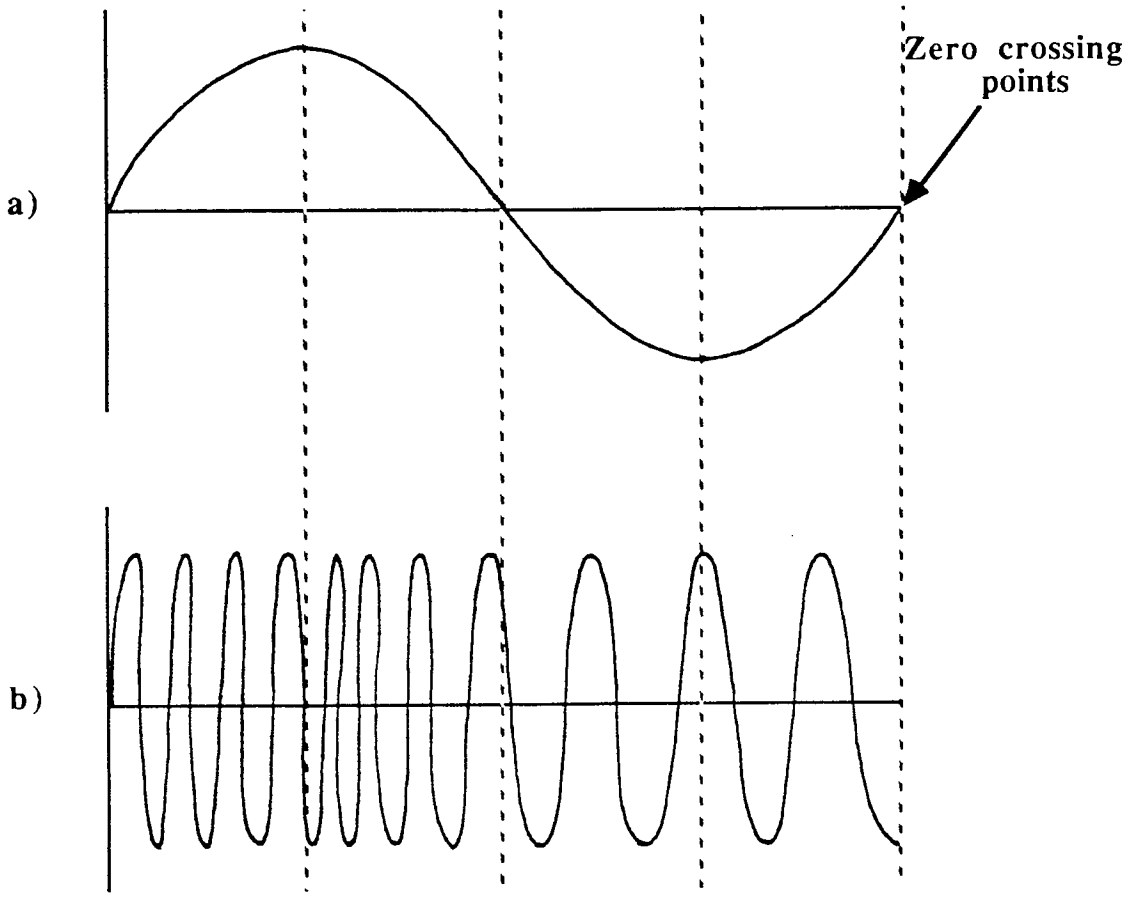

Figure 1.9: FM modulation; a) Input signal to frequency modulator, b) Frequency modulated signal which is subsequently recorded on the magnetic medium.

combination of moving head and tape the required tape-head speed can be obtained. Consumer and professional machines run at 200 and 1000 inches per second respectively. The movement of the heads is achieved by supporting them in the drive on a rotating aluminium drum or scanner which spins as the tape passes. In VHS machines the passage of the tape around the head is known as two headed wrap which covers three quarters of the drum (1). There is no break in operation as two to four heads are positioned on the rotating drum. The drum is positioned at an angle to the tape drive, so that the head scans diagonally across the tape. The resulting tape tracks are shown in Figure 1.10. The angle is such that each track describes one complete television field. The angles of the gap of the two heads are different so that the recorded tracks are at a significantly different angle, thereby eliminating the need for a guard band between tracks. This increases the packing density of the tape and allows a longer playing time for a given length of tape (45).

1.6 Methods of head wear measurement

The abrasivity of the tape and the wear resistance of the head are two properties which will always require quantification in order to obtain the correct balance of head wear. The amount of wear occuring to the head has to provide a balance between maximising the life of the head and removing debris, transferred layers and surface damage. The following section gives a brief description of the more popular methods of wear measurement.

The difficulty of measuring wear in situ, especially in the case of the video head, led to the development of methods using simulated head samples in the shape of bars or cylinders over which the tape would be drawn under simulated conditions of tape tension, wrap angle and pressure. Carroll and Gotham (46) were the first to use a "rod wear" test, in which the tape sample is run over a rod of radius 6.4mm under a wrap angle of 45 degrees. Wear is measured by the weight loss of the rod. Barsotti and Hyland (47) took the method one stage further, developing a tester consisting of several rods of different

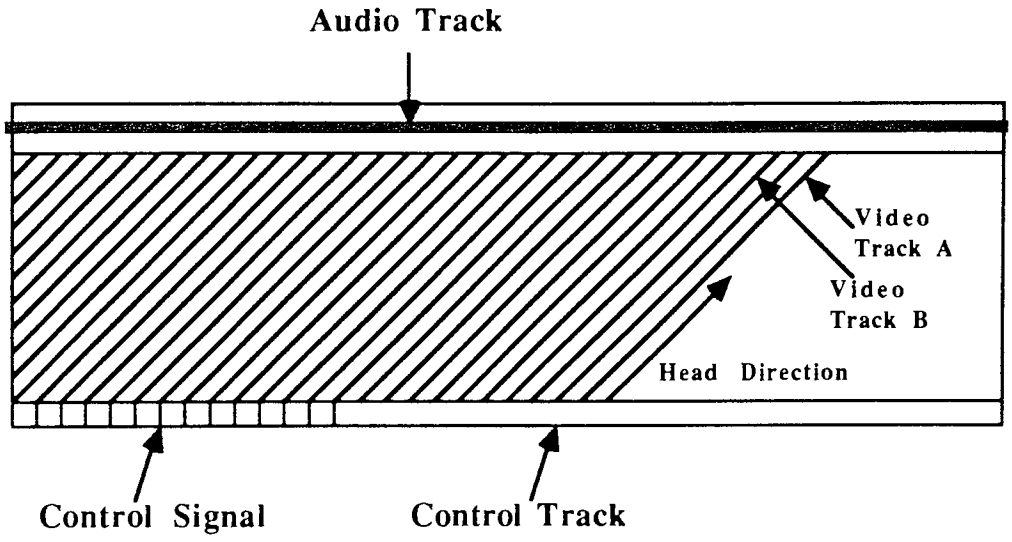

Figure 1.10: Position of audio and video tracks described on standard format VHS video tape.

radii and materials mounted on a wheel around which the tape is wrapped. Thus one tape sample could be run over several rod samples. The main problem with this method is the transfer of debris from one test specimen to the next. This is likely to alter the resulting wear rate by increasing the occurrence of three body abrasive wear.

Kehr (48) developed an accelerated version of the original test using the single rod. By using a smaller cylinder (2.5mm radius), a higher contact stress can be produced and the test is accelerated. Versions of the rod wear test were developed which did not include measurement of the weight of the rod. For example, Hahn (49) used a stylus profilometer to measure wear, which was dragged across the wear scar formed on the rod. This method can also be used directly on the head. Traces of the head are taken before and after wear, and the wear is calculated from the change in profile. The accuracy of this technique depends on how the surface of the head has worn, since the surface may not have a good enough finish to allow small changes to be measured. Alternative tests used a square bar as opposed to a rod, in which the tape is passed over one edge of the bar and the "flat" which appears with wear is measured optically. A Problem with this method is the breaking of the edge, which is exacerbated by performing the test under a high normal pressure to accelerate the test (50). Also the initial quality of the edge of the bar is variable and could alter the results.

Other methods of measuring wear occuring to a rod shaped sample include the "Russian" method which uses indentation as the method of wear measurement. A round brass rod is indented with the pyramid shaped diamonds and the wear measured as a function of the decrease in length of the square diagonals (51). Measuring the diagonals is problematic after wear, as the edges of the indent tend to become smeared. The "Scat" method uses the same technique but substitutes a coated indentation (51). Each indent is covered with a ceramic coating which is sputtered over the bar. The presence of the coating overcomes the smearing of the edges. A variation on this method includes wearing down a flat on the rod and positioning indentations on the scar before continuing

the wear test. This test uses the square Vickers diamond and a layer of sputtered ceramic material.

The rod/bar tests are a quick and simple way of comparing the abrasivity of various tape samples but bear little resemblance to the actual tape drive situation. The wear that occurs during head-tape interaction is a complex process, and is dependent on the materials as well as parameters such as speed and pressure. Other factors which cannot be simulated using a simple bar or rod include the variation in pressure due to the contoured shape of the head and the change in this contouring with wear, and the flash temperatures occuring at the head-media interface (52,53,54). The interface temperature is an important factor affecting the wear mechanism and is likely to be different for the rod or bar than for the actual magnetic head. For a test to provide accurate results, the surface to be worn needs to have the same contours, physical size, hardness and thermal properties as a real head. In addition, the correct wrap angle and normal pressure must be simulated. The production of such specialized samples is time consuming and would increase the price of the test. If only the relative abrasivity of a particular head-tape material combination is required, then the rod wear test provides sufficient information. However, the technique is not suitable for serious or detailed wear studies.

The Radicon Corporation (USA) developed a method of wear measurement using a specially made radioactive recording head (51,55). The head is made of Kovar, an alloy of nickel (23-30%), cobalt (17-30%), manganese (0.6-0.8%), and iron the remainder. The head is then irradiated to produce radioactive cobalt. As the head wears the radioactive material is transferred onto the tape and the amount transferred is measured by monitoring the tape using standard radioactivity counting techniques. The method assumes that all material worn from the head is transferred to the tape which may not be the case. Other disadvantages of the method include the need for a specially made head, the use of additional counting equipment, and health hazard associated with the use of radioactive material. The only advantage is the measurement of wear of authentic head material and head dimensions.

Hahn (56) reports on a method based on the change in resistance of a thin alloy film as it wears away. A thin metal alloy film of a chosen hardness is deposited onto a non-conducting ceramic substrate. The sample is polished and contoured to resemble the sliding surface of the head. The film forms part of an electrical bridge arrangement, allowing its electrical resistance to be monitored in situ. As the film wears away the resistance changes. A similar method is reported by Cash and Pagel (57), called the Fulmer Abrasivity test. Advantages of the method include the reproducibility of the results, and the fact that the wear is in situ and is monitored continuously. However, authentic head material is not worn and again the test is used to determine the abrasivity of various tape samples relative to a 'standard' tape. The "Shim" method is similar to the thin film method in that a layer separating the head and the tape is worn (51,55). In this case a thin brass shim of known hardness is positioned between tape and head, creating a head-to-tape spacing with corresponding signal loss. The increase in reproduction level (L) due to removal of the brass with wear is used to determine the amount of wear using the following equation, derived from the spacing loss formula (equation 1.2);

$$\text{Shim wear} = (\lambda \times L)/54.6 \qquad (1.3)$$

where λ is the recording wavelength = tape velocity/recording frequency.

The shim is worn to a conforming radius before the test and it is possible to create a finish similar to a real head. Nevertheless, the real head material is not being worn.

The duration of the test appears to be a prime factor in the design of a majority of the methods. The ability to obtain a relative abrasivity measurement in a very short time is desirable; and similarity of the test to the real life situation appears secondary. Broese van Groenou (58) reports a quick test using accelerated wear using increased pressure. The moving magnetic tape is pressed against a stationary flat polished sample by either a

cylindrical or spherical load. The resulting wear scar is then measured using a profilometer. This test was used by Schaake (59) to monitor the head wear rate due to chromium dioxide video tape. Although the test accelerates the wear dramatically, the difference in wear mechanism between an iron oxide and a chromium dioxide tape is apparent in the minutes it takes to perform the test. Schaake reports that the transfer of tape material dominates the wear of the head material in the case of the iron tape. In general accelerated wear tests appear to bear little relation to the actual situation.

Indentations have been used to measure wear in several of the tests described (50,55). Indentations can also been used to measure wear directly, for example, wear to authentic audio heads (60) and magnetic media has been recorded by directly indenting the surface. The indentation made on the surface to be worn is pyramidal, and as the surface is worn the diagonals of the indentation decrease. The change in diagonal length is related to the apex height of the indentation and thus the reduction in surface height by the apex angle. The accuracy and sensitivity of the technique can be enhanced by the use of a Knoop diamond indenter. The Knoop indentation is characterised by one long diagonal. The ratio of apex height to main diagonal is 1:31, hence the change in apex height of the indent as a measure of the wear can be very accurate (60). Another advantage of the technique is that the indentations can be positioned at various points on the surface to be worn. Using this technique it is possible to monitor wear which has occurred in situ to an authentic head. However, due to the nature of a tape and disc drives the head would have to be removed from the drive in order to measure the indentations.

The main priority for the methods of wear measurement reviewed above is the assessment of the abrasivity of the tape sample, rather than the head, providing wear values which bear little relation to real head wear. The main disadvantages of the methods reviewed are a failure to use authentic head materials and the reliance on the simulation of drive conditions, as opposed to in situ wear testing.

1.7 General principles of friction and wear

In this section the basic principles of friction and wear are presented. The sliding surfaces to be studied in this project are a filled polymer (the magnetic medium) and the ceramic head surface. The friction and wear of polymers, filled polymers and ceramics are also briefly reviewed.

1.7.1 Friction

When two surfaces slide relative to one other the resistance to motion that is experienced is known as friction. Two fundamental laws of friction are attributed to Amontons (1699) (61. The first states that the frictional force (F) is proportional to the normal load (W). From this relationship the coefficient of friction (μ) is defined as follows;

$$F=\mu W \qquad (1.4)$$

where μ is a constant for a given pair of materials under a given set of environmental conditions.

The second law states that the frictional force between two bodies is independent of the apparent area of contact. This law arises from the fact that nearly all surfaces are rough on a microscopic scale and the contact between two surfaces takes place at the tips of the asperities (62). As a consequence, the real area of contact (Ar) may be very much smaller than the apparent area of contact (A_{app}). Hence, both Ar and F are independent of A_{app} (63,64,65). The laws are generally true for metals but do not necessarily hold for polymers.

If two surfaces are loaded together under a normal pressure, the load is supported by the contacting asperities and the stress on the individual areas is relatively high. Initially, the summation of all the individual contact areas is insufficient to support the

load. Thus the asperities will deform plastically until Ar can just support the normal load (W). For an ideal plastic-elastic material

$$Ar.po=W \qquad (1.5)$$

where po=yield pressure. In general, for two surfaces in contact, po is the yield pressure of the softer metal (66). As W increases the number of contacting asperities increases. The deformation of the asperities in the case of metal contact is plastic or non-recoverable, whereas in the case of polymers the deformation may be partly elastic and some recovery may occur after the load has been removed. Thus the final contact area is dependent on the nature of the two surfaces, as well as the normal pressure. In general all friction and wear phenomena are a function of the highly stressed and localised interactions occuring within the real area of contact.

When two surfaces move relative to each other, it is widely accepted that the two main contributions towards the resulting friction are the shearing of the adhesive bonds formed over the real area of contact (Fad), and the displacement of the softer material by the asperities of the harder material (Fdef). The latter contribution can take the form of elastic displacement or plastic displacement (ploughing) of the softer material resulting in cutting of the bulk material.(63,64,65,66).

Adhesive component: If two metal surfaces are loaded together, strong adhesive bonds will form in the real area of contact. Since plastic flow occurs at the tips of the asperities they are in effect welded together and the bond is often called, in the case of metals, a cold weld. For relative sliding to take place the junctions must be sheared, and this gives rise to the adhesive component, which is dependent on the shear strength of the junctions (s) as follows;

$$Fad = Ar.s \qquad (1.6)$$

The adhesive component includes only the interfacial region between asperities but involves relatively large strains and rates of strain. (67).

Ploughing component: The ploughing term (Fp) is the main contribution to friction during abrasive processes. Ploughing occurs when either a hard asperity in one surface penetrates a softer material, or when a hard particle ploughs through one or both surfaces in contact (three body situation). The contribution to frictional force occurs through the resistance to ploughing. The simplest model to describe this contribution to friction assumes the asperity to be a conical slider with an angle Ø in contact with the softer material, where the friction force due to ploughing (Fp) is given as follows;

$$Fp=(2/\pi)\tan Ø \qquad (1.7)$$

Ploughing contributes further to the frictional force in two ways; first by creating wear particles which affect subsequent friction and wear; and second, as the asperity ploughs through the softer material debris may build up in front of the slider rather than being removed from the groove being formed (68).

Deformation component: If two asperities come into contact, in order for motion to continue the softer material will have to deform. This term involves small strains and large volume deformation which may be either plastic or elastic depending on the materials. This contribution to friction is largest when two metals slide against each other since there is no elastic deformation of the asperities. This contribution is responsible for the main part of static friction (65,69).

Figure 1.11 shows the contributions to the displacement term. If it is assumed that the two contributions to friction do not interact, then the total frictional force can be written as follows;

$$F = F_{ad} + F_{def} \qquad (1.8)$$

Factors which affect the total friction have been shown to be the surface topography, the type of motion (i.e. sliding or rolling), and the mechanical properties of the materials (61).

1.7.2 Friction in polymers

Polymers exhibit viscoelastic-plastic behaviour, they have low bulk moduli and low melting points. Thus the deformation term is more significant than for metals, and they are more sensitive to applied loads, sliding velocity and temperature (70,71). Bowden and Tabor (66) suggest that, in the case of unlubricated polymers, the adhesion term is predominant due to the elastic nature of the deformations.

Adhesion term: The proximity of the asperities results in an adhesive joint as with metals. The bond is either physical (Van der Waals forces) or chemical (ionic or electrostatic bonding) (22,72,73). Van der Waals forces are long range forces present between all atoms, and arise from the fact that at any instant the centre of the negative charge of the electrons travelling round the nucleus may not coincide with the centre of the positive charge. The atom is in effect a small dipole and the bond is a dipole-dipole interaction, and is therefore relatively weak. Ionic or electrostatic forces originate when two dissimilar heteropolar surfaces come into contact. Electrostatic forces are produced by one or more electrons transferring completely from one atom to another. Thus neutral atoms are converted to charged atoms and these mutually attract forming ionic bonds. Whilst the

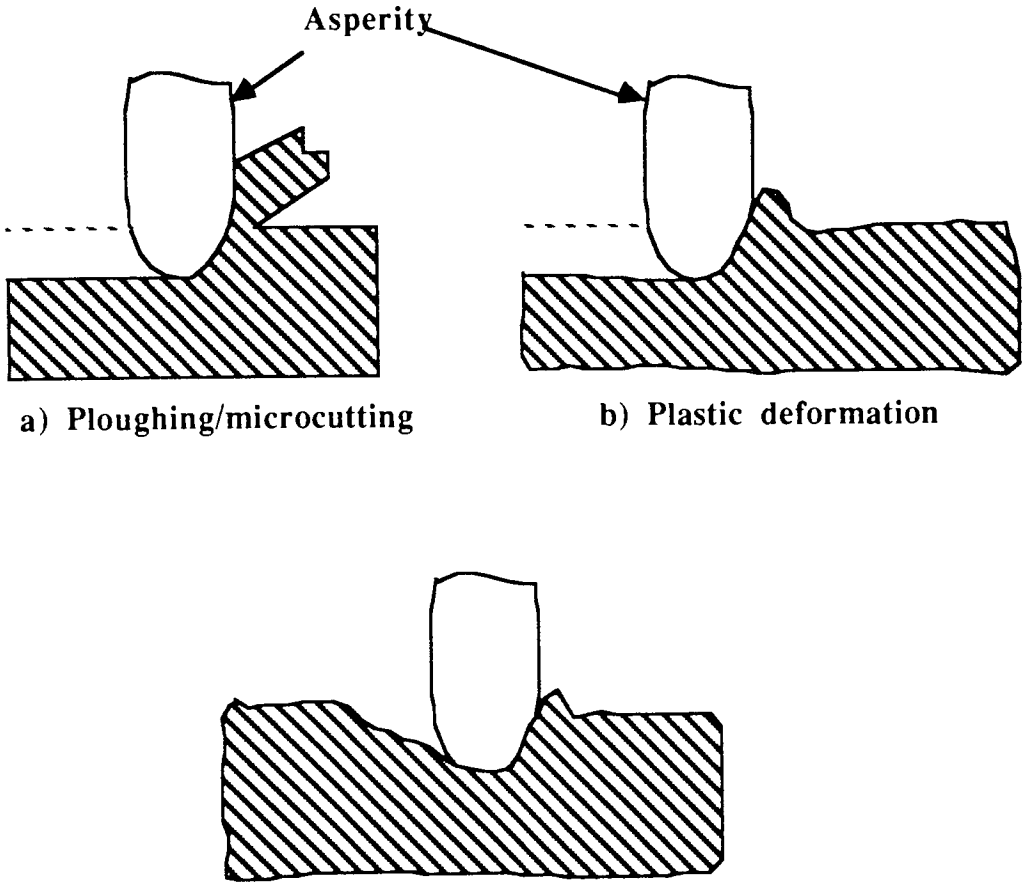

Figure 1.11: Contributions towards the deformation component of friction

Van der Waals attraction is a physical bond, the ionic bond is chemical and only forms within the real area of contact.

Van der Waals forces are effective from relatively large surface separations (approximately 500Å) to close contact. Hence, the forces also increase the real area of contact by drawing the two surfaces closer together. During sliding, the asperities are continually loaded and unloaded. At each point bonds are formed and sheared as the surfaces slide. Polymer binders are soft and deformable, and can stretch appreciably without rupturing. This also has the effect of increasing the contact area. In the case of polymer sliding, although the bonds themselves are weak, large areas of intimate contact are established and the overall adhesive force is high. In general, the smaller the real area of contact, the lower the friction.

Deformation term: In the case of polymer friction the deformation term is further divided depending on whether the deformation is plastic or elastic. If a hard asperity is sliding over a polymer surface, energy is fed to the polymer ahead of the asperity and is partly recovered elastically behind (74,75). The energy released behind the asperity helps to push it forward, although the energy released here is still less than that supplied during deformation. Hence, a tangential force is still required to continue the relative motion (Figure 1.12). The deformation is not entirely elastic as plastic deformation may occuring resulting in grooves forming in the surface. Under high sliding speeds thermal effects may play an important part in friction. Polymers have low thermal conductivity, and the heat build up may alter the elastic modulus and the shear strength of junctions thereby affecting the friction. When the velocity of sliding is relatively high the heating effects at the interface may never reach a steady state due to the continually oncoming cold surface (67,76).

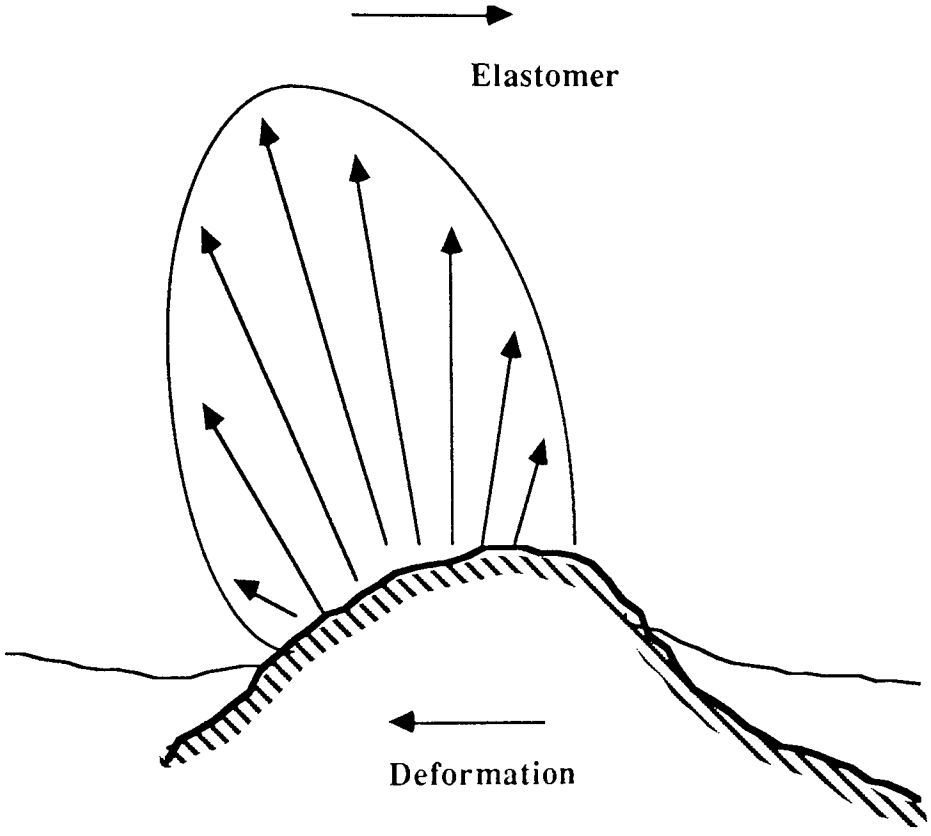

Figure 1.12: Deformation of an elastomer in the path of an asperity demonstrating the hysteresis component of friction in polymers.

1.7.3 The wear of polymers

In the context of polymer wear five mechanisms are identified; these are abrasive, erosive, fatigue, corrosive and adhesive (61,65,66).

Abrasive wear: Abrasive wear is characterised by the ploughing of a harder material through a softer surface. This may be the result of either the sliding of a relatively rough hard surface over a softer surface, which is known as the two body case, or a loose particle trapped between two surfaces which is termed three body abrasion. Material is removed from the softer material by ploughing or cutting during sliding and grooves may be formed in one or both surfaces. Not all the material in front of the slider is ploughed out of the groove. Plastic deformation also occurs in the formation of the groove and is a prerequisite of abrasive wear (77). In the simple model of ploughing, assuming the hard asperity to be a conical slider with an angle of Ø to the surface, the volume of material removed by the asperity (V) in abrasion can be expressed as follows;

$$V = (KWD \tan Ø)/H_d \qquad (9)$$

where D is the distance of sliding, H_d is the hardness of the material removed, and K is a constant which accounts for the fact that not all the material is removed as debris, a substantial amount may be plastically displaced (70).

The mechanical property of a polymer most relevant to abrasive wear is the work required to rupture the material during sliding. This is measured as the area under the stress/strain curve for that polymer, but is also approximately equal to the product of the breaking strength (S) and the elongation at break (e). Thus, wear rate is proportional to 1/Se (70,78).

Erosive wear: This term is used to describe damage caused by the impinging of solid particles present in a fluid on a surface. The wear rate is dependent on the angle of incidence of the particles and on whether the solid surface is brittle or ductile. For a ductile solid the mechanism is similar to abrasion and fatigue, depending on the angle of impingement. For brittle materials, surface cracks are formed which propagate and intersect to give wear particles (61,63).

Fatigue wear: For a range of materials in sliding contact, with surface topography varying from very rough to smooth, it is not easy to decide the point at which abrasive wear, characterised by plastic deformation and cutting changes to fatigue wear. In general fatigue wear results from the repeated stressing of a given area, but often overlaps substantially with the abrasive process. In fact, a large amount of what is termed abrasive wear may in fact be fatigue wear. The difference is that fatigue wear occurs through continuous asperity contact, whereas abrasive wear results from a single micro-cutting action. Ideal conditions for fatigue wear occur where the surfaces are separated by a lubricating film. In this case no adhesive or abrasive wear can take place but the opposing surfaces experience stresses transmitted through the lubricant during sliding. Another example is the distinction between wear caused by a surface composed of relatively sharp asperities, and wear caused by a surface composed of more rounded asperities. For the latter the cutting of the surface is far less evident and fatigue on a localised scale is considered to be the predominant wear mechanism (61,63).

Corrosive wear: For corrosive wear to occur relative motion must be taking place in a corrosive environment which is either gaseous or liquid. Under these conditions, surface reactions may take place and the products are left on one or both sliding surfaces. The reaction products do not usually adhere strongly to either surfaces and are removed with further sliding. The presence of a lubricant usually protects a surface from corrosive wear, however, it is not unknown for products corrosive to the surface to be present in the lubricant.

Adhesive wear: Adhesive wear occurs where strong intermolecular forces are created between the two surfaces. In the case of polymers in contact with a smooth hard surface, the load or pressure is supported by the deformation of the asperities of the polymer. However, the polymer is more deformable than a metal, and larger real areas of contact are established. For relative sliding to take place the bonds formed have to shear. If the bond between the polymer and the counterface is relatively weak, shearing takes place at the interface. If the bond is stronger than the polymer bulk, then the shearing takes place away from the interface in the bulk of the polymer and a portion of the polymer will be transferred to the counterface. During repetitive sliding of polymers against metals transfer of polymer film to the metal is often observed (79). The film developed depends on the polymer and also dictates the ensuing contact between the two surfaces (78). A rigid polymer such as polyester transfers in irregular lumps creating a relatively rough surface and increasing the wear rate of the remaining bulk polymer. A more ductile polymer will form a smoother transfer film, as repeated sliding will deform the transferred polymer. In this case the wear rate decreases with time. Transfer is more likely to occur with polymers above their glass transition temperature (Tg). However, at high sliding speeds surface heating may increase the interfacial temperature above the Tg of the polymer. Once transferred, repeated sliding over the layer may detach the film, which will eventually be displaced from the counterface and will appear as loose debris. In general the following considerations are important in the transfer of polymer films (75);

a) The nature of the initial adhesion.

b) The mode of failure of the polymer.

c) The structure and thickness of the transferred layer.

d) The bonding between the transferred layer and the counterface.

e) The mechanism of the film removal.

1.7.3.1 Filled polymers

Fillers are often added to reduce wear of the polymer. This is especially effective in the case of the polymer sliding against a relatively smooth surface. Addition of a filler usually increases S, and greatly reduces e. Hence, the polymer is not necessarily more resistant to abrasive wear. It would appear in the case of PTFE and HDPE that the addition of fillers increases the adhesion of the transferred layer to the counterface which contributes to the reduction in wear rate of the filled polymer. The increased adhesion of the transferred layer is a product of the particles of the filler material acting as temperature intensifiers which causes local polymer melting and increasing the intimate contact between the polymer and the counterface (78). Another factor in the reduction in wear rate of the filled polymer is the support the filler gives to the polymer at the interface. The filler rich surface effectively supports the load and separates the polymer from the counterface (80). The polymer operates as a boundary lubricant. In the case of adhesive wear due to the sliding of two very smooth surfaces, the addition of a filler will abrade the counterface and may provide the optimum roughness to provide minimum wear. The parameters relevant to the choice of a filler are the shape and size of the filler particle and the relative hardness. Very little can be generalized concerning the wear of filled polymers. Definitive trends in wear can only be established by testing a particular polymer composite-metal pairing.

1.7.4 Wear of ceramics

Ceramic materials generally exhibit low friction and wear. The properties which contribute towards low friction include a high level of hardness, which results in low deformation and low adhesion since ceramics are chemically inert over a wide range of environmental conditions. Ceramics are used in both polycrystalline and single crystal forms. In the polycrystalline form the hardness, and consequently the wear resistance, increases with decreasing grain size (41,48,81). In the single crystal form the material

exhibits anisotropic behaviour (38,43). Magnetic heads are produced in both forms.The single crystal form is usually chosen for video recording because of the increased wear resistance obtained by choosing the crystal directions. The coefficient of friction is lowest when sliding occurs along the close packed planes and directions. The lower coefficient of friction in this direction arises from the lower surface energy exhibited by a close-packed system, and the higher level of hardness of the close packed system. The planes which exhibit the best wear resistant characteristics were described in section 1.4.

The high strength of the ceramic usually results in brittle failure, fracturing with little or no evidence of plastic deformation. However, plastic flow has been observed for ceramics such as magnesium oxide and aluminium oxide under relatively low wear conditions of sliding contact (82). The friction and wear of ceramics are affected by the presence of surface films (82,83). Surface films or absorbed layers affect both the adhesion and the amount of plastic deformation that occurs. The extent of plastic deformation is also dependent on the contact pressure. Miyoshi and Buckley (82) report different modes of wear occuring to a silicon carbide surface in sliding contact with a diamond slider. Under relatively low contact pressure neither cracking of the silicon carbide or groove formation due to plastic flow were observed. Under a low range of contact pressures the main contribution to friction originates from adhesion and the coefficient of friction (μ) is related to the load (W) by the following expression

$$\mu = kW^{-1/3} \qquad (1.10)$$

At higher contact pressures the effect of load on the friction characteristics is totally reversed. The formation of plastically deformed grooves and cracking of the silicon carbide surface is observed and the relationship between load and friction changes to the following;

$$\mu = kW^{0.3\text{-}0.4} \qquad (1.11)$$

The exponent depends on the crystal orientation of the silicon carbide. At even higher pressures gross surface fracture, subsurface cracking and plastic deformation are observed (82).

The wear of ceramics has also been examined under conditions of sliding against a material consisting of hard abrasive grits embedded in resin (the two body condition) (82). A Mn-Zn ferrite oxide ceramic was used and the abrasive grits of silicon carbide and aluminium oxide were seen to cut grooves in the ferrite, using a ploughing and microcutting mechanism. To achieve a large number of such grooves it would appear that relatively few abrasive particles need to come into contact with the ferrite. The same type of abrasive wear can occur due to three body abrasion where a third particle harder than one or both of the surfaces becomes trapped between them. In this case, material from one or both of the surfaces may be removed. Two different sizes of abrasive grits were also examined and different abrasion mechanisms were observed for the two sizes. In the case of grits which were approximately 15μm in size brittle fracture was seen to occur, whereas at 4μm plastic deformation was predominant (82).

1.8 Previous work on tape and head wear

Improving the durability of the tape and the life time of the head have always been the objectives of research into wear. The nature of research into tape and head wear has changed over the past 30 years as electronics technology has become more sophisticated. Improvements in technology have demanded better and smoother finishes to both tape and head surfaces. The stage has now been reached where the limiting factor to improved performance is not the electronics of the system but the tribology. This is especially true of video recording where the operation is in-contact to the extent that the head protrudes into the tape. Under these conditions, wear to both surfaces is unavoidable. In order to obtain good signal reproduction, close head-tape contact must be maintained under conditions of continual wear. To achieve a system which allows maximum contact to be

maintained the wear mechanisms must be fully understood. Miyoshi (84) claims that little has been learned about fundamental mechanisms of friction and wear involved in the interaction between tape and head. The following section describes some existing theories of tape and head wear, with an emphasis on head wear.

It is widely agreed that the first sign of wear to a magnetic head is the appearance of small scratches or grooves over the sliding surface, formed in the direction of sliding (42,85,86,87). The occurrence of this phenomenon has led to the assumption that wear to the head is predominantly abrasive. However, other wear phenomena are present, such as the build up of frictional polymer films, which reveal that a certain amount of adhesive wear also occurs (73,86,88). The following sections discuss the origin and effects of abrasive and adhesive wear.

1.8.1 Abrasive wear

The width of the scratches or grooves in the ferrite surface, on average 0.1μm, has been shown to be almost the same as the diameter of the oxide particles of the magnetic coating, (42,73,85). Thus, it is generally accepted that the damage is caused by the acicular magnetic particles of the tape (89). Another factor contributing towards such damage may be air-borne debris becoming trapped between the two surfaces and creating deformation by the process of three body abrasion (23). Potgiesser and Koorneef (85) report that, even if the tape drive is isolated from the environment so that no air borne debris reaches the head, the scratching appears with the same frequency. Hence, deformation caused by the magnetic particles appears to be dominant. However, isolation of the tape drive does not completely eliminate the occurrence of three body abrasion as debris produced by wear from either the tape or head may also become trapped (90,91).

An additional source of the scratching which has now been largely eradicated is glass chips in the magnetic coating. The use of glass pearls in the milling of the magnetic slurry before coating led to the occurrence of tiny chips of glass in the coating itself (85).

The coating was filtered to remove them, though any particle similar in size to the magnetic particles would not be filtered out. In most cases glass beads have now been improved or replaced.

Experiments were performed by Hahn (92) to compare wear caused by tape which was smoothed using a cleaner blade as it approached the head with wear occuring under normal operation. Asperities were also counted electronically. The cleaner blade reduced the number of asperities as intended, which reduced the wear to the head by a factor of four. The severity of the scratching to the head was much improved as shown by photomicrographs in the paper. Hahn (92) concluded that the deep scratching of the head is caused by isolated asperities on the tape surface present as deformations on the tape. Hahn's observations concur with work performed on the general wear of ceramics against resin filled with abrasive grits (82). As mentioned in section 1.7.4, only a few abrasive particles need contact the counterface in order to cause a large number of scratches or grooves on the surface.

Over the first few hours of use of a new head the reproduction signal is seen to degrade, and this correlates with the appearance of the plastically deformed,or grooved surface. Polleys (87) found that the degradation develops more quickly than visible damage, which implies that the degradation results from changes occuring on a micro-scale. The signal degradation is characterised by a loss in sensitivity of short recording wavelengths. After the first few hours the sensitivity remains constant in most cases. The loss in signal is the result of two phenomena; first, change in the surface of the head as it wears over the first few hours which may include the build-up of polymeric material transferred from the tape or damage to the ferrite surface itself, either of which will produce a head-to-tape spacing and loss in signal; second, damage to the gap. The gap length dictates the minimum recorded wavelength, hence removal of material from the gap will reduce the sensitivity of the head to short wavelengths. These effects are discussed in greater detail later in this section.

Polleys (87) found that plastic deformation of the surface within the first hours of use can lead to a damaged surface layer of ferrite with reduced magnetic properties, (i.e. a dead layer). This results in head-to-tape spacing with corresponding signal loss. The removal of material from the head surface results in strain fields associated with the grooves formed on the wear surface. In the case of ceramics, the strain appears to be compressive and can have a value close to the breaking strength of the material, which for ferrites is 3000N/mm^2 (85). The strain field around such a scratch can be seen using Lang's method of X-ray topography (93). The technique uses a diffraction image to show any abnormalities in crystal structure, including strains and dislocations. The strain field results in a layer of disturbed magnetic properties in the region of strain. The head is often covered in a number of grooves each with their associated strain field, which gives rise to the formation of a layer of disturbed properties, a dead layer, and a head-to-tape spacing.

Polleys (87) suggests that the stress caused by the removal of material from the head in the form of strips or grooves by the tape is the same as that achieved when an indenter is applied to the surface of the material. The indenter has a sharp apex and corners to its shape. As it is loaded onto the specimen, the deformation is plastic, that is irreversible, and the sharp corners initiate surface cracks which propagate out from these points. As the indenter is unloaded the cracks close up, but a residual stress field remains. As the indenter is completely removed, subsurface cracks are initiated, and it is assumed that these originate from residual stress in the plastic deformation zone. Figure 1.13 shows the resulting stress field. Each groove in the surface is associated with a stress field along its length, and a number of such scratches are associated with the loss of performance of the surface layer.

To investigate the change in magnetic properties of the dead layer, the surface of worn heads have been examined using several techniques. The Kerr effect utilizes the effect of magnetization on polarized light. A beam of polarized light is reflected against the magnetic material, the angle of rotation of the polarised light being proportional to the

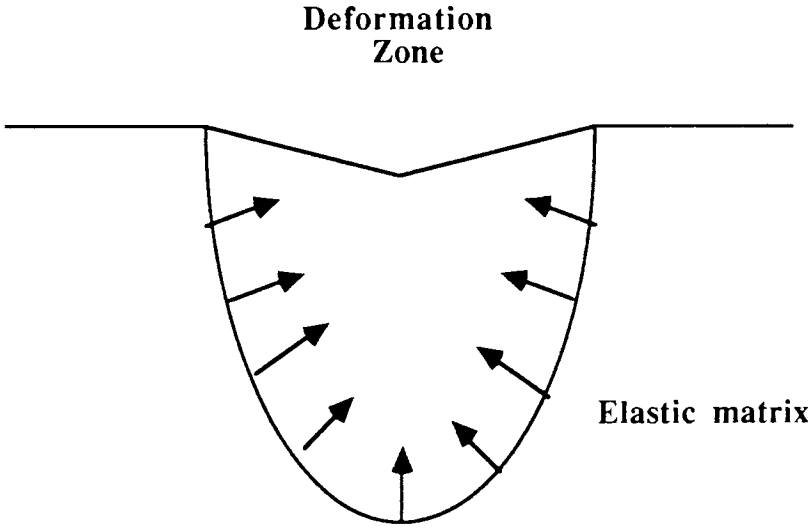

Figure 1.13: Residual stress present after the withdrawal of a sharp indenter.

magnetization of the sample. Using the magneto-optic Kerr effect, the reduction in magnetic properties of the surface was examined by Potgiesser and Koorneef (85). As the head was worn the angle of rotation was found to decrease, showing a reduction in magnetization. Thus the reduced magnetic properties of the surface due to deformation of the ferrite surface were demonstrated. In addition, using reflection electron diffraction the wear surface has been shown to be almost completely amorphous (85). In order to establish the depth of the amorphous layer, the surface was etched with hydrochloric acid at 50°C for 0.1μm at a time. The diffraction pattern after etching for 0.1μm showed evidence of plastic deformation. Crystallinity was observed after etching for 0.3μm and the bulk crystalline structure was observed after etching for 0.6 μm. Plastic deformation of the ferrite surface appears therefore to create an amorphous layer of reduced magnetic properties, the depth of the layer being between 0.3 and 0.6 μm. Miyoshi (42) suggests that the deformed layer is the critical factor in signal degradation over 2.5dB, loss in performance due to tape wear being 1dB or less. Another property of the deformed surface is work hardening due to the residual stresses involved. This also has the effect of increasing the wear resistance of the surface (87).

The mechanism of removal of material from the head is not widely discussed. Potgiesser (85) claims that scratching can only occur if the local normal pressure is sufficiently high and that this will only occur under an asperity. The presence of an asperity will raise the local pressure above the breaking strength of the material and scratching will be initiated. The indentation of such a brittle surface by sharp indenters involves fracture involving both radial and lateral crack propagation. Plastic deformation of the surface is a product of the lateral crack propagation. Polleys (87) suggests that lateral cracks extend to and then along the grain boundaries until the intersection with other cracks results in pull-outs. Hence, a major source of material removal is the propagation of subsurface cracks. It is interesting to note that this form of crack propagation and material removal is a product of a sharp indenter similar to acicular magnetic particles. A blunt edged indenter would act only on subsurface cracks already

established. Hahn (86) also reports the occurrence of pull-outs, especially in the case of video recording where the head is under high speeds and pressures. Under these conditions grain pullouts occur as a result of cumulative fractures and fatigue. Again the result of the removal of material is a work hardening of the surface.

Given the production of damaged ferrite layers, it would appear that a certain amount of wear is necessary, not only to remove debris from the surface, but also to remove or inhibit the development of layers of damaged ferrite. Wear is also necessary to remove or inhibit the development of polymeric films caused by transfer from the tape. This is especially important in the case of video recording where wear is unavoidable, and deformed and deposited layers must be controlled or removed in order minimise losses due to head-tape spacing. This creates a paradox, because in general a high wear rate is not desirable for any magnetic recording situation. The life of the head is an important factor especially for professional duplicators and a high wear rate is therefore undesirable. Commercial tape products vary widely in terms of wear rate depending on the magnetic pigment chosen. A chromium dioxide tape will exhibit approximately twice the hardness of an equivalent iron oxide tape . Using the Knoop hardness test the following hardness measurements have been taken at (13°C); Chromium dioxide 225 Mpa; Iron oxide 118 Mpa. These figures are for tapes made with a polyester-polyurethane binder system which also contributes towards the overall hardness (84). Chromium dioxide media have an inherently higher wear rate so that softer particles such as Zinc oxide are often added to the coating to reduce the wear rate (59). Iron oxide tapes fall into the low wear category.

1.8.2 Adhesive Wear and the effect of adhesion on friction.

Adhesive wear is characterized, in the case of head-tape interaction by the transfer of polymeric debris from the tape to the head. The resulting transferred layers are sometimes referred to as frictional polymer films (86). The origin and mechanism of transfer of the film is not fully understood due to the complex nature of the tape. However, it is probable

that the film is transferred from the soft portion of the binder system. This conclusion is reached by considering the possible transfer mechanism. Bonding between the tape and the head surface occurs within the real area of contact, which in the case of a polymer can be relatively large due to the ability of the polymer to deform. Although bonds may be weak the overall adhesive force may be high. Removal of polymer from the tape surface occurs when the bonds between the two surfaces are similar in strength to those of the bulk polymer. In this case, the shearing process may tear out a fragment of polymer. This is more likely to occur for the softer portion of the binder system, as the bonding of the soft binder is weaker than the semi-crystalline hard binder. If the tape surface were not lubricated this would occur continually and the friction involved would make the system inoperative. Despite the presence of the lubricant it appears that some polymeric debris may be transferred to the head (86). The result of the polymer build-up on the head is head-tape spacing with corresponding signal loss. However, the film is extremely wear resistant making it a desirable property from this point of view. The transfer of polymeric debris to the head surface usually involves either ion-dipole or ion-induced dipole electrostatic bonds. Once a layer of the polymer has built up on the head the adhesive mechanism changes. Polymer-polymer bonding consists of dipole-dipole or dipole-induced dipole bonds which are much weaker adhesive bonds reducing the adhesive wear and therefore creating a wear resistant layer (22).

The adhesive component of friction and wear is also responsible for sticking problems presented by very smooth magnetic tapes (23). It is desirable from the point of view of signal reproduction and wear to have both surfaces as smooth as possible. This is to provide close head-tape contact and to avoid abrasive wear. However, the large real area of contact created by smooth surfaces, one of which is a polymeric material, presents high adhesion and sticking problems (23). The problem can be controlled, to some extent by choosing a binder system with low surface energy. In general a non-polar polymer has a lower surface energy than a polar polymer, and therefore provides lower friction. The problem can also be controlled by lubrication of the surface to reduce the friction.

However, it would appear that a compromise is required in terms of roughness in order to avoid high adhesion due to large real areas of contact. Another alternative is to increase the elastic modulus of the polymer, reducing the real area of contact, and consequently, the friction and wear (72).

1.9 Environmental effects on wear to the head

Environmental conditions, such as temperature and humidity, under which magnetic tape is operated or kept may affect the wear to both surfaces in contact. Under conditions of humidity above 40-45% RH, head wear is seen to increase, as shown in Figure 1.14 (94). Although this is generally accepted, the mechanism underlying such a sharp increase is not clear. The tape itself is hygroscopic, and in equilibrium at high humidities will contain a high percentage of water. There is, however, no dramatic increase in hygroscopic properties above 45% RH which corresponds to the increase in head wear (94). The effect of a high water content within the bulk of the tape is a breakdown of the soft binder segment by hydrolysis (73,95,96), as shown in Figure 1.15.

The degradation products are of a lower molecular weight, and can migrate through the coating and exude onto the surface flowing over the asperities. This increases the Van der Waals forces, and also the adhesion and wear. The adhesive process occuring under these conditions can lead to stiction. By definition stiction only occurs where there are changes in the surface chemistry, as in the case of hydrolitic degradation. Here the bonds formed are strong covalent or electrostatic bonds as opposed to the Van der Waals and weak electrostatic bonds. The main difference between stiction and friction is that, for stiction, a measurable force is required to pull the tape from the tape drive (22). The occurrence of stiction has been known to result in the failure of the tape to move across the head. Hydrolytic degradation of the binder system does not necessarily result in gummy products on the surface of the tape. If the chain scission of the polymer has an element of regularity, crystalline products may be formed and generated as debris which

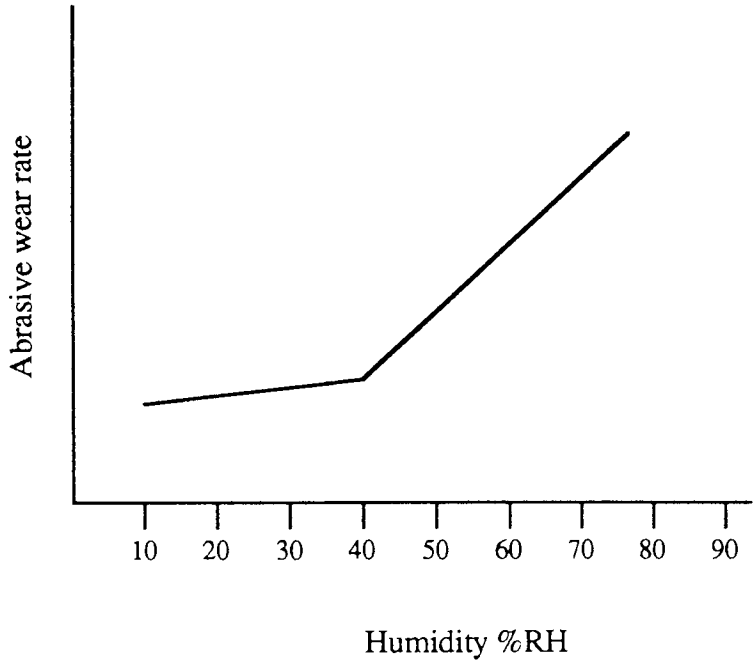

Figure 1.14: Abrasive wear rate plotted against humidity

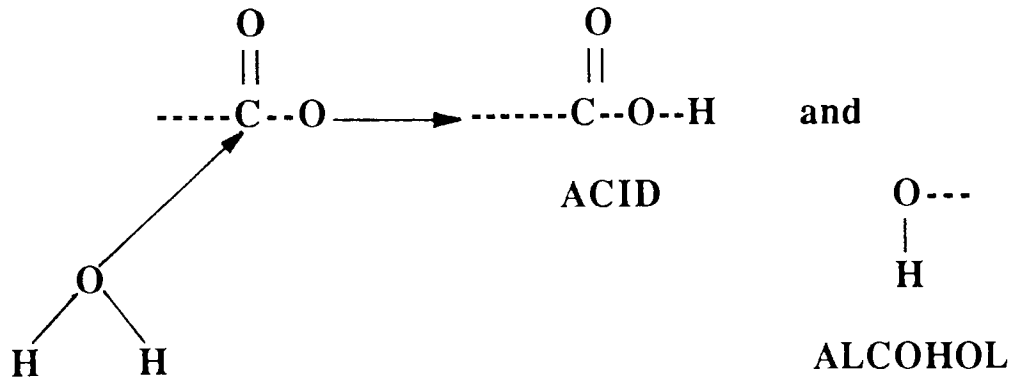

1.15. Hydrolysis of the ester group of the binder system to produce an acid and an alcohol.

does not affect the friction properties. Also, the migration of low molecular weight products may be slowed or stopped by strong interaction between the degradation products and the metal oxide. Prior absorption of dispersants inhibits the interaction and allows exudation. If the products which exude and spread out over the surface are completely random in size, they are less likely to form a crystalline debris and will increase the adhesion of the surface due to the increased polarity of these small fragments.

Carroll and Gotham (97) performed a number of experiments to establish whether the cause of increased wear at high humidity was due to the tape or the head. By localising the humidity, they found that the increase in wear was a property of the head and independent of the tape surface, although the tape dictates the magnitude of abrasive wear. Larsen-Basse (90,98) suggests a mechanism of moisture assisted fracture of the grains of the head, which causes more grains to come into contact with the tape. However, Carroll and Gotham (97) suggest that the fracture or break-down of abrasive grains is due to the mechanical action of the tape, and occurs without increased humidity.

Under conditions of low humidity, below 25% RH, the phenomenon of 'Brown stain' occurs (23). The phenomenon is characterised by a brown or sometimes blue coloured polymer film over the head. The variation in colour is produced by interference and is a function of film thickness (23). Chemical analysis of the film has been inconclusive (86). The film can only be removed by mechanical means, which suggests that the mechanism producing the staining occurs under all conditions of humidity but is only allowed to build up under the low conditions of wear found with low humidities.

The change in wear rate with humidity necessitates that magnetic tape recorders should be operated and tapes stored at a level of humidity between 25%-30% and 40%-45% RH. In known adverse conditions the recorder is often placed in a sealed unit with a set humidity range dependent on the temperature. However, the domestic consumer is unlikely to operate the machine under controlled atmospheric conditions.

Once again there is a paradox in terms of head wear; a smooth highly polished tape exhibiting minimal abrasivity is more likely to 'stick' to the head and result in transfer of polymeric debris to the head. This results in head-tape spacing and loss of signal at short wavelengths. Contributions to the effect come from the increased area of contact and therefore increased Van der Waals forces, and the lack of abrasive wear. However, this type of tape-media interaction is desirable for the length of head life, the build up of the polymer being wear resistant and further increasing the life of the head.

1.10 Research Programme

The overall objective of the research programme is to establish the mechanisms of wear occuring to the video head in sliding contact, in particular with iron oxide tape. This will be achieved by examination and quantification of wear occuring to the head, in-situ, in a standard domestic video recorder. The effect of varying the type and level of the head cleaning agent on the wear mechanisms will also be examined. Various techniques will be used to examine the wear to the head including X-ray Photoelectron Spectroscopy (XPS), Secondary Ion Mass Spectroscopy (SIMS), Scanning Electron Microscopy (SEM), Transmission Electron Microscopy (TEM), and Interferometry.

From the literature it is clear that the interaction between magnetic media and heads is not well understood. This is particularly true of video recording, where the head is physically much smaller than any other recording system and protrudes into the tape such that wear to the head is unavoidable. The mechanisms of wear to the head need to be fully understood in order to realise the full potential of the technology behind video recording. One of the reasons behind the lack of understanding of the wear mechanisms occuring to the video head stem from the fact that few studies have examined heads worn in situ, that is, in the tape drives and using authentic head materials. One of the main aims of this project is to study wear occuring in-situ in order to establish the wear mechanisms. There does not appear to be a satisfactory method of wear measurement, in particular for

the measurement of wear occuring to an authentic head. Thus the aim is to develop a method of wear measurement which monitors wear occuring in situ.

It is only recently with the development of surface analysis techniques such as XPS and SIMS, that it has been possible to analyse the top few layers of a surface. With these techniques, insight into the transfer of material in this and many other tribological situations can be observed.

Another area which has not been adequately addressed in the literature is the study of the effects of adding a head cleaning agent to iron oxide formulations. These particles are added to increase the head wear to the manufacturers specifications. There appears to be no definitive statement on the optimum head wear necessary for any head-media interaction. Thus a second aim is to examine the effect of the addition of the HCA, to establish any change in wear mechanism with their addition, and to establish the optimum HCA level for the interaction between a single crystal Mn-Zn ferrite video head and iron oxide video tape.

Chapter 2:

Equipment and experimental methods

2.0 Introduction

This chapter is divided into four main sections, each section describing the method and techniques used at different phases of the research. The first section describes the pilot research performed at 3M (UK) plc, at the video technical centre in Swansea. This work focussed on a study of the performance and basic wear characteristics of several commercial brands of video tape. The aim of this preliminary study was to isolate the general characteristics of head wear and to establish a course of further research.

The second section describes the work carried out to develop and test a method of head wear measurement to be used throughout the project. The aim was to find an accurate in-situ method which could be used in conjunction with other measurements. The method involved the direct indentation of the video head with a knoop diamond.

The third section describes the methods used in the main experimental work, in which the role of the head cleaning agent (HCA) within the magnetic coating was examined. The performance of a standard iron oxide formulation containing variations in the concentration and type of HCA was examined using the wear measurement technique developed in the previous section, and also by monitoring the signal degradation over several hours. The aim was to establish the optimum use of the HCA.

The fourth section gives an overview of the methods of surface analysis used throughout the project. At each stage of the project the surfaces of both the tape and head were examined to monitor any physical or chemical changes. The results were used to establish the wear phenomena, in particular those relating to the head.

2.1 Pilot research

The first period of the project was spent at the 3M laboratories in Swansea. This period was primarily used to build up a knowledge of the structure, properties and manufacture of video tape, in particular iron oxide tape. An understanding of the problems occuring with the technology was also developed, including those identified by customer complaint. The origin of customer complaints was commercial duplicators rather than the domestic video user. At the time this project was set up, customer complaints of poor signal degradation and the appearance of scratching on the video head associated with the use of the iron oxide formulation containing Cr_2O_3 as the HCA were being reported. This prompted an immediate course of investigation into the interaction between the video head and tape. The object of this investigation was to isolate the problematic characteristics of head wear and to establish a correlation between these phenomena and the degradation of the playback signal. This was achieved by close examination of the video heads before and after a period of wear with one brand of video tape. The aim of this initial study was to provide feedback to the manufacturing plant, possibly leading to changes in the commercial product. The results were also to be used as the basis for a longer term project, the main aim of which was to establish the mechanisms of wear of the video head, and to look into the effect of the HCA on performance and wear characteristics of the tape.

2.1.1 Experimental method.

The pilot investigation consisted of the examination and characterisation of video heads before and after sliding contact with one brand of video tape. The tests were run on JVC 7000 video machines. Each brand was run over a new video head in record mode for a total of six hours.

The signal carrying the video information is a collection of radio frequencies (RF). The RF is normally quoted as the logarithmic ratio between the input and output RF signals in decibels (dB) and therefore offers a quantification of the ability of the head to reproduce the input RF signal. In order to monitor the response of the head over its first six hours of use the RF signal and the signal-to-noise (S/N) ratio were measured at regular intervals. The degradation of the RF signal was the fall in RF as the head wears. The full range of frequencies are recorded and then replayed and the ratio between the two signal levels is obtained in dB as 20 log(input/output). This measurement was performed using a Farnell auto-ranging R.F. millivoltmeter which featured a dB scale. The S/N ratio is also a measure of the ability of the head to re-record after a period of use. The ratio is obtained by recording and playing back a single RF frequency. As the signal is played it is decoded or subtracted from itself to leave the noise. The S/N ratio was determined at the beginning of the test and at several points during the test, from which the degradation in the ratio could be obtained. Plots of signal degradation against time were produced and the total degradation occuring in 6 hours was derived. In some cases the 'degradation' is referred to as positive, where the use of the head resulted in an improvement rather than a decay in the signal reproduced by the head. Table 2.1 shows a summary of the video tapes examined in the pilot experiment. Each brand was in the form of standard 180 minute cassettes. Virgin tape was used for each test. The video heads were examined both before and after testing, using the following techniques;

a) Photomicroscopy

Optical photomicrographs were taken of each head (two per video drum) at a magnification of X450. The area photographed clearly shows the magnetic gap, glass inserts and part of the two ferrite pole pieces. The purpose of the microscopy was to monitor the visible degradation of the ferrite surface in this area, and also to show any damage to the gap. Figure 2.1 shows a photomicrograph of the gap area before wear.

Tape	Magnetic Pigment (Percentage by weight)	HCA Oxides (weight %)	Other Metals (weight %)
A	Iron oxide (80.5%)	Cr (5.7%)	Cl (6.3%),Co (5.7%)
B	Chromium dioxide (97.6%)	-	Fe (2.3%)
C	Iron oxide (85.6%)	Cr (2.1%)	Cl (3.0%),Co (7.5%)
D	Iron oxide (81.9%)	Al (1.2%),Si (1.5%) Ti (1.9%)	Cl (7.5%),Co (5.4%)
E	Iron oxide (85.7%)	Al (3.8%)	Cl (3.6%),Co (6.2%)
F	Iron oxide (89.8%)	-	Mn (2.8%), Co (6.2%)

Table 2.1: Summary of video tapes studied in the pilot experiment

Figure 2.1: Optical photomicrograph of the video head before wear.

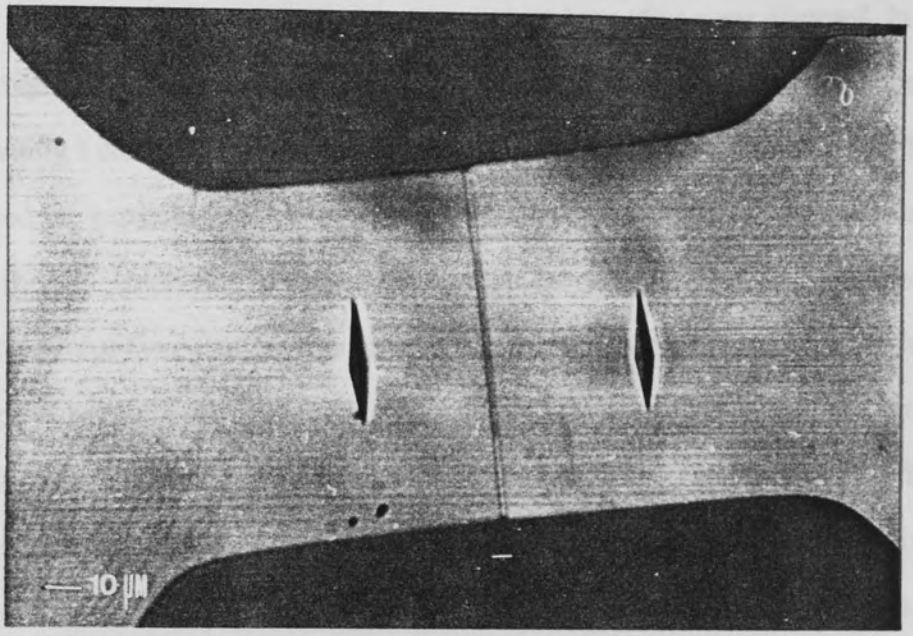
10 μm

b) Interferometry

The technique of computer analysed optical interferometry was used to produce three dimensional contour maps of the video head, concentrating on the area around the gap. The construction and operation of the Mirau optical interferometer are described in section 2.4.3. Figure 2.2a shows a typical interferogram of the gap area before wear. In the area analysed, the border between the glass regions and the ferrite can be seen, as can the gap itself. Using the interferogram, the relative uniformity of ferrite surface, glass and gap could be determined, and any major changes in topology after wear detected. In addition, the technique allows a cross-sectional profile to be extracted from either the x or y axis. By extracting a central cross-section, from a point on the x-axis, a profile which intersected the gap could be produced. Figure 2.2b shows a typical cross-sectional profile through the gap. Inspection of cross-sections taken from interferograms obtained before wear showed that there is often a mismatch between the two pole pieces of the head. The difference in height between the two pole pieces could be measured from the cross-sectional plots. Examination of a range of new heads showed that the initial difference in height of the two pole pieces ranged from 0 to 7μm. Interferograms were obtained for each head before and after testing. Cross-sectional plots were extracted for each sample and the change in the pole piece height difference with wear was recorded.

c) Wear Contour measurement

After six hours of testing a change in the contouring of the surface of the head was evident in the form of a wear 'scar' or 'contour' extending either side of the gap. The contour provided an immediate impression of the position and extent of the head-media contact. The contour was sketched and its extent measured with respect to the gap. To achieve optimum performance the maximum head-media contact must occur at the gap. This would result in a wear contour centred at the gap. The distance of the centre of each wear contour from the gap was therefore derived and compared with the signal degradation.In addition to the examination of the head before and after wear the following

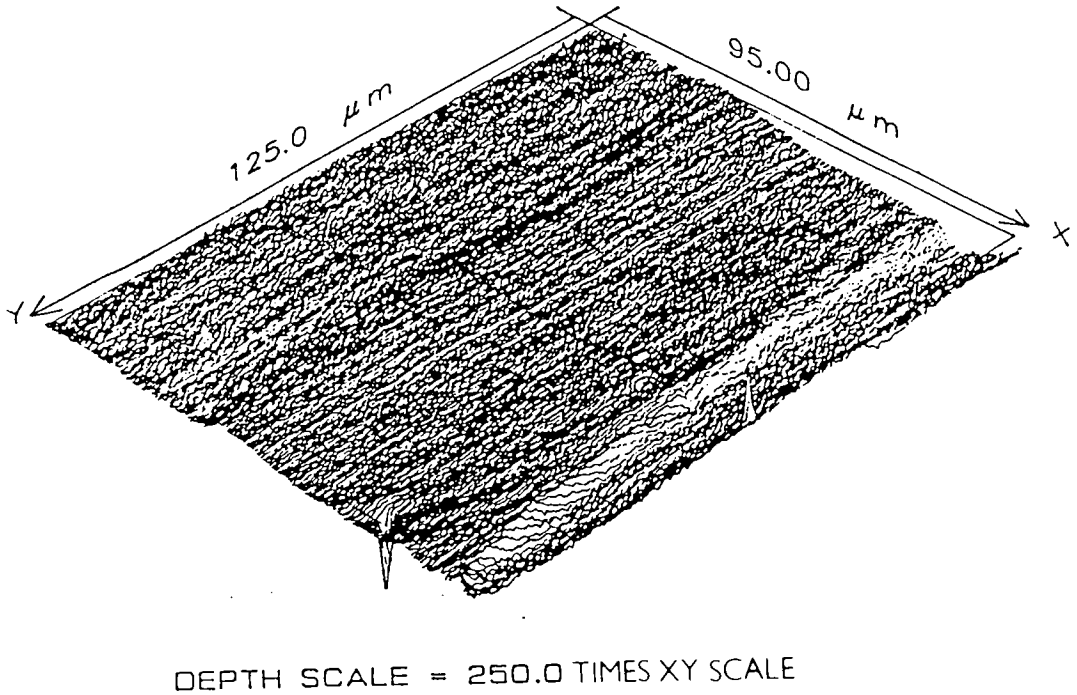

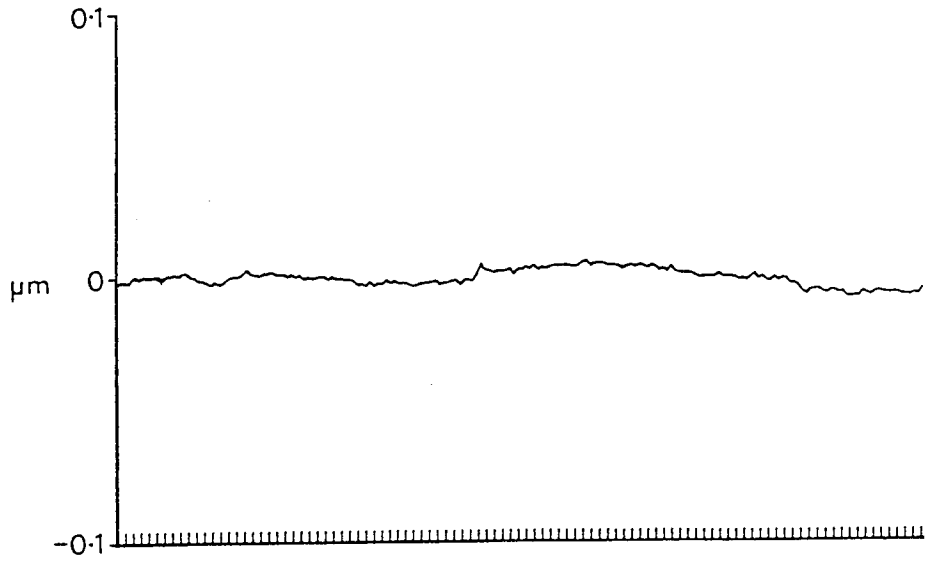

Figure 2.2: a) Typical interferogram of the gap area of the video head. b) Typical cross-sectional profile taken from the interferogram across the gap.

physical parameters of the tape were measured; tape thickness; flexibility of the tape in both the machine and cross directions; and the roughness of the tape surface. The roughness values were obtained from interferograms of the tape surface, as explained in section 2.4.3.

2.2 Development of a method of wear measurement.

From the results of the pilot research the structure of the main project was formed. One point which emerged from the pilot experiment was the need for a method of head wear measurement. Thus the following section covers the experiments performed to evaluate one particular method. In the following experiments, and those performed later in the programme, specialized samples were required in addition to samples of tape manufactured for commercial use. In the following section the production of samples for the whole project is discussed.

2.2.1 Tape samples.

All the iron oxide based tape samples used in the main project were produced by 3M, Swansea. The standard iron oxide samples used were part of a single batch produced at the commercial manufacturing plant. A pilot plant was also available for the production of specialized samples. The pilot process is identical to the commercial manufacturing process but on a much smaller scale. Hence, all samples containing a variation in the standard product were produced in the pilot plant.

The pilot plant samples were coated with the standard product formulation, but with variations in the type or the level of HCA. Two types of HCA were examined; green chromium (Cr_2O_3); and alumina (Al_2O_3). The HCA is added to the magnetic slurry before coating on to the PVC backing coat. Percentage values were quoted for each tape sample depending on the level of HCA they contained. The percentage represents the

percentage of HCA particle with respect to the iron oxide concentration and not the magnetic slurry as a whole. The sample tape was slit and reeled into 180 minute cassettes in the same way as the commercial product. Elemental analysis was performed on each sample using a scanning electron microscope (JSM 35 MKII) in conjunction with a Kevex 7000 system. Figure 2.3 shows a typical trace obtained using x-ray electron spectroscopy (XES) and Table 2.2 shows the data obtained from this analysis. If all the elements within the tape are specified, the data show the percentage of each element present, adding up to a total of 100%. The HCA is measured with respect to the iron oxide concentration. Having obtained one full analysis of the surface, subsequent data showed only the percentage of iron to that of chromium or alumina, depending on the particle present. It should be noted that when the slurry is mixed the weight percentage of both constituents is that of the oxide and not of the element recorded by the analysis. This should not produce errors as the element to oxide ratio is 2:3 for all three oxides (iron,aluminium and chromium oxides). The elemental analysis should relate directly to the weight percentage of HCA in the magnetic coating, and should be able to confirm the value. One point which should be noted is that the x-ray analysis penetrates approximately 1μm of the surface, and does not therefore sample the whole of the magnetic coat. This should not alter the percentage analysis if the HCA particles are evenly distributed throughout the magnetic coating.

The HCA particle sizes were specified by the supplier in the form of a sedigraph plot, as shown in Figure 2.4. The two particles examined ($Cr_2O_3$and Al_2O_3) were quoted as being the same size, or size range of 0.50μm. As shown by the plot, these figures represent the equivalent spherical diameter of 50% of the total volume. The range of sizes can be seen by the plot. In addition to the tape samples mentioned, a chromium dioxide tape was used in the evaluation of the method of head wear measurement. This sample was a standard E180 commercial product.

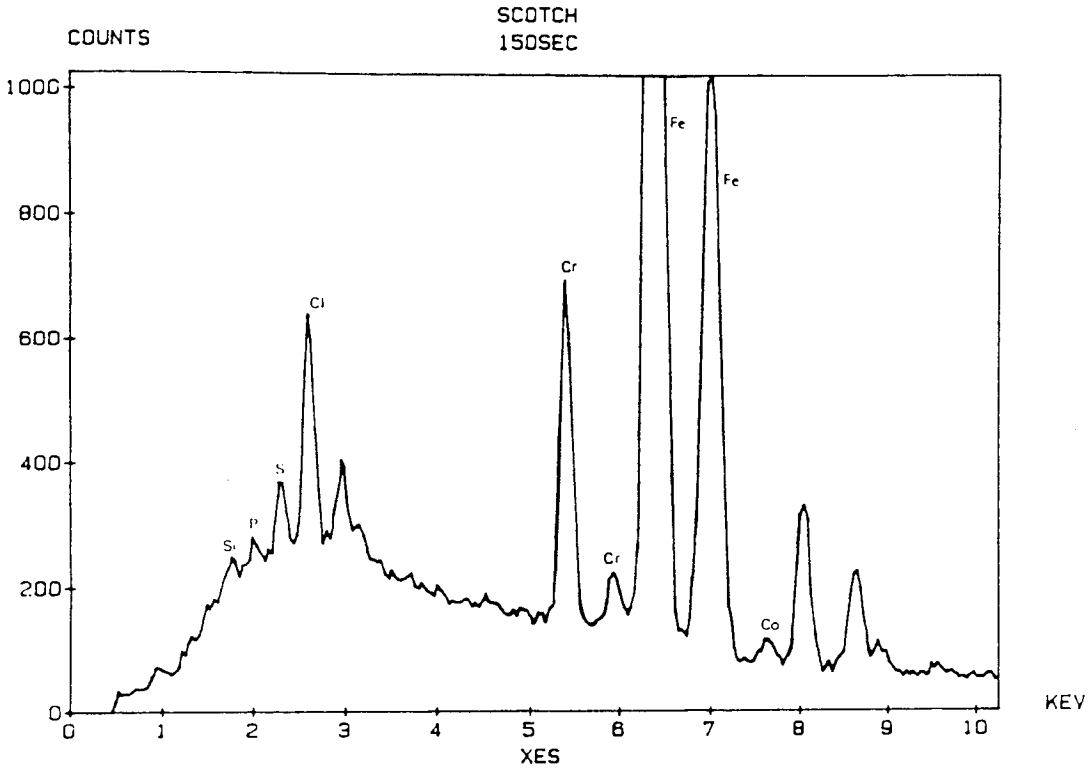

Figure 2.3: XES spectrum taken of the standard commercial iron oxide tape showing the elemental composition of the magnetic coating.

Element	Weight Percent	Atomic Percent
Si	0.15	0.29
P	0.24	0.43
S	0.68	1.17
Cl	2.21	3.42
Cr	3.77	3.96
Fe	85.72	84.02
Co	7.23	6.71

Table 2.2: Relative composition of the tape surface by weight and atomic percentage of the most abundant elements.

Missing page(s) from the bound copy

2.2.2 Selection of method of head wear measurement.

The pilot study did not include the measurement of wear rate. However, the appearance of a wear contour, enabled the relative abrasivity of each tape to be determined. The relative sizes of the wear contours demonstrated the large difference in abrasivity between a chromium oxide tape and an iron oxide tape, which represent the extremes in terms of wear rate. However, the method was neither accurate nor sensitive. The main part of the project demanded a method of wear measurement which could differentiate between subtle changes in the formulation of the standard iron oxide formulation tape. A method was required which would have sufficient sensitivity to detect variations in already low wear rates. A method using diamond indentation was developed which allowed the measurement of wear of the head in-situ . The measurement of in-situ wear has not so far been achieved in the case of video heads.

In section 1.6 various methods of wear rate measurement were reviewed and their relative advantages and disadvantages discussed. Since the main priority for previous methods of wear rate measurement has been to assess the abrasivity of various tape samples they often have little in common with real head wear. The small size of the video head has always made the measurement of in-situ wear difficult. This has encouraged the development of specially formulated 'head' samples in the shape of bars or cylinders, often made of materials similar but not identical to the head material. These methods rely on the simulation of conditions of the video tape drive, notably the wrap angle and tape tension. They do not allow for the variation in wear rate over the head due to the conformation of the tape to such a small head. A method of measurement of in-situ wear was required to examine the effect of wear on an authentic video head, at the same time comparing the abrasivity of tape samples.

Several of the methods described in section 1.6 used an indentation technique, for example the Russian and Scat methods (51). Here a pyramidal shaped indentation is made in the surface to be worn. Wear values are obtained from the reduction in length of the

indentation diagonal, the diagonal length being related to the apex height of the pyramid via the base angle. The change in apex height represents the wear to the material at that point. Different forms of this technique have been used in magnetic media research to measure the wear to floppy discs, video tape, and the heads of the disc drive. In this project the method was used to measure the wear to the video head. This was achieved by directly indenting the video head and then wearing the heads in-situ.

2.2.3 Knoop diamond indentation

Indentation techniques vary in terms of the dimensions of the diamond used to make the indentation. Maximum sensitivity for the technique was derived from the use of the Knoop diamond indenter. The Knoop diamond is characterised by the elongation of one diagonal. The ratio of apex height (h) to diagonal length (l) for the Knoop diamond is 1:30.51 (see Figure 2.5), compared with an average ratio of 1:7 for a square based indenter used, for example, in the Russian method. The larger ratio allows small amounts of wear to be recorded, as well as increasing the accuracy of the readings. Apex height and diagonal length are related by the apex angle as follows;

$$\text{Tan } 3°45' = 2h/l \qquad (2.1)$$

The change in apex height (Δh), and consequently the wear at that point, are derived from the change in length of the main diagonal (Δ);

$$\Delta h = (\Delta l \text{ Tan } 3°45')/2 \qquad (2.2)$$

The equipment used to indent the samples was not specific to head wear. A standard microhardness tester was employed, fitted with a Knoop diamond indenter. Positioning the indentation on the head surface was achieved using a set of cross wires aligned to cross at the apex of the indentation. The system was aligned under the microscope. The stage was then swung away from the sample and the indentation arm was swung in on the same axis. Both arms were clipped and held in the same position.

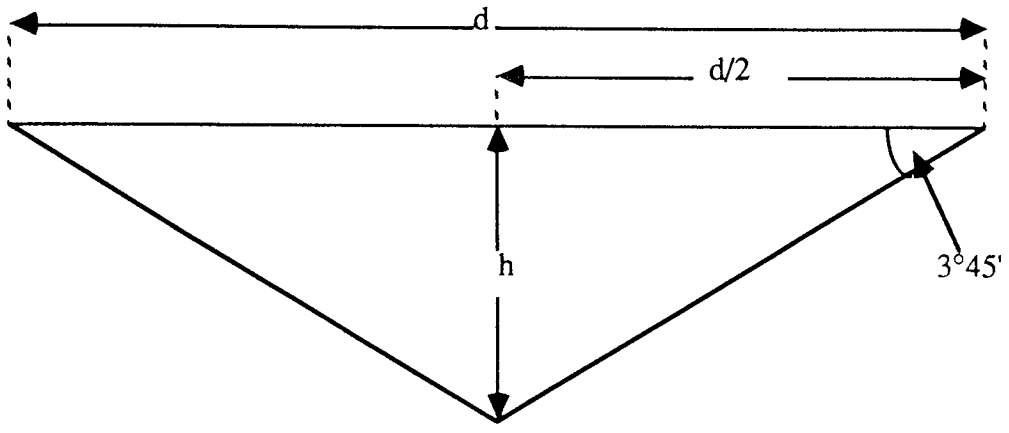

Figure 2.5: Geometry of the Knoop diamond indenter.

The pressure on the diamond, and therefore the size of the indentation, was set by adding plate weights to the indentation arm. The video heads were indented under a pressure of 50 ponds which produced an indentation with an average main diagonal length of 26μm. In order to avoid distortion, constraints were imposed on the positioning of the indentations on the video head because it is a small narrow surface. First, the minimum distance between the centres of two indentations was set at two diagonals. Second, at least half a diagonal length must have remained intact between the indentation and the edge of the sample, on all sides of the indentation (99).

The curvature of the head presented another constraint in the positioning of the indentations. The head is curved in both directions away from the gap, and as wear is most likely to occur along the ridge where the centres of curvature meet, the indentations must include this area. Hence, positioning the indentations centrally along the length of the head was also critical.

2.2.4 Experimental methods for use in Experiments IN1 and IN2, the evaluation of the diamond indentation technique.

Experiments were performed in order to establish the accuracy, ease of use and speed of diamond indentation technique as a method of wear measurement. In experiment IN1 two possible orientations of the indentations were compared with a control head which had not been indented. The two orientations examined are represented in Figure 2.6. Figure 2.6a shows the indentations with their main diagonals oriented along the sliding direction of the head. Figure 2.6b shows the indentations with their main diagonal oriented perpendicular to the sliding direction. In the experiment two types of tape sample were run over the heads. The samples were a) the standard iron oxide tape containing 4% green chromium (Cr_2O_3) as the HCA, and b) a pilot plant produced iron oxide tape varying from the standard only in terms of the head cleaning agent, containing 4% Al_2O_3 as the HCA. The alumina was also included to provide a preliminary investigation into the use of alumina as an HCA.

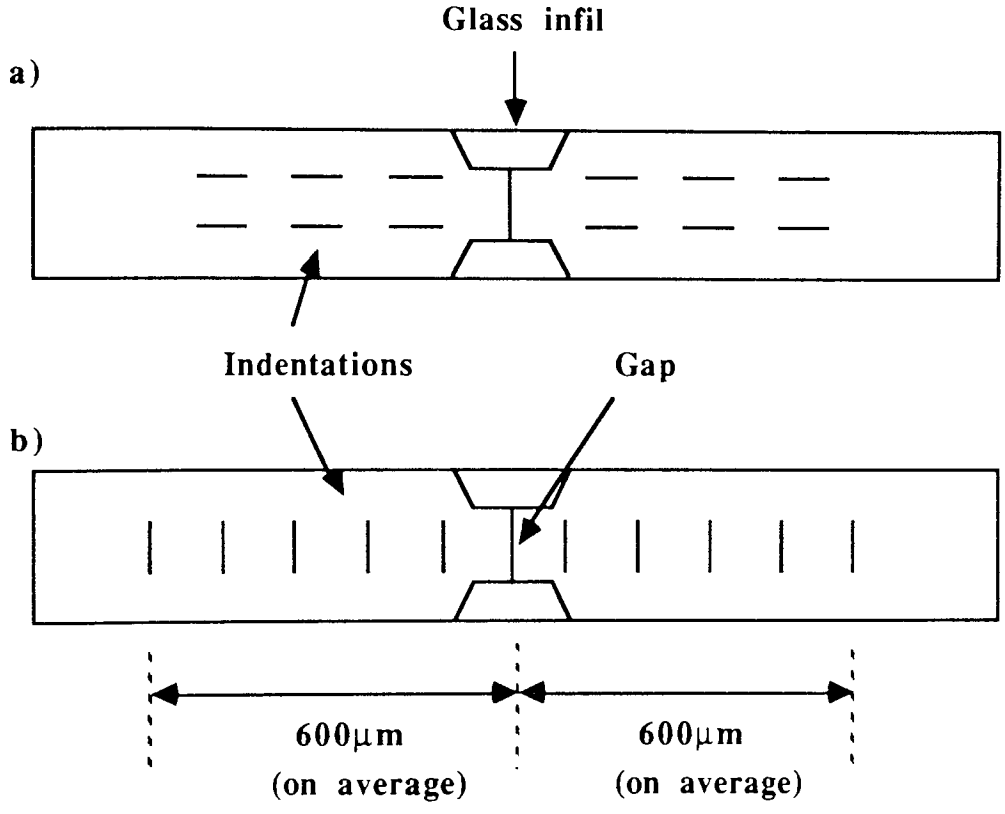

Figure 2.6: Orientations of the knoop diamond indentations, a) indentations oriented with their main diagonals along the sliding direction of the head, and b) indentations oriented with their main diagonal perpendicular to the sliding direction.

Each tape sample was run over a set of three heads, two indented and one control, for a total of six hours. New heads were used for each test and virgin tape was used throughout. The RF signal was monitored during the experiment as detailed in section 2.1.1. From the results of this experiment which are reported in section 3.2, it was clear that the most accurate results were achieved using indentations oriented perpendicular to the sliding direction. This orientation was subsequently used for all experiments and wear measurements. For ensuing experiments, the indentations were positioned along the head, five on either side of the gap, with the furthest indentation approximately 750μm from the gap. Absolute accuracy in spacing the indentations was unnecessary, and would anyway be difficult to achieve using a mechanically operated hardness tester. After indentation the length of the main diagonal and the exact position of each indentation relative to the gap were recorded. Six measurements were taken of each indentation, and the mean value was used to calculate the wear rate. From the duration of the test the wear per hour was derived for each indentation, and this value was the value used for comparison of results in the ensuing experiments.

Having established the optimum orientation of the indentations, the accuracy and limits of the technique were examined. From the pilot research it would appear that the chromium dioxide tape (tape B) produced the greatest wear over six hours. In order to test the use of the technique under conditions of high wear, in experiment IN2 the chromium dioxide tape was compared with two iron oxide samples produced at the pilot plant, one containing 4% Al_2O_3 and the other containing 4% Cr_2O_3 as the HCA. The tape samples were tested against new indented heads and run in record mode for six hours. Again, the tape samples were run against plain un-indented heads which provided a control. During the test the RF signal was monitored. The wear data were calculated for each sample and wear profiles were produced for each head, that is, two per tape sample. Table 2.3 summarizes

	Tape samples		Video heads		
			Indentation		Plain
	Pigment	HCA	Parallel#	Perpendicular#	
IN1	Iron Oxide	4% Alumina*	6hrs	6hrs	6hrs
	Iron Oxide	4% Chrome	6hrs	6hrs	6hrs
IN2	Iron Oxide	4% Alumina*		6&12hrs	6&12hrs
	Iron Oxide	4% Chrome*		6&12hrs	6&12hrs
	Chrome Dioxide	none		6&12hrs	6&12hrs

*** Pilot plant produced samples.**

 # The designations "parallel" and "perpendicular" refer to the orientation of the diamond indentations in relation to the sliding direction.

Table 2.3: Summary of tests performed in experiments IN1 and IN2 on the evaluation of the diamond indentation technique as a method of head wear measurement.

the experiments performed to evaluate the indentation technique as a method of wear measurement.

The following section gives a brief analysis of the accuracy of taking the average of six readings, allowing the sensitivity of the technique to be estimated (100). Table 2.3 shows two sets of indentation measurements taken before wear. The two data sets correspond to the two the heads (shown as blue and green) on a single drum. There are ten indentations on each head. The table shows the measurements taken, the mean (x), the standard deviation (σ) showing the uncertainty in any one observation, and the error in the mean ($\sigma/\sqrt{n}$), where n is the number of observations. The last column indicates the accuracy of using the mean for calculations. These data were generated for each set of indentation measurements, taken before wear and after wear, throughout the project.

From the examples shown in Table 2.4, the highest standard deviation from the mean is 0.243, which gives the largest error in the mean of 0.099. The vernier scale allows the indentations to be measured within 0.1μm which coincides with the error in the mean. Hence, the error in taking the mean of six readings is ±0.1μm and each reading has an error of approximately ±0.25μm. Thus in theory the knoop diamond indentation technique is able to detect a minimum change in wear of 0.5μm in the 6 hours of a test. This represents a wear rate of approximately 0.3×10^{-2}μm/hour.

2.3 Examination of the effect of the head cleaning agent on head wear.

Having established a method for wear measurement, the method was then used to examine the effects of varying the concentration and type of head cleaning agent (HCA) within the magnetic coating on the wear to the head. The present HCA in the standard iron oxide formulation tape is green chromium (Cr_2O_3) at a concentration of 4%. Although alumina has been used in the past as the HCA, this was replaced with green

Blue head

							x	σ	σ/√n
1	26.6	26.8	26.8	26.8	26.5	26.6	26.68	0.133	0.050
2	26.5	26.8	26.6	26.6	26.7	26.8	26.67	0.121	0.049
3	26.3	26.3	26.2	26.5	26.5	26.8	26.43	0.216	0.088
4	26.0	25.6	25.4	25.9	25.5	25.5	25.65	0.243	0.099
5	26.1	26.0	25.9	25.8	26.0	26.2	26.00	0.141	0.058
GAP									
6	25.8	25.6	26.0	25.8	26.0	25.9	25.85	0.152	0.062
7	26.5	26.2	26.3	26.5	26.2	26.2	26.32	0.147	0.060
8	26.1	26.5	25.8	26.0	26.0	26.1	26.08	0.232	0.095
9	26.0	26.1	26.0	25.4	26.1	26.2	26.13	0.151	0.061
10	26.4	26.6	26.0	26.4	26.3	26.3	26.33	0.197	0.080

Green head

1	26.1	26.1	26.5	26.0	25.9	26.1	26.12	0.204	0.083
2	26.2	26.4	26.8	26.6	26.4	26.6	26.50	0.210	0.086
3	26.0	26.3	26.0	25.9	26.3	26.0	26.08	0.192	0.070
4	26.6	26.4	26.5	26.6	26.2	26.2	26.42	0.183	0.075
5	26.5	26.7	26.6	26.4	26.6	26.7	26.58	0.117	0.048
GAP									
6	26.6	26.1	26.1	26.2	26.1	26.5	26.27	0.225	0.092
7	26.4	26.6	26.3	26.6	26.4	26.6	26.48	0.133	0.054
8	26.4	26.2	26.5	26.7	26.6	26.6	26.50	0.179	0.073
9	26.5	26.4	26.4	26.4	26.6	26.5	26.47	0.082	0.033
10	27.5	27.5	27.8	27.5	27.7	27.5	27.58	0.133	0.054

Table 2.4 Examples of initial indentation measurements for two sample heads on the same scanner.

chromium following customer reports of severe scratching of the ferrite heads. The HCA was believed to be responsible, and so the alumina was replaced following a short program of research.

The study was designed to investigate variations in concentration either side of the standard HCA formulation of the commercial iron oxide formulation used in this project. Two types of HCA particle were examined; the standard green chromium (Cr_2O_3)and alumina (Al_2O_3).

In evaluating the method of wear measurement, samples containing both alumina and green chromium HCA were tested. The results of these preliminary tests showed that samples containing alumina exhibited good wear characteristics compared with samples containing green chromium. Hence, a more extensive examination of this particle as an HCA was performed.The alumina product used for the experiments reported in this project was a different grade to that originally used for commercial purposes. The new grade is claimed, by the manufacturers, to be a vast improvement on the original.

2.3.1 Experimental equipment and procedure for monitoring head performance.

The following equipment was used to monitor RF for all experiments,including those already described in the section 2.2.4 on evaluation of the diamond indentation technique.

A new drum supporting two heads was used for each test. After every six hours of use the drum was removed and the head surfaces were examined under the optical microscope. This procedure involved the continual removal and re-alignement of the drum in the tape drive, the procedure for which is described in section 2.3.1.2. The performance of the head was monitored in terms of the RF signal and the following section describes the equipment required to perform these measurements.

2.3.1.1 Equipment.

All experiments were performed using standard domestic video recorders. The model used was the JVC domestic model HR-D170E/EG/EK VHS cassette recorder. All wear occurred in-situ, although the video drums had to be removed from the machine in order to measure the wear occuring to the head and to monitor debris and damage to the surface of the head. Hence, the tape tension and wrap angle used for the experiments were as fixed by the manufacturer. In the VHS machine a two headed wrap is used, which takes the tape around approximately three quarters of the drum. In addition, the heads are aligned on the drum such that they protrude into the tape surface so that the wrap angle is dictated by the height of the head above the drum, that is, the tip height. The tape tension is set at 25gm at the input (just before the tape reaches the head) and 50gms at the output (tension of the tape leaving the drum).

The recorders were adapted so that the pure RF signal could be measured directly. This was achieved using a 3M bridging amplifier, which also acted as a buffer protecting the video recorder. Figure 2.7 shows the circuit diagram for the buffer amplifier. The RF signal input to the amplifier was taken almost directly from the head. In order to view the signal on the oscilloscope a timing signal was required, which was also taken directly from the recorder. The pulse was used as an external trigger when viewing the RF signal on the scope. The circuit was supported in a box at the back of the video recorder, the signal being delivered via a BNC terminal.

The RF signal was fed directly to an auto-ranging RF millivoltmeter (Farnell TM8) where the signal was measured directly in dB. The meter was calibrated in dB from -50 to -20dBm. The value measured represented the overall response and did not differentiate between the two heads. For the duration of each test the recorder was set in record mode, and the RF reading was performed by replaying a few seconds of the recorded signal. The signal was provided by a Philips PM 5515 colour TV pattern generator. The signal was chosen to cover the maximum frequency range, and

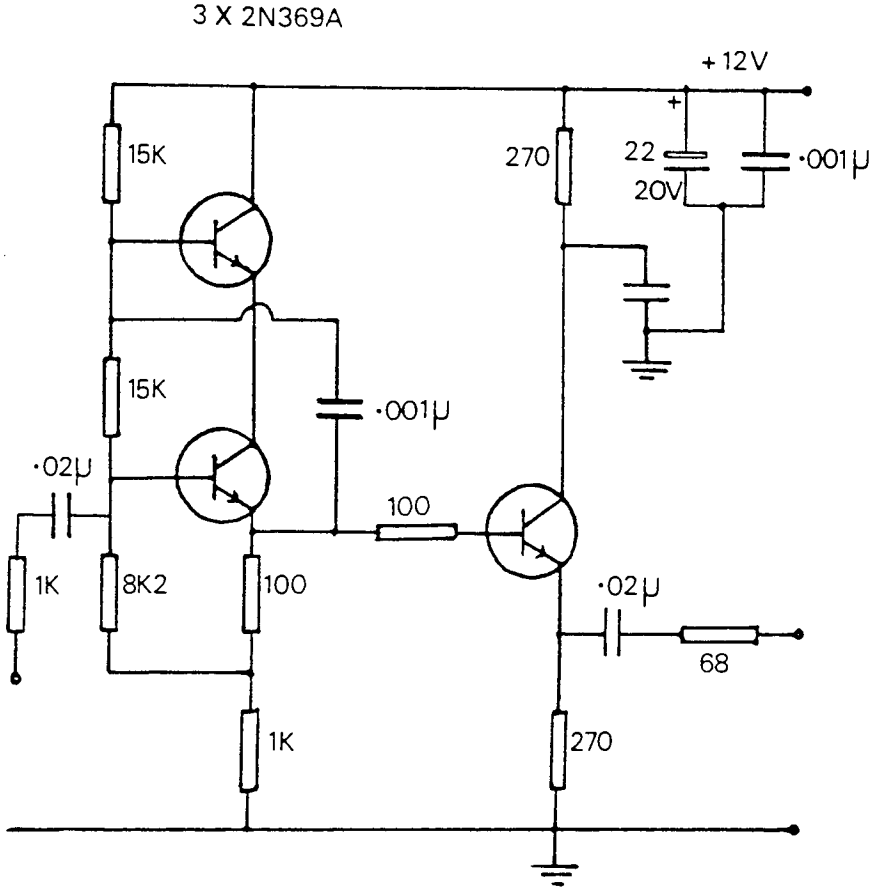

Figure 2.7: Circuit diagram of the buffer amplifier used to enable RF to measurements to be obtained directly from the head circuit.

simple colour bar but instead a shifted colour staircase with the appearance of a multicoloured checker board. Figure 2.8 shows a schematic diagram of the equipment used to monitor the RF signal as the head was worn in-situ in the video recorder. The TV monitor was used to view the signal as it was recorded and played back through the video recorder, allowing any problems with the equipment to be noticed immediately. The temperature and humidity of the test environment were recorded using a Comark hygro-thermometer. The hygrothermometer was a general purpose probe for measuring both humidity and temperature. The humidity probe was a capacitive thin film sensor, calibrated in the range 0-98% RH. The temperature probe was a platinum resistance (PT 1000) thermometer calibrated in the range -10 to 70°C.

2.3.1.2 Removal and replacement of the drum assembly

The video heads were supported in the tape drive on an aluminium drum or scanner. The drums used in this project supported two video heads (more advanced machines may hold four), and the heads were held on the drum using brass supports. The supports were colour coded, one blue and one green, in order to differentiate between the two heads. During manufacture the brass supports are carefully aligned on the drum. The precision with which the heads require alignment and also the small size of the brass support and head dictated that all work was carried out with the heads still supported by the drum. The heads were examined, indented and measured whilst on the drum and only removed when they were no longer required for testing in the machine. Removal from the drum was eventually necessary for a majority of head samples, as the drum itself was generally too large to fit into the high vacuum chamber or entrance chamber of surface analysis equipment (see section 2.4.2.3). A new video drum was used for each test, and was removed and examined after every 6 hours of testing. Each time the drum was repositioned it required resoldering and alignment. The procedure to replace the video drum in the machine was as follows; The drum supporting the heads forms the upper drum assembly.

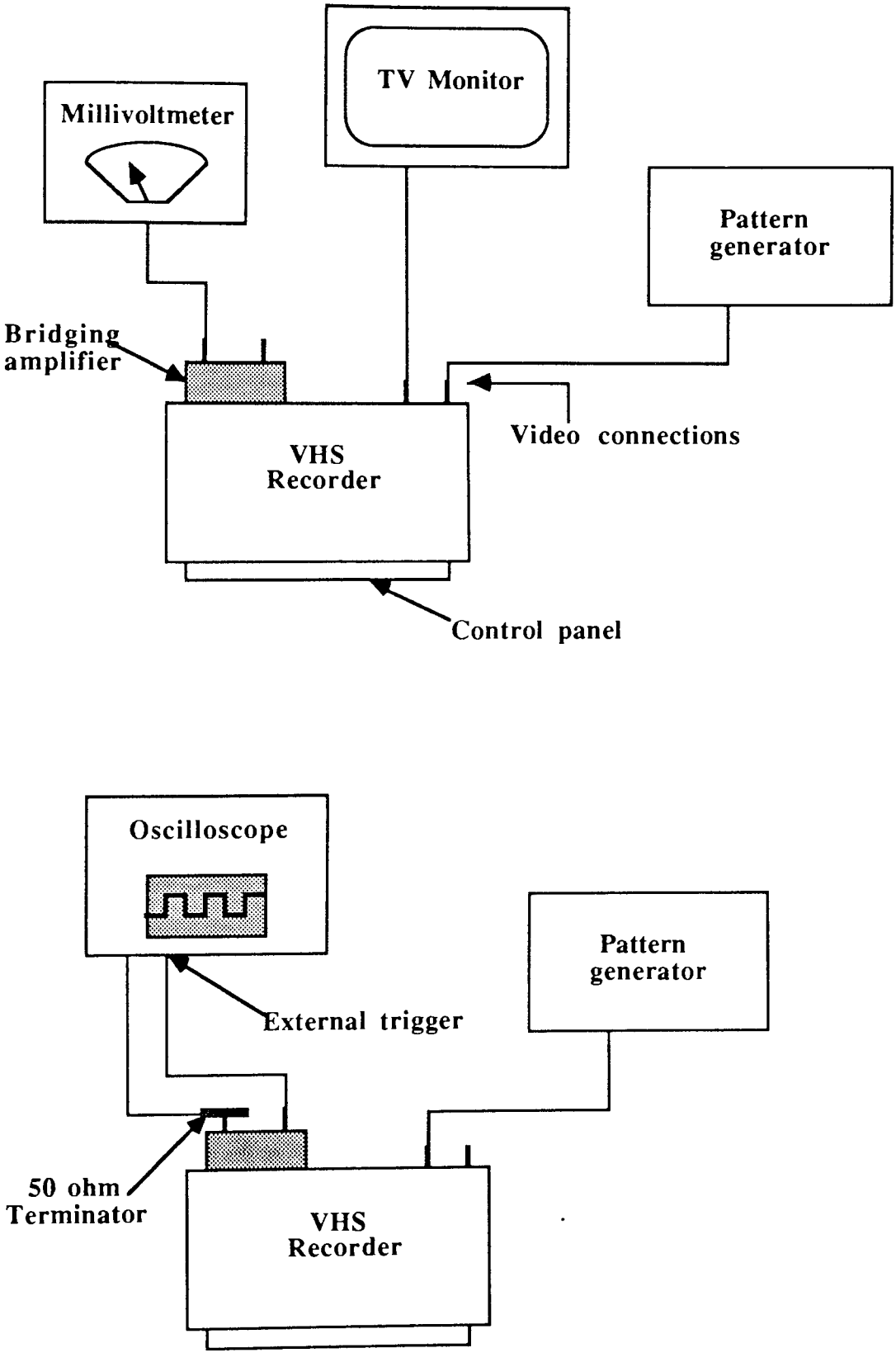

Figure 2.8: Schematic diagram of the equipment used a) to monitor the RF signal and b) to check the recorder performance after head replacement.

In operation, the upper drum fits tightly over the lower drum assembly and rotates with the inner section of the lower assembly, as shown in Figure 2.9. The lower assembly is built at an angle to the tape drive to produce the required recording pattern. Two screws hold the upper drum to the lower drum. Having lowered the upper drum over the lower drum, the screws are tightened in a balanced manner. The relay pins from the lower drum protrude up through holes in the upper section. A small circuit board, the drum PWB, was fitted over the upper drum, and once the relay pins of both drums were soldered to it, connections between the two assemblies were complete. Finally the brush assembly was screwed into its original position, as shown in Figure 2.9.

Before the newly positioned drum was used the alignment was checked as follows; the eccentricity of the drum was checked using an eccentricity gauge. By loosening the holding screws and tapping the drum lightly to position it centrally any slight eccentricity was corrected. In a domestic video machine the upper drum assembly fits so closely to the lower that the eccentricity had to altered very rarely.

To achieve in contact recording the video heads are aligned so that they protruded from the drum and push into the tape as it passes. The maximum height the head attains above the drum is termed the tip height and the eccentricity gauge was also used to measure these heights for each new head. This was performed to ensure that the protrusion of the two heads on the same drum were similar. In measuring small amounts of wear a difference in protrusion of a few microns between heads would produce different wear results for each head. If the two heads on a drum were found to have tip heights differing by above 5 μm the drum was not used for wear measurement. The maximum height the head attains above the drum for a VHS machine is typically 38μm. With an old or well used machine, the tip height can reveal whether the head is worn to the extent that it needs replacing. If the tip heights are not measured a worn head is often wrongly diagnosed, and is replaced when the problem was merely clogging of the gap or debris accumulating on the head.

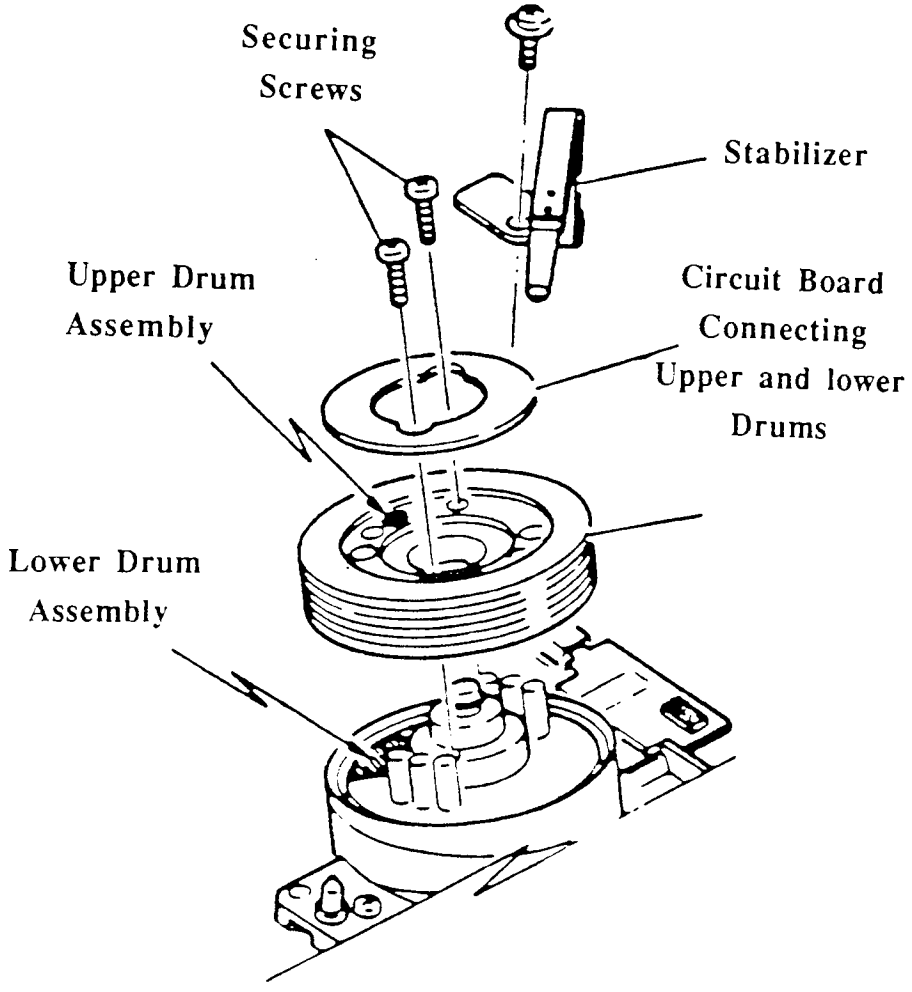

Figure 2.9: Upper and lower drum assemblies as fitted into the tape drive of a standard domestic VHS video recorder

Before electrical alignment procedures were performed the drums were cleaned using a solvent, Flurorsil, on a long stemmed cotton bud. Cleaning was required as the drums were handled at each stage of removal, and during photographing and measurement. During these operations touching the heads was carefully avoided.

Having aligned the head physically in the machine, the correct operation of the tape transport was then checked using an oscilloscope. Due to the nature of the experiments the alignment procedures were cut to a minimum to avoid wear to the head. The coloured checker board signal was played back for a few seconds and the RF waveform viewed on the oscilloscope. The signal was taken via the bridging amplifier to the oscilloscope and was triggered externally using the square wave pulse from the video recorder itself. The ideal shape of the RF signal is shown in Figure 2.10. The signal height was checked and by switching from a positive to a negative leading edge on the oscilloscscope the wave forms of both heads were viewed alternately. With identical tip heights the wave forms for both heads should not differ.

The performance of each video recorder was checked thoroughly at regular intervals throughout the project, by replacing the original video head and running through the checking procedures given in the manufacturers service manual (101). These included the measurement of tape tension, and FM and video responses. The checking procedures were performed with the aid of a standard video alignment tape.

2.3.1.3 Experimental procedure

Photomicrographs were taken of the heads of each new drum at a magnification of X600. For those drums which had been indented, the indentations were measured and the average measurement for each indentation was recorded. From the results of the pilot study, the signal to noise degradation did not provide any additional information as to the degradation in RF signal. Hence, only the RF was measured in dB. Each test was

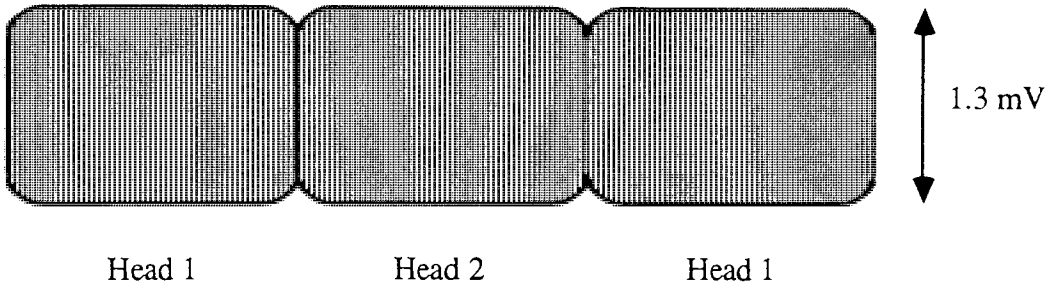

Figure 2.10: Ideal RF signal showing the response of both heads on the drum.

performed in record mode. The recorded colour bar signal was replayed for several seconds while the RF reading was taken. The RF readings were taken after 0,5,10 and 20 minutes of recording, continuing with readings every 10 minutes for the first hour and then every 20 minutes after that for the 12 hours of the test. This duration represents the total recording time and did not take into account the head to tape contact occuring during playback when the RF readings were taken. The average time to take the reading was 10 seconds. A total of 41 readings were taken during each experiment adding a total of 410 seconds to the duration of head to tape contact (6.83 minutes). Over 12 hours this represented an error of less than 1% of the duration.

The video drums were removed for examination after 6 hours of wear and then after the full 12 hours of the test. At each stage the heads were photographed at a magnification of X600, and the indentations were remeasured. The surface of the head was examined for debris, deformation of the ferrite surface, quality of the gap, and any other noticeable features of the wear process.

The results of the pilot research revealed the presence of a wear scar or contour which can be seen after the first 6 hours of wear. Under a magnification of X150 the entire head can be seen and the wear contour is clearly visible. Using an eye piece with built-in scale the wear scar could be measured. For each test, the position of the scar was sketched and measured with respect to the gap. These measurements provided confirmation of the extent of wear measured using diamond indentation. They also confirmed that sufficient indentations had been positioned either side of the magnetic gap to record the extent of the wear occuring over the head during the 12 hours.

The temperature and humidity of the test environment were recorded alongside each RF measurement to monitor any changes during the test, since very high or very low conditions of humidity would potentially alter the wear rate, as discussed in chapter 1. The humidity in the test environment was not controlled, but no tests were performed if the humidity was above 45% RH or below 25% RH. There is usually no sudden change

in wear rate either side of these values, although outside of this range the wear rate begins to rise (94).

2.3.2 Experiments performed

From the results of the experiments performed to evaluate the diamond indentation technique as a method of wear measurement, it appeared that the iron oxide tape containing alumina HCA performed better in terms of signal degradation than the standard iron oxide tape containing the green chromium HCA. Hence, it was decided that the use of alumina as an HCA should be investigated further. The results of the pilot work suggested that, in general, a high wear rate resulted in better signal degradation than a very low wear rate, although a high rate of wear is not desirable property for prolonged head life. In addition, the standard iron oxide tape containing 4% green chromium HCA produced the lowest wear of the tapes tested and the greatest signal degradation. The severe signal degradation correlated well with the severe damage to the gap and ferrite surface that was observed. Thus one aim of this part of the work was to examine the effect of varying the level and type of HCA, in particular to raise the HCA level above the present level of 4% to examine whether this increases head wear and decreases surface damage and signal degradation. The second aim of this work, which was the main aim of the project as a whole, was to establish the mechanisms of wear occuring to the video head. Levels of HCA were chosen on either side of the current commercially used level, and a sample containing no HCA was also produced. Thus two series of samples were produced at the pilot plant containing two types of HCA, as follows;

		Percentage HCA content by weight					
GC1	Green chromium	0	2	4	6	8	10
AL1	Alumina	-	2	4	6	8	10

A second series of green chromium samples was also produced with an HCA levels of 8% to 16%. This second series also included an overlap of the first series in order to test the reproducibility of the pilot plant samples. Hence, the second series of iron oxide tapes containing green chromium was as follows;

GC2 Green chromium 8% 10% 12% 14% 16%.

The series took the level of HCA above the level which would be commercially viable. The maximum level of HCA used in the magnetic coating is restricted by the cost of the HCA, and problems of dispersion at high loading levels. Hence, a level of above approximately 8-10% would not be used commercially.

The drums were saved after the completion of the experiments, to be used for surface analysis. Head samples were required for SEM, XPS and SIMS analysis which are described in later sections. The heads had to be removed from the drums and the brass holder had to be reduced in size in order to produce a sample suitable for the vacuum chamber of these techniques. Hence, the heads could not be re-used after surface analysis.

2.4 Surface analysis

2.4.1 Optical microscope analysis

At each stage of testing photomicrographs of the video heads were taken. An Olympus model BHC microscope was used which was fitted with a model PM-6 camera. It was necessary to adapt the microsope in order to accommodate the video drum and to provide support for the drum holder underneath the lens system. The main stage of the microscope was removed, and part of the base was inverted to provide a base for the drum support. Figure 2.11 shows the apparatus used to support the drum. Plastic screws were used to secure the drum and a clearance was provided at the bottom of the support

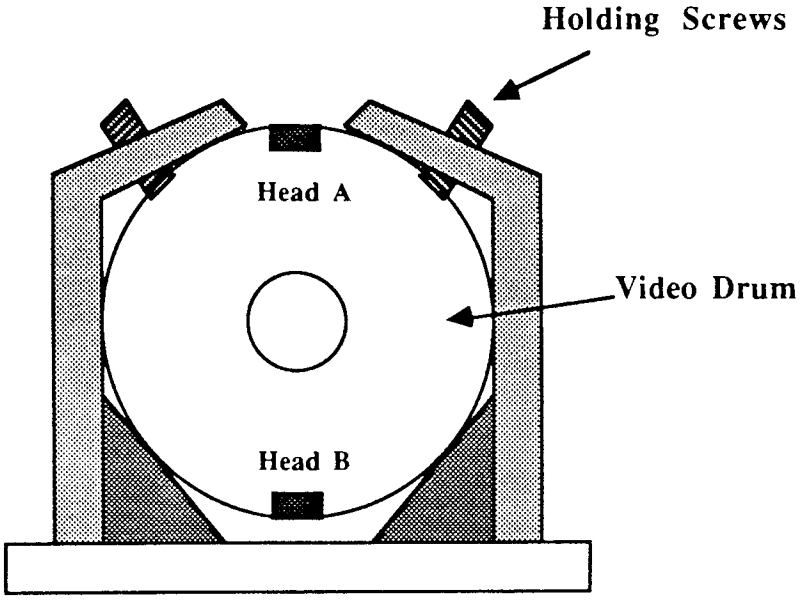

Figure 2.11: Apparatus used to support the video drum for examination under the optical microscope.

where the second head was positioned. The heads were examined under the microscope for debris and visible degradation. Under a low magnification (X75) the entire length of the head could be viewed and the wear scar clearly seen. The dimensions of the wear scar were measured using an eye piece with a built in scale.

The diamond indentation measurements were made using the optical microscope attached to a microhardness tester. A vernier system attached to the microscope allowed very accurate submicron measurements to be made. Since the average size of an indentation made on a video head was 26μm, the vernier provided the minimum sensitivity required. Because of the nature of the hardness tester, the distance between sample and lens system could be varied over a larger range than on a standard optical microscope, and this easily accommodated the video drum. The drum was supported by a solid block, as shown in Figure 2.12. The drum was screwed to the block so that it protruded approximately 1cm above the support.

2.4.2 Electron Microscopy

Transmission Electron Microscopy (TEM) and Scanning Electron Microscopy (SEM) are both well established techniques. An overview of the principles and applications of these techniques can be found in publications by Wells, Wischnitzer, and Godhew and Humphreys (102,103,104). Samples from this project were prepared for analysis under both SEM and TEM, as described in sections 2.4.2.2 and 2.4.2.3.

2.4.2.1 Transmission Electron Microscopy (TEM)

TEM was used to study the magnetic video tape in cross-section.The aims of the analysis were as follows;

a) To identify the HCA particle and to study any variations in its shape and size.

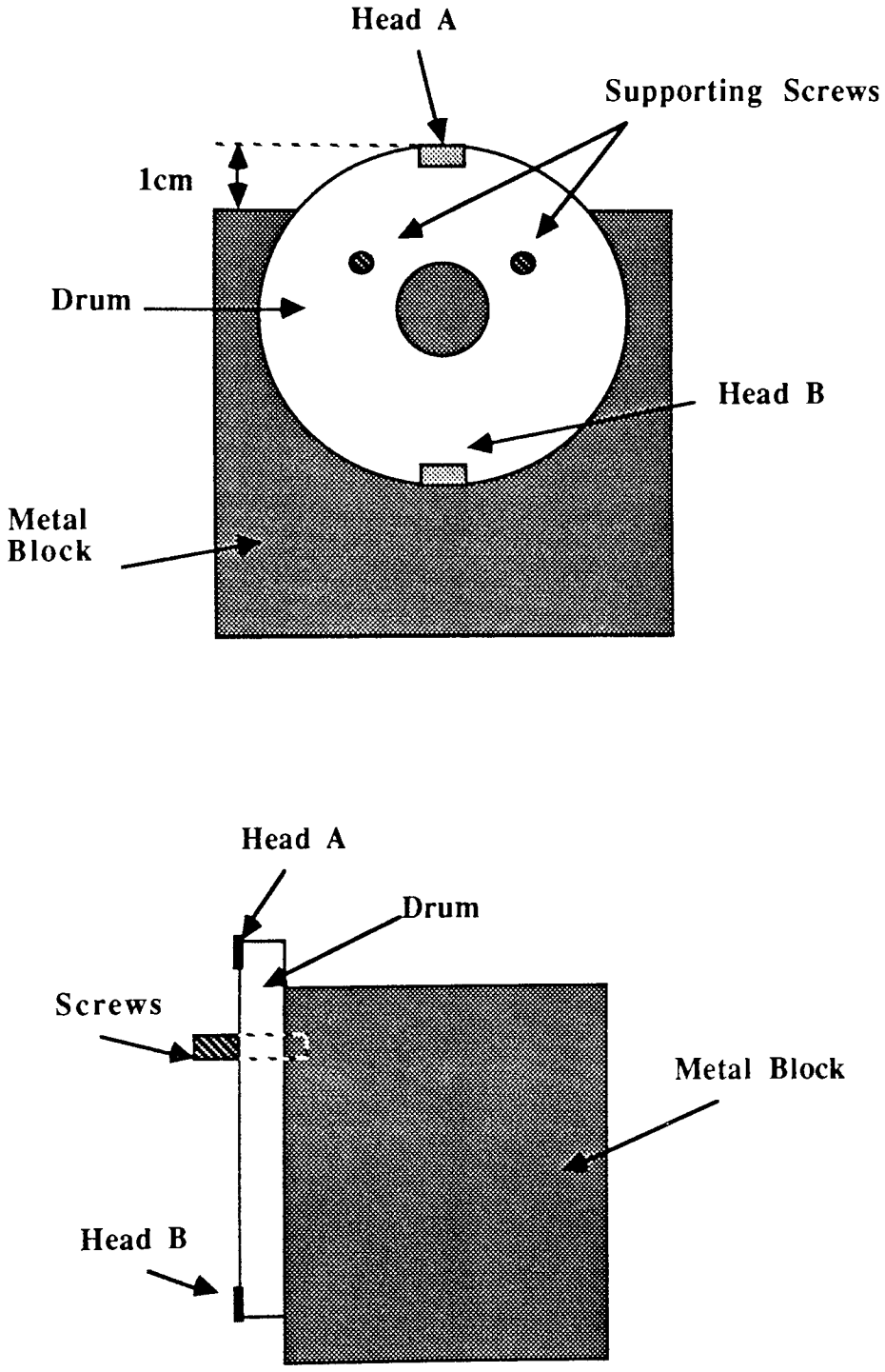

Figure 2.12: Block used to support the video drum during indentation and all indentation measurements.

b) To study the position of the HCA particles in the bulk, in particular their proximity to the tape surface.

c) To study the dispersion of the particles within the magnetic coating.

The position and proximity to the surface of various non-magnetic particles are thought to have an influence on the performance and wear characteristics of the tape (105). Knowledge of the relative particle positions may identify those particles most likely to influence the wear processes occuring to the head, such as the particles likely to initiate deformation of the ferrite surface.

2.4.2.2 Sample preparation for TEM

To achieve an image of reasonable resolution under the TEM, samples must be no thicker than 150 Angstroms. The samples were prepared and cut into very thin sections using microtome sectioning equipment and were then mounted on the TEM 3.5mm grids. The tape was not rigid enough to be sectioned without support, so small samples of tape were embedded in an epoxy resin before sectioning as follows;

Samples of tape were sliced into pointed shards of approximately 0.5cm in length. The shards were then embedded in Araldite CY 212. The Araldite was mixed with an equivalent volume of the activating (hardening) agent Dodecenyl succinic anhydride (DDSA). The hardness of the resulting resin could be controlled by substituting either Dibutylphalate (DBP) to soften the resin, or Methyl nadic anhydride (MNA) to increase the hardness of the resin. The chosen liquid was substituted for an equivalent volume of DDSA in the mixture. Various degrees of hard and soft resins were produced and sectioned. The most effective resin in terms of quality of cut samples was found to be a hard resin made from substituting 1ml of MNA to the mixture. Too soft a resin tended to produce wrinkled samples and adhesion to the block from which the sample was being

cut. The tape shards were set in the liquid resin in small moulds and was baked at 60°C for 24 hours.

After a further 24 hours the blocks were ready to be sectioned. The block was first trimmed to a rough four-sided pyramid using a glass knife as shown in Figure 2.13a. The block was shaped in this way to increase the likelihood of a ribbon of sections being obtained. The trimmed block was then sectioned using a diamond knife, since a glass knife was not able to produce sections of the desired thickness. The trimming and sectioning were performed using a microtome, which operates by dragging the mounted block vertically down onto the cutting surface. The block is gradually fed towards the knife, as its surface is cut away, using thermal expansion of the rod supporting the block. The diamond knife is mounted with a comparatively large trough behind it to collect the ribbon of sections as it forms. This trough is filled with a mixture of distiled water and acetone. The resin is slightly soluble in acetone, so that the sections flatten out as they form. The ribbon of sections is picked up from the trough using the mounting grid, as shown in Figure 2.13b. The optimum position of a sample would be with the tape slice in the centre of a grid square supported by the resin film. Several grids of sections had to be made to provide one such sample. Finally, the specimens were carbon coated to avoid charge build up. This was likely to occur as both the resin and the tape base film are insulators.

2.4.2.3 SEM

Sections of video tape were cut from the tape and affixed to the sample stub using a double sided tape. To avoid charging of the sample due to the insulating base film, each sample was made conductive to the base using silver paint and were then gold coated.

The drum supporting the video heads was too large for the vacuum chamber of the SEM and this prevented the heads from being examined during the experiment. After completion of testing the heads were removed from the drum for analysis.

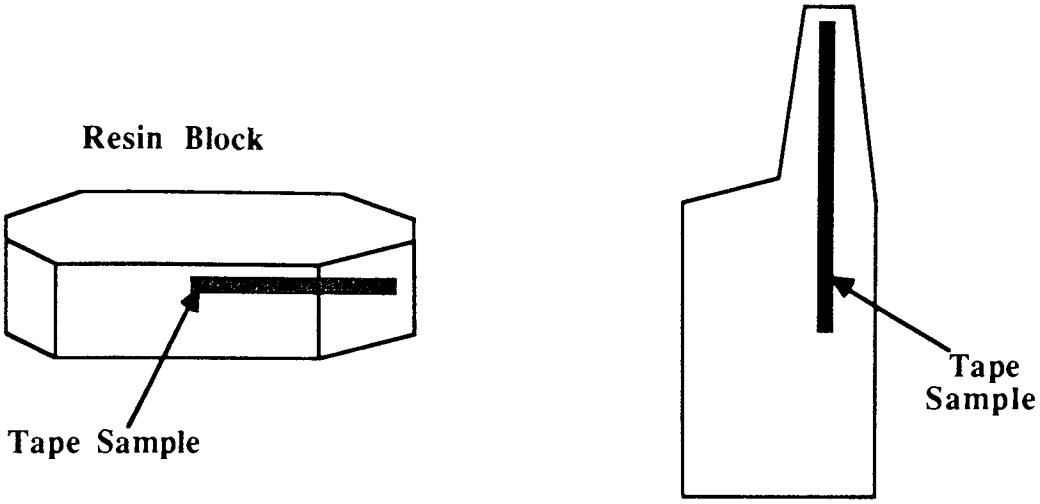

Figure 2.13a: Resin block as moulded and then trimmed with a glass knife around the embedded tape sample.

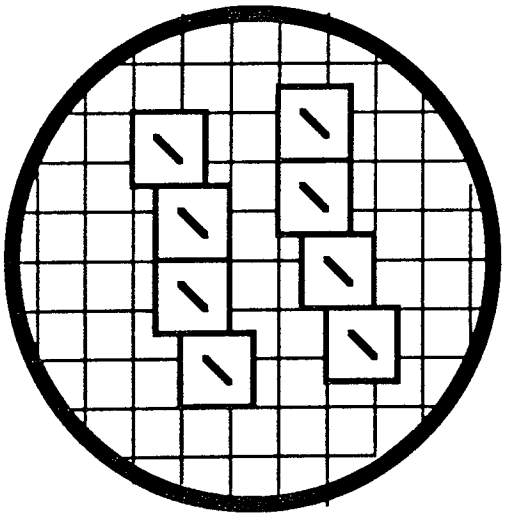

Figure 2.13b: Ribbon of resin sections containing a section of tape sample and supported by a copper mounting grid for TEM analysis.

Figure 2.14a shows the head and brass support removed from the drum. In order to view the head on the sliding surface, the brass support had to be further trimmed until the final sample was approximately 0.5 cm in height (Figure 2.14b). The samples were then checked under an optical microscope before use to ensure that no damage had occurred during the removal of the bottom of the brass support. Once again a conductive paint was used to create a good contact between sample and stub.

The SEM was used to compare the surfaces of commercial produced and pilot plant produced tape samples. After testing, several video heads were examined for debris, damage to the ferrite surface and to the magnetic gap. A variety of magnifications were used up to 200K.

2.4.3 Interferometry

Computer analysed optical interferometry was used to examine the surfaces of both video head and tape. This technique scans a microscopic area of the surface measuring the minute vertical displacements of a relatively smooth surface. The product is a three dimensional contour map of the scanned area. The technique is also capable of providing a quantitative roughness analysis of the surface, and was therefore used to provide a roughness value for each tape sample used throughout the project (106). It should be noted that only a microscopic area of the sample is scanned, and a roughness value taken from this may not accurately describe the entire surface.

The technique involves the interference of two coherent beams of light; a reference beam and a second reflected by the specimen. Figure 2.15 shows the path of the beams through the system (107,108,109). Incident light is reflected(1) towards the specimen and focussed by the objective lens of the microscope (2). The light is then split into two coherent beams by the beam splitter (4). The reference beam is reflected towards the reference plate (3) and the second beam continues towards the specimen. The reference beam is reflected by the mirror incorporated in the reference plate, whilst the second beam

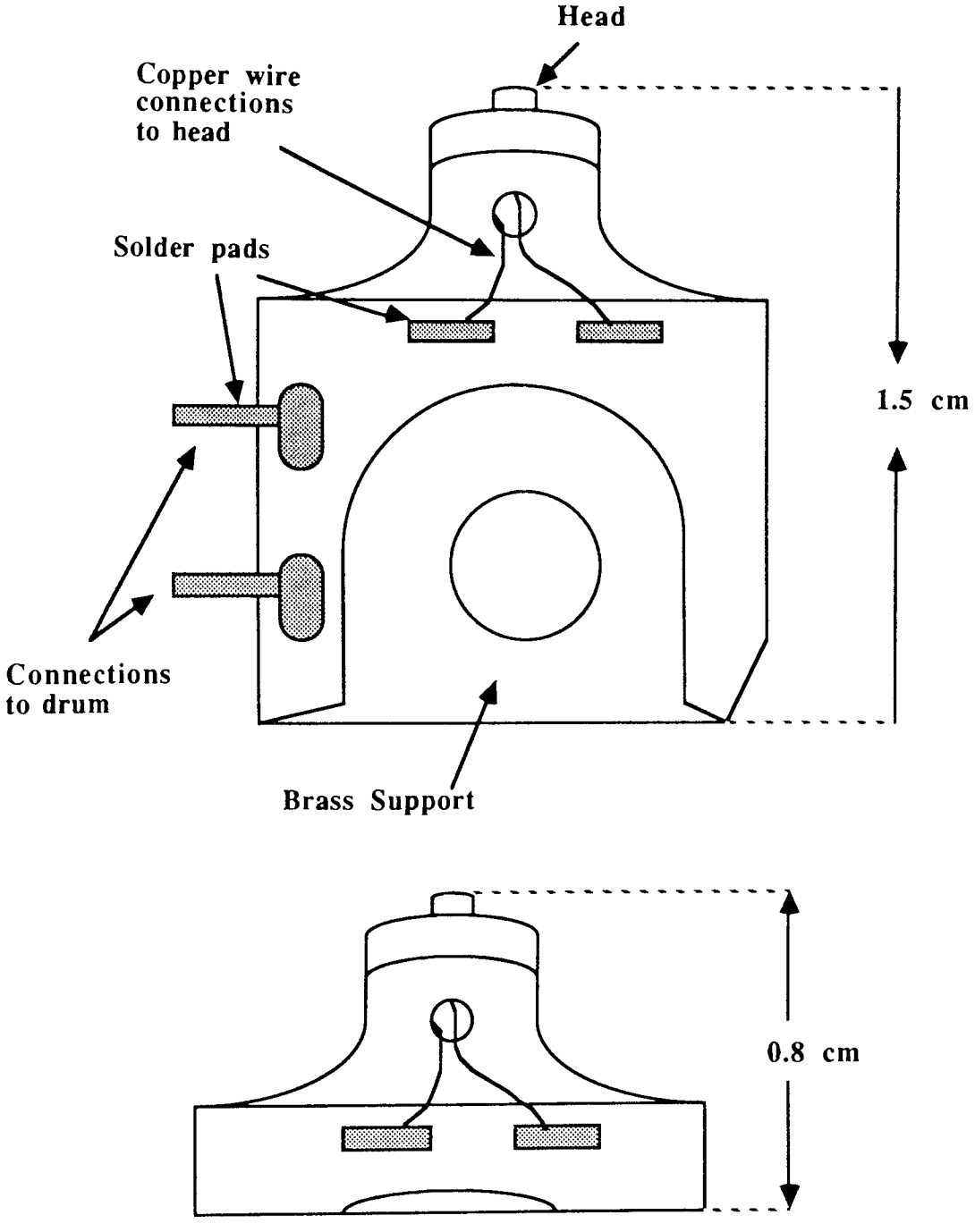

Figure 2.14: a) Head and brass support removed from the video drum. b) Head and support cut to fit the entrance chamber of the surface analysis facilities; XPS and SIMS.

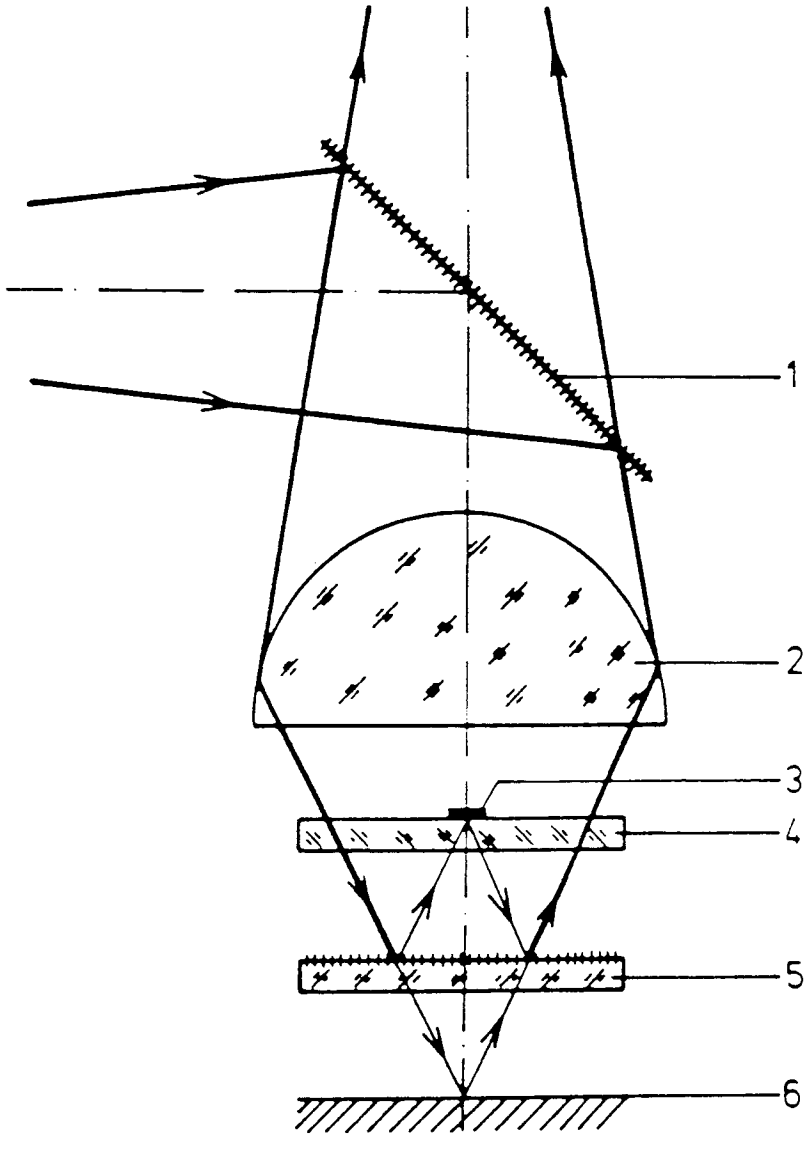

Figure 2.15: Path of light beams through the Mirau interferometer

is reflected by the specimen. The mirror and the specimen are at an equal distance from the beam splitter. If the specimen surface is completely smooth the beams will be in phase when they combine and will continue back towards the objective. Any irregularities in the surface will produce a phase shift determined by the vertical height or depth of the irregularity. The result is a system of interference fringes. Direct phase measurement is performed by the computer at each point on a grid of 200 by 200 points. The result is a 40,000 point three dimensional image of the sample surface. Taking a point on the specimen surface, the interference between the reference and specimen beams can be represented as;

$$I = I'[1 + \gamma \cos \alpha] \tag{2.3}$$

Where I = Intensity of the combined reference and specimen beams.

I' = Intensity at the objective with no interference.

α= The phase difference between the reference and specimen beams.

γ = Interference contrast for the point, $0 \leq \gamma \leq 1$

Shifting the phase of the specimen beam in steps of $\pi/2$, the relative intensities are as follows;

$$A = I' [1 + \gamma \cos (\alpha + 0)] = I' [1 + \gamma \cos \alpha] \tag{2.4}$$

$$B = I' [1 + \gamma \cos (\alpha + \pi/2)] = I' [1 - \gamma \sin \alpha] \tag{2.5}$$

$$C = I' [1 + \gamma \cos (\alpha + \pi)] = I' [1 - \gamma \cos \alpha] \tag{2.6}$$

$$D = I' [1 + \gamma \cos (\alpha + 3\pi/2)] = I' [1 + \gamma \sin \alpha] \tag{2.7}$$

Rearranging equations 2.4 and 2.6 gives:

$$I' = A - I'\gamma \cos\alpha \qquad (2.8)$$

and $$I' = C + I'\gamma \cos\alpha \qquad (2.9)$$

Equating 2.8 and 2.9 gives:

$$\cos\alpha = (A-C) / 2I'\gamma \qquad (2.10)$$

Similarly, from equations 2.5 and 2.7:

$$\sin\alpha = (D-B) / 2I'\gamma \qquad (2.11)$$

Hence:

$$\tan\alpha = (D-B)/(A-C)$$

or $$\alpha = \tan^{-1}[(D-B)/(A-C)] \qquad (2.12)$$

A peak in the surface is detected if the phase difference is larger than zero and a trough if the difference is less than zero (109,110). Finally, a phase shift of 2π corresponds to a change in height on the surface of $l/2$ so the height at that point is:

$$Z = (l/4\pi).\alpha \qquad (2.13)$$

2.4.4 Secondary Ion Mass Spectrometry (SIMS)

This surface analysis technique was used to examine the top surface layers of the video head and to identify the chemical changes in these layers as the head is worn. The aim was to isolate species being transferred from the tape to the surface of the head. A build up of transferred material, such as, a polymer from the binding system of the tape, may

create spacing loss and hence signal degradation. A polymer layer may also alter the wear characteristics of the surface and the rate of wear.

The technique involves the bombardment of the surface to be studied by a beam of monoenergetic primary ions. The ions are usually rare gas ions, but liquid metal ions or oxygen are sometimes used. The primary ion beam, of energy typically between 1-20 KeV, penetrates the surface a distance of the order of 10nm. Here the ions transfer their energy to the lattice in a series of inelastic collisions. This sets up a cascade of collisions resulting in the emission of positive and negative secondary ions, electrons and atoms from the top two monolayers of the surface. The ions are then subjected to mass spectrometry to determine their mass to charge ratio and their relative abundance. The secondary electrons generated are used to produce an SEM image of the surface, and which provides a means of directing the beam. The first two monolayers of the surface are removed, which means that the SIMS technique is destructive in contrast to other techniques such as AES and XPS (these techniques become destructive if depth profiling by sputtering is performed). The destructive nature of the technique is offset by its superior detection sensitivity, the detection limits being related to the amount of material being sputtered away;

$$I^{\pm} = I_p S^{\pm} hc \qquad (2.14)$$

where I_p = primary current.

$S^{\pm}$ = secondary ion yield (positive or negative).

h = the instrumental factor.

c = fractional atomic concentration.

A high primary current will lead to higher detection limits, but more material will be removed. Although this is well established, the mechanism for the production of the secondary ions is less certain (111,112,113).

The resulting mass spectra consist of a positive and a negative spectrum. The atomic ions of electropositive elements are found with greatest intensity in the positive mass spectrum, and those of electronegative elements in the negative mass spectrum. The spectra yield species of atoms, compounds and clusters. The yield of secondary ions depends upon the nature, energy, current density and angle of incidence of the primary ion beam, and also upon the composition and chemical environment of the surface. In Dynamic SIMS a high primary ion current is used ($>10^{-6}Acm^{-2}$) and the erosion of the surface provides an inherent depth profiling mode. In this mode, the secondary ion yield is measured as a function of time. It is possible, using Static SIMS, to probe only the surface of the sample by using a small ion current ($10^{-9}Acm^{-2}$). The surface erosion in this case is negligible, and to overcome the corresponding loss in signal intensity a broad primary ion beam is required, covering a large area of sample. Using Imaging SIMS a current of $10^{-6}Acm^{-2}$ is used to bombard an area of approximately 300 μm in diameter. The instrument is tuned to one particular mass and a map of one particular element is produced. As with most bombardment techniques when examining electrical insulators surface charging occurs with SIMS. The technique of Fast Atom Bombardment Mass Spectrometry (FABMS) overcomes this problem by using neutral particles for the primary beam (114,115,116).

The technique was used to examine the surface of the video head before and after wear with a number of different samples. One of the aims of the analysis was to establish the presence of any organic material on the surface of the head. This may have been transferred directly from the tape or from other parts of the video tape drive and carried to the head via the tape. The optimum detection of thin layers of organics on the head surface would have been achieved using the FABMS technique. However, the small size of the head surface did not allow sufficient sensitivity, and prevented the use of this technique. Therefore, the surfaces of the video heads were analysed using static SIMS. A compromise was also made in the use of this technique by reducing the primary beam size at the expense of sensitivity. The apparatus used was the VG SIMSLAB at UMIST.

The ion source was a FAB61 gun which could provide a beam of inert gas ions or atoms with energy varying from 100eV to 5KeV. Positive and negative spectra were obtained for each sample, as well a SIMS image of the head where the distribution of a particular element over the surface was required.

2.4.5 X-ray Photoelectron Spectroscopy (XPS)

This technique was used to obtain additional information about the change in the surface of the video head after wear. XPS is one of the few methods of surface analysis which yields chemical information as well as elemental resolution of the first 2-20 atomic surface layers. The technique can detect the change in binding energy of an atom due to its chemical environment. The shift in binding energy allows chemical state and compound information to be obtained. The method is not inherently destructive and is sensitive to the first few atomic layers of the surface.

The excitation used for this technique is X-rays, usually either the Al Ka line at 1487eV, or the Mg Ka line at 1254eV. The incident X-ray photon transfers all its energy to a photoelectron. Part of this energy is used in overcoming the binding energy (BE) of the electron, the remainder of the energy appearing as the kinetic energy (KE) of the photoelectron. Each element can be identified from its characteristic energies, and all elements except for hydrogen and helium can be detected in this way. The information is obtained in the form of a Kinetic energy/Binding energy distribution of the photoelectrons produced. The energy spectra contain elemental peaks which are well resolved from the background. Although an element can be associated with more than one peak, spectral overlap should not present a problem with the use of an analyser of sufficiently high energy resolution. Chemical information is obtained from the technique as a result of the influence of the chemical environment of the atom on the binding energy of a given core electron. The effect produces a chemical shift in the resulting spectra. In general, an increase in the effective positive charge of an atom, for example from oxidation, will

create a more tightly bound electron, and the spectral shift will be towards a higher binding energy. However, an electronegative increase will create less tightly bound electrons and the shift will be towards the lower binding energies. Only one atomic level is involved in the production of photoelectrons, so the shift is easily related to the chemical environment (111,112,114,116,117)

XPS was used to examine the organic species on the surface of the head before and after wear. Thus the chemical shift in the carbon and oxygen spectra was monitored. Standard XPS provides an x-ray beam of approximately $1mm^2$ with collimation. Since the video head was approximately 0.3 mm wide, standard XPS could not be used (118). It was not possible to use gold masking to surround the head surface because of difficulties encountered in obtaining contact between the gold leaf and the head surface. Additionally, the large gold to ferrite ratio would create problems in that the carbon and oxygen signals may be confused by the contamination and oxidation of the gold surface. Hence, the small spot XPS facility at the University of Surrey was used to examine the surfaces of video heads before and after wear. The beam size for the small spot facility was 0.5 mm^2. Surfaces examined using this technique included a new head and a head worn for thirty hours with standard Scotch and then cleaned using Fluorosil to remove any loose debris. The spectra acquired for each sample were a wide scan covering binding energies from 0 to 1000eV, and then spectra covering from 275 to 300eV to monitor the carbon, 525 and 550eV for the oxygen.

Chapter 3:

Presentation of results

3.0 Introduction

In this chapter the results from all sections of the work are presented. In the first section the results from the pilot project are presented, and the succession from this work to the main project is discussed. The results of the two main experiments performed in evaluating the diamond indentation technique as a method of wear measurement are presented in the next sections, followed by the results of the three main experiments which examine the effect of a variation in the type and level of the head cleaning agent. The later sections describe the results of the analysis which was performed alongside all the experiments, including XPS, SIMS, SEM and TEM. The final section presents an analysis of the pilot plant samples, this was performed after experimental results were obtained which indicated possible variation in samples from the pilot plant.

3.1 Pilot Research

The six commercial tapes (A-F) tested in the pilot experiment are listed in terms of their elemental content in Table 2.1. From the results of the pilot experiment, the performance of the six tape brands divided naturally into three groups, which can be summarised as follows:

a) The surfaces of the heads worn with tapes B and D were smooth and undamaged and the resulting signal degradation was low. In addition a large wear scar was produced, suggesting high wear.

b) Tapes A,E and F produced a slightly smaller wear contour and some damage to the gap and the ferrite surface could be seen. The signal degradation for these samples was average, that is, between -0.3 and -1.8dB (S/N degradation).

c) The ferrite surface and the gap of the heads worn with tape C were badly damaged and the resulting signal degradation was the highest of all the tapes tested. The wear contour was by far the smallest, suggesting the lowest wear.

The results obtained from one brand of tape from each of the three groups is presented in this section as follows; Tape D from group a; Tape A from group b; and finally Tape C from group c. However, the results obtained for the remaining tape brands are included in the graphs plotted in this section. Although each drum supported two video heads, the results for two heads worn with the same tape brand were similar for every sample. Thus the results for only one head, the blue head in each case, are presented.

3.1.1 Optical Photomicroscopy

Under the optical microscope the condition of all new heads was found to be similar. Examination of the heads after 6 hours wear concentrated on the change in appearance of the gap, the ferrite surface and the glass regions. Figure 3.1 shows the photomicrographs of the heads worn with the following tape brands; Figure 3.1a, Tape D; Figure 3.1b, Tape A; and Figure 3.1c, Tape C. A correlation was found between the extent of damage to the head surface and the signal degradation measured. The head worn with Tape D was found to be in a similar state to the original unworn head surface. The ferrite, glass regions and gap were all undamaged and the signal degradation was correspondingly good. The RF degradation for this sample was +0.5 dB, indicating that the interaction had improved the performance of the head to a small degree. In the case of the head worn by Tape C, the ferrite surface showed deformation which took the form of wear tracks or scratches spreading along the length of the head. The surface of the glass region appeared to be 'roughened' after wear. Under the optical microscope it was not clear whether the change in appearance was due to removal or deposition of material. The gap also showed damage characterised by the chipping of its edges. The physical state of the head worn by Tape C was reflected in the poor signal degradation, an RF degradation of -4.2 dB was recorded. The sample Tape A, exhibited wear characteristics between the two extremes of Tapes D and C. Some

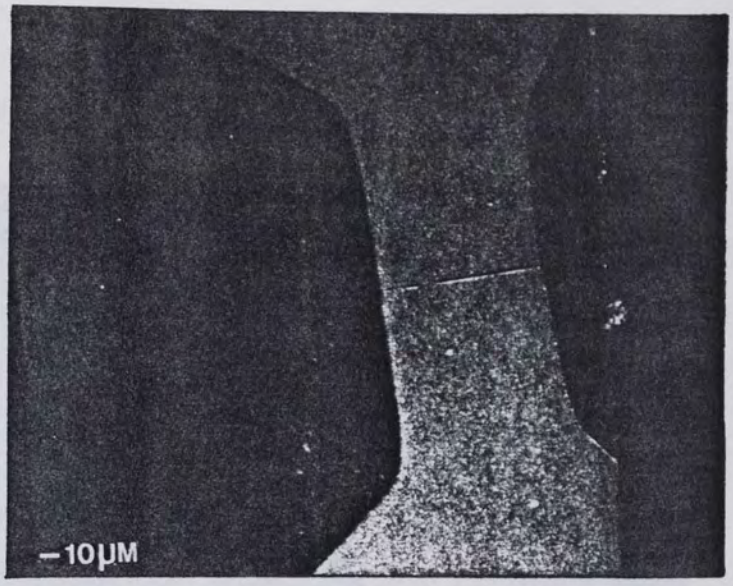

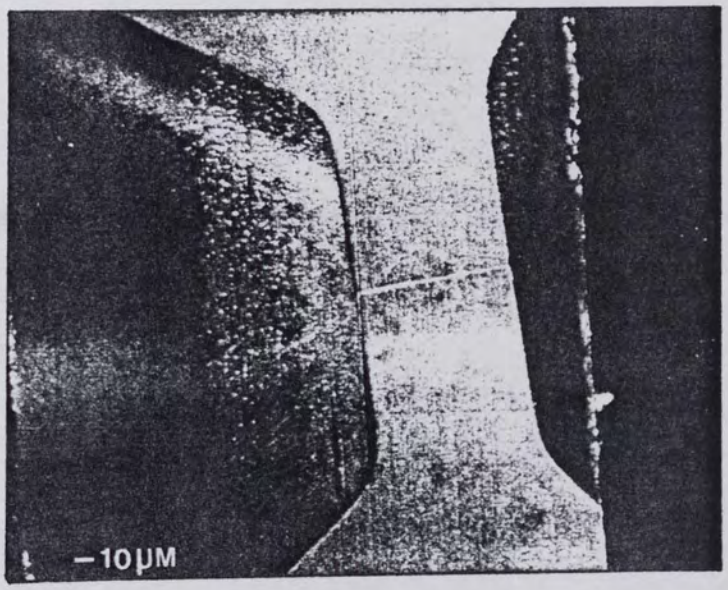

Figure 3.1: Photomicrographs of a) video head after 6 hours wear with Tape D, b) video head after 6 hours wear with Tape A.

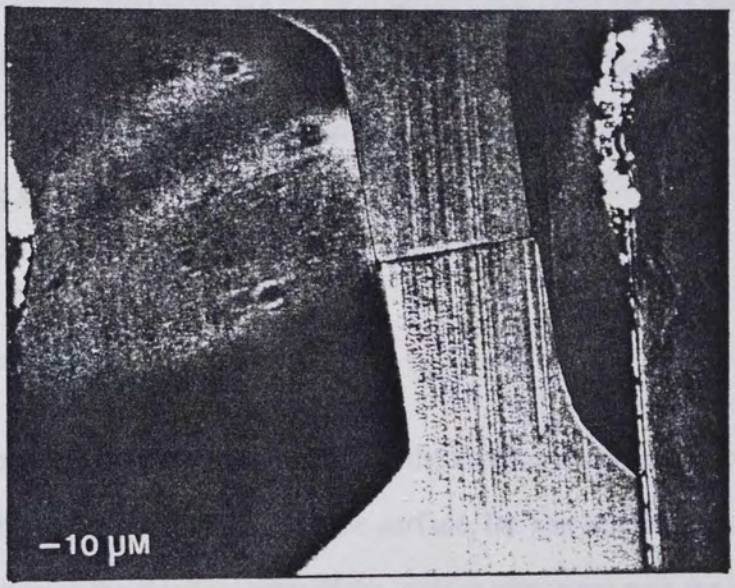

Figure 3.1c: Photomicrograph of video head after 6 hours wear with Tape C

damage to the head could be seen, including a roughening of the glass region but the signal degradation was relatively good at -0.9 dB.

The physical state of the surface of each head appeared to correlate with the resulting signal degradation. However, it was clear from an examination of the interferograms and the wear contours for each sample that other factors had contributed towards the performance of the head. The physical state of each head was examined in more detail using the surface maps or interferograms, the results of which are reported in the following section.

3.1.2 Interferometry

Each interferogram presented a detailed map of the asperities and general contours of the area surrounding the gap. Changes in the surface, the gap and the glass region could be seen by comparing the interferogram of the surface after wear with the interferogram of the original surface. Figure 3.2 shows the two interferograms for the head worn with Tape D. The resulting surface is very smooth, even compared with the original contours of the head. The head appears to have been worn down so that the gap, which can be seen clearly in the original interferogram, is difficult to distinguish after wear. This effect was examined more closely by taking a cross-section through the interferogram crossing the gap. Figure 3.3 shows two cross-sections from the head worn with Tape D. The original head showed a difference in the height of the pole pieces of approximately 5nm. The head after wear shows no difference in pole piece height. Hence, one effect of wear to the head has been to resolve the difference in pole piece height. It is likely that the resolution of the pole pieces is responsible for the slight increase in signal degradation.

Figure 3.4 shows the two interferograms for the head worn with Tape A. The roughening of the glass region after wear can be seen clearly. The raised contours suggest that it is a deposit rather than a removal of material. Figure 3.5 shows the

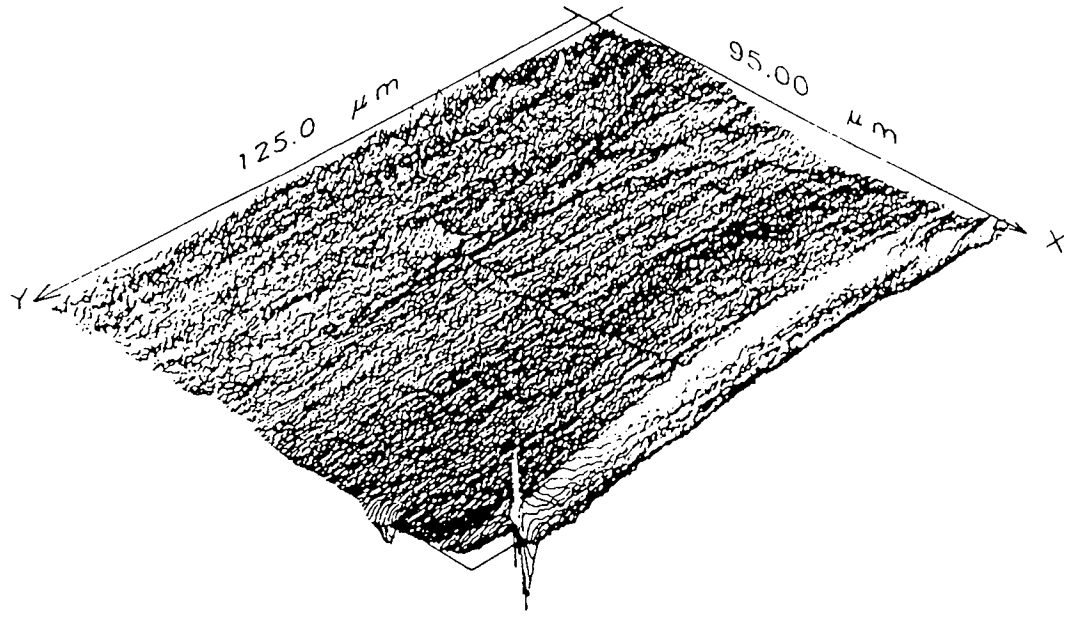

DEPTH SCALE = 250.0 TIMES XY SCALE

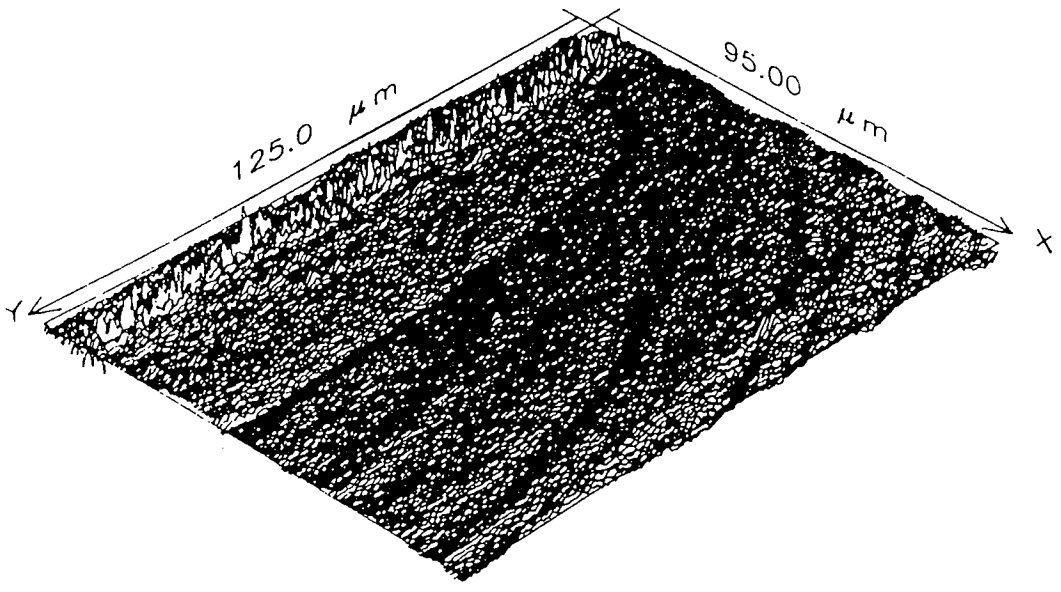

DEPTH SCALE = 250.0 TIMES XY SCALE

Figure 3.2: Interferograms of the gap area of the video head a) before and b) after 6 hours wear with Tape D

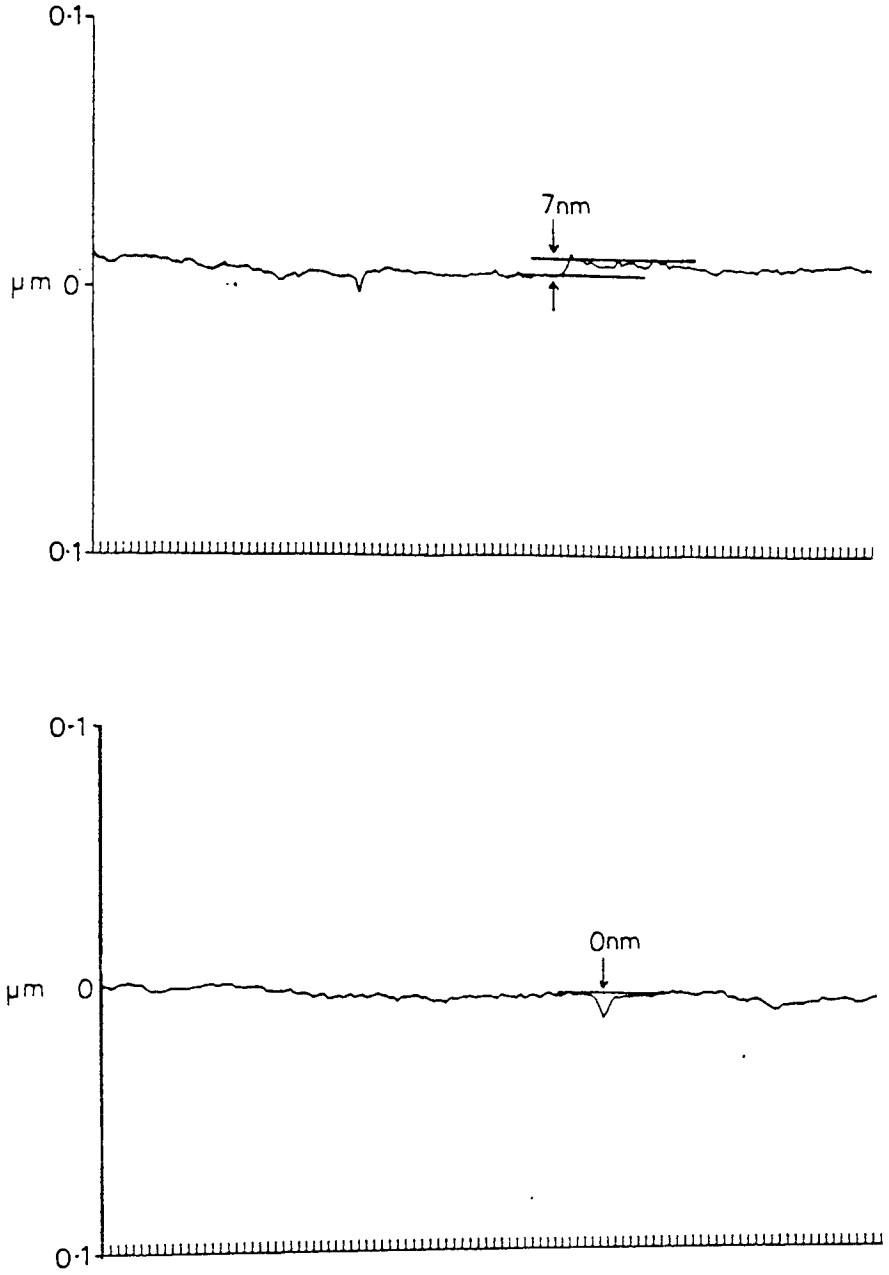

Figure 3.3: Cross-sectional plots taken from the interferograms of the gap area of the video head a) before and b) after 6 hours wear with Tape D

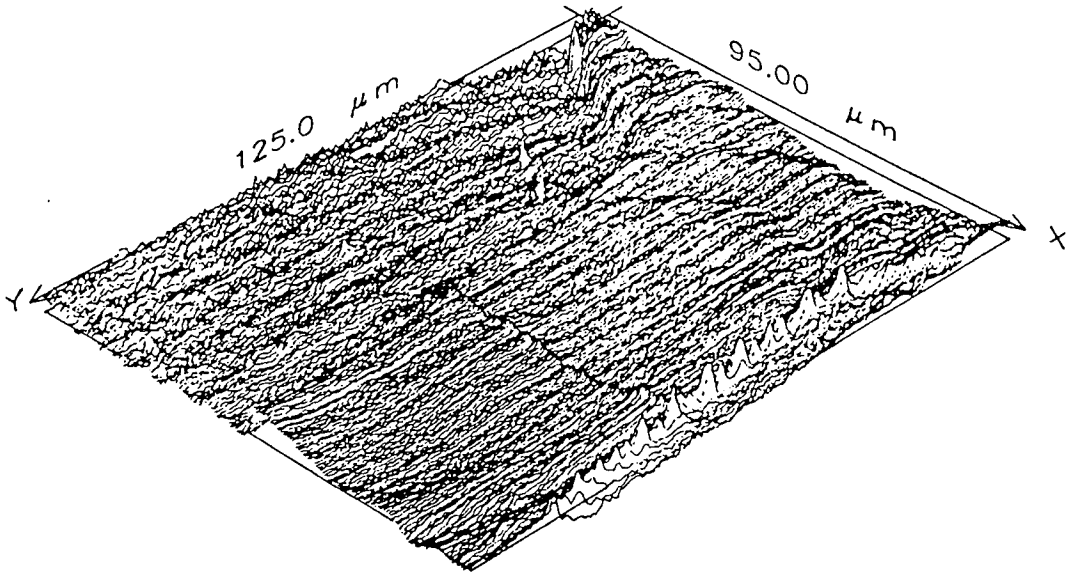

DEPTH SCALE = 250.0 TIMES XY SCALE

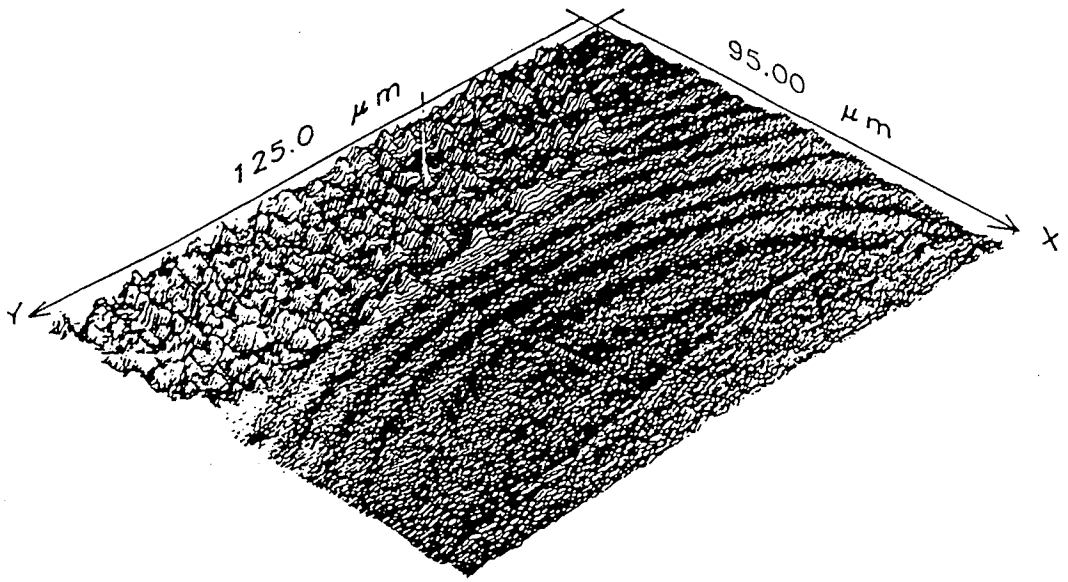

DEPTH SCALE = 250.0 TIMES XY SCALE

Figure 3.4: Interferograms of the gap area of the video head a) before and b) after 6 hours wear with Tape A

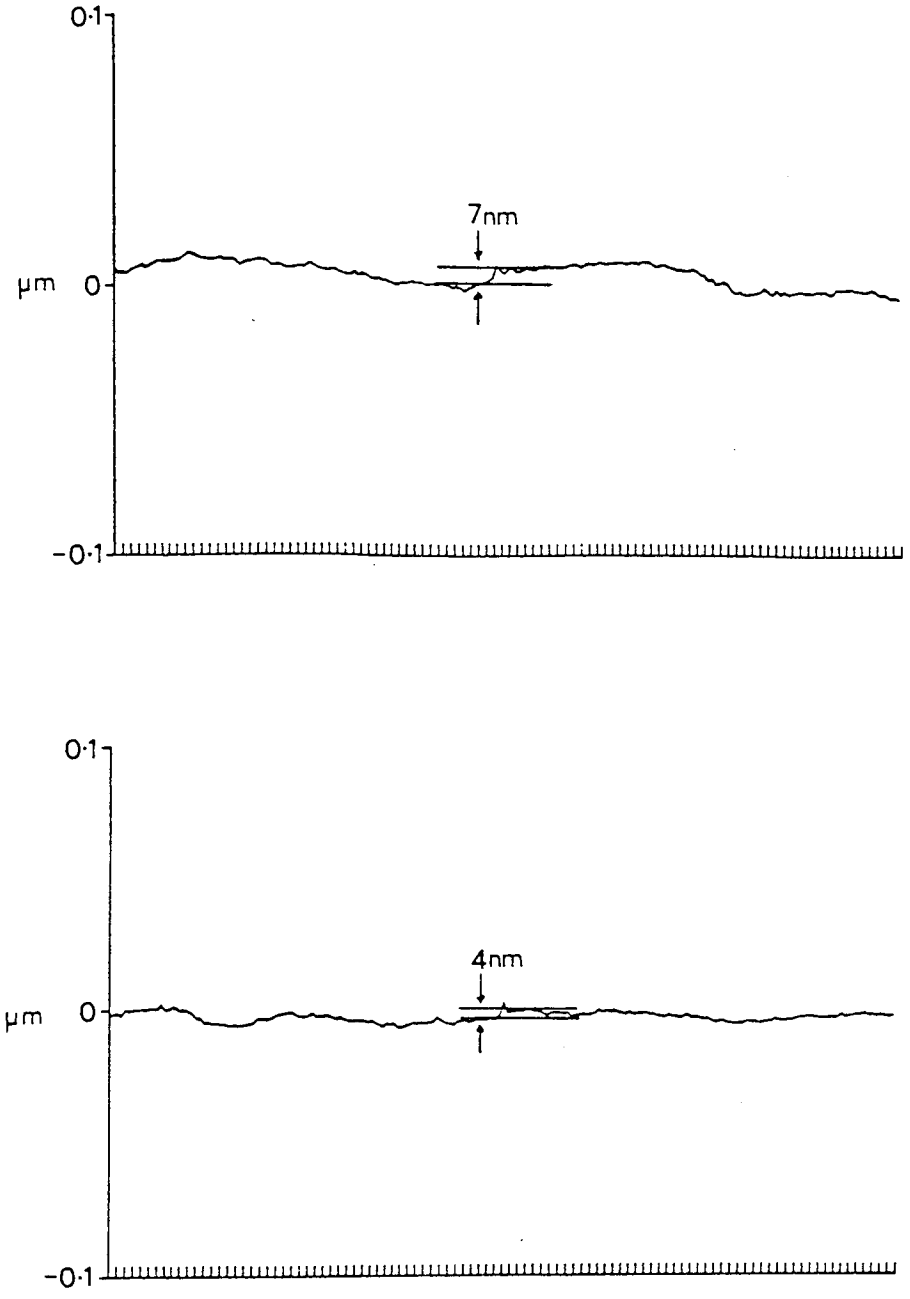

Figure 3.5: Cross-sectional plots taken from the interferograms of the gap area of the video head a) before and b) after 6 hours wear with Tape A

cross-sections taken from these interferograms. The wear to the head has resulted in an reduced difference in pole piece height, although the difference has not been resolved.

The interferograms for the head worn with Tape C are shown in Figure 3.6. The interferogram taken after wear shows a dramatic change in the contouring of the head. It should be noted at this point that the image provided by the interferogram is strongly dependent on the processing of the data and some features may be exaggerated. From the interferogram it would appear that a large volume of wear has occured to the trailing pole piece, and this is confirmed in the following section by the position of the wear contour. However, the interferogram may be slightly misleading in this case, as the large pit described by the contours is unlikely to occur in the form shown. The occurrence of such a feature would also be visible under the optical microscope and was not observed. Thus the interferogram should merely be taken to indicate the existence of a change in contouring of the head, possibly involving the removal of material. In addition to the change in contouring, it can be seen from the interferogram that the magnetic gap was degraded with wear. However, the scratching of the ferrite surface can not easily be distinguished, as the contours of the interferogram run along the head, in what would be the same direction as the wear tracks. The wear feature is therefore absorbed into the background. Also, the technique leaves an impression of the interference rings on the head which appear on the interferogram. Figure 3.6 shows this clearly, and demonstrates how difficult it would be to distinguish between scratching to the head and the image of the interference fringes. Figure 3.7 shows the cross-sectional plots from the interferograms. It appears that, in the case of the head worn using Tape C, the wear has increased the difference in pole piece height.

The change in pole piece height difference was derived for each sample tested and plotted against the RF degradation, as shown in Figure 3.8. The plot was produced using data from all six tape samples tested and from both video heads. The plot shows a

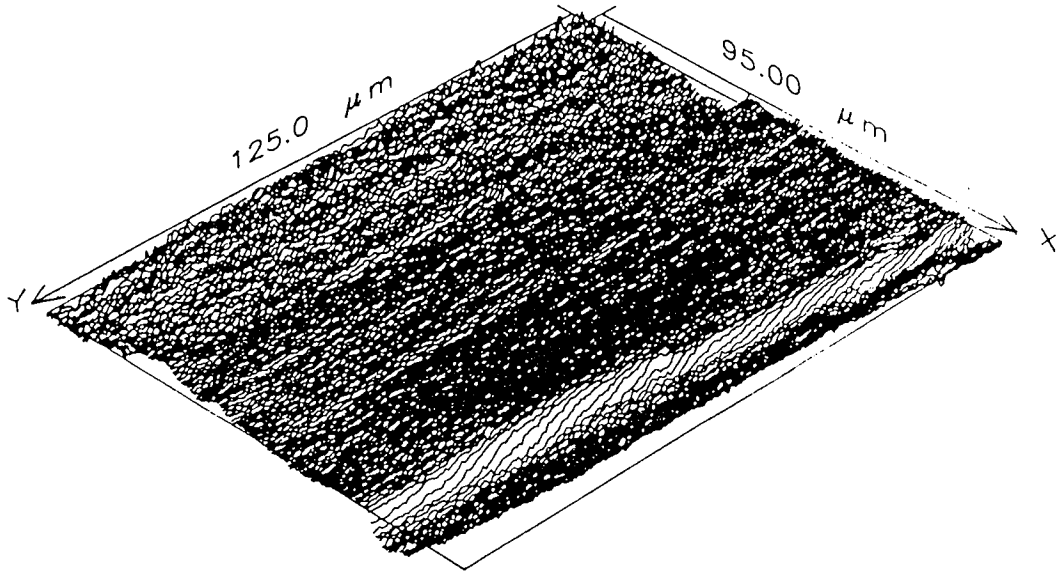

DEPTH SCALE = 250.0 TIMES XY SCALE

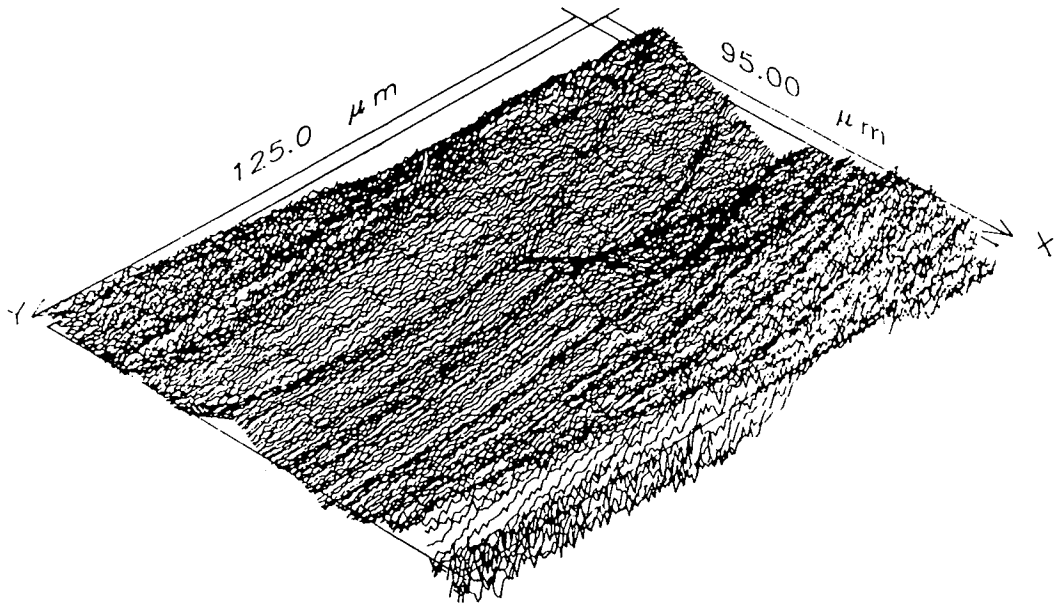

DEPTH SCALE = 250.0 TIMES XY SCALE

Figure 3.6: Interferograms of the gap area of the video head a) before and b) after 6 hours wear with Tape C

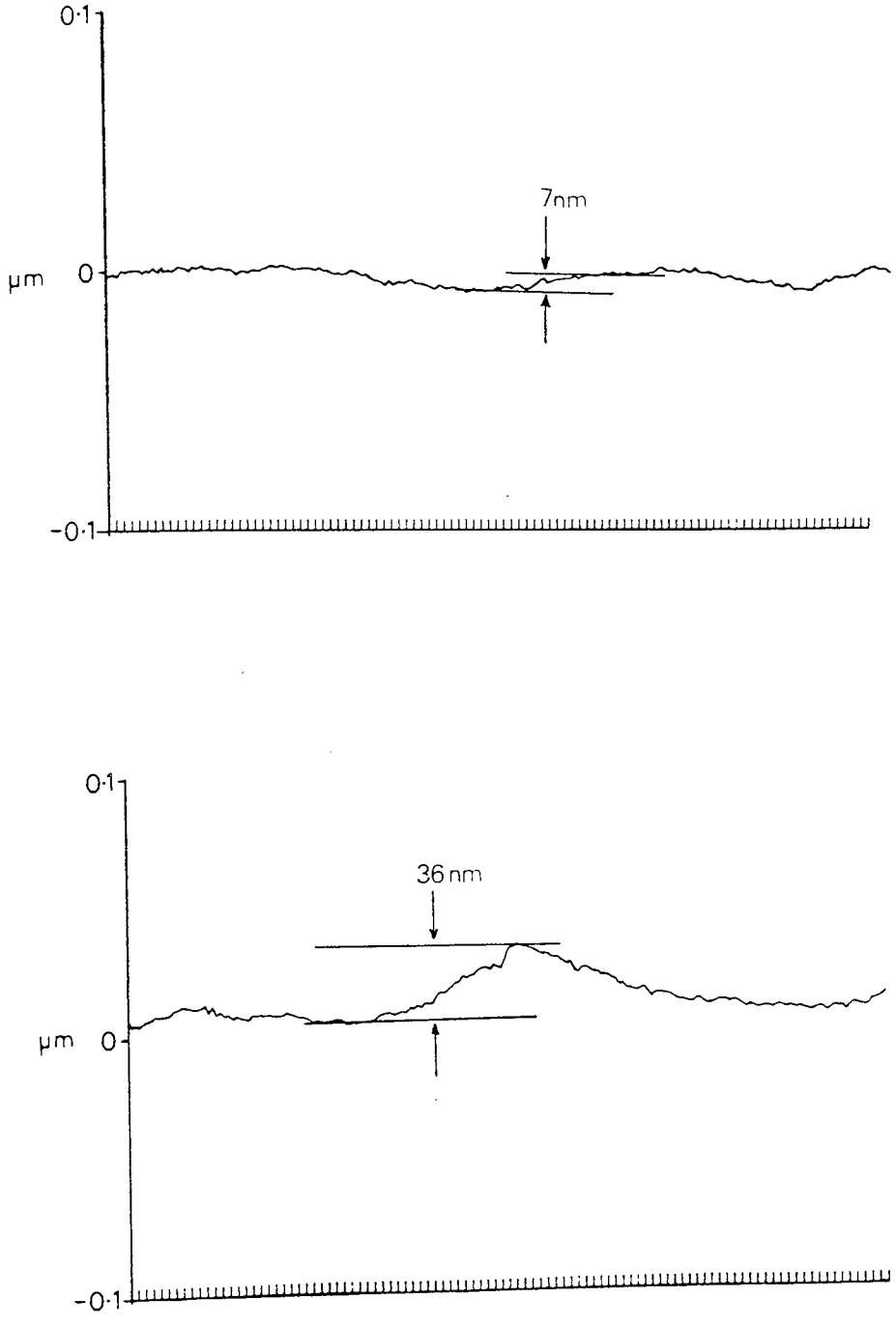

Figure 3.7: Cross-sectional plots taken from the interferograms of the gap area of the video head a) before and b) after 6 hours wear with Tape C

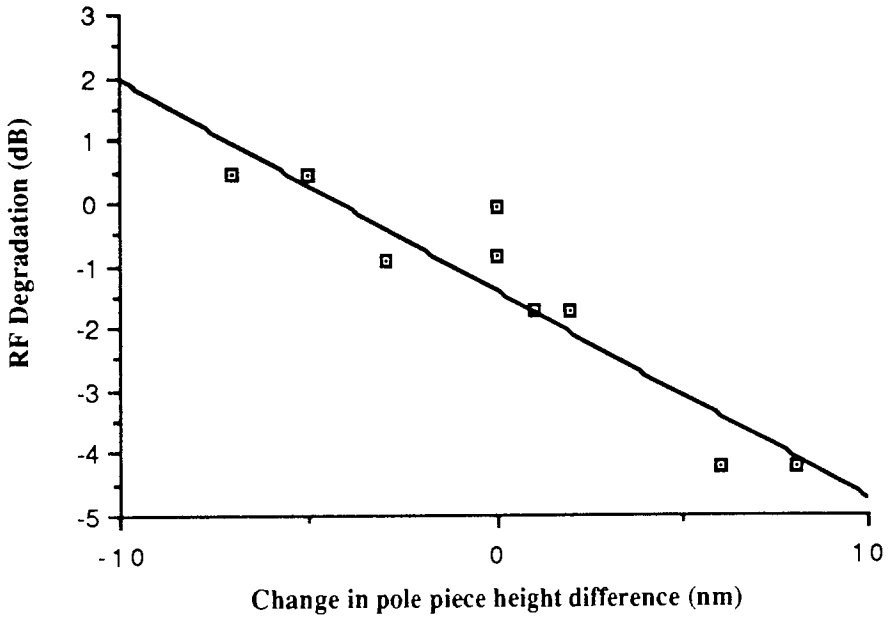

Figure 3.8: RF degradation plotted against change in pole piece height difference.

positive correlation between the change in pole piece height difference and the signal degradation.

3.1.3 Wear contouring

Examination of the worn heads under the optical microscope revealed the presence of a wear 'scar' or 'contour' extending either side of the gap. The contour provided an immediate impression of the position and extent of the contact between the tape and the head. Figure 3.9 shows sketches of the contours for Tapes D, A and C. The dimensions of the contours are also indicated. The relative size of the wear contours gave an indication of the abrasivity of each tape brand. These showed Tape D to be more abrasive than Tape A, and Tape C to be the least abrasive of all the tapes tested. The position of the wear contour in relation to the gap provided an image of the way in which the tape had wrapped or conformed to the head. The wear contours for Tapes D and A extend over both pole pieces either side of the gap with the wear biased towards the trailing pole piece. The contour produced by Tape C showed wear exclusively to the trailing pole piece. The preferential wear shown to one pole piece correlates with the increase in pole piece height difference. The position of the contour also correlates with the change in contouring of the trailing pole piece shown on the interferograms. It is assumed that the optimum conformity would centre on the gap, with the wear contour extending the same distance along both pole pieces. In the case of Tape C the tape has conformed badly and created uneven wear to the head. To study the relationship between head performance and the position of the wear contour, the position (in μm) of the centre of each contour in relation to the gap was derived and plotted against RF signal degradation (dB). The plot is shown in Figure 3.10, showing the results for both heads and for all samples tested were used to plot the graph. The conformity of the tape to the head is a product of several physical parameters of the tape, such as the thickness and stiffness in both machine and cross directions.

a)

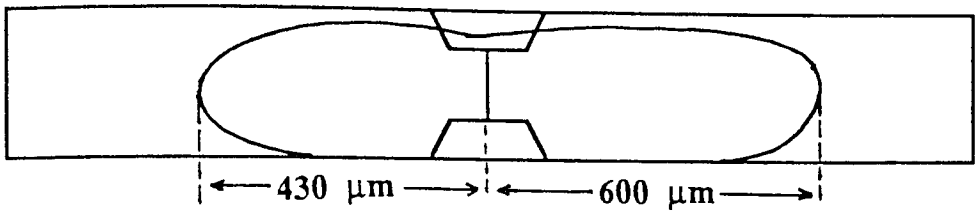

b)

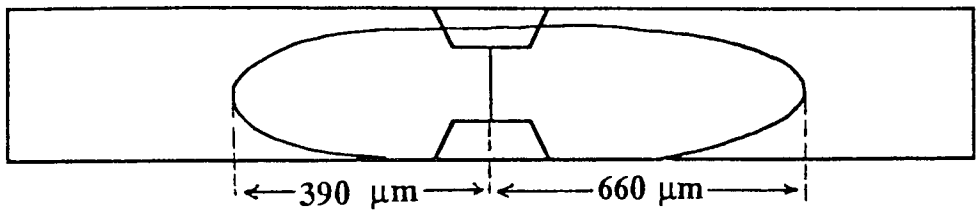

c)

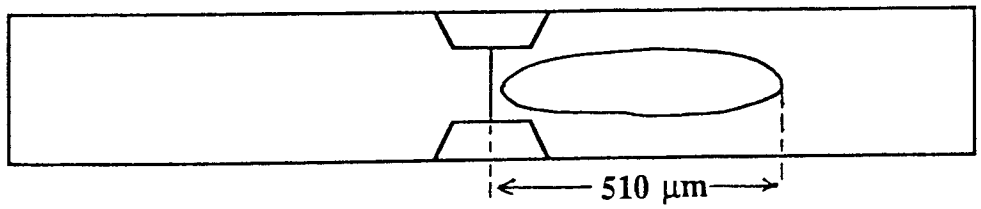

Figure 3.9: Wear contours formed on the head surface after 6 hours wear with the following samples:

a) Tape D

b) Tape A

c) Tape C

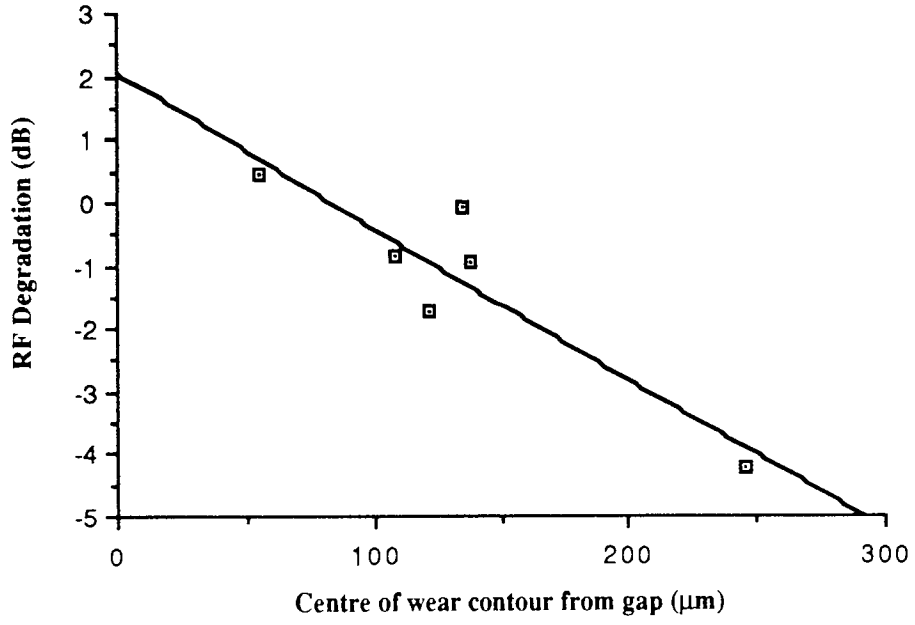

Figure 3.10: RF degradation plotted against the centre of the wear contour from the gap.

3.1.4 Signal degradation

The degradation of the RF signal was monitored at regular intervals during the test and plots were produced of the degradation (dB) against time (minutes). Figure 3.11 shows the degradation plots for Tape D, Tape A and Tape C. The total degradation after 6 hours was derived from the results and used to provide correlations with the physical wear phenomena. The plots show whether the final degradation figure is representative of the change in degradation over the 6 hours. They also reveal other features of the degradation in signal, such as a sharp decline in response over the first few minutes in the case of Tape D. As wear continues the performance is recovered, to the extent that the final degradation figure is positive, that is, the performance of the head has been improved. This correlates well with the physical improvements to the head mentioned in the previous two sections. The plot representing the degradation of the head worn with Tape C shows a steady decline in performance with no indication of a level being reached in 6 hours. The plot for the Tape A shows little decline in performance and levels off after a short time. Since in some cases the signal was still degrading after 6 hours of wear the experiments performed in the main project were continued for a further 6 hours.

The first aim of the pilot experiment experiment was to isolate the causes of bad signal degradation and to identify to the tape parameters which could be changed to improve performance. In order to do this the physical parameters of the tape samples were considered. Table 3.1 shows the RF degradation (dB) for each sample, together with the roughness RQ (nm), the thickness (μm), and the flexural modulus of the tape in both machine (MD) and cross directions (CD). The flexural modulus is quoted in kg/m^2 The magnetic particle in each sample dictates the relative abrasivity of the tape. Hence the type of particle used is also tabulated together with the head cleaning agent if present. All the values stated are for the standard E180 product for each sample (118).

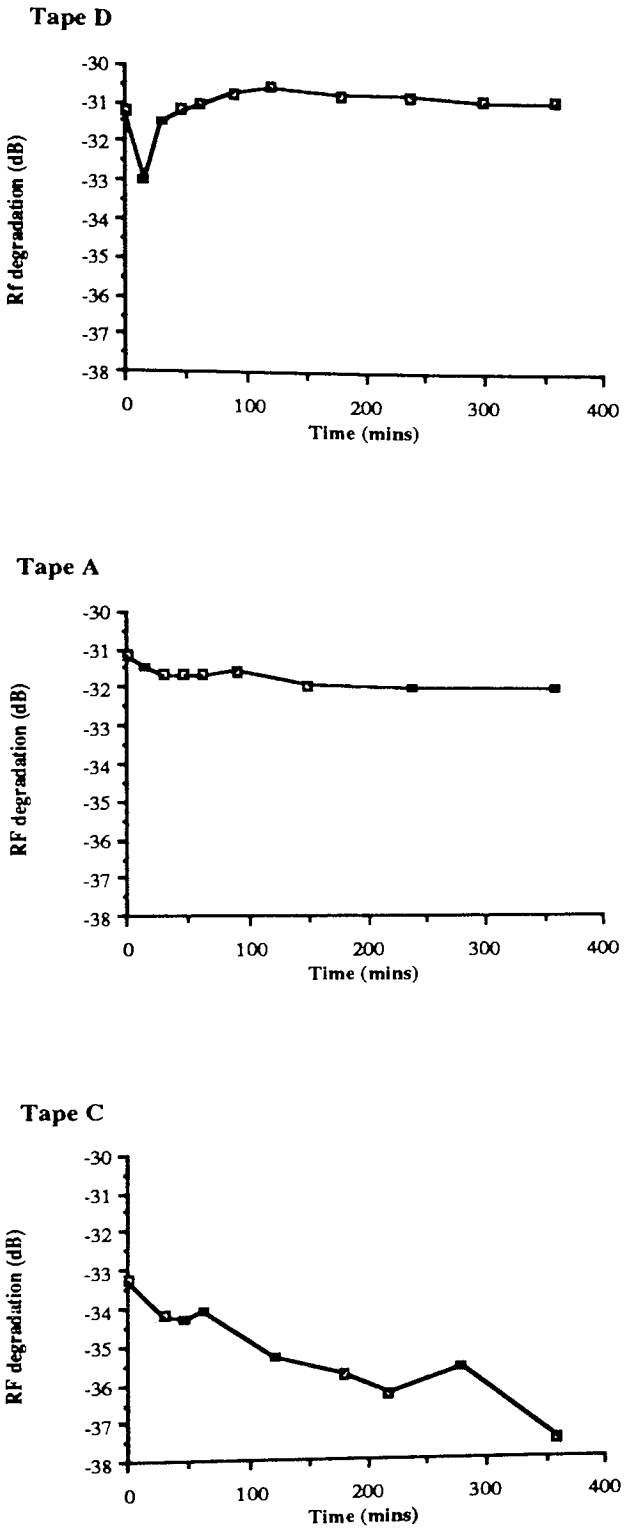

Figure 3.11: RF Degradation plotted against time for a) Tape D, b) Tape A and c) Tape C

Tape	RF Deg. (dB)	RQ (nm)	Caliper (µm)	Flexural Mod. (Kg/m^2) MD	CD	Magnetic pigment	Head cleaning agent
A	-0.9	14.3	18.78	1.83	1.35	Iron	Chromium
B	-1.7	21.6	18.53	2.11	1.49	Chromium	—
C	-4.2	14.8	18.02	1.65	1.44	Iron	Chromium
D	+0.5	8.4	18.53	1.78	1.88	Iron	Aluminium Silicon Titanium
E	-0.8	18.0	18.27	2.09	1.44	—	—
F	0	15.7	18.27	2.23	1.25	Iron	—

Table 3.1: Summary of physical tape parameters for tape samples examined in the pilot project

The second aim of the pilot experiment was to establish a programme of research which would examine in greater depth the mechanisms of wear occuring to the video head. In order to build up an accurate and full picture of the wear mechanisms occuring to the video head a more systematic examination of both surfaces before and after wear was required. Following the pilot research the research concentrated on Tape C, this was an iron oxide formulation containing 4% green chrome as a head cleaning agent. From the results of the pilot project, this formulation appears to produce by far the lowest wear, and extensive surface damage with the corresponding bad signal degradation. Hence, one aim of the main project was to investigate methods of increasing the wear caused by this formulation with a view to improving its performance.

3.2 Experiments IN1 and IN2: Evaluation of the Knoop diamond indentation technique

The diamond indentation technique was selected as a method of head wear measurement for this project. Before it could be used in the main part of the project, the optimum use of the technique as well as its accuracy in determining head wear had to be established.

In experiment IN1 the two orientations of the indentation, parallel and perpendicular to the sliding direction, were examined. Controls were included in the form of plain heads which were not indented. The aim of the experiment was to establish the most accurate indentation orientation, and to compare the performance of the head with and without indentation. The tape samples used in the examination were the standard Iron oxide tape containing 4% green chrome HCA and a pilot plant sample containing 4% alumina HCA.

Problems became immediately apparent with the main diagonals oriented parallel to the sliding direction. The indentations became increasingly distorted the further from the gap they were positioned due to the curvature of the head. The

distortion was characterised by a shift in the position of the apex of the indentation, which was no longer the centre of the main diagonal. Since the distortion was likely to produce errors, only indentations positioned close to the gap provided accurate results. Further problems with this orientation became apparent after testing with the standard iron oxide tape. With the indentations oriented along the sliding direction, there was a tendency for any scratching produced during wear to the head to lengthen the main diagonal. Figure 3.12 shows a photomicrograph of an indentation which has been lengthened during wear of the head. The method of wear measurement was dependent upon the reduction in length of the main diagonal. The deformation made the indentations difficult to measure and inaccuracies were introduced.

3.2.1 Calculation and use of the wear rate results

Each indentation measurement was repeated six times, and the mean was used in the derivation of wear rate. If X_0 is the original mean length of the indentation and X_6 the mean length after six hours, then the change in length of the main diagonal (Δd) is;

$$\Delta d = X_0 - X_6 \qquad (3.1)$$

The change in apex height (Δh) is related to the base angle as shown in chapter 2, such that;

$$\Delta h = (\Delta d \text{ Tan } 3°45')/2 \qquad (3.2)$$

This represents the change in height of the surface, (i.e. the wear), occuring over six hours. The wear is expressed in terms of wear rate per hour. The wear rate per hour (H) was derived for each indentation, as follows;

$$H = \Delta h/6 \qquad (3.3)$$

Figure 3.12: Optical photomicrograph of indentation oriented parallel to the direction of sliding and lengthened during wear.

In the evaluation of the indentation technique the tests were terminated after 6 hours. In the main experiment a further 6 hours of testing was performed. For the results obtained after 12 hours the indentation measurements were treated as above, with the mean readings for the indentations after 12 hours (X_{12}) being substituted for X_6. In addition, in deriving the wear rate the duration was taken into account, as follows;

$$H = \Delta h/12 \qquad (3.4)$$

The distortion of the indentations oriented parallel to the sliding direction meant that only the indentations positioned nearest to the gap could be accurate enough to be considered. Hence, only the wear rate at the gap could be compared for the two orientations.

In Experiment IN1 the samples tested were the commercial iron oxide formulation and an iron oxide formulation produced at the pilot plant containing 4% Al_2O_3. Table 3.2 shows the wear rate at the gap after 6 hours of wear, for the experiment. The value shown is the average wear rate for the two heads in μm/hr.

	Wear Rate (μm/hr) $X10^{-2}$	
	Indentation parallel to S.D	Indentation perpendicular to S.D.
4 % Al_2O_3	1.66	1.18
Standard tape (4% Cr_2O_3)	0	0

Table 3.2: Experiment IN1: Wear rates for tape samples after 6 hours wear

In six hours no measurable wear was recorded for the standard iron oxide sample for either orientation of indentation. Wear was recorded using both orientations for the alumina sample. Considering the accuracy of the technique, which was calculated as ± $0.3x10^{-2}$ μm/hr (see section 2.2.4), little difference in wear rate was recorded between the two orientations.

The wear rates for each indentation were plotted against the position of the indentation relative to the gap, which were recorded when the original measurements were made. Figure 3.13 shows the wear rate plot for the sample containing the alumina HCA, in experiment IN1. The wear rate data for the plot were taken from the indentations oriented perpendicular to the sliding direction. The results of both the blue and the green heads are shown to confirm the similarities between the two heads on a single drum wear. On the plots the gap is indicated to show how the wear is distributed over both pole pieces. Also, the positions of the edges of the wear contour are indicated to confirm that the visible extent of the wear corresponds to that measured using diamond indentation.

The plot describes the variation in wear along the head, and therefore the conformation of the tape to the head in some detail. In the pilot research, the position of all wear contours was biassed towards the trailing pole piece, to varying degrees. Figure 3.13 shows that the maximum volume of wear occurred on the trailing pole piece in close proximity to the gap, with the wear rate decreasing towards the gap. However, that the minimum point of contact did not occur at the gap. A sharp increase in wear rate was also apparent on the leading pole piece corresponding to the edge of the wear contour.

3.2.2 RF degradation

The total RF degradation figures are shown for the set of six tests of experiment IN1 in Table 3.3 . It appears that heads worn with tape containing alumina HCA performed

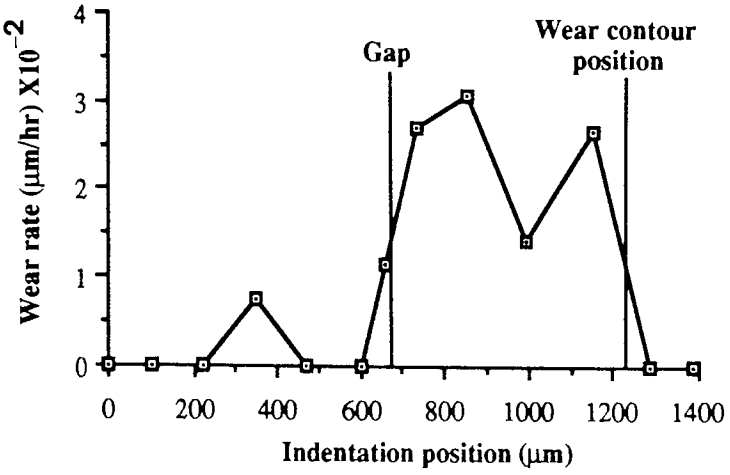

a) blue head

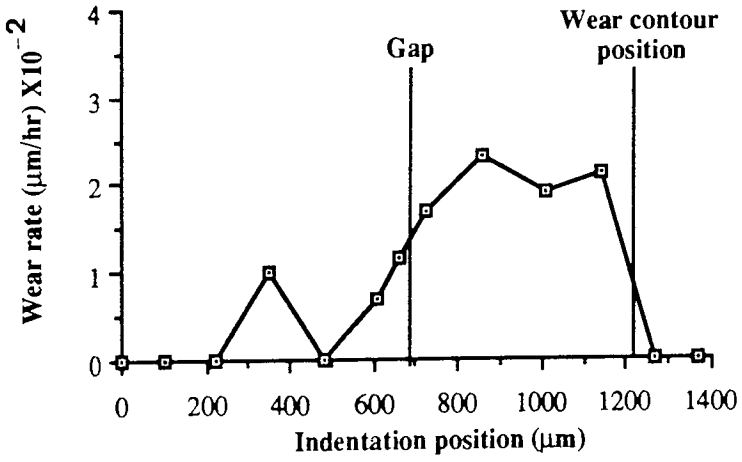

b) green head

Figure 3.13: Wear rate plotted against indentation position for the heads worn with the iron oxide formulation containing 4% alumina. (Experiment IN1)

better than those worn with the standard product. However, the sample containing alumina was a pilot plant sample is being compared with the standard commercial product. Although they are ostensibly the same formulation except for the HCA, their different origin of manufacture may contribute to differences in performance. Thus in experiment IN2, iron oxide samples are compared which were both produced at the pilot plant.

	RF degradation (dB) Type of indentation		
Sample	Perpendicular to S.D	Parallel to S.D	Not Indented
4 % Al_2O_3	-0.50	-1.50	+0.25
Standard tape (4% Cr_2O_3)	-2.00	-3.10	-2.30

Table 3.3: Experiment IN1: RF degradation after 6 hours wear

The results of Table 3.3 also show that heads with indentations oriented parallel to the sliding direction exhibited slightly worse degradation than the perpendicular orientation. Hence, indentations oriented with the main diagonal perpendicular to the sliding direction appear to be preferable for optimizing accuracy of wear rate and degradation measurement. This orientation eliminated the effect of the curvature of the head and the distortion caused by wear phenomena, and was therefore used for all further experiments in the project.

Each set of indentation results was used to derive the wear rate at the gap and the maximum wear rate on the head. These were then plotted against the position of the indentations to provide a wear rate profile over the head. It was also decided to examine the performance of the alumina particle as an HCA in more detail.

3.2.3 Experiment IN2: Further evaluation of the indentation technique, including testing of a chromium dioxide formulation.

In experiment IN2, two iron oxide based tapes were compared with a chrome dioxide tape. This experiment was performed to test further the indentation technique as a method of wear measurement and to examine the limit of its use in measuring wear caused by abrasive tapes such as a chrome dioxide formulation. The iron oxide tapes were produced at the pilot plant and varied only in HCA, one tape containing 4% green chrome, the other 4% alumina. The total RF degradation after 6 hours wear for the three tape is shown samples in Table 3.4 . The tapes were run over both indented and non-indented heads as a control.

		RF Degradation (dB) After 6hrs Wear	
Tape	HCA	Head Indented	Head Plain
Iron Oxide	Cr_2O_3	-3.00	-3.75
	Al_2O_3	-0.35	+0.25
Chrome Dioxide	-	-0.75	-1.20

Table 3.4 Experiment IN2: RF degradation after 6 hours of wear

The high wear produced by the chrome dioxide tape compared with the iron oxide became apparent after just 6 hours of testing. The extent of wear to the head worn by the chrome dioxide tape was such that indentations situated at positions of greatest wear were rendered too short to be of further use. Hence, the test was not continued for the chrome dioxide sample, whereas the iron oxide samples were run for a further 6 hours, giving a total test duration of 12 hours.

The wear results for the experiment are shown in Table 3.5. The wear rate, relative to the initial readings, was calculated after both 6 and 12 hours of wear and values are given for both the wear rate at the gap and the maximum wear rate. The wear rate profiles were also plotted. The profiles after 6 hours for all three tape samples (blue heads only) are shown in Figure 3.14a, and in Figure 3.14b the profile for the iron oxide samples after 12 hours of wear is shown.

Examination of the wear rates show that wear caused by the chrome dioxide tape is approximately ten times the wear rate per hour of the iron oxide samples. When all three samples are compared the difference between the two pilot plant iron oxide samples containing different HCA's appears negligible.

3.3 Examination of the effect of varying the head cleaning agent (HCA)

One aim of the project was to establish the optimum use of the HCA green chrome. The results of the pilot research showed that the iron oxide tape containing 4% green chrome exhibited a very low wear rate compared with other competitive products. This was evident from the very small wear scar produced. The iron oxide particle is relatively soft and does not provide a head cleaning action without the addition of an HCA. However, the volume of HCA required to provide the tape with a satisfactory head cleaning action is not well established. The addition of an HCA has mostly concentrated on improving the durability of the tape rather than on the wear of the head.

	Wear Rate (μm/hour) X10	Fe_2O_3				$Cr O_2$	
		Al_2O_3		Cr_2O_3			
		Blue	Green	Blue	Green	Blue	Green
6 hours wear	gap	0.98	1.27	1.66	1.69	10.42	8.92
	maximum	2.47	2.41	2.93	2.25	15.27	12.67
12 hours wear	gap	1.24	1.06	1.27	1.40	---	---
	maximum	2.98	2.88	1.99	1.66	---	---

Table 3.5: Experiment IN2: Summary of wear results after 6 and 12 hours of wear

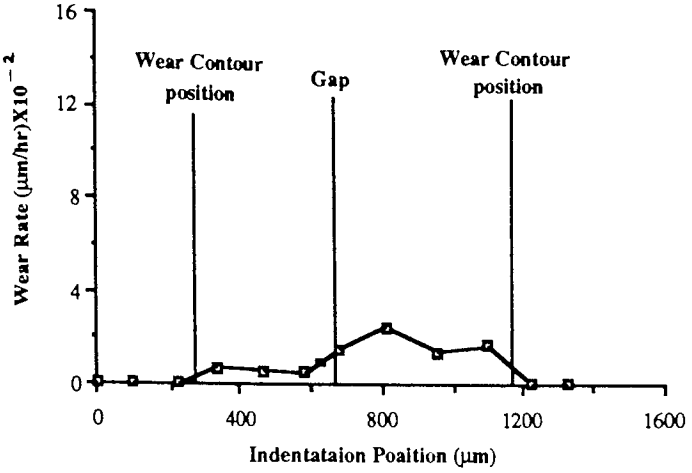

1)

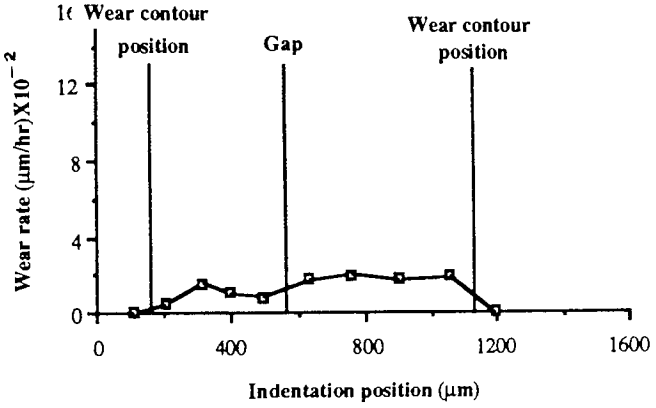

2)

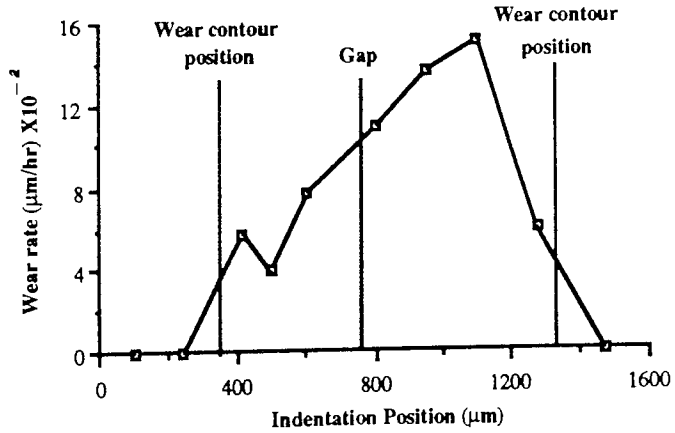

3)

Figure 3.14a: Wear rate after 6 hours plotted against indentation position for the three samples of Experiment IN2, 1) iron oxide containing 4% Al_2O_3, 2) iron oxide containing 4% Cr_2O_3, 3) chromium dioxide.

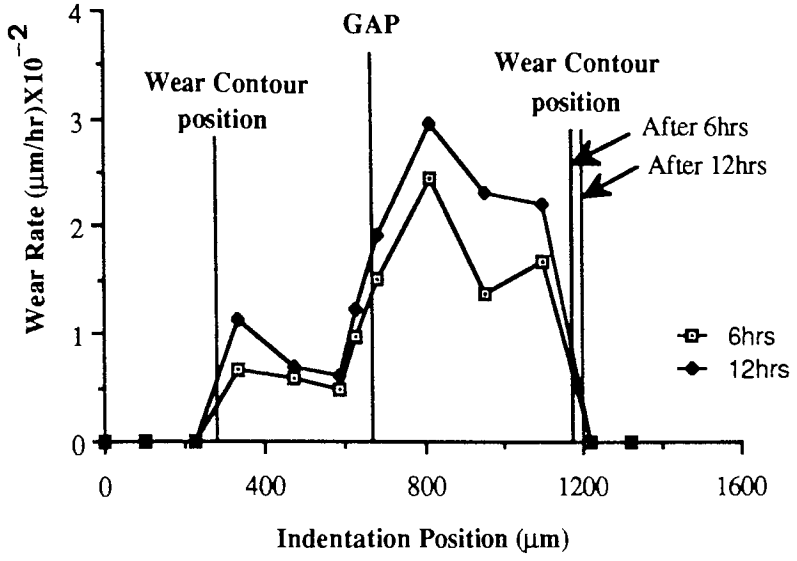

1)

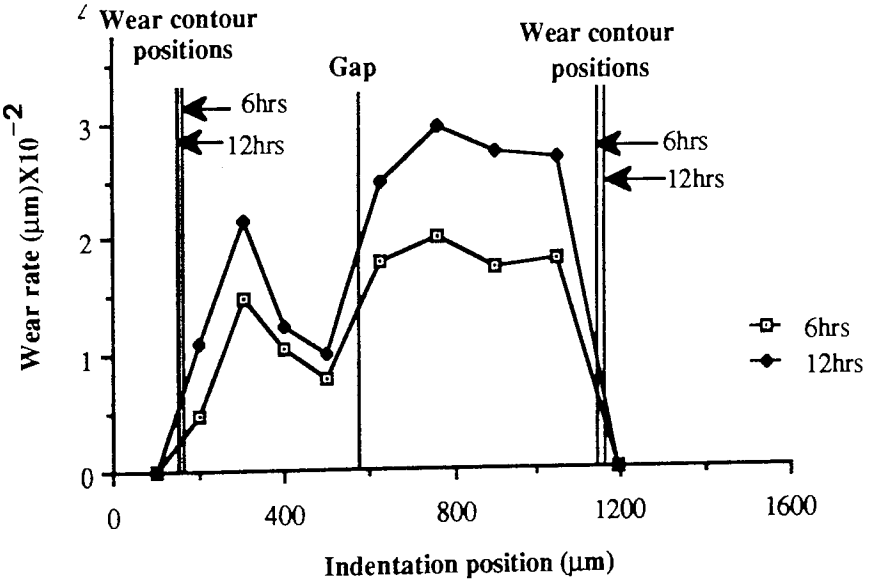

2)

Figure 3.14b: Wear rate after 6 and 12 hours plotted against indentation position for the samples of Experiment IN2, 1) iron oxide containing 4% Al_2O_3, 2) iron oxide containing 4% Cr_2O_3

3.3.1 Variation in green chrome from 0% to 10%.

In experiment GC1 the percentage of the HCA, green chrome within the magnetic coat was varied from 0% to 10%, in steps of 2%. Results were obtained after 6 hours and after 12 hours of wear for each of the six tape samples.

3.3.1.1 RF degradation

The degradation curves for each of the six experiments are shown for the complete 12 hours of the test in Figure 3.15. From these results the total degradation after 6 and 12 hours was derived, and is tabulated in Table 3.6. Each plot shows an approximately exponential fall in performance of the head. After 6 hours the degradation is still falling, whereas towards 12 hours of wear the degradation levels and in the case of the 10% sample improves slightly. The bulk of the degradation appears to take place within the first 6 hours of wear and is followed by a relatively steady state. In Figure 3.16 the total RF degradation after 6 and 12 hours is plotted against the percentage of green chrome. The sample containing no HCA shows surprisingly low degradation. Little variation in performance was evident between 2% and 6% and at 10% the performance of the head appeared to be improving. For samples containing green chrome the RF degradation ranged between -3.10dB and -4.75dB.

Examination of the surface of each head under the optical microscope showed deformation of the ferrite and very bad degradation of the gap. The features of wear were similar for each head worn with samples containing differing HCA concentrations. Figure 3.17 shows the photomicrographs of two heads one worn with a sample containing 6% green chrome and the other worn with a sample containing 10% green chrome after 6 hours wear. Severe damage to the gap can be seen in both cases, together with some deformation of the ferrite surface. Figure 3.18 shows the head worn with the sample containing no HCA. The surface of the ferrite is severely damaged, and

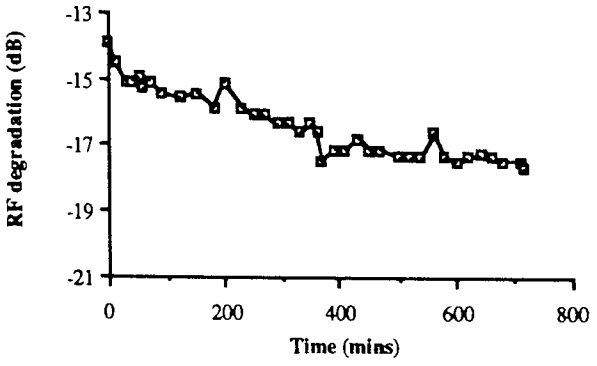

a) 0% HCA

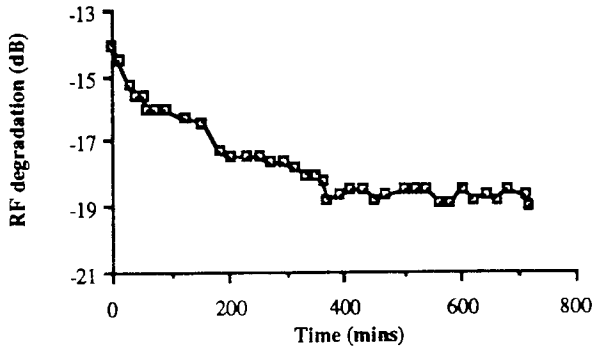

b) 2% green chrome

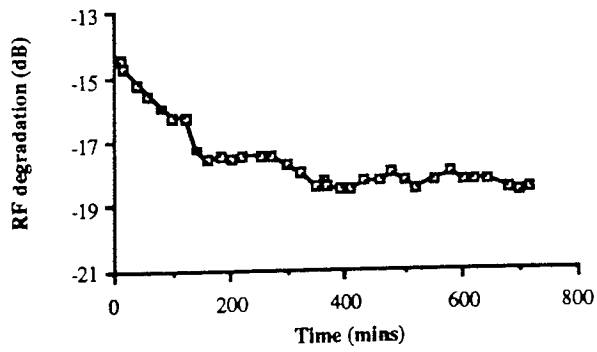

c) 4% green chrome

Figure 3.15: RF degradation plotted against time for the samples of experiment GC1, iron oxide samples containing 0%, 2% and 4% Cr_2O_3 HCA.

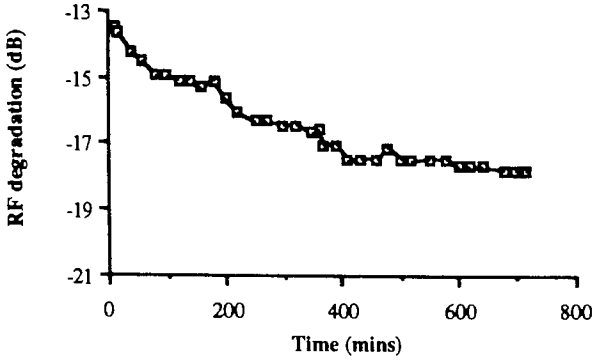

d) 6% green chrome

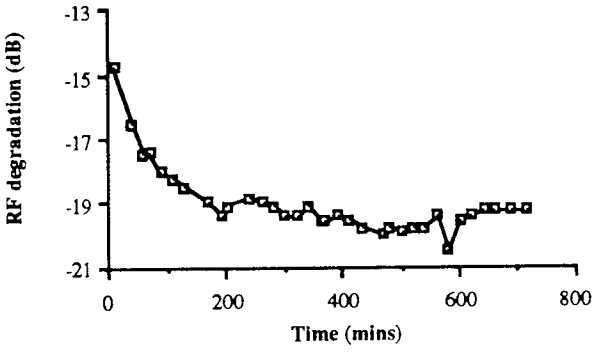

e) 8% green chrome

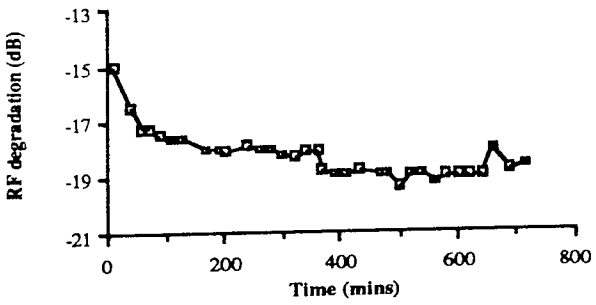

f) 10% green chrome

Figure 3.15 continued: RF degradation plotted against time for the samples of experiment GC1, iron oxide samples containing 0%, 2% and 4% Cr_2O_3 HCA.

			Wear rates (μm/hour)X10^{-2}				
	RF degradation (dB)		After 6 hours		After 12 hours		
Percentage HCA	6 hours	12 hours	At the gap	Maximum	At the gap	Maximum	Roughness (nm)
0	-2.10	-3.20	0	0.78	0	0.48	13.522
2	-3.70	-4.50	1.17	1.66	0.75	1.08	12.770
4	-3.75	-4.10	3.07	4.28	2.21	3.05	14.077
6	-3.00	-4.25	1.68	2.56	1.34	1.83	11.994
8	-4.25	-4.50	2.53	4.05	2.42	3.32	13.201
10	-3.10	-3.60	4.68	6.64	4.55	5.51	13.471

Table 3.6: Experiment GC1: variation in Cr_2O_3 from 0% to 10%: Summary of results for 6 and 12 hours wear.

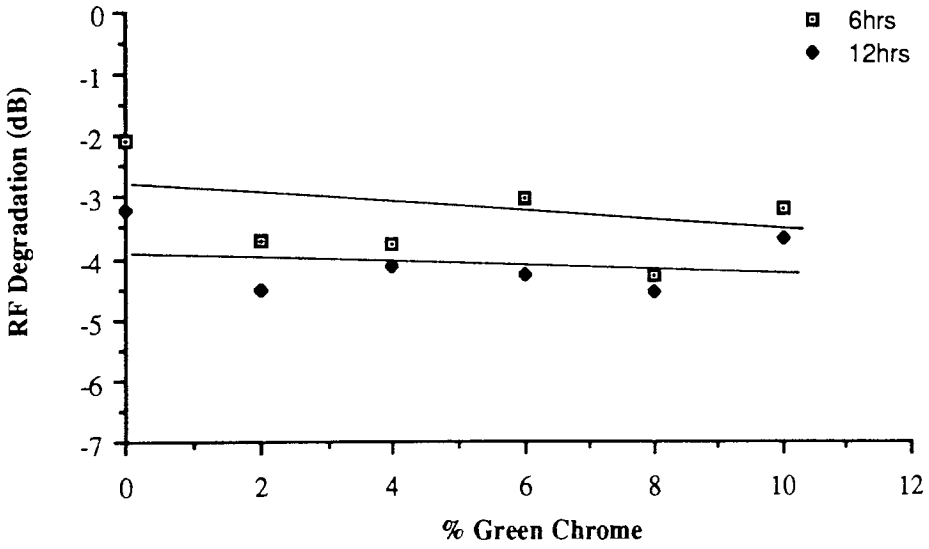

Figure 3.16: RF degradation against percentage Cr_2O_3 after 6 and 12 hours wear (Experiment GC1).

Figure 3.17: Photomicrographs of video heads after 6 hours wear with the iron oxide formulation containing:

a) 6% Cr_2O_3 as the HCA

b) 10% Cr_2O_3 as the HCA

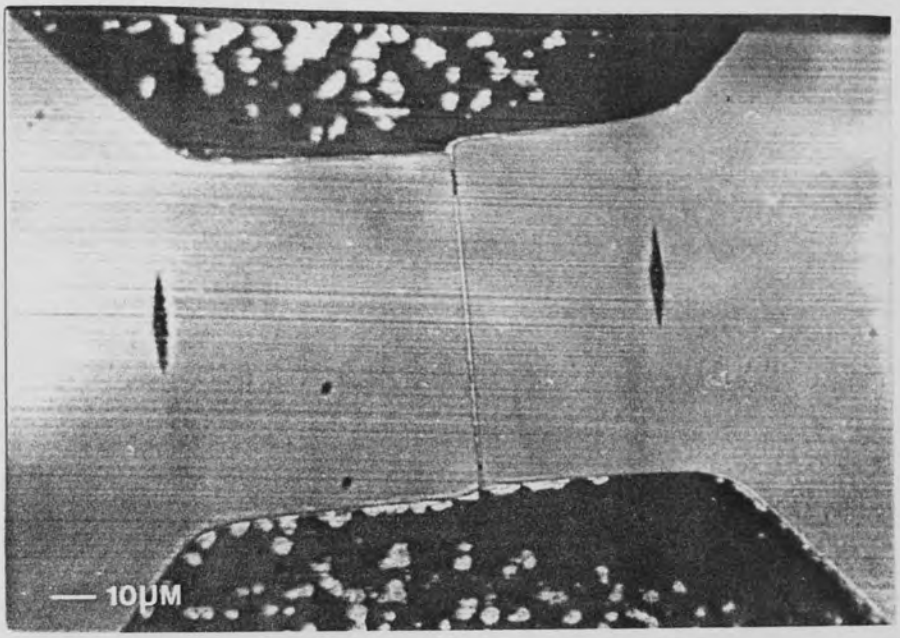

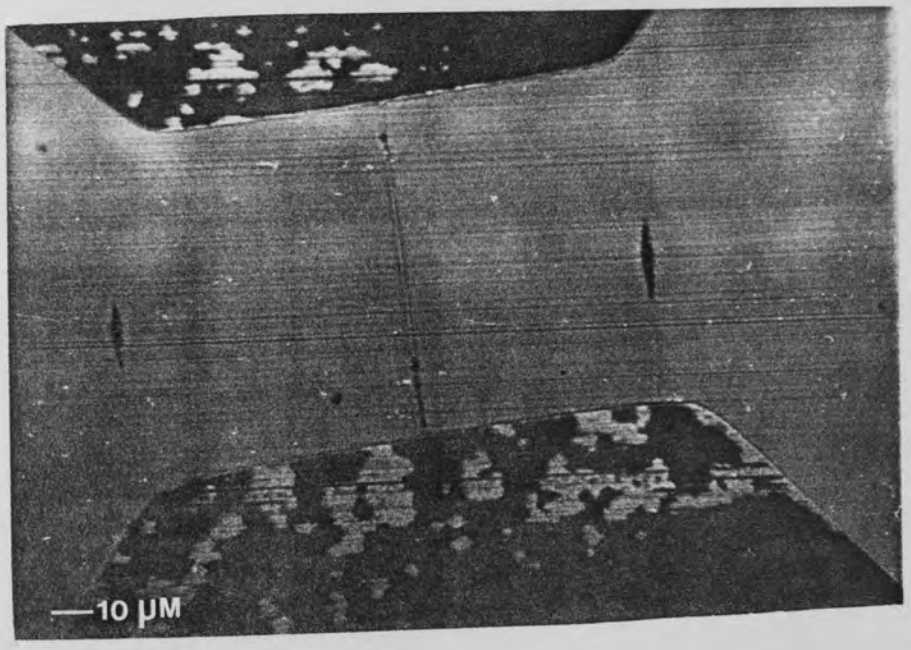

Figure 3.18: Photomicrograph of video head after 6 hours wear with the iron oxide formulation containing no HCA.

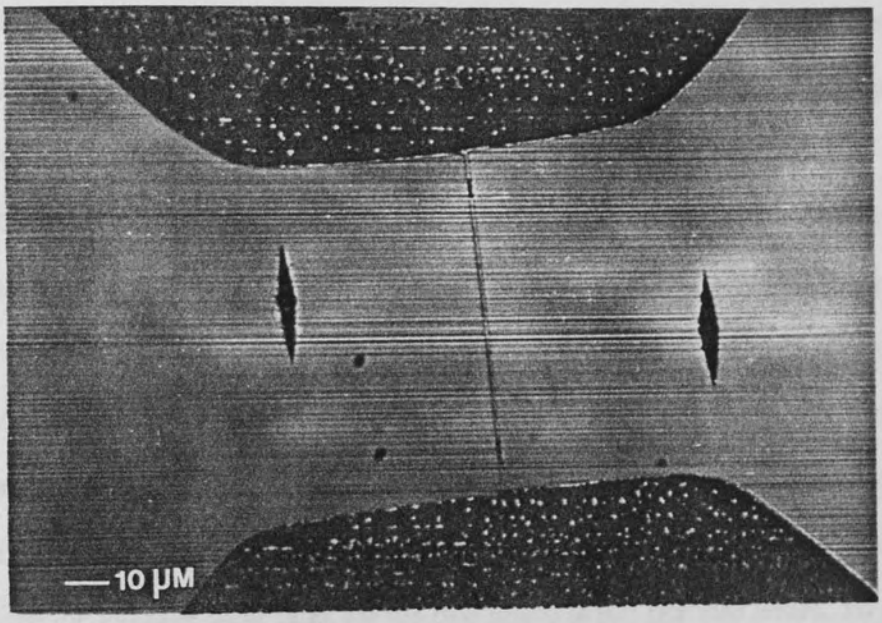

is covered in wear tracks or grooves. The gap itself has remained relatively undamaged, considering the damage to the ferrite surface. The RF degradation for this sample was lower than for samples containing green chrome which showed severe gap damage but less surface deformation.

3.3.1.2 Wear rate measurements

Plots of wear rate against the position of the indentations along the head after 6 hours are shown in Figure 3.19. The results for the blue head only are presented, one head for each sample. The general profile of wear was similar to that reported in experiment IN1, with a large percentage of the wear occurring on the trailing pole piece. Measurable wear was recorded for only one indentation from the head worn with the 0% sample after 6 and after 12 hours. Hence, no plots could be produced for this sample. In general the wear rates increased with increasing percentage of green chrome. This trend was interupted by the sample containing 4% HCA in which the wear rate was higher than would be expected. The wear rate at the gap and the maximum wear rate were derived for each sample, and are shown in Table 3.6. The values quoted in the table are the average wear rates for the two heads in μm per 100 hours. To show the general trend in wear the wear rate at the gap and the maximum wear rate were plotted against the percentage HCA as shown in Figure 3.20. The plot shows an increase in wear rate with percentage HCA and an abnormal rise in wear rate for the 4% sample. A possible explanation for the rise in wear rate may be found from the relative roughness of the samples, also shown in Table 3.6. The roughness for the 4% sample is the highest of this batch of samples. Figure 3.21 shows roughness plotted against percentage green chrome. From this plot it can be seen that the roughness of the 4% sample was high even compared with the 10% sample. Also, the roughness of the 6% sample is lower than would be expected. From the literature it is clear that the wear characteristics of the head are related to the roughness of the media (106), which

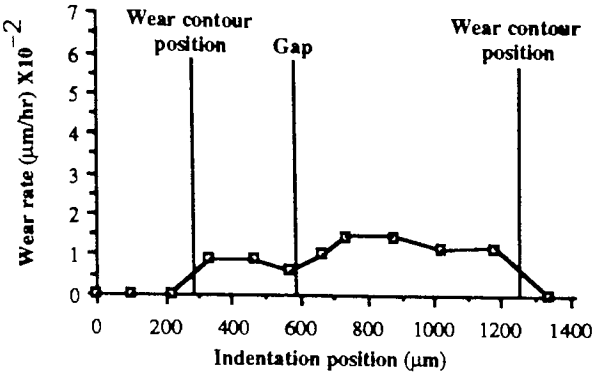

a) 2% green chrome

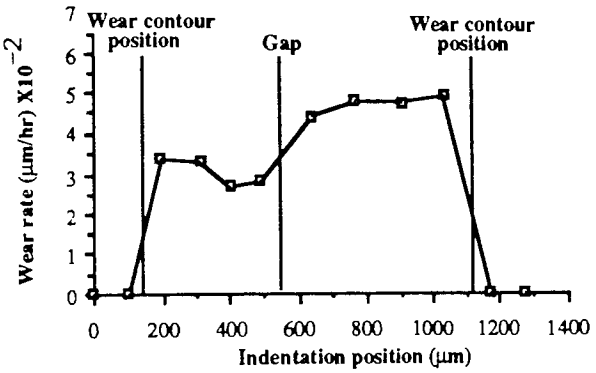

b) 4% green chrome

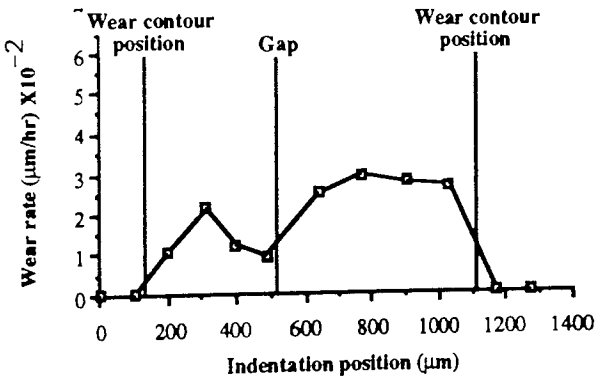

c) 6% green chrome

Figure 3.19: Wear rate after 6 hours plotted against indentation position for samples of Experiment GC1, iron oxide samples containing 2%, 4% and 6% Cr_2O_3.

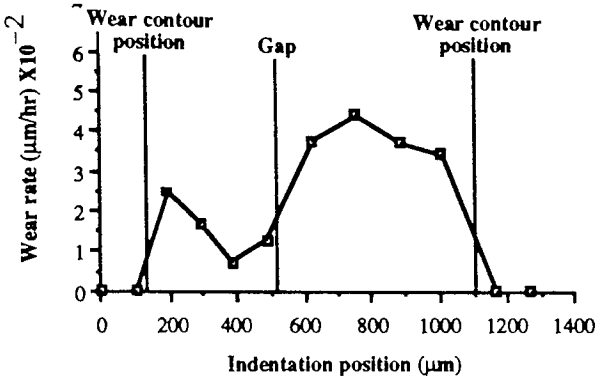

d) 8% green chrome

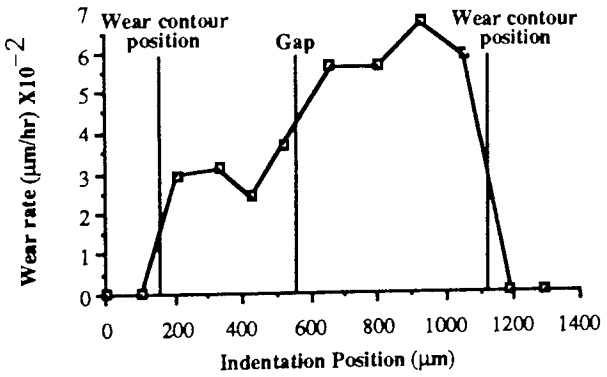

e) 10% green chrome

Figure 3.19 continued: Wear rate after 6 hours plotted against indentation position for samples of Experiment GC1, iron oxide samples containing 8% and 10% Cr_2O_3.

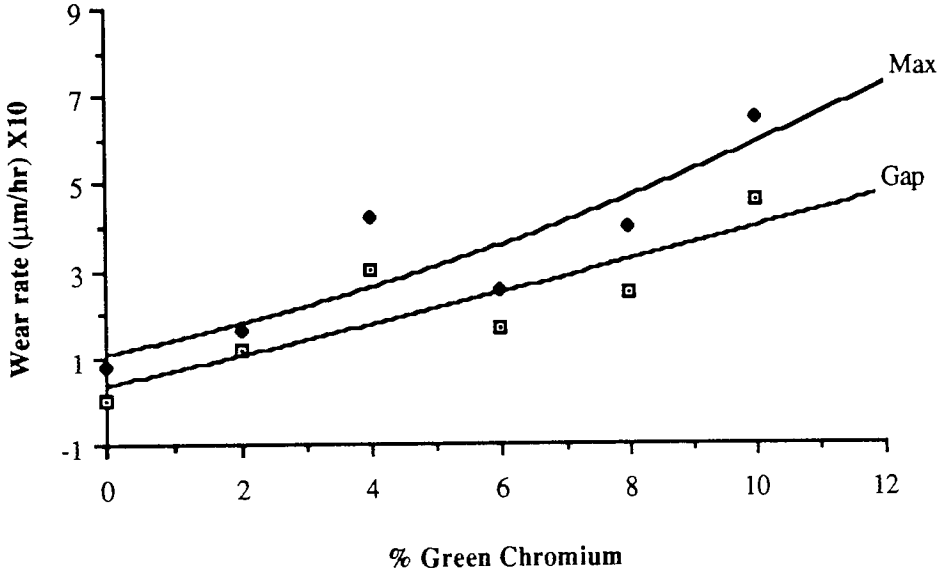

Figure 3.20: Wear rate at the gap and the maximum wear rate after 6 hours, plotted against percentage concentration of Cr_2O_3 for the samples of Experiment GC1

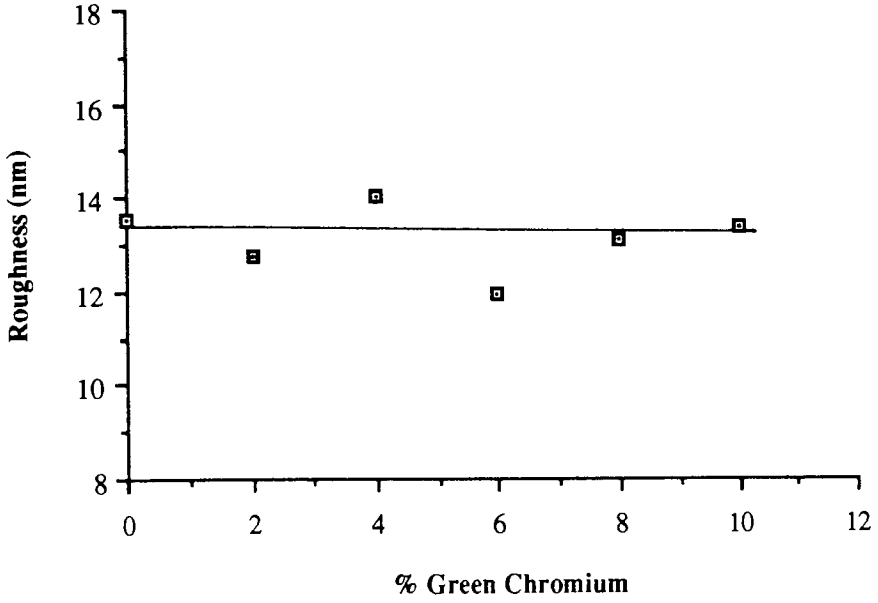

Figure 3.21: Roughness (RQ) plotted against percentage Cr_2O_3 for Experiment GC1

that the increase in roughness has produced a corresponding increase in wear rate for the 4% sample. However, the wear rate is not directly related to roughness. The resulting wear rate is a product of both the roughness and the type and concentration of the HCA, and cannot be explained solely in terms of increased roughness resulting from increased HCA loading. It must be pointed out that ideally the roughness of all the pilot samples should be the same, since the calendering process through which the tape is taken is designed to produce tape of consistant roughness. The pilot plant appears to produce a greater variation in roughness than would be acceptable in commercial production.

The wear rate curves given in Figure 3.19 show only the wear after 6 hours. The wear rate at the gap, the maximum wear rate and the degradation results after 12 hours of wear are also shown in Table 3.6. Figure 3.22 shows the wear rate curves for 12 hours overlaid on the 6 hour plots for the samples containing 4% and 10% green chrome. From these plots it is clear that the wear rate has decreased with time for each sample. The change in wear rate after such a small amount of wear suggests that the wear which has occured has resulted in a more wear resistant surface than the original ferrite surface. Two possible causes of an increased resistance to wear, which are discussed in Chapter 4 are; first, the deposition of a polymer film on the head; and second, work hardening of the surface due to deformation. Whatever the cause, it was clear that in order to understand the wear processes occuring, the head had to be examined in more detail; first, under high magnification to study the deformation of the surface and any wear particles produced; and second, chemical analysis of the surface to establish any transfer of material from the tape. Both types of analyses were performed, and are discussed later in this chapter.

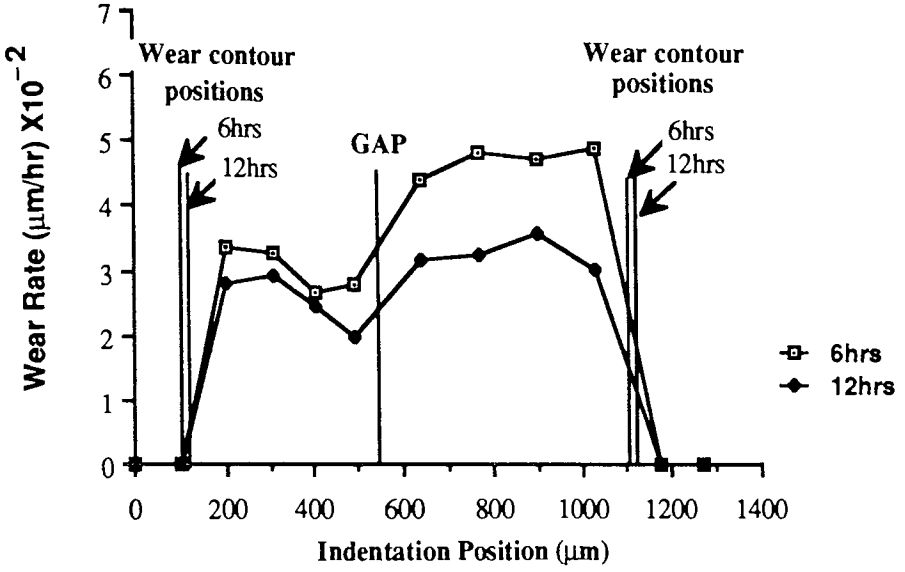

a) 4% green chrome

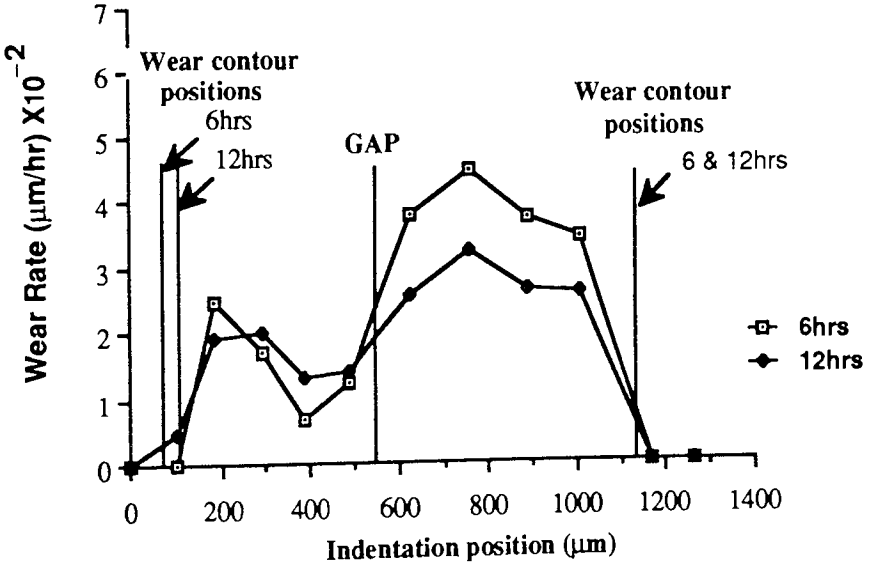

b) 8% green chrome

Figure 3.22: Wear rate against indentation position after 6 and 12 hours wear with a) iron oxide formulation containing 4% Cr_2O_3, b) iron oxide formulation containing 8% Cr_2O_3.

3.3.2 Experiment GC2: Variations in green chrome from 8% to 16%,

In experiment GC2 the performance of tape samples containing concentrations of green chrome from 8% to 16% in steps of 2% was examined. The experiment was designed to ensure continuity between experiments GC1 and GC2 by repeating two of the HCA levels, and thus examine the reproducibility of the pilot plant samples. The experiment included concentrations up to 16% which is a relatively high concentration which provided an opportunity to examine the dispersion of the HCA within the magnetic coating, and the ability of the binder system and dispersive agents to spread the increasingly larger concentrations of HCA evenly throughout the magnetic coating. At higher concentrations it may be the case that levels of other constituents in the tape require alteration in order to accommodate the increase in HCA particles.

The experimental procedures followed in experiment GC1 were maintained for experiment GC2. Hence, a similar set of results were obtained for the second set of green chrome concentrations. Table 3.7 gives a summary of the results of experiment GC2, showing the total degradation, the wear rate at the gap, the maximum wear rate after 6 and after 12 hours and the roughness value of each sample.

Examining the RF degradation the overall signal degradation for this batch of samples was low compared with GC1, until 16% concentration was reached. The appearance of the video heads under the optical microscope again reflect the measured signal degradation. Figure 3.23a shows a photomicrograph of the head worn with the 16% sample and reveals damage to the gap in several places. Figure 3.23b shows the head worn with the 14% sample which shows some damage to the gap and one particularly deep groove. Surprisingly the gap was not badly damaged where it is traversed by the deep groove.

The lowest degradation was shown by the 10% sample. The head surface was badly deformed whilst the gap remained virtually undamaged (see Figure 3.23c). Closer inspection reveals that the worst damage was to the glass region and not the

			Wear rates (μm/ hour) $X10^{-2}$				
	RF degradation (dB)		After 6 hours		After 12 hours		
Concentration HCA (%)	6 hours	12 hours	At the gap	Maximum	At the gap	Maximum	Roughness (nm)
8	-1.85	-2.75	0.35	1.03	0.20	0.90	12.828
10	-0.90	-1.10	0.57	1.86	0.52	3.03	13.021
12	-1.50	-2.50	0.44	2.57	0.22	2.13	13.978
14	-1.10	-1.35	1.26	4.04	1.11	4.92	16.724
16	-2.50	-4.60	1.11	4.06	0.76	2.07	12.558

Table 3.7: Experiment GC1: variation in Cr_2O_3 from 8% to 16%: Summary of results after 6 and 12 hours wear.

Figure 3.23: Photomicrographs of video heads after 6 hours wear with the iron oxide formulation containing:

a) 16% Cr_2O_3 as the HCA

b) 14% Cr_2O_3 as the HCA

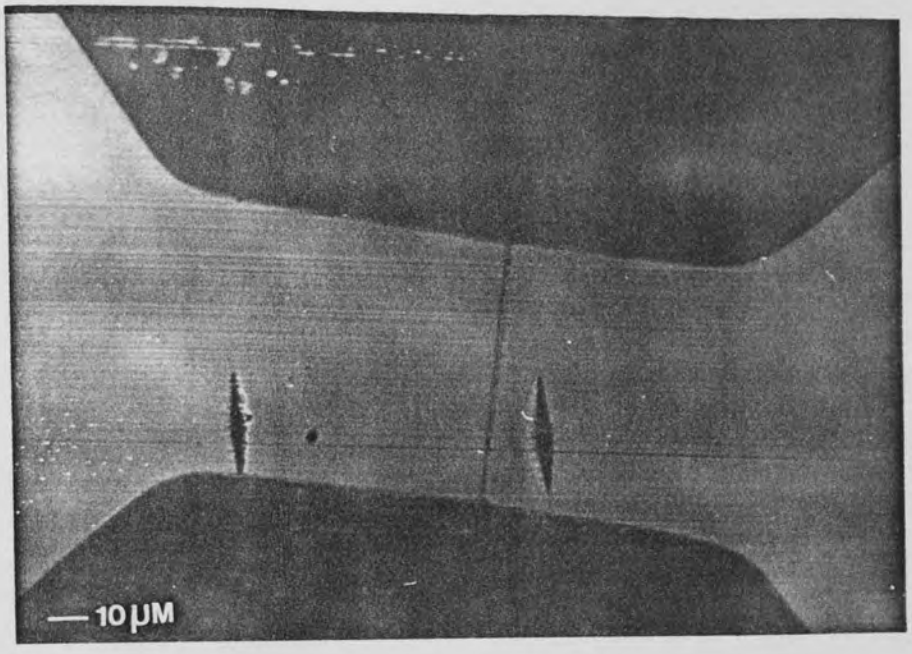
— 10 μM

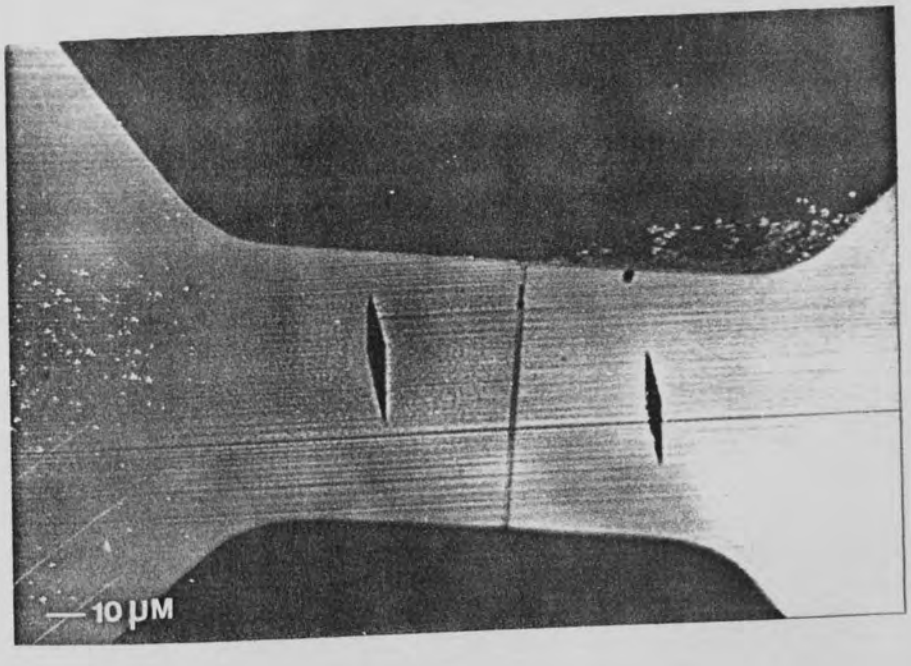
— 10 μM

Figure 3.23c: Photomicrograph of video head after 6 hours wear with the iron oxide formulation containing 10% Cr_2O_3 as the HCA. (Experiment GC2)

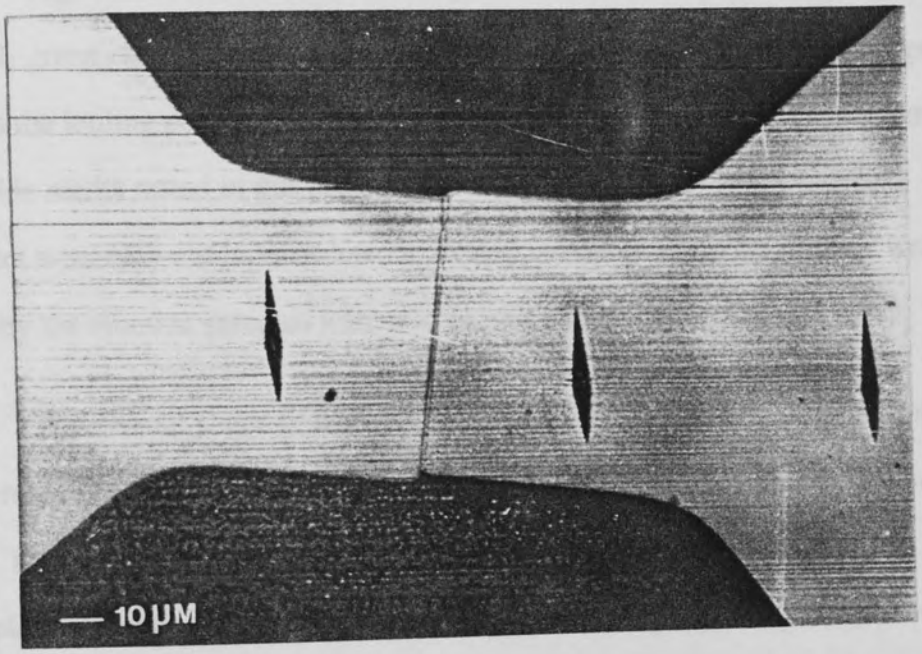
— 10 µM

ferrite. The relationship between the RF degradation and the concentration of green chrome is plotted in Figure 3.24. An improvement in performance of the head occured from 8% to 10% HCA loading, as was found in experiment GC1. The degradation then fell with increasing green chrome content. Figure 3.25 shows the roughness plotted against percentage of green chrome. The overall roughness was high for this batch of samples but varied little between samples apart from the 14% sample which was abnormally high and produced correspondingly high wear rates.

Figure 3.26 shows the wear rate profiles for the samples containing 8%,12% and 16% green chrome after 6 and 12 hours wear. The wear to each head was greater towards the trailing pole piece, a feature which was found repeatedly on examination of iron oxide media tested in this project. The wear rates were also very low, and sufficient wear may not have occured to extend to both pole pieces. The low wear rates shown by the alumina samples were also heavily biased to one side of the gap.

The general shape of the wear profile was similar to previous experiments and the decrease in wear rate with time found in experiment GC1 was also evident in these results. Figure 3.27 shows the wear rate at the gap and the maximum wear rate after 6 hours plotted against the concentration of green chrome. The wear rate increased with increasing HCA content. The increase in wear rate at the gap is small compared with the overall increase in wear. No increase in wear occured between 14% and 16% green chrome.

At this stage it became obvious that continuity had not been maintained between the two batches produced at the pilot plant for experiments GC1 and GC2. There was a period of at least a year between their production. In order to establish whether the difference in performance of the two batches was a product of experimental procedure or pilot plant production, several experiments from GC1 were repeated after the completion of experiment GC2. The results fell within the accuracy of the methods and did not explain the difference in sample batches. Thus physical data was compiled,

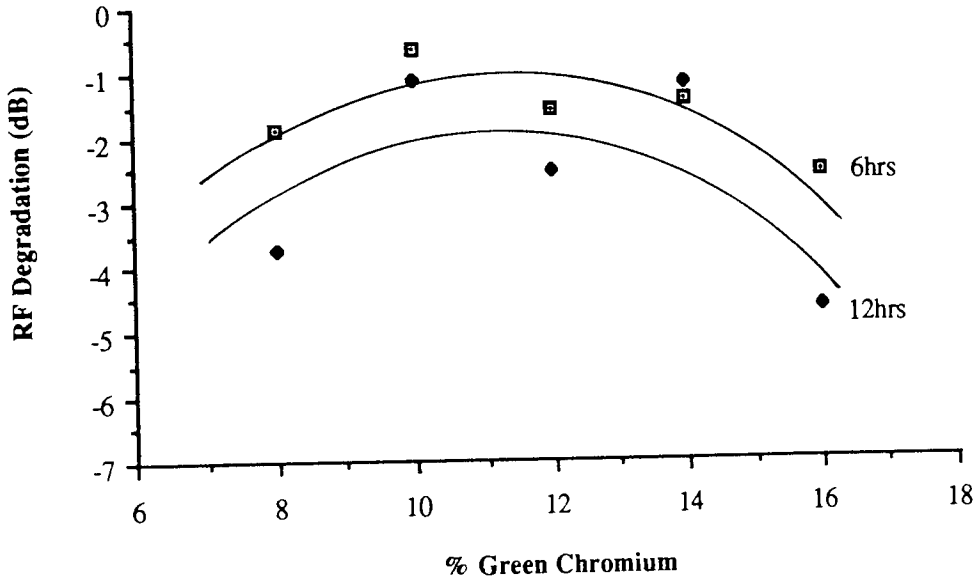

Figure 3.24: RF degradation against concentration of Cr_2O_3 after 6 and 12 hours wear (Experiment GC2).

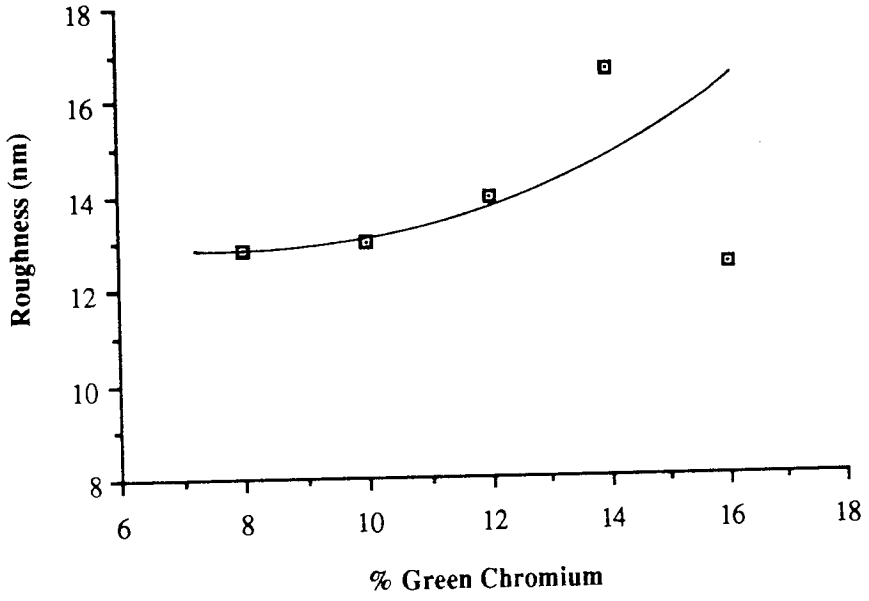

Figure 3.25: Roughness (R_Q) plotted against percentage Cr_2O_3 for Experiment GC2

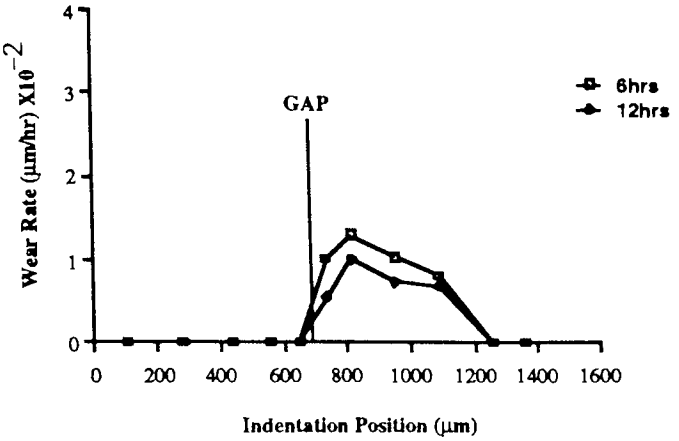

a) 8% green chrome

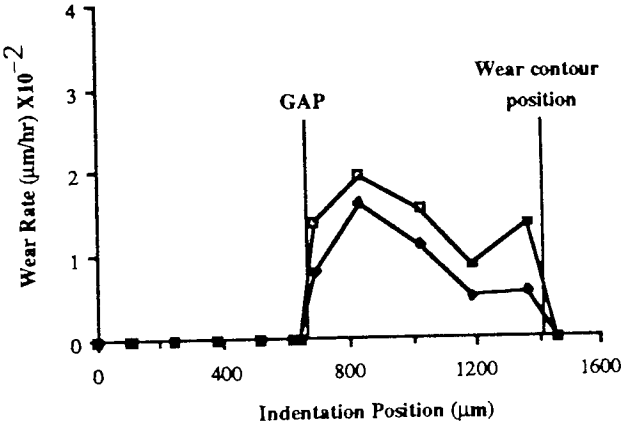

b) 12% green chrome

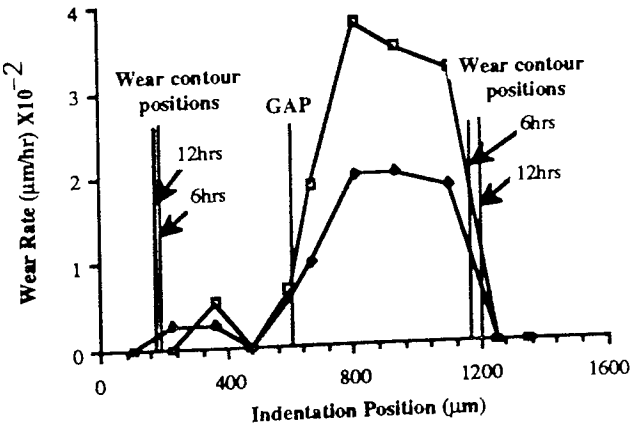

c) 16% green chrome

Figure 3.26: Wear rate against indentation position after 6 and 12 hours of wear with iron oxide samples containing a) 8%, b) 12% and c) 16% Cr_2O_3. (Experiment GC2)

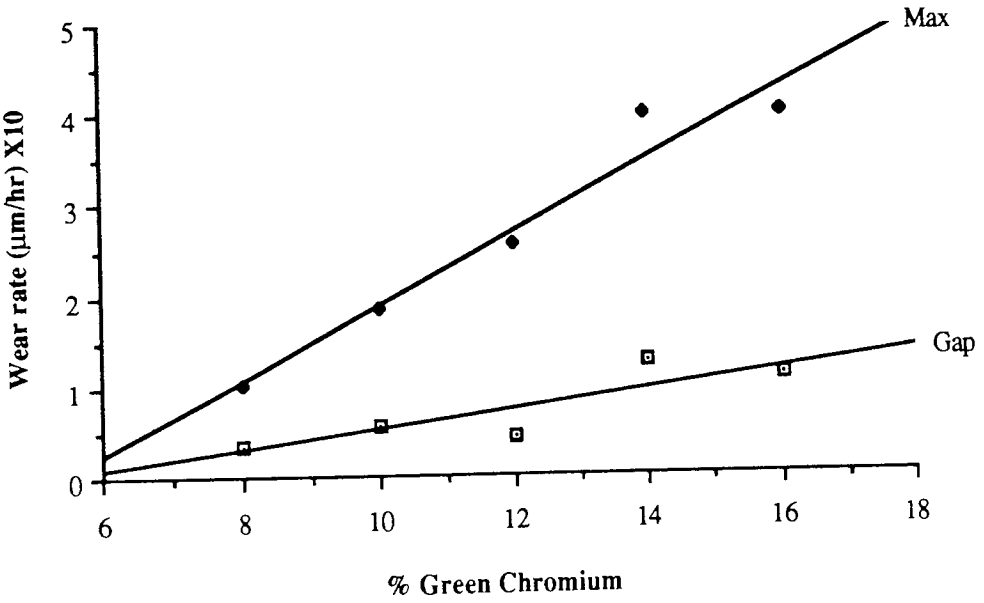

Figure 3.27: Wear rate at the gap and maximum wear rate plotted against percentage concentration of Cr_2O_3 for the samples of Experiment GC2

for all samples including thickness and flexibility in both machine and cross direction. These results will be discussed in section 3.8.

3.3.3 Experiment AL1: Variation in alumina from 2% to 10%

In experiment AL1 the effect of varying the concentration of the HCA alumina (Al_2O_3) was examined. The concentration was varied from 2% to 10% in stages of 2%. The procedures for testing the samples were identical to experiment GC1. Two sets of results were achieved for the head after 6 hours and after 12 hours of wear. Table 3.8 shows a summary of the results. The table includes, for both 6 and 12 hours of wear; the total RF degradation; the wear rate at the gap; and the maximum wear rate. The roughness of each sample is also tabulated. No wear was recorded for concentrations of alumina under 8%. In experiment IN1 a 4% alumina sample was tested and produced a small but measurable amount of wear in 6 hours. In this experiment the 4% sample produced no wear. Examination of the roughness of the relevant surfaces provides a possible explanation. In experiment IN1 the roughness of the 4% alumina sample was 12.749 nm, whereas the roughness of the commercial iron oxide sample in experiment IN1, for which no wear was recorded, was 11.700 nm. From Table 3.8 the roughness of the 4% alumina sample in experiment AL1 is only 8.089 nm. The fact that no wear was recorded for the sample is consistent with the roughness of the surface, that is, the lower roughness producing the lower wear.

The RF degradation (as shown in Table 3.8) for the alumina samples was very low despite the low wear conditions encouraged by the low roughness of the sample surface. Figure 3.28 shows the RF degradation after 6 and after 12 hours plotted against the percentage of alumina. The plot appears to show little variation in degradation, the lowest degradation occurring with the 4% alumina sample. However, the variation is very slight, the maximum and minimum degradation figures varying by only 0.65 dB. Since the accuracy of the measurement is 0.5 dB, there was little

			Wear rates (µm/hour)X10^{-2}				
	RF degradation (dB)		After 6 hours		After 12 hours		
Percentage HCA	6 hours	12 hours	At the gap	Maximum	At the gap	Maximum	Roughness (nm)
2	-0.75	-1.00	0	0	0	0	11.061
4	-0.10	-0.70	0	0	0	0	8.089
6	-0.30	-0.40	0	0	0	0	9.351
8	-0.40	-0.60	0.31	1.97	0.32	1.20	12.908
10	-0.50	-0.50	1.24	2.79	1.96	5.12	12.542

Table 3.8: Experiment AL1: variation in Al_2O_3 from 2% to 10%: Summary of results for 6 and 12 hours wear.

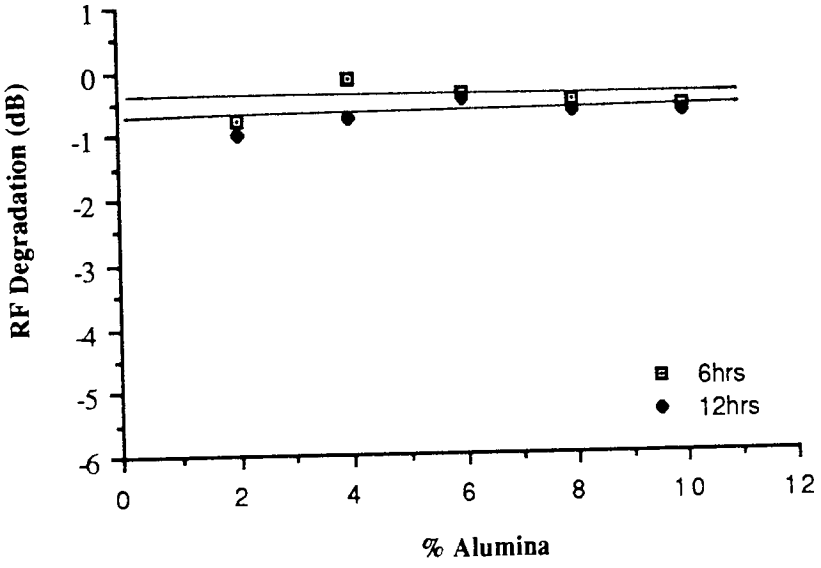

Figure 3.28: RF degradation against concentration of Al_2O_3 after 6 and 12 hours of wear

variation in performance between the alumina samples. The alumina samples presented lower RF degradation in all cases than the green chrome samples of experiment GC1. Examining the surface of the head under the optical microscope, the damage to the gap was found to be minimal for heads worn by the alumina samples. Figure 3.29 shows photomicrographs of heads worn by the samples containing 4% alumina and 8% alumina. Both surfaces show deformation of the ferrite, the 8% sample showing the greater damage. The surface worn by the 4% sample has remained in a good condition, and a correspondingly low signal degradation was observed. The physical state of the head worn by samples containing alumina was closer to the original appearance of the head than those worn by samples containing green chrome, the main difference being the condition of the gap.

Figure 3.30a shows the wear at the gap and maximum wear after 12 hours plotted against the concentration of alumina in the coating. Measurable wear was recorded for the 8% and 10% samples only, and the wear results for these two samples showed an increase in wear with increasing HCA content. For those heads which showed measurable wear, the shape of the wear profile was similar to that found with iron oxide media in Experiments IN1, IN2, GC1 and GC2. Figure 3.30b shows the roughness plotted against the HCA concentration. Below 8% the roughness is low compared with the commercial product which has a roughness of 11.7 nm, this may contribute to the fact that no wear was recorded below 8% Al_2O_3. Figure 3.31 shows the plots of wear rate for both 6 and 12 hours overlaid, against indentation position for the 8% and 10% alumina samples. The plot for the 8% sample shows wear only on the trailing pole piece. The wear is very small and as the maximum wear rate has been shown to occur on this pole piece it follows that wear would be recorded in this area first. The plot for the 10% alumina sample shows wear on both pole pieces, but it is heavily biased towards the trailing pole piece. This implies that sufficient wear has occured such that the wear has spread to include both pole pieces. The change in wear rate from 6 to 12 hours shows that with alumina the wear rate increased with time. With

Figure 3.29: Photomicrographs of video heads after 6 hours wear with the iron oxide formulation containing:

a) 4% Al_2O_3 as the HCA

b) 8% Al_2O_3 as the HCA

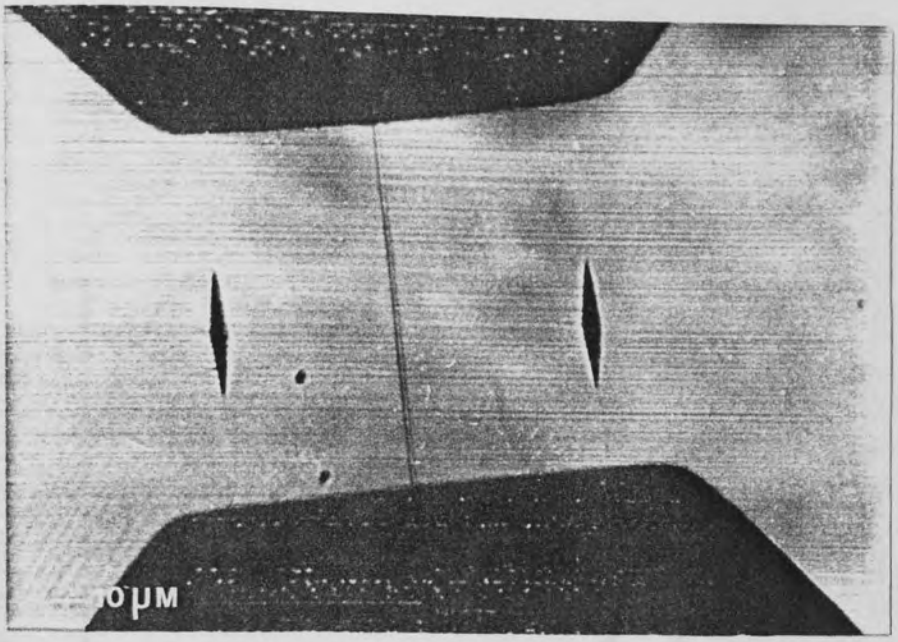
10 µM

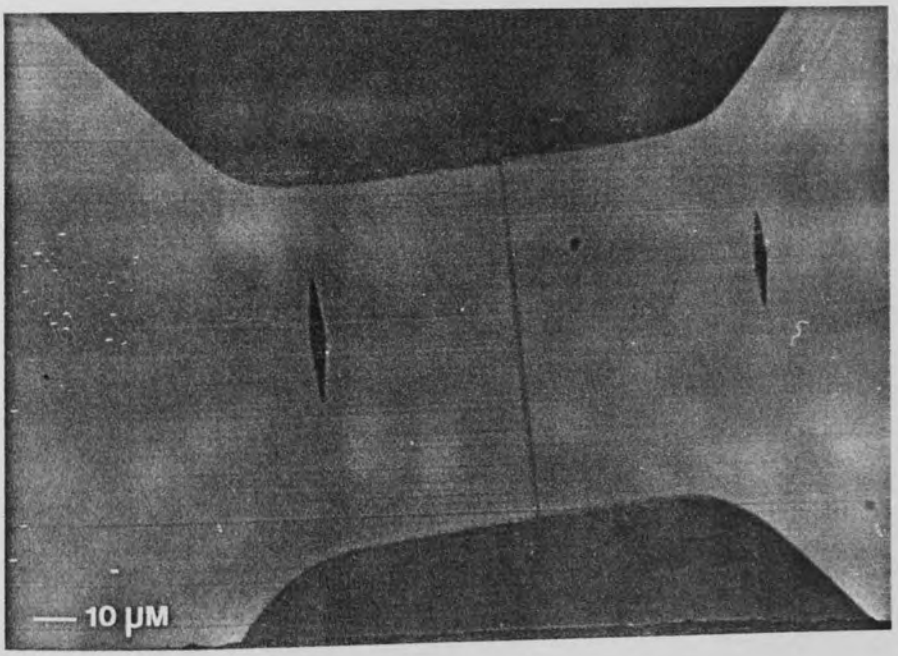
10 µM

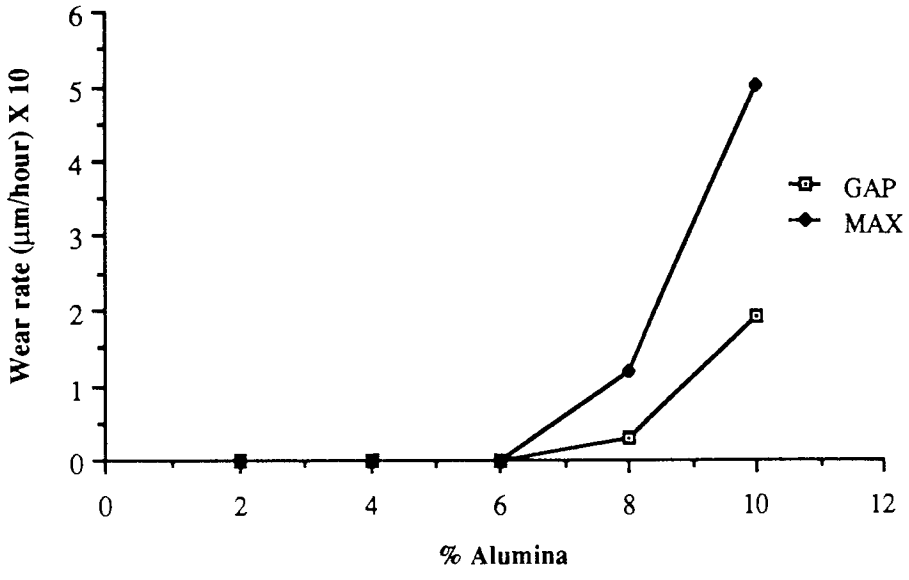

Figure 3.30a: Wear rate at the gap and maximum wear rate plotted against percentage concentration of Al_2O_3 after 12 hours wear.

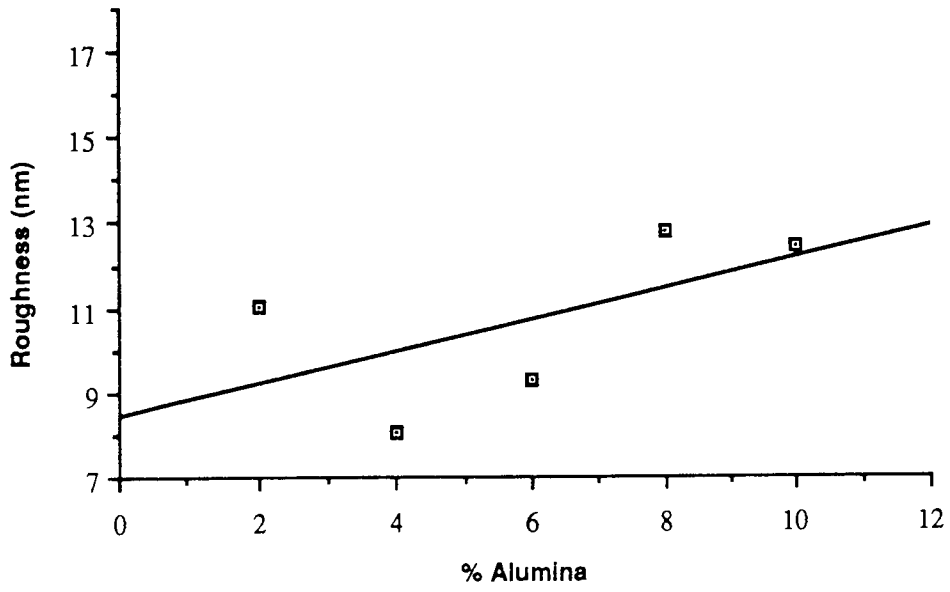

Figure 3.30b: Roughness (RQ) plotted against percentage concentration of Al_2O_3

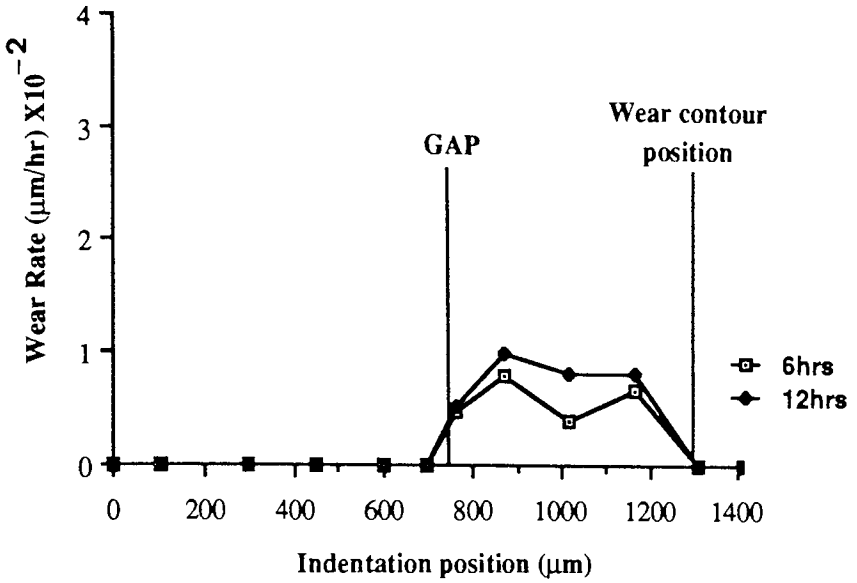

a) 8% alumina

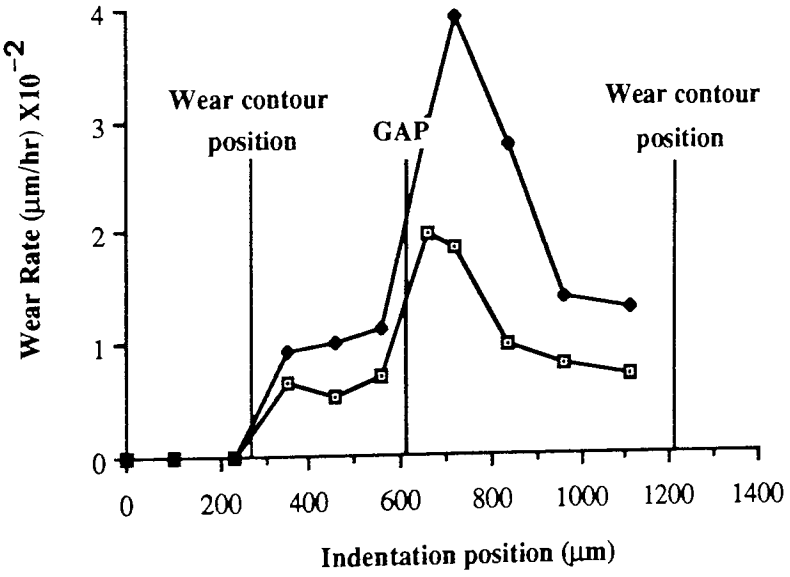

b) 10% alumina

Figure 3.31: Wear rate against indentation position after 6 and 12 hours wear with a) iron oxide formulation containing 8% Al_2O_3 and b) iron oxide formulation containing 10% Al_2O_3

the green chrome samples in Experiment GC1 the wear rate was seen to decrease with time.

From the results of Experiments GC1 and AL1 it appears that the change of HCA from green chrome to alumina evokes a change in wear mechanism. Also although low wear rate can be said to be responsible for bad signal degradation in certain circumstances, the wear mechanism occurring to the head is more relevant and may not necessarily encourage bad performance of the head. Finally, the wear rate is related to the sample roughness, although the wear mechanism occurring to the head also affects the rate and roughness is not directly related to wear rate. For example, a sample containing green chrome would not be expected to produce the same amount of wear as a sample containing alumina of the same roughness. Instead the pevailing wear mechanisms determine wear rate.

3.3.4 Surface concentration of HCA

The values of HCA concentration quoted represent the volume of HCA added to the magnetic slurry before coating. The percentage weight of the HCA was also measured using X-ray electron spectroscopy, as described in section 2.4.5. The measured values were all lower than the expected concentration. One disadvantage of surface analysis is that only a small area of the surface is analysed, which may not necessarily be representative of the whole surface. The percentage weight by XES is a representation of the HCA present in the top few layers of the surface. The technique penetrates several monolayers but not the complete thickness of the magnetic coating. The analytical figure is therefore the percentage HCA directly in contact with the head and the difference in expected and measured percentage needs to be examined. The expected concentration for each of the Experiments GC1,GC2 and AL1 is tabulated alongside the percentage weight by analysis in Table 3.9.

Experiment GC1 Green chrome 0%-10%		Experiment AL1 Alumina 0%-10%		Experiment GC2 Green chrome 0%-10%	
Expected % concentration	Weight % by XES	Expected % concentration	Weight % by XES	Expected % concentration	Weight % by XES
0	0	2	2.04	8	4.30
2	0.88	4	3.11	10	6.48
4	2.03	6	5.41	12	8.81
6	3.99	8	6.76	14	9.92
8	5.13	10	7.22	16	8.72
10	6.44				

Table 3.9: Expected and measured concentrations of HCA for experiments GC1, GC2 and AL1. .

Figure 3.32 shows the degradation after 6 hours for experiment GC1, plotted against the measured concentrations of green chrome. Comparing Figure 3.32 with Figure 3.16 for expected green chrome concentration, although the measured concentration curve is lower, the general shape of the graph is unchanged. Although the difference in concentration is apparent the conclusions drawn from the results remain unchanged. The measured concentrations also provide an indication of the quality of the dispersion within the magnetic coating. In the case of the 16% green chrome sample the measured value of concentration fell lower than that of the 14% sample indicating dispersive problems with the higher concentrations. A detailed examination of the measured values showed that the separation between expected and measured concentration was lower for each of the samples containing alumina than for those containing green chrome. The average percentage difference between the two readings for the samples of Experiment GC1 is 42.0%, for Experiment GC2 is 36.4% and for Experiment AL1 is 18.8%. This suggests that the alumina particle is easier to disperse throughout the coating. The dispersion of the HCA particle within the magnetic coating was examined using TEM, the results of which are presented in section 3.6.

3.4 Secondary ion mass spectrometry (SIMS)

In this section the results of the SIMS analysis performed at the SIMSLAB at UMIST are presented. The results presented include an analysis of the following;

a) An unused video head.

b) A head worn for thirty hours with a commercial iron oxide tape containing 4% green chrome HCA.

c) A head worn as in b) and then cleaned using Fluorosil to remove the visible debris.

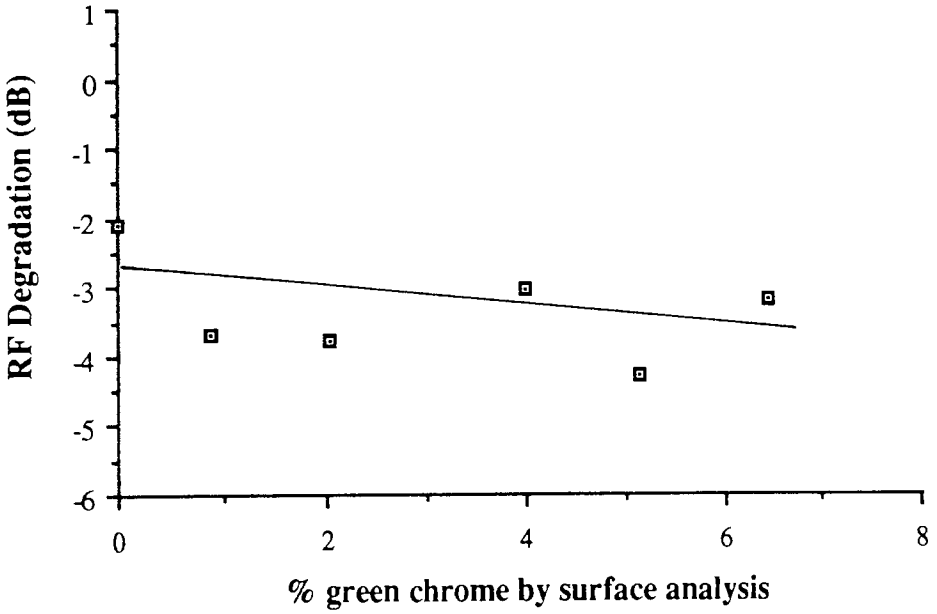

Figure 3.32: RF degradation after 6 hours for Experiment GC1 plotted against the concentration of Cr_2O_3 measured using XES

d) A head worn for 12 hours with an iron oxide based tape, produced at the pilot plant, and containing no HCA, then cleaned using Fluorosil.

Figure 3.33 shows the positive and negative spectra for the unused head. The main features of the positive spectrum are the high iron and manganese peaks. These elements are constituents of the head material. The head is a manganese-zinc ferrite containing approximately 70% Fe_2O_3, 23% MnO and 7% ZnO. The large galium peaks observed in all spectra are an artefact of the primary beam (m/z 69 and 71). Sodium and potassium can also be seen, these are elements which are common on SIMS spectra due to contamination from handling and because SIMS is very sensitive to these elements. The negative spectrum shows a high oxide content from the ferrite composition and high chlorine, which is also a contaminant from handling.

Figure 3.34 shows the spectra obtained from the head worn with the commercial iron oxide product. Here, the manganese is lower relative to the iron and we have the appearance of aluminium. In addition, there is a greater insidence of hydrocarbon peaks with this head. The lower manganese peak indicates that the ferrite surface may be covered by a deposit. The iron-manganese ratio did not remain the same since debris transferred from the tape, is likely to contain iron oxide and the iron peak may therefore increase with the deposit of debris. Hence, although iron is the main constituent of the head, the signal cannot be used as a reference. The aluminium is most likely to come from the drum itself, or even the tape guides. It is likely that the aluminium is worn by the tape, and lodges on the tape to be deposited on the head. The aluminium is not likely to be deposited as the metal but more likely to be transferred to the head surface with the binder or other debris in the form, for example, of an oxide. The increase in hydrocarbons suggests an organic layer on the surface. The negative spectrum shows the appearance of phosphate residues. A possible origin of these ions is the wetting agent which is used to break up agglomerates of magnetic particles and to encourage the best possible dispersion. The wetting agent used in the iron oxide

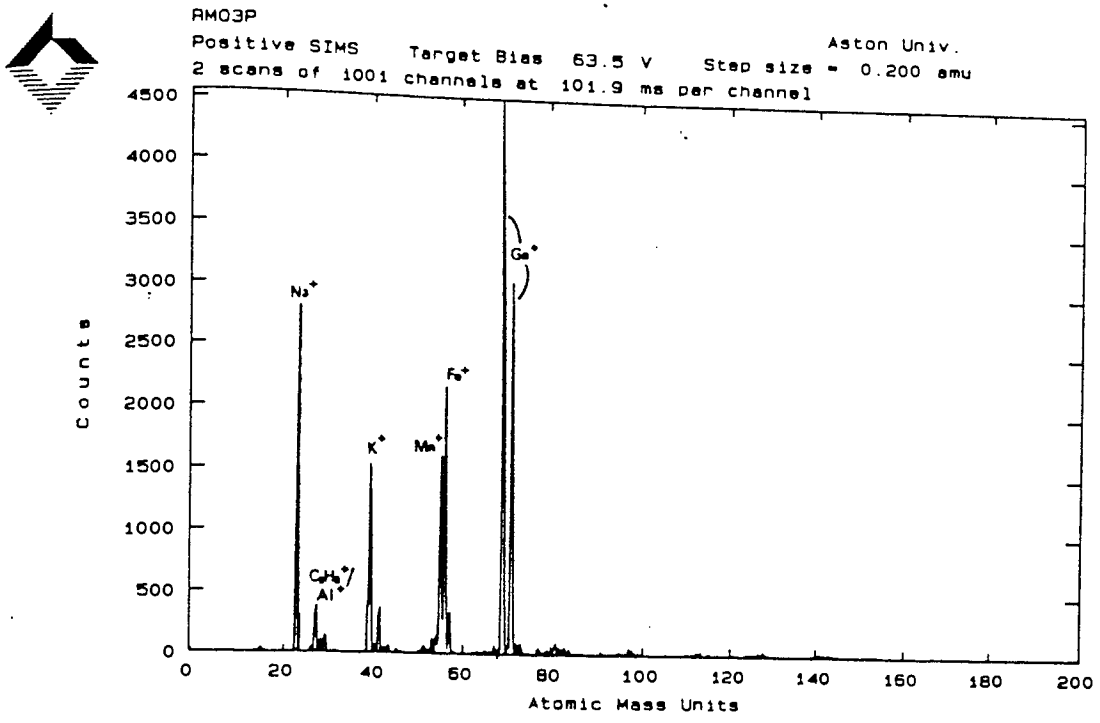

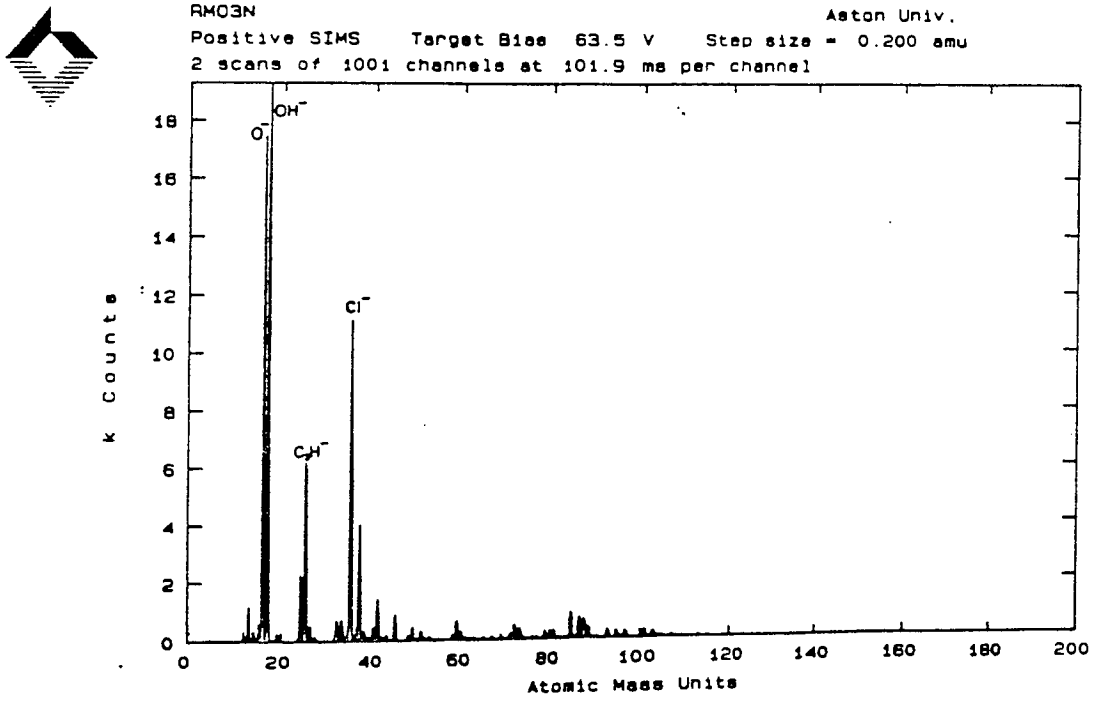

Figure 3.33: Positive and Negative SIMS spectra of an unworn video head

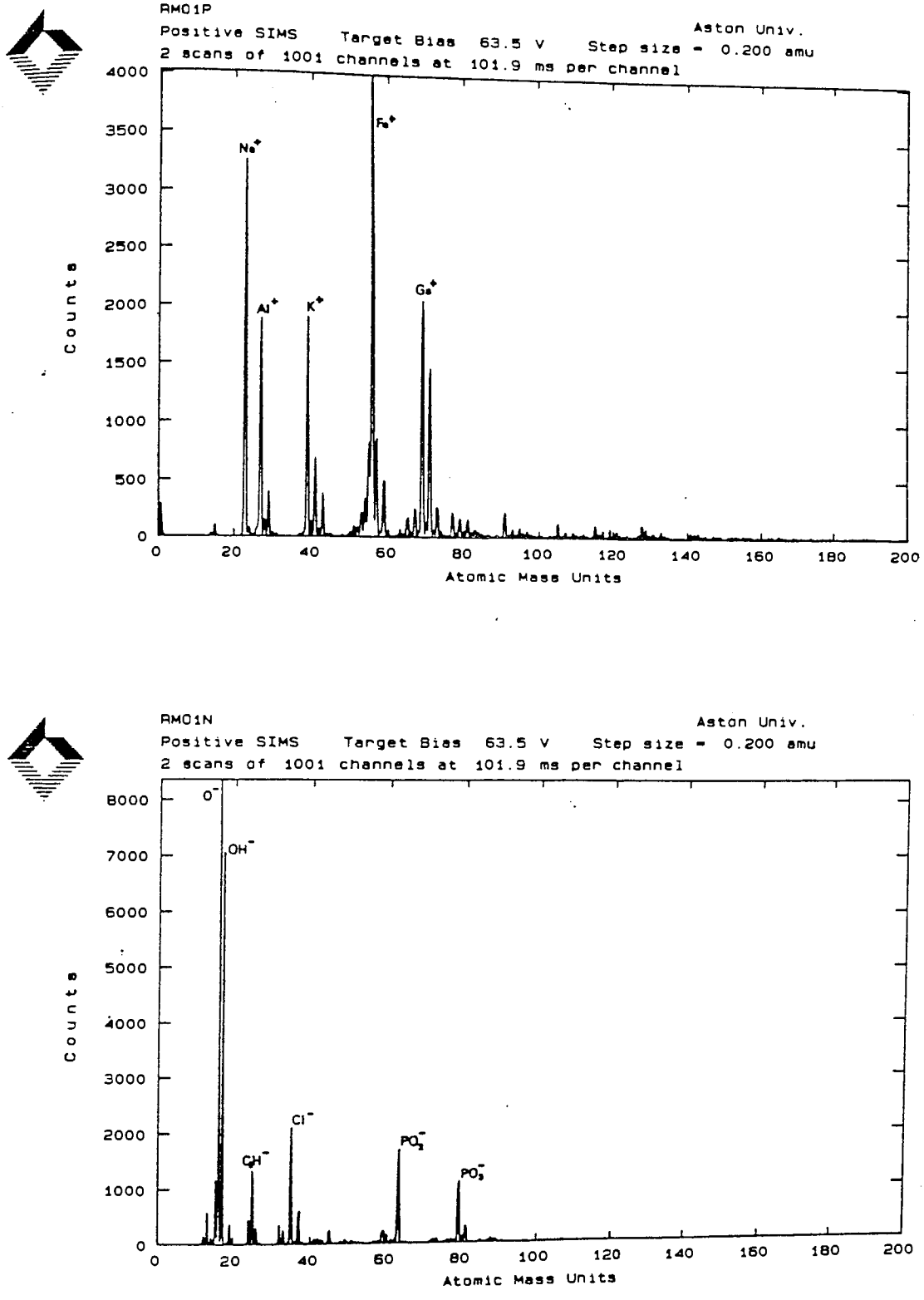

Figure 3.34: Positive and Negative SIMS spectra of a head worn using the standard commercial iron oxide formulation containing 4% Cr_2O_3 HCA

product is POCA II, the chemical formulation of which is shown in Figure 3.35. If this agent is exuding to the surface of the tape and is then being transferred onto the head, it would increase the level of organic material detected. Before the acquisition of the spectra, while the correct signal level was being selected from the area to be analysed, myristate ions were detected at 227 amu. By the time the system had been set up and the spectra acquired, the ions at this mass had been sputtered away, so that the spectra were acquired up to 200amu only. However, it would appear that a small amount of lubricant was present on the surface of the head.

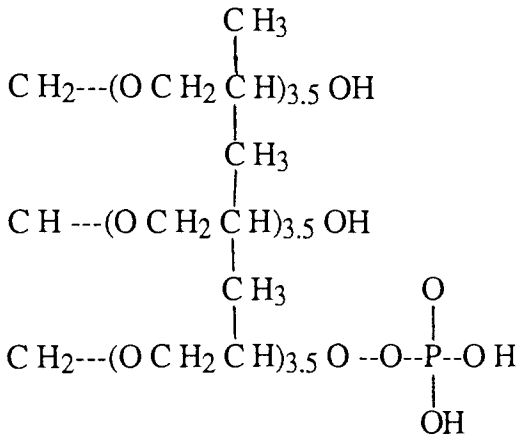

Figure 3.35: Chemical formula of the wetting agent used in the standard commercial iron oxide tape POCA II.

Figure 3.36 shows the spectra from the head worn with the commercially produced iron oxide tape (4% green chrome HCA) and then cleaned with the solvent Fluorosil to remove any visible tape debris. The aims of the analysis of this head were first, to detect material on the head which can only be removed by mechanical means, and second, to establish whether the solvent leaves any residue on the head. The positive spectrum showed a higher organic to Fe ratio than the unworn head and the manganese was also very low. The low manganese and iron signals suggest two features; first, the surface of the head is covered by an organic layer; and second,

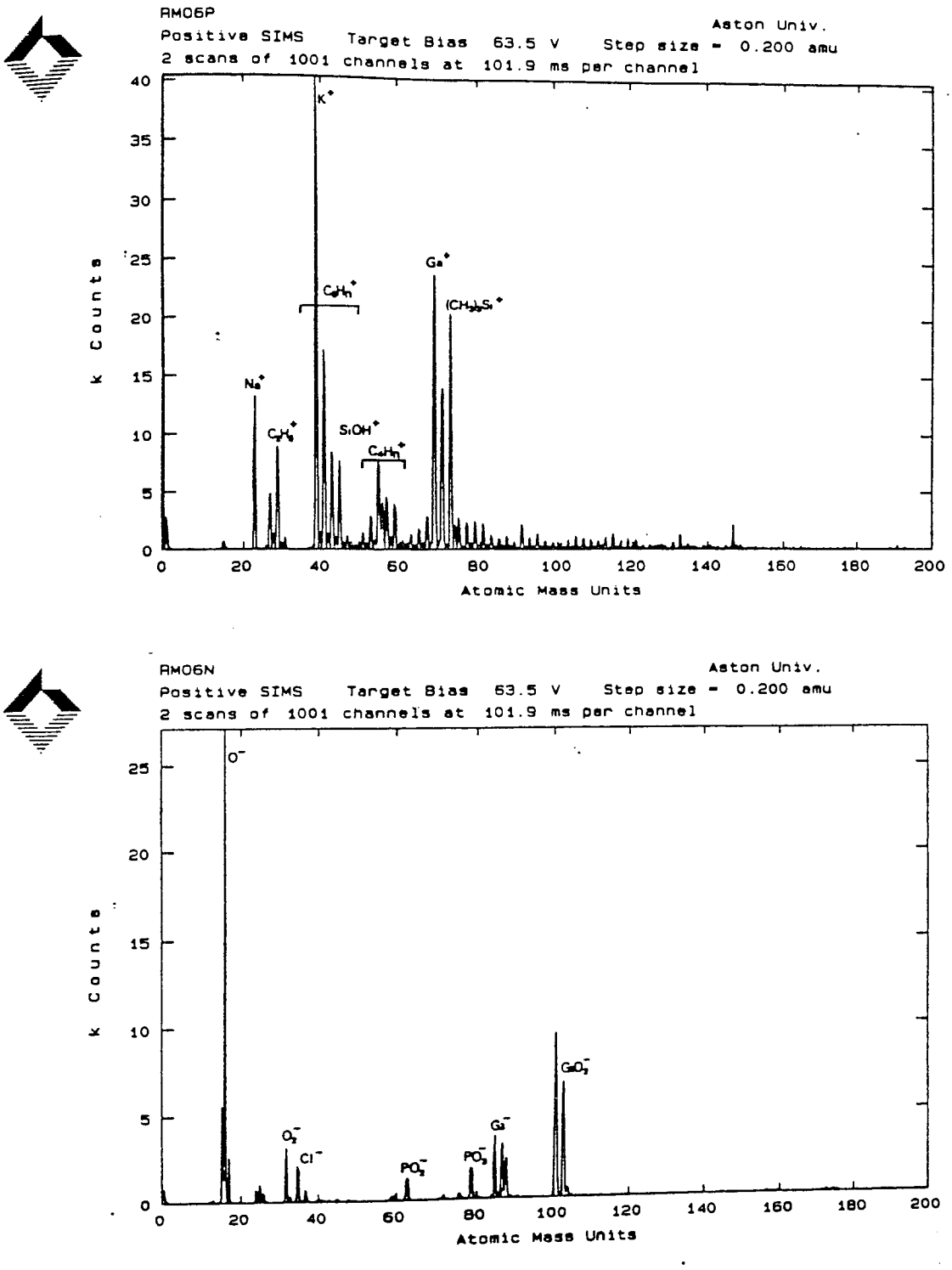

Figure 3.36: SIMS spectra of a head worn with the commercial iron oxide tape (4% Cr_2O_3 HCA) and then cleaned with the solvent Fluorosil to remove any visible tape debris.

cleaning has removed rolls of tape debris which can be seen on the surface of the head. It is likely that the debris which had been removed contained particles of iron oxide pigment, which would increase the iron peak. The debris is completely removed on cleaning, such that the iron signal detected, in this case, comes from the ferrite surface only. The ratio of the iron peak to organic peaks was low suggesting the presence of organics on the surface. No fluorocarbon residues or F^- ions were detected, indicating that the solvent completely evaporates and does not leave any residue.

The negative spectrum from the head worn with the commercial iron oxide tape and then cleaned shows the existence of phosphate residues and a highly oxidised surface. Also detected were various silcone ions as shown in Figure 3.36b. It would appear that a silicone oil is used to grease the guide rollers of the video cassette, and is likely to be the origin of these deposits.

Figure 3.37 shows the spectra from the head worn with the pilot plant sample containing no HCA and then cleaned with fluorosil to remove the loose debris. The negative spectrum is very similar to that of the head worn with commercial iron oxide formulation and then cleaned. The iron and manganese signals are high, suggesting that there is little or no organic deposit on a head worn under these conditions. Aluminium is present, as are residues of the wetting agent, suggesting that aluminium from the drum and the wetting agent have transferred to the head, but there has been no build up of polymeric material transferred from the binder.

3.5 X-ray photoelectron spectroscopy

The size of the head provided problems in the analysis of the surface. Standard XPS could not be used because the spot size of approximately 1mm diameter would extend beyond the sample and the spectra might be confused with signal from the holder. The results which are presented here were obtained using the small spot XPS facility at the

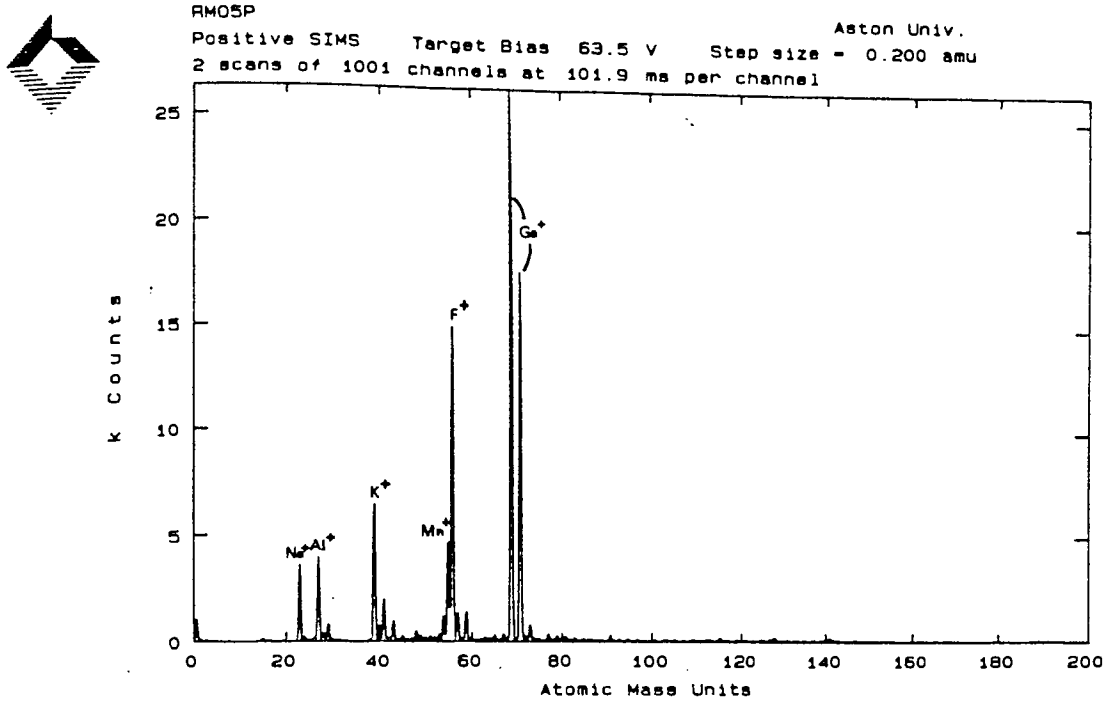

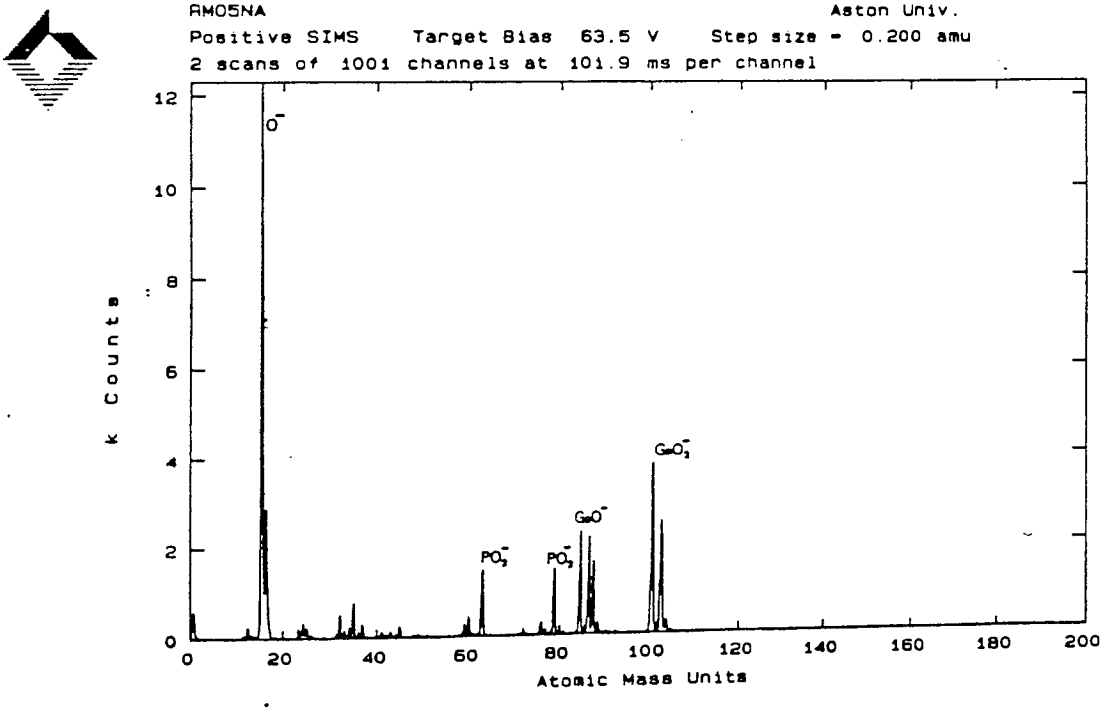

Figure 3.37: SIMS spectra of a head worn with iron oxide tape containing no HCA and then cleaned with the solvent Fluorosil to remove any visible tape debris

University of Surrey. With small spot XPS the sensitivity is low, and so the pass energy for the analyser was set to 100eV in order to obtain a sufficient signal. However, using the analyser at this level gave poor resolution of the peaks.

The purpose of the analysis was to observe any changes in the surface content after wear and to find evidence of material transfer from the tape to the head, by comparing new and used heads.

Figure 3.38 shows the wide scans for a) the unworn and b) the worn head. The carbon, oxygen and iron peaks can be clearly seen above the background of the spectrum for the unworn head. For the worn head, the iron peak is diminished and is difficult to determine from the background. The reduction in the iron peak suggests that the surface may be covered by a deposit after wear. The examination of single peaks provides more detailed information on the change in the surface with wear. Figure 3.39a and b show the carbon and oxygen spectra acquired from the surface of the unworn head. The full width at half maximum of the carbon peak is 2.9 eV, which is too large for a single peak and would suggest that the peak is a composite peak. In this case the shift in binding energy due to the chemical state of the carbon atom is not sufficient for the instrument to resolve the peaks. Hence, a single composite peak is recorded. Figure 3.40 gives the deconvoluted carbon spectra which show that the peak is composed of three separate but overlapping components. Peak 1 at 285.6 originates from C-C and/or C-H groups. This peak should be situated at 284.6 eV, the difference being caused by the charging of the surface. Peak 2 is situated at a slightly higher binding energy, 287.0 eV. This shift is due to the oxidation of the carbon which causes the carbon atom to be more electropositive and hence more tightly bound. Therefore, peak 2 shows the abundance of C-O groups. The third group shows the abundance of C=O and O-C-O groups, since both give a similar binding energy (Briggs and Seah). Carbon is present in all three forms on the surface of the unworn head. However, it should be noted that the technique is very sensitive to absorbed water and

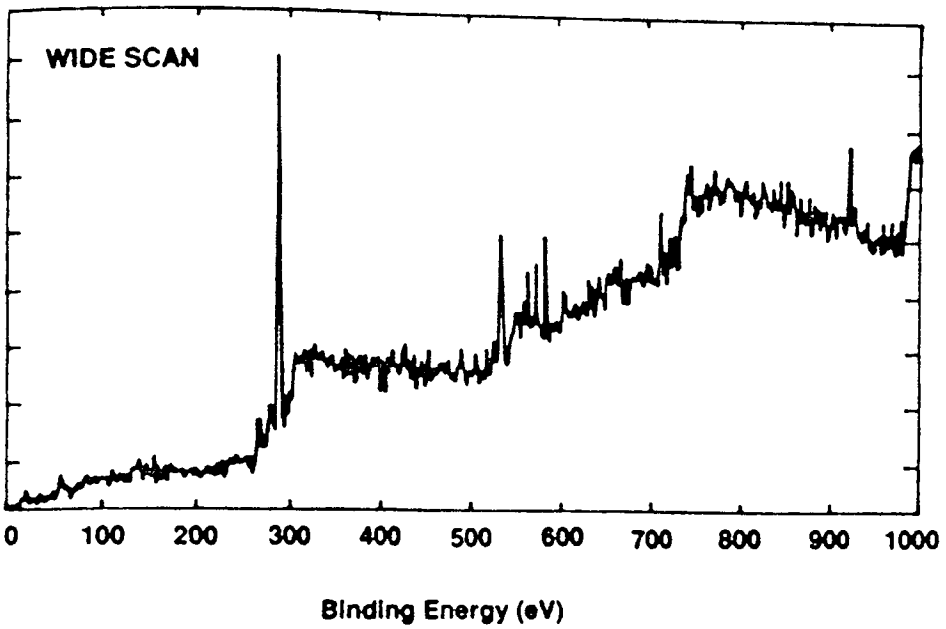

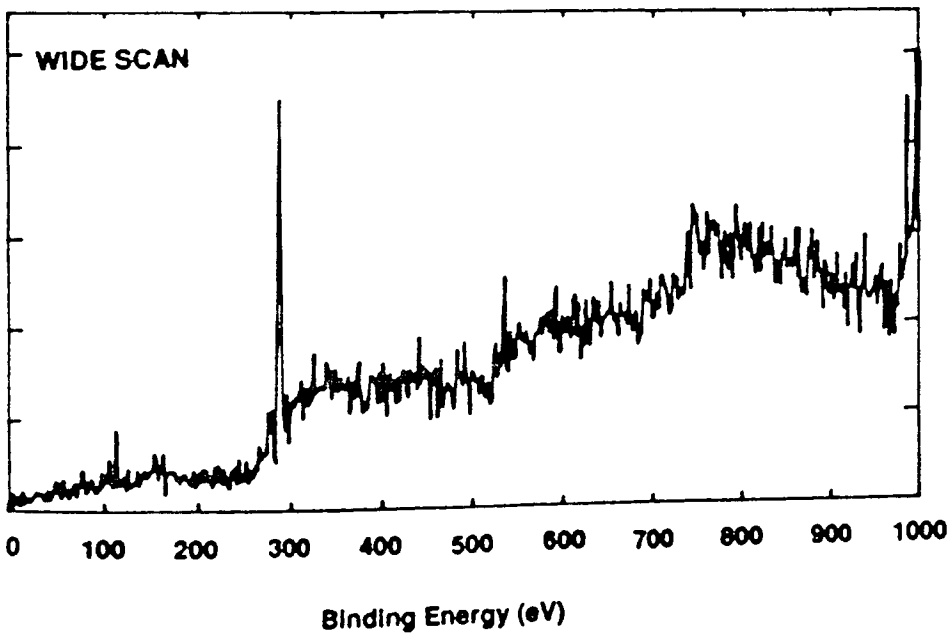

Figure 3.38: XPS wide scan spectra of video heads a) Unworn and b) worn with the commercial iron oxide formulation

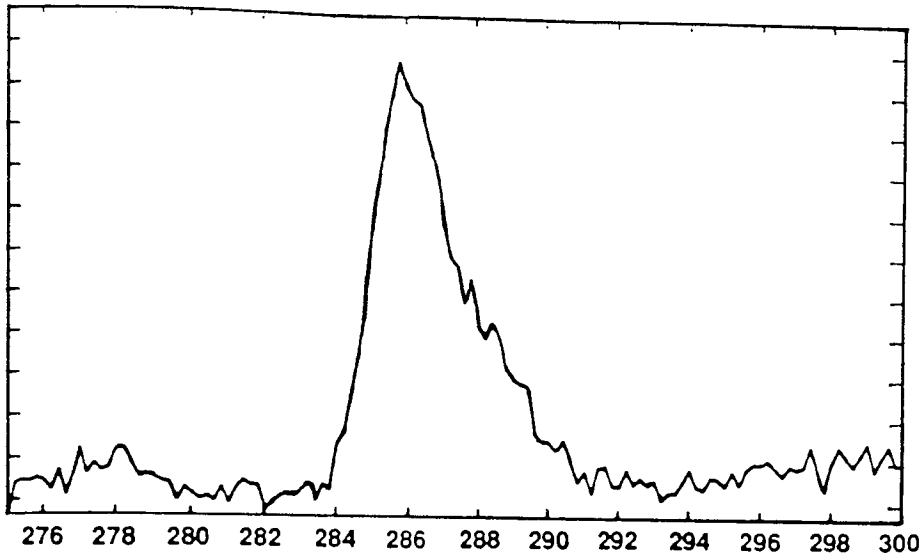

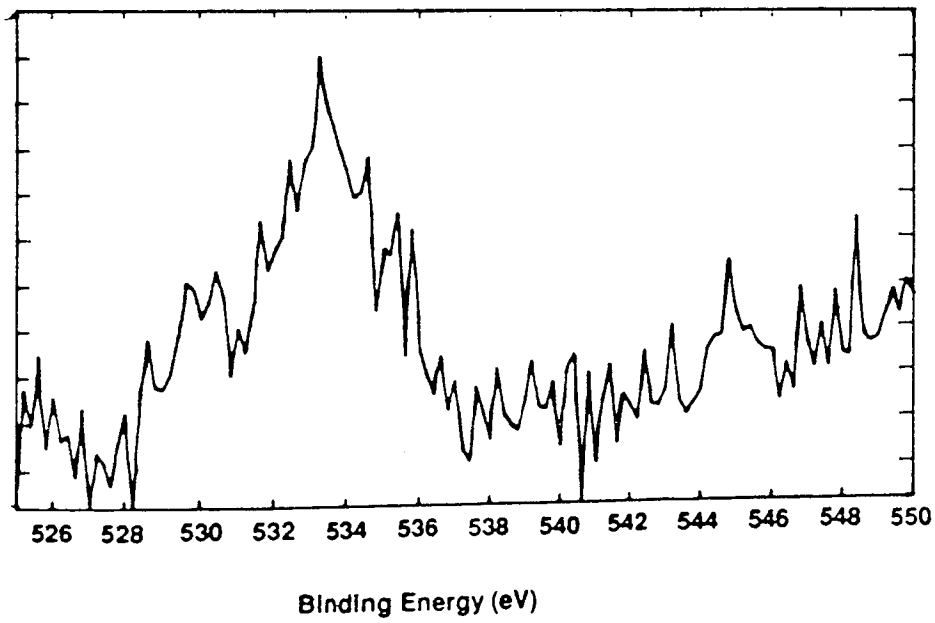

Figure 3.39: XPS spectra showing the abundance of a) carbon and b) oxygen on the surface of an unworn video head.

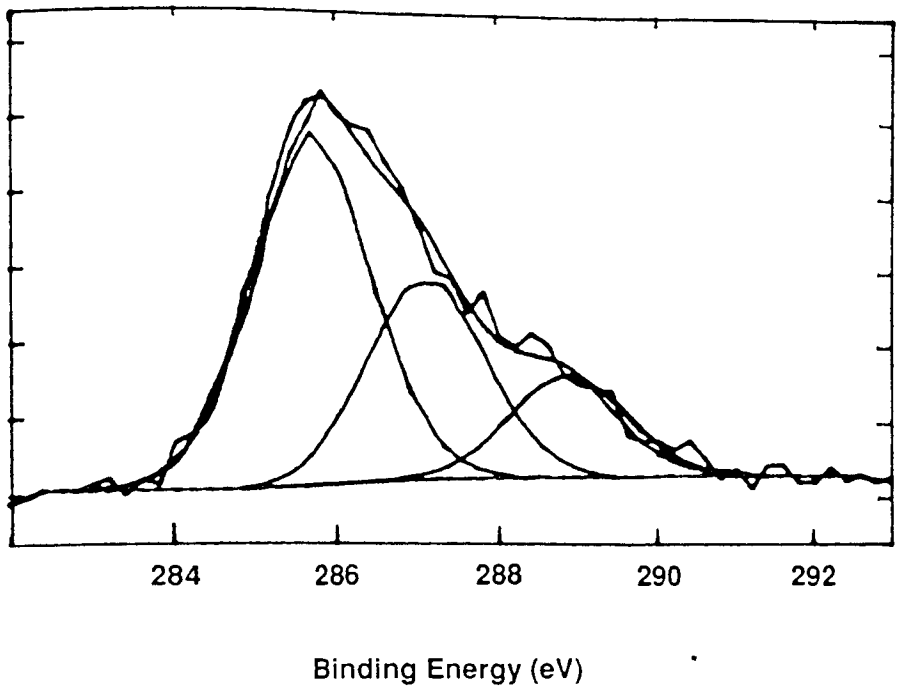

Figure 3.40: Deconvoluted carbon spectra showing the abundance of organic species on the surface of an unworn head

Peak	Centre (eV)	FWHM (eV)	%Area	Ratio to C-C Peak
C-C/C-H	285.6	1.70	54	1
C-O	287.0	1.70	31	0.57
C=O	288.7	1.70	16	0.30

Table 3.10: Composite carbon peak data for unworn head

hydrocarbons. Therefore the C-H signal is likely to be high, and part of the C-O may be present due to contamination. Table 3.10 shows the position of the peaks, the full width at half maximum (FWHM), the percentage areas, and the ratio of carbonyl to hydrocarbon groups. The counts for oxygen spectra are low and the resulting spectra are noisy. From the FWHM of the peak it would appear the oxygen peak is also a composite. Because of the noise level no deconvolution was performed. Sufficient information can be gained from the carbon spectra.

Figure 3.41a and b show the carbon and the oxygen spectra taken from the surface of the head worn for thirty hours with the commercial iron oxide sample containing 4% green chrome as the HCA. Both spectra show that the levels of the various organic groups have changed substantially with wear. Figures 3.42 show the deconvoluted carbon spectra, and Table 3.11 shows the positions, FWHM, % areas and the carbonyl ratios for the peaks. The occurrence of C-C and C-H groups has decreased compared with the carbonyl groups. The ratio C-C : C-O has doubled, whereas the ratio C-C : C=O is nearly three times that observed before wear. The group containing the double bond is more significant since it is less likely to originate from contamination. The oxygen spectrum also shows a high carbonyl peak around 535 eV, compared with a relatively low oxide peak around 531.5 eV. The results indicate that there is an increase in the occurrence of organic species on the surface of the worn head.

3.6 TEM analysis

In this analysis sections of video tape were examined in cross-section, under high magnification, in order to examine the relative sizes, shapes, and most importantly, the distribution of the various particles within the magnetic coating. The aim of the analysis was to isolate any features within the coating which may affect the performance and wear characteristics of the tape.

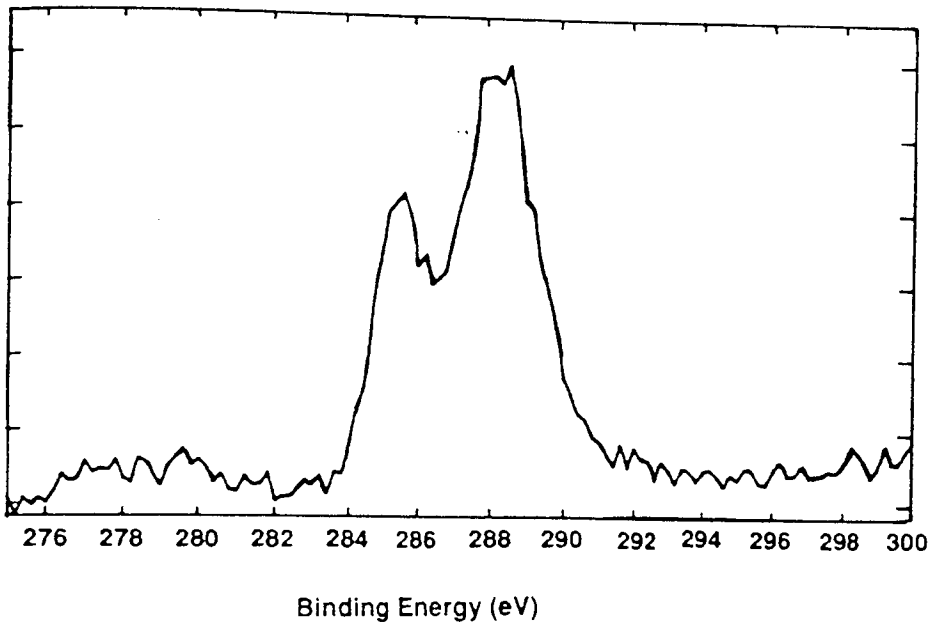

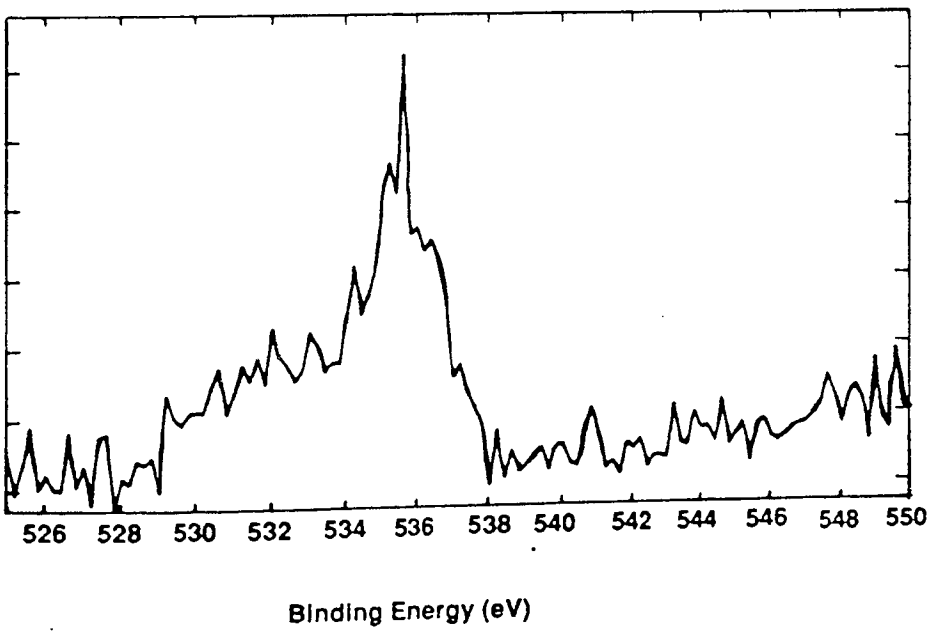

Figure 3.41: XPS spectra showing the abundance of a) carbon and b) oxygen on the surface of a video head worn with the commercial iron oxide sample containing 4% Cr_2O_3 HCA.

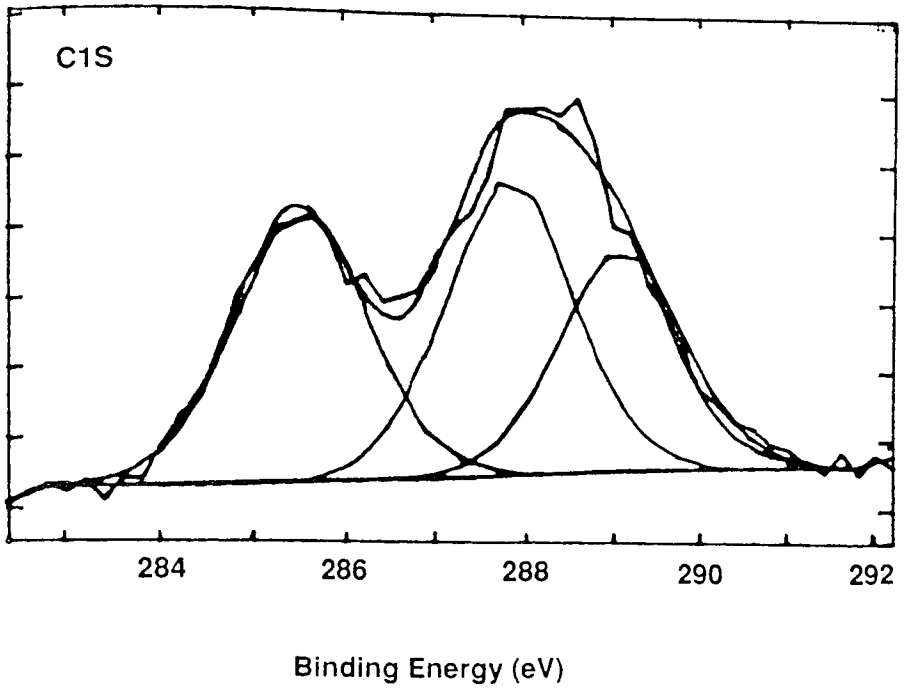

Figures 3.42: Deconvoluted carbon spectra showing the abundance of organic species on the surface of a head with the commercial iron oxide sample containing 4% Cr_2O_3 HCA.

Peak	Centre (eV)	FWHM (eV)	%Area	Ratio to C-C Peak
C-C/C-H	285.6	1.70	54	1
C-O	287.0	1.70	31	0.57
C=O	288.7	1.70	16	0.30

Table 3.11: Composite carbon peak data for worn head

Figure 3.43 shows a cross-section through the entire depth of the magnetic coating of the commercial iron oxide tape, containing 4% green chrome. The acicular magnetic iron oxide particles can be seen to be roughly aligned parallel to the tape surface. At this magnification it is not easy to identify particles other than the magnetic pigment. Figure 3.44 shows a single particle of Cr_2O_3 found in a section of the commercial iron oxide tape. The particle was confirmed as a chrome particle using the EDAX system attached to the SEM. From the photomicrograph the hexagonal shape of the particle can be seen clearly. Measurement of the particle showed it to be approximately 0.1μm in diameter. The particle size quoted by the suppliers of the green chrome pigment is 0.35μm, which represents the equivalent spherical diameter of 50% of the volume. A number of HCA particles were isolated and their diameters measured. The size variation was found to be wide ranging from 0.1μm to 0.4μm, and from those measured the average size was found to be lower than the size quoted. The size of the iron oxide pigment is quoted as 0.02μm X 0.2μm.

During examination of the various sections of tape it became apparent that it was more common for HCA particles to be found in groups than as single particles. The groups usually consisted of a number of different sized particles. Figures 3.45 and 3.46 show examples of typical groups or agglomerates of green chrome particles within the commercial product. Figure 3.47 shows a closer view of a group of three or possibly four green chrome particles. It should be noted that care was taken to find single particles as it was clear that groups of particles would be easier to observe and might lead to an overestimation of the frequency of their occurrence. However, the large number of groups of particles found is significant with or without the occurrence of single particles of green chrome and may affect the performance and wear characteristics of the tape. Figure 3.48 shows a single particle in the midst of the iron oxide pigment, indicating its distinctive shape within the bulk of the magnetic coating. One effect of the formation of agglomerates of HCA particles within the coating is immediately apparent. The iron oxide particles are magnetically aligned during

Figure 3.43: Cross-section through the magnetic coating of the commercial iron oxide tape containing 4% Cr_2O_3 HCA

Figure 3.44: Single particle of Cr_2O_3 found in a section of the commercial iron oxide tape

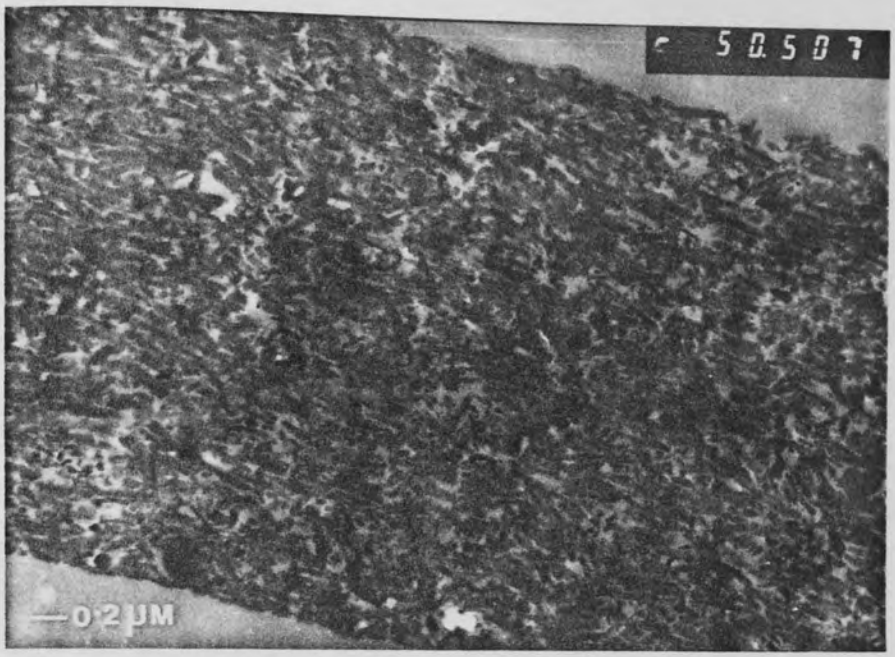
50507
0·2 μM


0·05 μM

Figures 3.45 and 3.46 examples of groups or agglomerates of Cr_2O_3 particles within the commercial iron oxide formulation

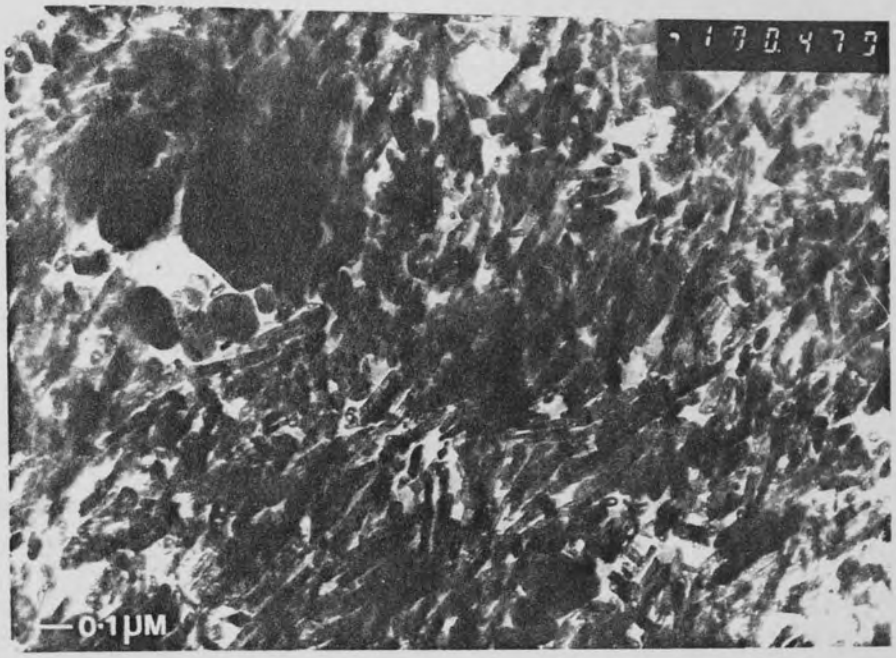
0·1 μM

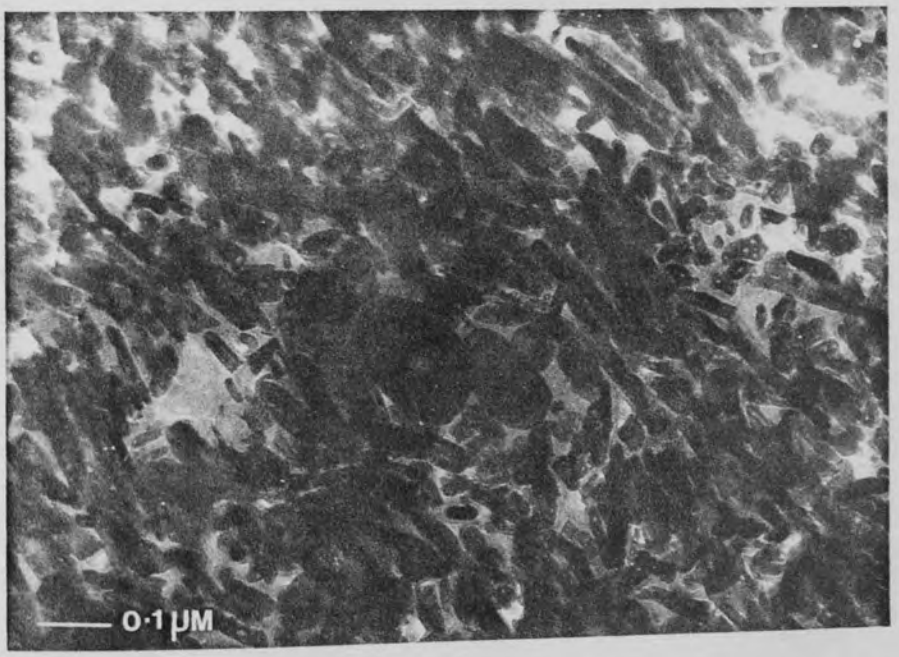
0·1 μM

Figure 3.47: Agglomerate of Cr_2O_3 particles causing iron oxide particles to deviate from alignement

Figure 3.48: Single particle of Cr_2O_3 showing its distinctive shape within the bulk of the magnetic coating

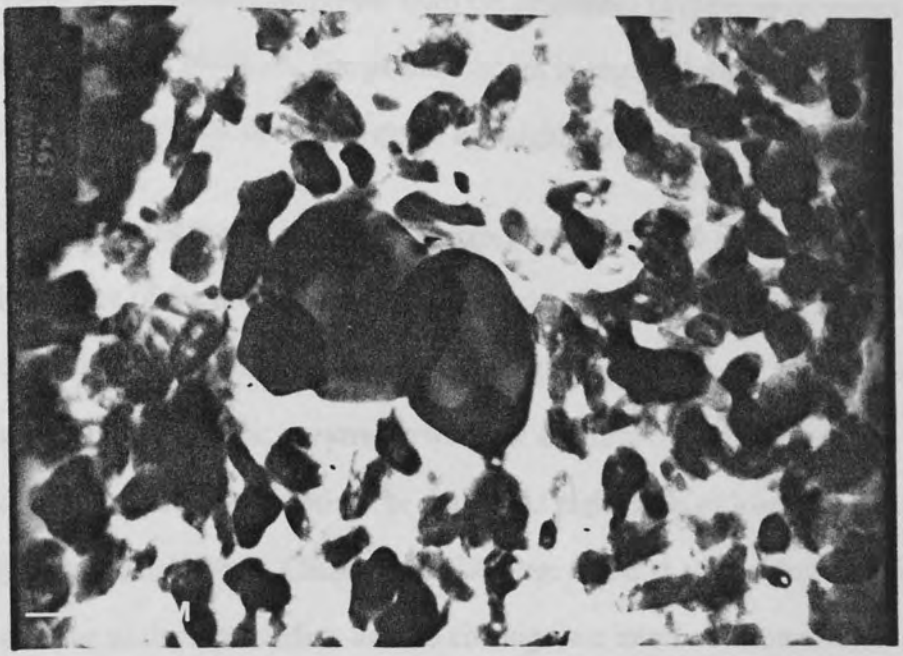

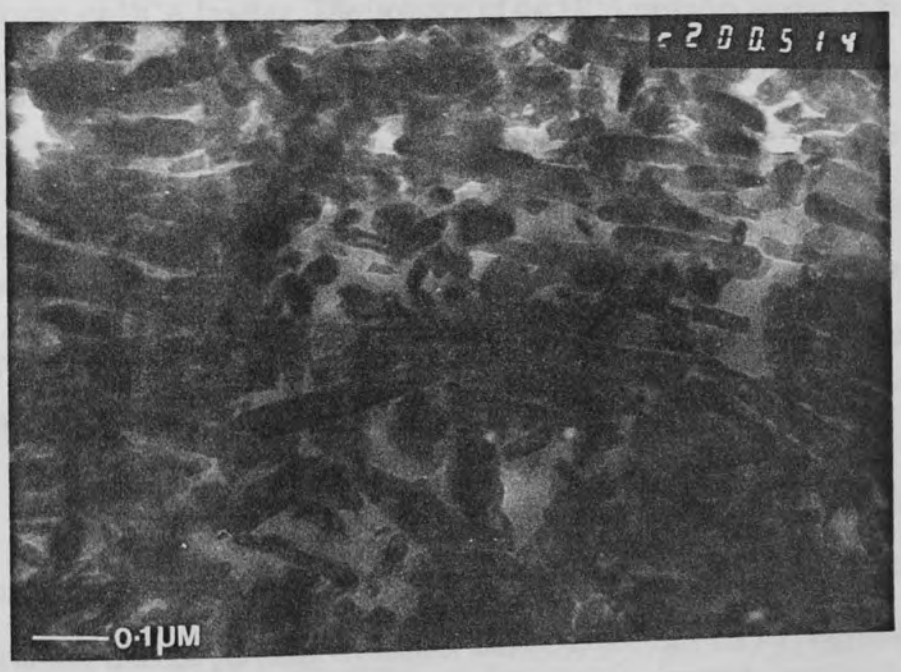
0·1μM

manufacture, just before the tape is dried. Close examination of Figure 3.46 shows that the iron oxide particles have to deviate from the alignment in order to surround the agglomerate of HCA particles. The particle shown in Figure 3.48 shows that a single particle has little effect on the alignment of its neighbouring particles.

Further observation of pilot plant tapes containing 2% and 10% green chrome revealed the state of the distribution of the agglomerates and single particles within the magnetic coating. With low HCA loading, although agglomerates of particles were noted, the frequency of their occurrence was low and firm conclusions on the distribution of the particles could not be drawn. At high levels of loading a pattern of distribution was established. Clusters of HCA were found at all positions within the coating relative to the tape surface and the coating-base interface. However, at a loading of 10% HCA it was clear that a greater number of groups of particles occured towards the coating-base interface than near the surface. Figure 3.49 shows a large cluster of green chrome particles on the interface of the sample containing 10% HCA.

Pilot plant produced tapes containing alumina HCA were also examined at various levels of HCA loading. The isolation of the HCA particles proved to be more difficult with samples containing alumina compared with those containing green chrome. The difficulty was thought to be due to the lower occurrence of agglomerates of HCA particles. Few groups of particles were found, the occurrence of a single particle or possibly two overlapping being most common. Figure 3.50 shows a typical cross-section through a tape containing 4% alumina. Even at higher HCA loading the occurrence of agglomerates found with green chrome was not seen.

Figure 3.51 shows a cross-section through a sample of chrome dioxide tape. Comparing this photomicrograph with those of the iron oxide particles, it would appear that the chrome dioxide particles are thinner and more uniform. As was explained in chapter 1, demagnetisation is reduced by using a long thin particle. The ability to form thin and uniform particles must only enhance the magnetic properties of this pigment.

Figure 3.49: Cluster of Cr_2O_3 particles at the coating-substrate interface

Figure 3.50: Typical cross-section through a tape containing 4% Al_2O_3

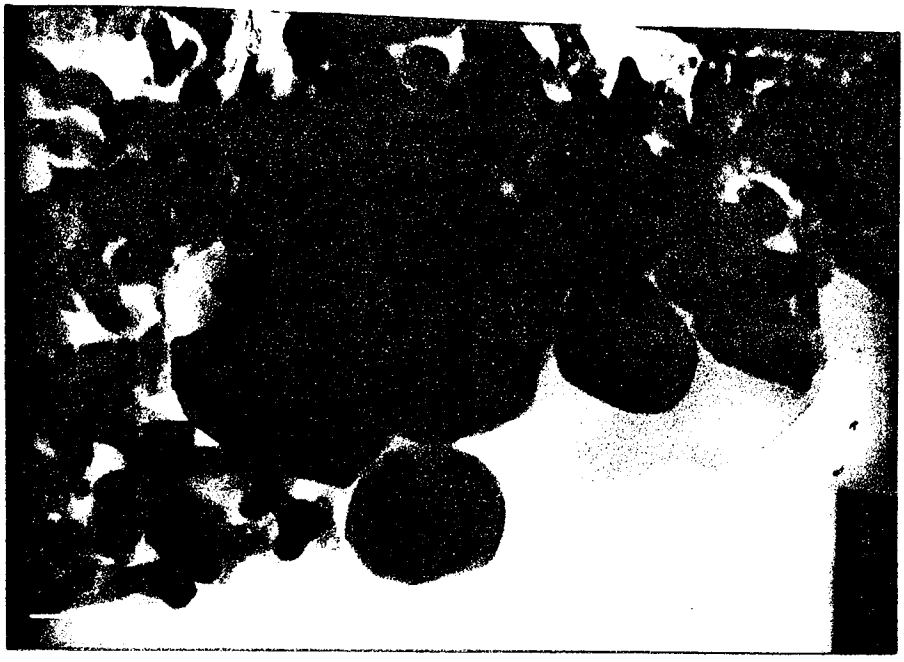


0·2 μM

Figure 3.51: Cross-section through a sample of chromium dioxide tape


0.2 μ

From the examination of cross-sections of iron oxide tape containing both green chrome and alumina as HCAs the results suggest that the green chrome has a tendency to agglomerate or not to disperse with mixing. The position of these agglomerates within the depth of the coating is biased towards the coating-base interface. The Al_2O_3 particles appear to disperse more evenly than the Cr_2O_3 whilst the chromium dioxide tape appears to have an overall better dispersion of magnetic particles.

3.7 SEM results

In addition to the analysis of debris SEM was used to obtain general photomicrographs of the head and also the examine the gap and ferrite surface after wear in more detail than was possible using a conventional optical microscope. Figure 3.52 shows a photomicrograph of the gap area after wear with an iron oxide tape produced at the pilot plant containing 8% green chrome as the HCA. Several features can be seen from this photomicrograph. First, the light area to the left is the edge of the glass insert which borders the gap, which can also be seen clearly. The glass does not stop abruptly at the edge of the ferrite but runs into the gap for a few microns. This can be seen on optical photomicrographs but is particularly clear in this case. Second, grooves formed in the ferrite are apparent, and seem to be most severe near to the glass region. Closer inspection reveals that the deepest grooves are not smooth and uncluttered, but contain lumps of debris. The third and most striking feature is the damage occuring specifically to the gap. Along the length of the gap the sides have been chipped away, however, in one particular region the damage extends away from the gap on both pole pieces.

In Figure 3.53 a second example of gap damage is shown. This time the head has been worn with a pilot plant produced iron oxide tape containing 6% green chrome as the HCA. Chipping of the gap is evident along the length of the gap, and once again a portion is badly degraded either side of the gap.

Figure 3.52: SEM photomicrograph of the gap area after wear with an iron oxide tape produced at the pilot plant containing 8% Cr_2O_3 HCA.

Figure 3.53: SEM photomicrograph of the gap area after wear with a pilot plant produced iron oxide tape containing 6% Cr_2O_3 HCA

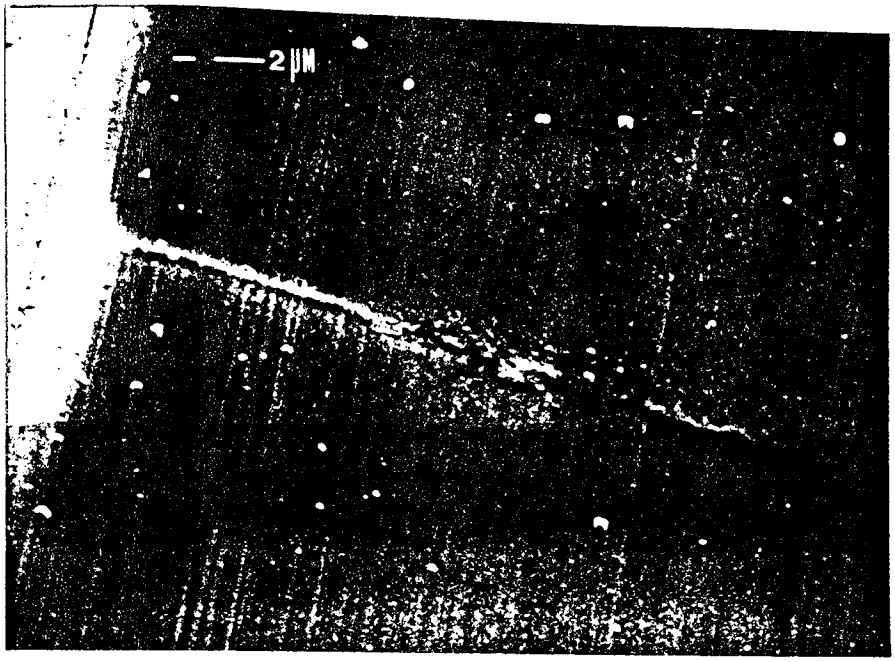
2 μM

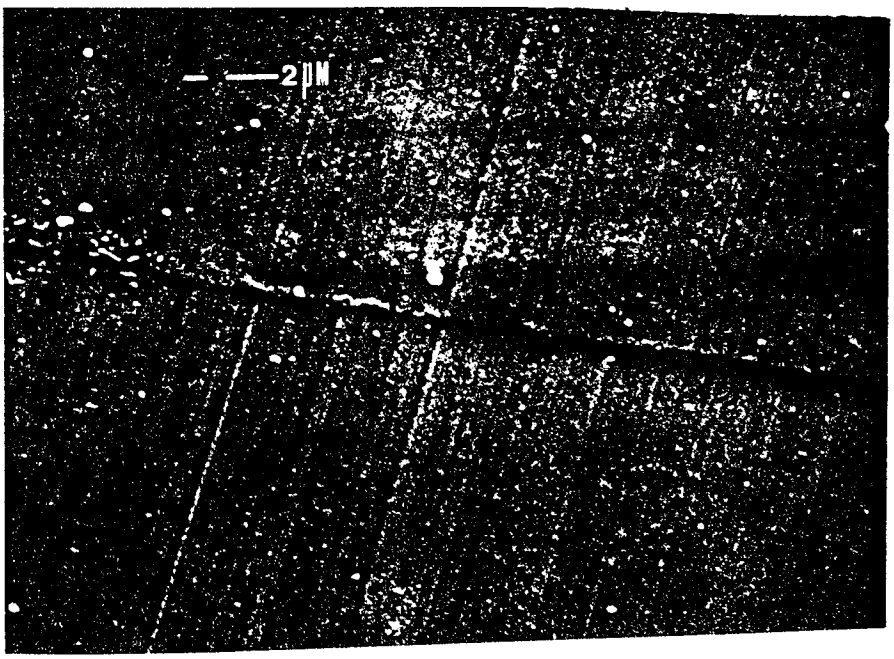
2 μM

Figure 3.54 shows the gap area of a head worn by an iron oxide tape produced at the pilot plant, this time containing alumina as the HCA. Deep grooves are present on the ferrite surface as observed with the sample containing 6% green chrome . However in this case the gap shows little or no damage even in the area where a deep groove has traversed the gap. Figure 3.55 shows the gap area of a head worn with the standard iron oxide formulation containing 4% green chrome as the HCA. This head reveals another feature of wear which was most obvious on heads worn with the commercial iron oxide product. The feature is characterised by a roughening of the ferrite surface. However, it is not clear from the photomicrograph whether the feature is a deposit or the removal of ferrite material. The commercial iron oxide tape also exhibited the lowest wear rate, suggesting that the wear surface shown in Figure 3.55 is characteristic of very low wear.

Microscopic examination of the gap areas of heads worn with different samples revealed several wear phenomena which appear to depend on both the wear rate and the type of HCA used. The appearance of grooves along the length of the ferrite occured for each sample. Examination of the signal degradation figures for each of the heads reveals a strong correlation between the damage to the gap and poor signal degradation. The lowest signal degradation was shown by the head worn with the iron oxide sample containing alumina as the HCA (-0.5dB), which showed little or no damage to the gap.

3.7.1 Analysis of debris

The pole pieces of each head used throughout the project were examined for debris after wear. Examination was performed using both SEM and the optical microscope. In general debris was deposited towards the edges of the pole pieces away from the gap, and often just outside the limits of the wear scar. Figure 3.56 shows an example of the accumulation of debris just beyond the wear scar. There is a definite boundary between

Figure 3.54: SEM photomicrograph of the gap area after wear with a pilot plant produced iron oxide tape containing 4% Al_2O_3 HCA

Figure 3.55: SEM photomicrograph of the gap area after wear with a pilot plant produced iron oxide tape containing 4% Cr_2O_3 HCA

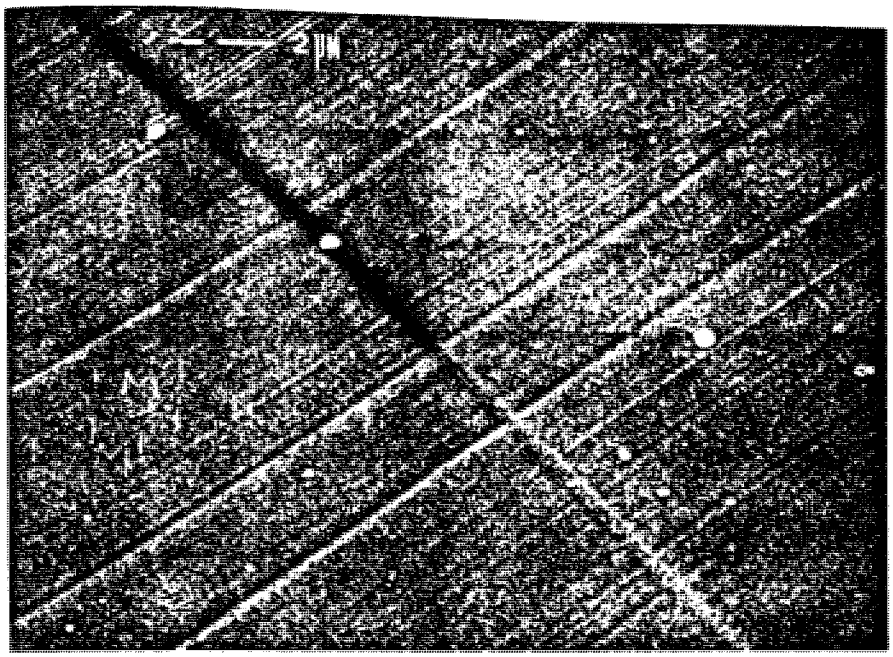
2 μM

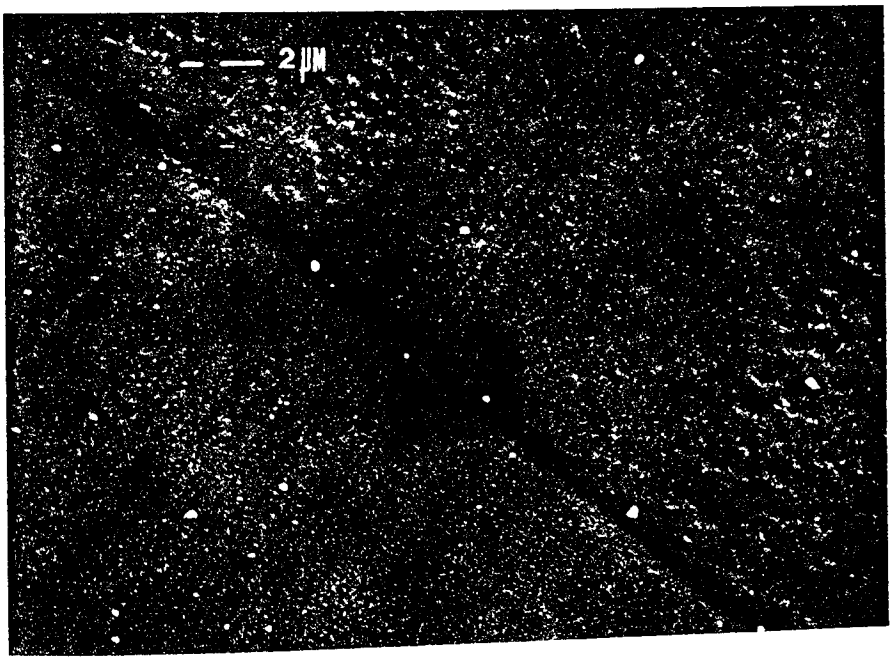
2 μM

the end of the wear scar and contact between the tape and the head, and the start of the wear debris. This may be expected as the head-tape contact is supposed to act as a self cleaning system and to remove wear debris and frictional films from the area around the gap. The debris shown in Figure 3.56 is particularly heavy and has collected after only six hours of wear on the trailing pole piece. Figure 3.57 shows the debris which has collected on the leading pole piece. As would be expected the leading pole piece was only lightly covered in debris.

Using the SEM the debris particles were examined at greater magnification. Figures 3.58a and b show examples of small debris found on both pole pieces. The debris particle appears to be a roll of material. Two main types of debris were observed, the rolls of material as already shown, and the clumps shown in close up in Figure 3.58c.

3.8 Examination of pilot plant samples

Variation in wear results between samples of the same HCA concentration brought into question the quality and reproducibility of the samples produced by the pilot plant. The samples received at the beginning of the project exhibited different wear results to those samples received over year later in the project. The main difference in the two batches was the average wear rate. The problem highlighted the difficulty in producing samples of the same standard from a pilot plant, over a period of three years. In order to determine the differences in tape production over the period of the project a full examination of all the samples used for the experiments was carried out. Data were compiled on the physical properties of the tape samples of the three Experiments GC1, GC2 and AL1. The examination also included a study of the production of the pilot samples, and the observation of any differences between the pilot process and commercial production. The parameters measured for each tape sample were as follows;

Figure 3.56: Accumulation of debris particles at the edge of the wear contour

Figure 3.57: Debris particles on the leading pole piece of a head worn with a pilot plant produced iron oxide formulation

A)

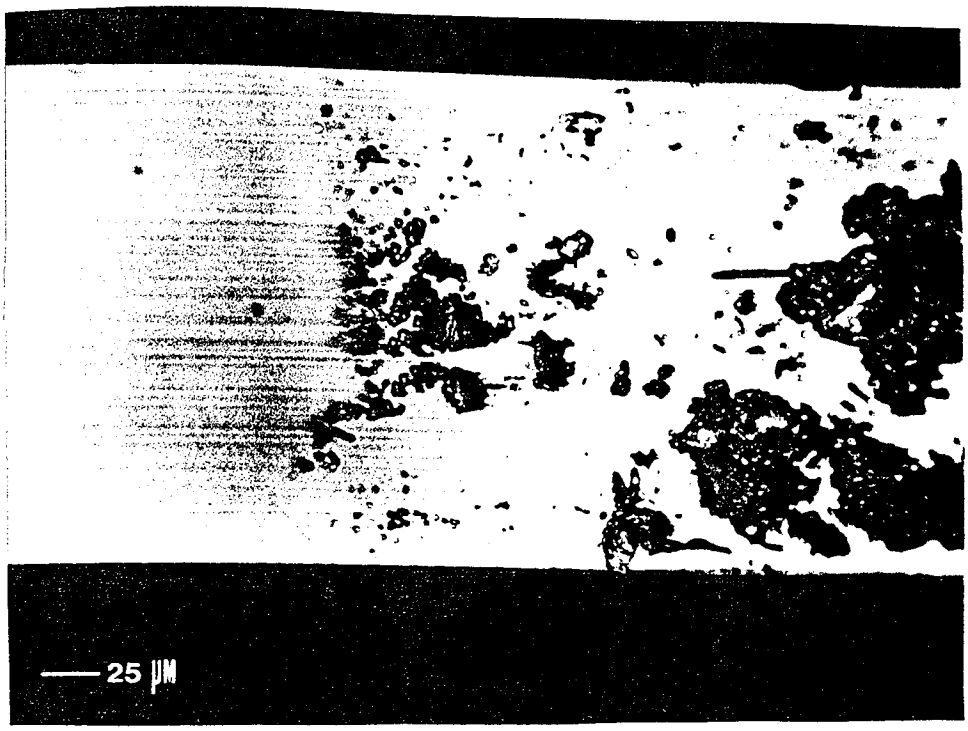

B)

Figure 3.58: Examples of debris particle types found on both pole pieces of the video head after wear

A)

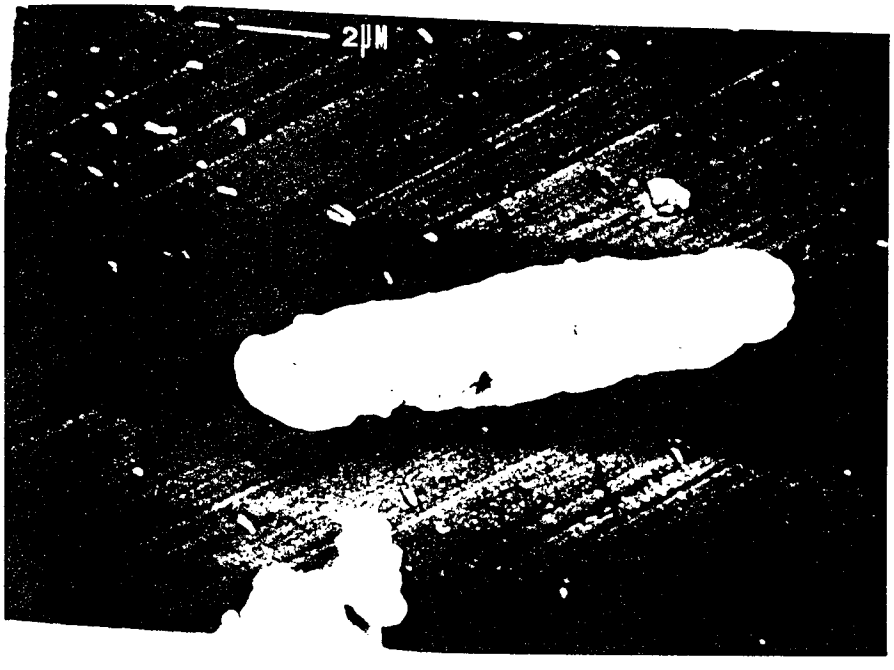

B)

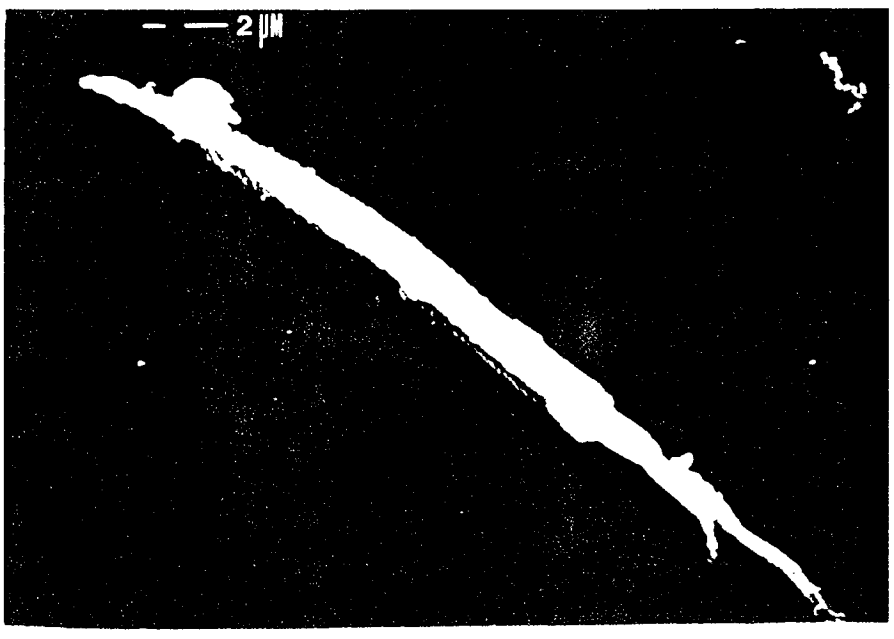

C)

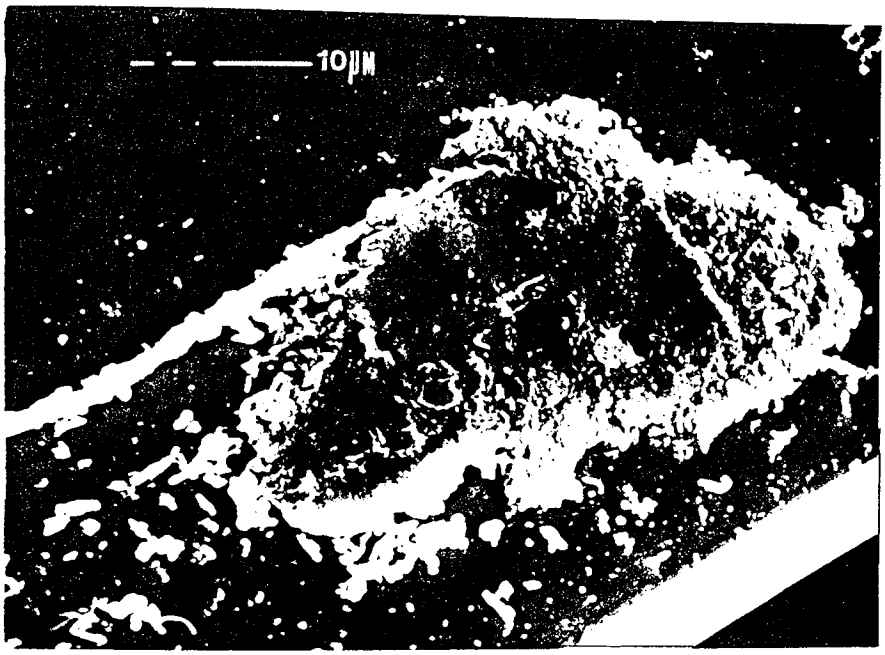

a) Thickness (μm) of the various layers of the tape, including thickness of the backing coat, the base film and the magnetic coat, as well as the overall thickness of the tape.

b) The flexibility (stiffness/thickness) in both the machine and cross directions.

Table 3.12 gives a summary of the average measurements taken for each of the three experiments.

In Experiment GC1 samples containing from 0% to 10% Cr_2O_3 were examined, whilst in Experiment GC2 samples containing 8% to 16% Cr_2O_3 were examined. The repetition of samples containing 8% and 10% HCA in both sets allowed a comparison of wear results of these samples to be made. The results of these two experiments showed that the samples of GC1 produced a series of higher wear rates than GC2. The average roughness of these two sample sets was similar, thus further examination of the tape properties was required. From the physical parameters it would appear that the largest difference between the two sets of samples (GC1 and GC2) is the flexibility in both machine and cross directions. Overall, the samples from Experiment GC1 show higher CD and MD moduli. In addition, GC1 samples are generally thinner than the GC2 samples. The effect of these differences will be discussed in chapter 4.

Experiment	Thickness (μm)	Flexibility (Kg/m^2)	
		CD	MD
GC1	17.1	17.76	15.77
GC2	17.7	16.27	14.22
A:L1	18.3	18.30	15.70

Table 3.12: Summary of the average measurements taken for Experiments GC1, GC2 and AL1

Chapter 4:

Discussion

4.1 Introduction

This chapter presents an evaluation of the research carried out in this project and discusses the more significant findings described in chapter 3.

First the results of the pilot research are discussed and general conclusions are made concerning the performance of some of the tape brands tested. The pilot research introduced the wear contour and the importance of the position of head-tape contact.

Next the use and advantages of the diamond indentation technique as a method of wear measurement are outlined and the significance of the results obtained using this technique are discussed.

The discussion of wear mechanisms to the head begins with the effect of transfer of polymeric debris from the tape to the head on signal degradation. The effect of varying the type and level of the head cleaning agent are then outlined. The wear mechanisms occuring to the head are then discussed with particular reference to the difference in wear produced by media containing only iron oxide, compared with media containing an HCA. A general wear mechanism is proposed for the situation occurring between iron oxide formulation media and the head. Finally a model for the progression of wear in the first few hours of wear of a new head is presented.

4.2 Pilot research

The tape brands which were examined in the pilot research included a range of predominantly iron oxide tapes and one chromium dioxide formulation. This range is representative of the video tape industry as a whole, as the market is dominated by the iron oxide formulation. This is partly due to historical reasons, chromium dioxide being a relatively new magnetic pigment for use in video tape. It may also be a product of the very high wear exhibited by chromium dioxide tapes, since the particle exhibits approximately twice the hardness of cobalt doped iron oxide and is therefore inherently

more abrasive. In the light of this, it was interesting to note that one of the iron oxide formulations,Tape D of the pilot experiment, exhibited very similar wear characteristics to the chromium dioxide tape. The results of the chromium dioxide tape which was tested in the pilot experiment (Tape B), were not presented in the results. However,the same chromium dioxide formulation was tested in Experiment IN2 and similar results achieved. The wear characteristics of both Tapes D and B included high wear relative to the other iron oxide formulations tested, the appearance of a smooth and undegraded gap, and ferrite surface with correspondingly good signal degradation. The high wear produced suggests that it is possible to produce an iron oxide formulation which exhibits a level of wear similar to the wear produced by a chromium dioxide formulation. A quantitative evaluation of wear rate would be required to confirm this, which was not attempted in the course of this work. Electron probe microanalysis of the surface of the iron oxide tape (Tape D) revealed the presence of aluminium, titanium and silicon in small amounts in addition to iron and cobalt. Cobalt is used to improve the coercivity of the iron oxide particles. It is assumed that the remaining metals are present as HCAs, and a complex combination of the oxides of these metals have created the high wear rate observed.

After wear with the chromium dioxide tape, Tape B, and the iron oxide Tape D the resulting head surface is heavily worn, but in a condition similar to, or smoother than the original surface. A photomicrograph of a head worn with CrO_2 is shown in Figure 4.1. This is ideal for good signal reproduction since high head wear does not allow the build up of any debris or contaminant layers on the head surface which cause spacing losses. These tapes are likely to be directed towards the domestic market where high head wear would not normally present a problem for three reasons; first, because of the relatively few hours the domestic user runs a video; second, because the tape looses its maximum abrasivity after a single play; and third, the domestic user does not necessarily play a single tape brand. It is notable that the manufacturers of both Tapes D and B have chosen to market a highly abrasive tape with inherently good head cleaning qualities.

Figure 4.1: Photomicrograph of head worn with chromium dioxide media.

Figure 4.2: Photomicrograph of worn head showing the presence of the wear contour

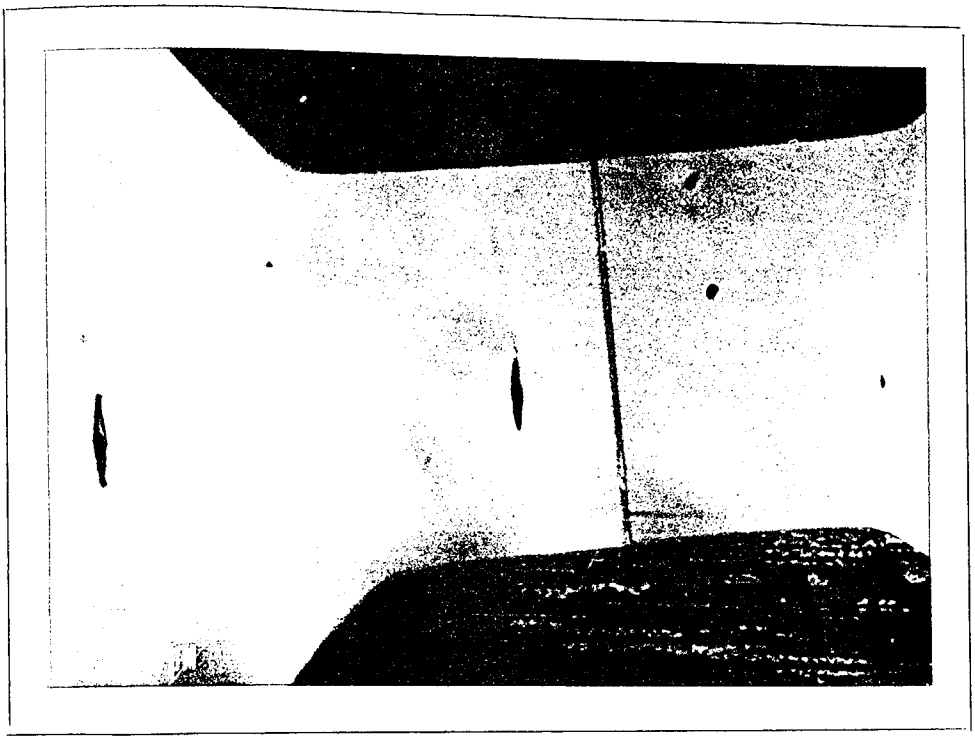

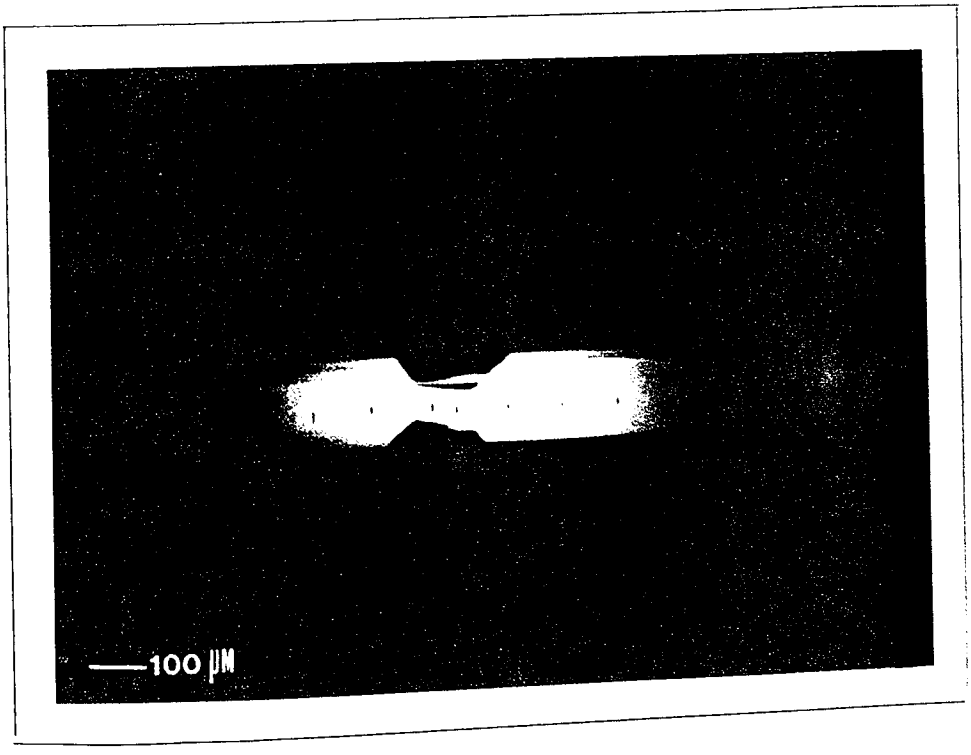
100 µM

However, for professional duplicators, the life of the head and the continued good condition of the head surface are more critical. A high wear tape would be unsuitable for the process of duplicating films where virgin tape is used continually. It is from professional duplicators that manufacturers of video media receive most feedback on head damage and tape performance.

The remainder of the tapes tested in the pilot experiment were iron oxide formulations containing various types and levels of HCA which all exhibited lower wear rates than those of Tapes D and B. The lowest wear was produced by Tape C, an iron oxide tape containing 4% Cr_2O_3 as the HCA. Although wear was low, the surfaces of the heads worn by this formulation exhibited gross abrasive damage to the ferrite and damage to the gap in the form of chipping. The head damage was accompanied by very high signal degradation. Excluding the high wear tapes (Tapes B and D) the damage to both ferrite and gap was observed on the heads worn by all tape brands with varying degrees of severity, and the signal degradation correlated with the visible surface and gap damage.From an initial examination of the heads it would appear that the dominant wear mechanism is abrasive. The deformation not only extends to the ferrite surface but also includes the glass region in most cases.

4.2.1 The wear contour

The wear contour formed in the first few hours of using new head provides an immediate indication of the position of maximum head-tape contact during operation. Figure 4.2 shows a photomicrograph of a contour. The formation and resulting shape of the contour is due to the curvature of the head which is contoured such that the surface curves away from the gap in both the sliding and cross directions, thereby encouraging maximum head-tape interaction to occur at the gap. Ideally maximum tape-head contact occurs at the gap to ensure good reproduction and to keep the area free from debris and deposits which would interfere with recording and reproduction (2). As the head wears the curved surface is flattened, resulting in a visible cigar shaped contour extending either side of the

gap in most cases, the size of which gives an immediate indication of the relative abrasivity of the tape.

Examination of the contours produced in the pilot experiment showed that the maximum point of normal pressure does not necessarily correspond to the gap. A correlation was observed between signal degradation and the distance of the centre of the wear contour to the gap. In general, the tapes which produced the highest wear exhibited contours with centres closest to the gap. However, it should be noted that all tapes produced a wear contour which was biased towards the trailing pole piece, regardless of volume of wear. The results suggest that the displacement of maximum pressure away from the gap is not necessarily detrimental to reproduction. In the case of Tape C, the bias towards one pole piece was so severe that contact did not occur at the gap at all. As a result, differential wearing of one pole pieces occurred causing an increase in pole piece height difference and an effective increase in head-tape spacing. In the next section the effects of wear to one pole piece are discussed, and the physical parameters of the tape which contribute towards the contact between the head-tape and the resulting contour are examined.

4.2.2 Signal degradation

The lowest signal degradation recorded in the pilot research project occured with the highest wear. In some cases the resulting degradation figures were positive showing that wear had improved the state of the original head surface, creating conditions for better reproduction of the signal. One way in which this may have occurred was through the levelling of pole pieces of originally different heights. For all samples tested, change in pole piece height correlated with signal degradation. The average pole piece height difference measured for a new head was 7nm. In the case of Tape D, which produced a large wear contour, the average change observed after 6 hours wear was -6.0nm. The

signal degradation was positive (+0.5 dB), showing an improvement in signal reproduction after wear.

A difference in height of two pole pieces produces a head-tape spacing, as illustrated in Figure 4.3. The effect of this spacing on the signal degradation can be examined using the Wallace spacing loss equation (8) which relates the loss in signal (dB) due to head-tape spacing (d), to the wavelength of the recorded signal (λ);

$$Spacing\ loss = 54.6.d/\lambda \qquad (1.2)$$

The length of the gap dictates the shortest wavelength which can be recorded by the head. Thus, spacing losses which are created by alterations to the gap are predominantly losses in short wavelength / high frequency response. Thus taking the recorded wavelength as 1 μm (the gap length is sub-micron) and the spacing of 7 nm, the following spacing loss would result;

$$spacing\ loss = 54.6\ (7\times10^{-9}/1\times10^{-6})\ dB$$

$$= 0.38\ dB$$

Thus the contribution of spacing loss towards signal degradation caused by the inherent difference in pole piece height is 0.38dB. If the pole pieces are then levelled by wear, there would be a corresponding increase in signal level. The highest signal degradation was exhibited by Tape C (-4.2 dB). The heads worn by this sample showed a large increase in pole piece height difference which may have contributed towards the bad signal degradation. One of the heads on the drum worn with Tape C had a difference in pole piece height of 36nm. The spacing loss resulting from this head-tape spacing, assuming λ = 1μm, is 1.96dB. Thus the contribution from spacing loss to the overall signal degradation observed for Tape C would be of the order of 2dB. This represents the maximum loss for this wavelength since the conformity of the tape over the gap created is not taken into account, as shown in Figure 4.3.

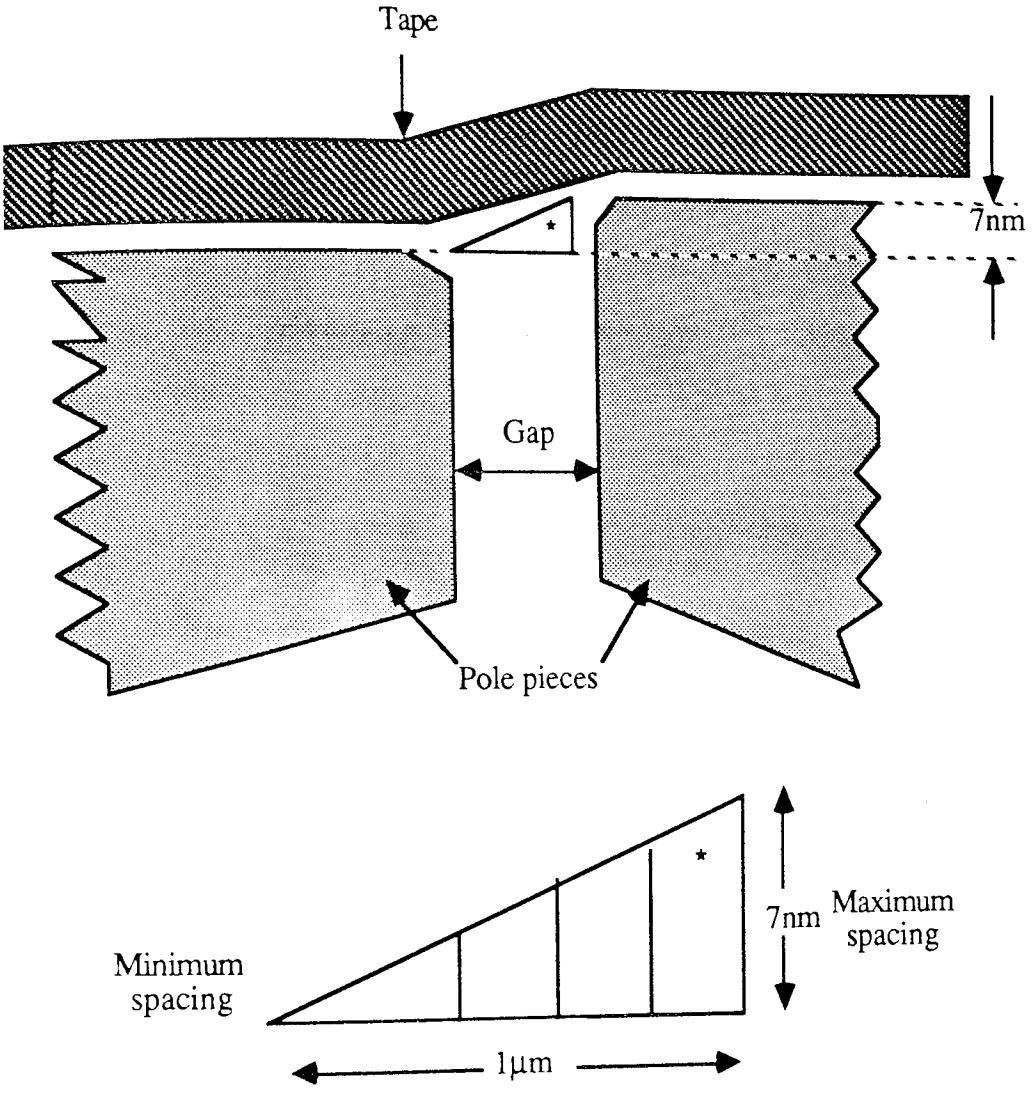

Figure 4.3: Head-tape spacing created by a difference in pole piece height

In addition to levelling of the pole pieces, there were indications that the good signal degradation exhibited by heads worn using Tape D may also be a product of the undegraded ferrite surface, the lack of damage to the gap and the removal of debris and transferred layers from the tape. Another reason for the improvement in signal reproduction observed under conditions of high wear stems from the dynamics of the head. High wear to the head continues to improve the performance of a head by reducing its throat height. The throat height of the head is illustrated in Figure 4.4a as the distance between a and b. Optimum reproduction is achieved at minimum throat height which occurs just before the head fails. At this point the concentration of flux per area of ferrite is at its highest (as shown in Figure 4.4b) and the head is at its most sensitive (121). Thus if we consider a situation of wear to the head which is not complicated by transferred layer removal or ferrite abrasion damage, the simple removal of ferrite with time would produce an improvement in performance of the head. The performance would continue to improve up to the point where the head failed. Although the best performance of the head is achieved in this manner, the life of the head is reduced to an unacceptable level.

Under lower conditions of wear the degradation was usually negative, which indicated a loss in signal reproduction. The largest change in signal degradation tended to occur within the first few hours of wear. For most of the tapes tested, the degradation had levelled off before the completion of a six hour test and the signal remained below the original reproduced signal level, for example 2 dB. Virgin tape was used throughout, so any change in signal degradation was not due to the loss of abrasivity of the tape, but to changes in the condition of the head. With Tape C it was observed that degradation was still occurring after six hours of testing. In this case a steady state had not been reached and new damage was still occurring to the head, resulting in degradation of the signal.

The results of the pilot research established a correlation between signal degradation and the physical properties of the tape. The pilot research was performed

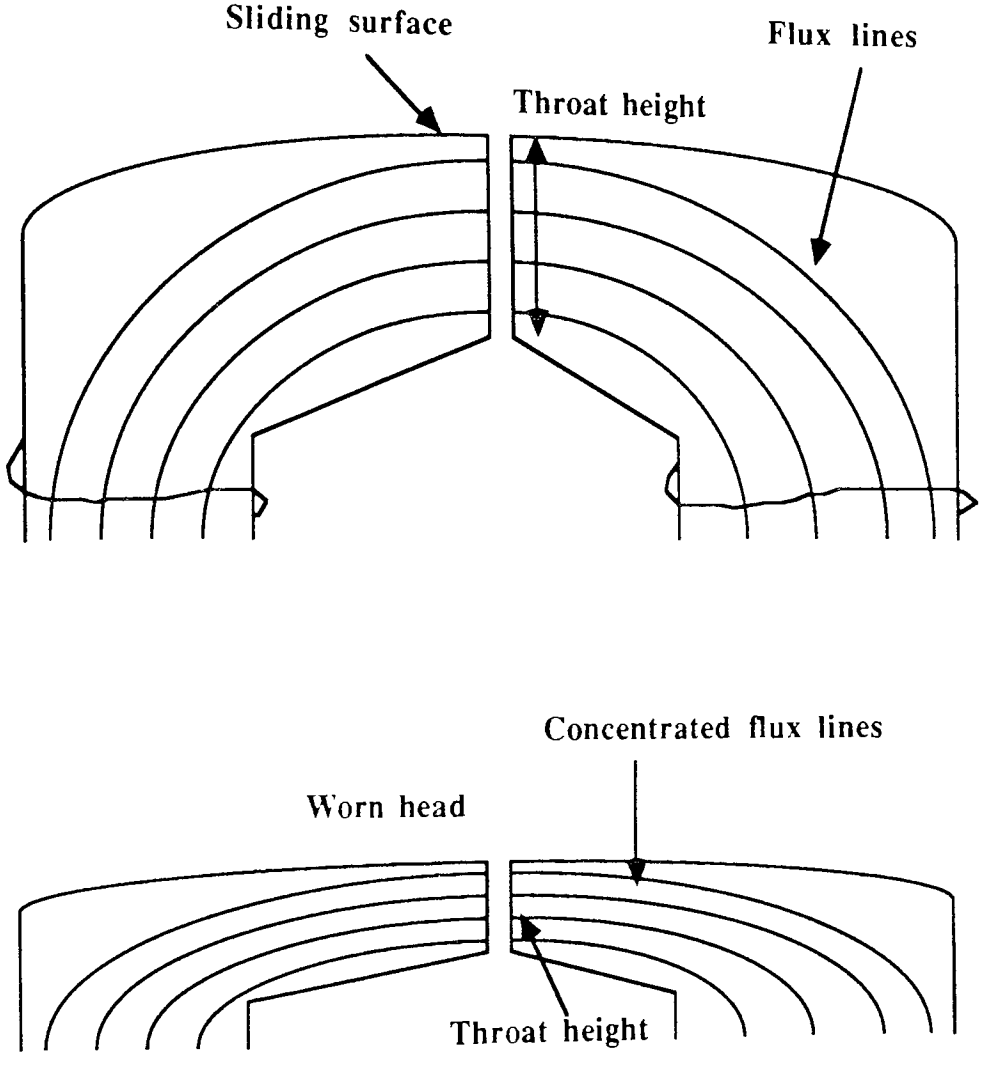

Figure 4.4: Effect of the reduction in throat height on the peformance of the video head

with the aim of suggesting immediate improvements to the commercial iron oxide product, Tape C. Tape C exhibited the lowest wear rate with consequent high signal degradation, and from the position of the wear contour, which was positioned over only the trailing pole piece and did not reach the gap, did not appear to make good contact with the head.

Factors affecting the contact between the head and the tape are the tape flexibility, thickness and surface roughness. These values are related in a semi-empirical formula by Suwarnasarn (122):

$$\text{Head/Tape spacing} = \frac{13182(\text{MD Flexibility})^{0.17}(\text{Tension})^{0.3}(\text{Roughness})^{0.35}}{(\text{Thickness})^{2.18}(\text{CD Flexibility})^{0.46}} \qquad (4.1)$$

Where MD Flexibility is a measure of the flexibility of the tape in the machine direction;

$$\text{Flexibility} = \text{Stiffness/Thickness}$$

and CD Modulus is the flexibility in the cross direction. Using this equation the head-tape spacing for each tape brand was calculated. Figure 4.5 shows a plot of head-tape spacing against RF degradation, which shows the expected increase in RF degradation with increasing head-tape spacing, as would be expected. In the head-tape spacing equation the most dominant parameters are roughness, thickness and cross directional modulus. Roughness has been acknowledged as a factor affecting head-tape spacing and wear (23,78), but from the point of view of commercial production both thickness and roughness are quite fixed. Hence, a change in the CD modulus is the only feasible parameter to alter in commercial production. From this work it was recommended that an increase in CD modulus would reduce the head-tape spacing and thus improve signal degradation of Tape C. Suwarnasarn's work concentrated on the head-tape spacing without considering the position of maximum or minimum spacing relative to the gap.

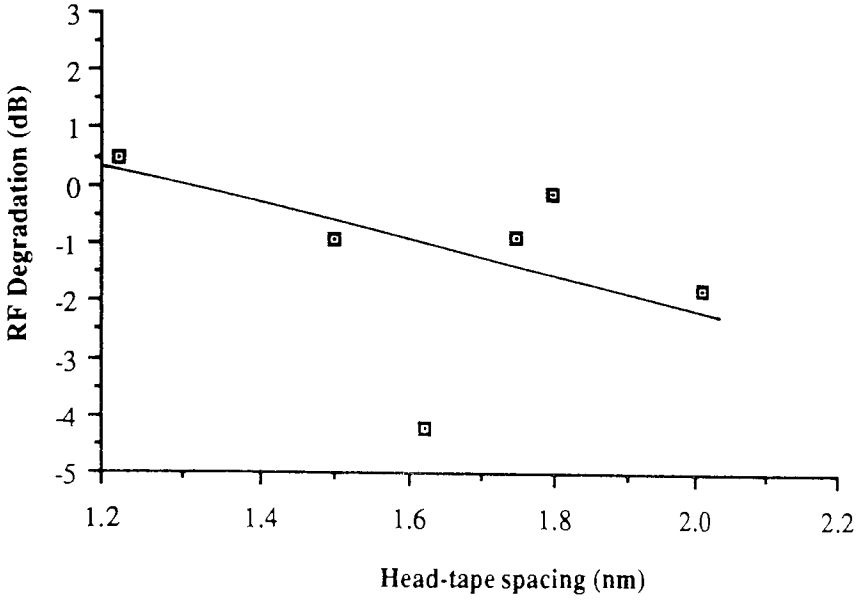

Figure 4.5: RF degradation plotted against head-tape spacing

Later in this discussion it is argued that the position of the contact is as important as the overall head-tape spacing.

An aim of the pilot research was to establish the research programme to be carried out in the main project. The pilot research was structured in such a way that general features of wear could be examined, such as the appearance of scratching, chipping of the gap, and their relationship with RF degradation. A programme of research was initiated which encorporated a more systematic examination of the wear to the head. The results of the pilot research indicated that, in general, a very low wear rate corresponded to high signal degradation, whereas those tapes exhibiting high wear exhibited low signal degradation. This can be seen to be a gross over simplification for two main reasons; first, no quantification of wear was attempted, and the majority of tapes did not exhibit either the abnormally low wear rate shown by tape C or the high wear rates shown by Tapes B and D; second, although there appears to be a direct relationship between wear rate and abrasive wear damage, the damage was observed on all heads (except for tapes B and D), even where good signal degradation was observed.

Tape C, which presented the lowest head wear, contains Cr_2O_3 HCA. Despite the addition of the HCA the wear is still very low. From the results of the pilot research it is reasonable to assume that an increase in wear rate reduces the signal degradation. Hence, in the main project the level of the HCA in the tape was varied either side of the standard concentration in order to examine the wear produced and its effect on the signal degradation.

A number of conclusions can be drawn about the wear observed in the pilot research. The action of the tape removes material from the head in an abrasive manner and changes the contouring of the head within the first six hours of wear of a new head. A large volume of wear, although undesirable, can produce a smooth surface similar to or in some cases better than the finish of the original surface. Under conditions of very low wear with some tape samples, damage to the head surface and the gap results in high

signal degradation. Wear to the head appears to be biased towards the trailing pole piece under conditions of both high and low wear.

4.3 Diamond Indentation Technique

In order to examine the wear produced by the different HCA levels an accurate method of measurement of wear was required. Many methods of head wear measurement were considered for the project but no existing method measured wear occurring to a real head in-situ. It was decided that the examination of wear occurring to an authentic head worn in the actual tape drive should be a priority. Thus a method of head wear measurement had to be identified which could measure wear occurring in situ, thereby producing results close to the real situation. Several methods were reviewed, but the only method which could be adapted for the measurement of wear of the video head, in-situ was the diamond indentation technique. In experiments IN1 and IN2, the diamond indentation technique was shown to be a simple and accurate method which enables a wide range of phenomena to be examined. Heads worn against all tape samples in the main project were examined using this technique and from the results a general profile of wear along the head emerged.

Figure 3.16b shows two typical wear profiles after 6 and 12 hours wear. The contact pressure was not uniform over both pole pieces, the minimum point of contact and minimum wear occurring on the leading pole piece in close proximity to the gap, though not actually at the gap despite the contouring of the head. The wear profiles confirmed that the maximum amount of wear occurred on the trailing pole piece in close proximity to the magnetic gap, with the wear decreasing towards the gap. A sharp increase in wear was also apparent on the leading pole piece corresponding to the edge of the wear contour. The shape of the wear profile suggests that the greatest head-media contact occurred either side of the gap, leaving an area of the head around the gap where the contact pressure was lower.

The wear figures used to compare various tape samples were the wear at the gap and also the maximum wear rate. The results confirmed the importance of measuring wear occurring in-situ in order to produce authentic results. The results obtained using the technique described the wear of the head, and not purely the abrasivity of the tape. Previous methods of wear measurement have relied on the simulation or reproduction of the conditions in the tape drive such as tape tension and wrap angle to simulate in-situ wear. From the results it can be seen that the size and contouring of the head, and the change in the contouring of the head with wear, are also critical in the progression of wear and must be taken into account. These conditions would be difficult to simulate, which emphasises the importance of measuring wear occuring in situ. Another equally important factor in performing the tests in-situ is the ability to correlate the wear rate with changes in the contours of the head, and to correlate features of wear damage with signal degradation.

By plotting wear rate profiles after 6 and after 12 hours of wear the variation in wear rate with time was examined. For iron oxide samples containing Cr_2O_3 it would appear that the wear rate decreases with time (see results of Experiment GC1). This can be attributed to the effects of several phenomena. As the wear contour spreads over the head (to be described further in section 4.9) the normal load is gradually distributed over a larger area of the head which produces a reduction in pressure per unit area. As a consequence, the rate of wear at any one point on the head decreases as the wear scar develops. In most cases, it was observed that the wear contour which developed in the first six hours of wear grew very little between six and twelve hours of wear. This suggests that the contribution of the change in pressure to the reduction in wear rate is negligible. The decrease in wear is most likely to be due to a build up of polymer frictional films or to the work hardening of the ferrite surface or a combination of the two. Both phenomena would provide the surface with a wear resistant layer. Work hardening of the ferrite surface is a product of the removal of material in the form of grooves by the abrasive mechanism, which creates a region of strain around the groove.

A surface covered in such grooves is work hardened and therefore more resistant to wear (87).

The sliding of polymers against a smooth hard surface is dominated by the transfer of the polymer to the counterface (79), and it is likely that transfer of polymer from the binder system to the head is occurring. The mechanisms of transfer wear of polymers were discussed in section 1.7.3. In general, transfer occurs where the adhesive junction between polymer and counterface is stronger than the bulk polymer. The polymer fails within the bulk and is transferred to the counterface. If transfer occurs, depending on the adhesion between the polymer and the counterface, the polymer may be removed by further traversals of the tape and may create debris in the form of polymer rolls, or remain on the head causing head-tape separation. The case of head-tape interaction is slightly different in that the polymer is filled with the iron oxide pigment. The filler reduces the wear rate of the polymer which is further reduced by the presence of a lubricant. One way in which the filler may reduce the polymer wear rate is by increasing the adhesion of the polymer to the counterface. This is caused by the filler particles acting as temperature intensifiers and causing localized polymer melting and as a consequence greater adhesion to the counterface (78). Once a polymer film is present on the head the wear rate decreases. This is because the interaction is now polymer-polymer, which involves dipole-dipole or dipole-induced dipole bonding as opposed to the stronger ion-dipole, or ion-induced dipole bonding which is characteristic of the polymer-head interaction (22).

Samples containing Al_2O_3 as the HCA, did not show a change in wear rate with time. This suggest that the heads worn with samples containing Al_2O_3 were not subject to subsurface damage to the same extent as those worn with tapes containing Cr_2O_3 HCA, nevertheless, the wear rates for the samples were similar, with tape containing Al_2O_3 showing slightly lower wear than tape containing Cr_2O_3. The difference in wear caused by the two different HCAs is examined more in section 4.6, where the quality of dispersion of all the particles in the magnetic coating is discussed in relation to the wear

mechanisms occurring to the head. In terms of change in wear rate with time; if the HCA particle is dispersed evenly throughout the coating the wear mechanisms of the tape are likely to be more predictable and a steady state will eventually be reached, after the head has been contoured by the tape. If the HCA does not disperse evenly the tape is likely to consist of many random asperities of varying size and frequency. Hence, wear to the head would be less likely to reach a steady state due to the random occurrence of asperities.

4.4 Transfer of debris and films from the tape to the head surface

XPS and SIMS were used to study the surface layers of the head before and after wear. From the results obtained with both techniques there was evidence to suggest that a layer of organic material was present on the surface of heads worn using the commercial iron oxide product. The advantage of the SIMS technique is the detection of ions in addition to elemental analysis. Thus, it should be possible to detect, for example, myristate ions originating in the lubricant ester butylmyristate. The myristate ion would be detected at 227 amu. From the spectra acquired myristate ions were not detected. During the setting up procedure, before the acquisition of the spectrum, myristate was detected at mass 227. From observations made at the time the analysis was performed, it would appear that there was a certain amount of lubricant on the surface of the worn head, which was sputtered away as the signal levels were being set. SIMS is a highly destructive technique, in which a compromise is often sought between sensitivity and the amount of material sputtered away. In setting the optimum sensitivity it is likely that some material will be removed before a spectrum can be acquired, as occured in this analysis. The ease with which the lubricant was removed would suggest that only a very thin layer was present. This indicates that the layer is continually being removed and replaced by the action of the tape. In short the layer is dynamic and does not build up on the surface. Therefore, it would appear that he transfer of lubricant is not a dominant factor in the creation of head-tape spacing.

On acquisition of the spectra, a layer of organic material was observed which had not been sputtered away within the same time as the lubricant. This organic layer remained even after cleaning with a solvent to remove loose debris. This would suggest that a layer which can only be removed by mechanical means is present. Organic films of this type have been recorded previously on the heads of magnetic recording systems, termed frictional films. In some cases the films were observed as coloured depending on the film thickness (86). However, there do not appear to be any descriptions of such films occurring on a video head in the literature. This is most likely due to the small size of the video head and the fact that the in-contact operation results in wear to the head surface. Thus it is unlikely that a film would build up on the video head to a thickness comparable with those observed for other recording systems. It is only recently that surface analysis techniques have been developed which are sensitive enough to detect organic material in such small quantities on the surface of such a small specimen. Therefore it would appear that a film similar in type and origin to those frictional polymer films found on other magnetic heads was observed.

Adhesive wear of polymers is most likely to occur with polymers above their Tg (78). The portion of the binder most likely to transfer to the head would be the softer polyurethane segment. At high speeds, surface heating is likely to increase the interfacial temperature above the Tg of the polymer (75). The hard phase of the binder system is crystalline and involves strong hydrogen bonding, thus even with frictional heating it is unlikely that this part is involved in transfer. It would appear that a certain amount of polymeric material is transferring to the head, possibly originating in the binder system.

The presence of phosphate residues was also recorded before and after cleaning the head surface. It is possible that some of the organic material may have originated from the wetting agent POCA II, as this is the most probable source of the phosphate residues. It is unlikely that all the organic material would come form this source and this is

endorsed by the results for the head worn using no HCA, which show the presence of phosphate residues but very little evidence of organic material on the surface.

The XPS included analysis of an unworn head and a head worn for 30 hours with the commercial iron oxide product. Since this technique concentrated on the organic components the spectra acquired were those of carbon and oxygen and iron only. The counts obtained for the oxygen spectra were very low, and accurate synthesis of the spectra could not be achieved. Examination of the wide scans before and after wear shows that the iron peak decreases with wear again suggesting the build up of a layer over the head surface, as was also detected using SIMS. From the carbon spectra the level of C=O and C-O were seen to increase after wear for thirty hours with the standard iron oxide product. Therefore, it would appear that both the binder and the POCA II wetting agent contributie to the increased concentration of organic material on the surface of the head.

Other species found on the surface of the tape were aluminium and silicone. The aluminium is most likely to have originated from the video drum or guide rollers, having been removed in an abrasive manner from these sources. The aluminium would not be deposited on the head as the metal, but is far more likely to have been transferred with the polymer. Silicone is well known as a lubricant and in this case originates in the oil used to grease the guide rollers and is transferred by the tape to the head. SIMS is not a quantitative technique, thus, the relative abundance of these species cannot be verified. However, it is probable that only small amounts of both alumina and silicone are transferred.

4.5 Use of the pilot plant

From the results it appears that the samples produced at the pilot plant varied in quality. There is no quality control associated with the pilot plant, so tape quality up until the findings of this project, remained unchecked. The plant is mostly used for one off

experiments, which would not normally necessitate the evaluation of similar batches of samples. In this project consistent samples were required over a period of three years. The pilot plant samples which were used in this project could be separated into two groups in terms of performance corresponding to the time they were coated in the pilot plant. At the beginning of the project two sample sets were acquired; one to evaluate the diamond indentation technique, which included samples containing Al_2O_3 as well as Cr_2O_3 (see Experiments IN1 and IN2); the second, a range of samples containing Cr_2O_3 from 0% to 10% (Experiment GC1). These samples were shown to be similar by comparing the results obtained for the iron oxide sample containing 4% Cr_2O_3 produced in the set used for Experiment IN2, with the results for the same sample (iron oxide, 4% Cr_2O_3) of the sample set used for the experiment GC1.

After approximately one year a second batch was obtained, consisting of two sets of samples; one set contained samples ranging from 8% to 16% Cr_2O_3 (experiment GC2); and the second set contained samples ranging from 2% to 10% Al_2O_3 (Experiment AL1). The main difference between the two batches of samples produced at different times was the wear rate. In general, the wear rates of the samples received towards the end of the project were lower than those of samples received at the beginning. However, if the average wear rates for the two sets of iron oxide samples are compared with the wear rates obtained for the chromium dioxide tape formulation, the relative difference in wear rate between pilot batches is minimal compared with the difference in wear between iron oxide and chromium dioxide formulations. Using such a sensitive technique as diamond indentation to measure wear, small differences appear significant.

In order to eliminate variation in experimental procedure or equipment over the year, samples remaining from the original batche were used to perform repeat experiments. The results confirmed a variation in samples rather than procedure. The variations in the physical properties of all the samples were then examined, and are discussed in chapter 3.

The average values for flexibility and stiffness for Experiments GC1, GC2 and AL1 are found in Table 3.12. The main variation between the two batches of samples was the flexibility in both the machine (MD) and cross directions (CD). A variation in flexibility would effect the head-tape spacing and consequently the wear in accordance with Suwarnasarn's formula for head-tape spacing (4.1). Comparing the average flexibility for Experiments GC1 and GC2, both the MD and CD moduli are higher for the samples of Experiment GC1. From Suwarnasarn's formula the CD flexibility is the more dominant term, and the head to tape spacing is inversely proportional to approximately the square root of this term. Thus an increase in the CD flexibility would create a decrease in the head-tape spacing, and therefore an increase in wear. Thus the higher wear exhibited by the samples of GC1 may be due to the higher flexibilty of the tape.

The pilot plant samples produced consistently higher head wear than the standard product, which suggests that aside from quality control to obtain consistency between pilot plant samples there exists differences between the pilot and commercial plants which are not acknowledged. One such difference likely to cause a variation in surface finish is the drying system. This is the one area where the pilot plant differs from the commercial production. After the pvc base has been coated on both sides, the tape is then dried in ovens, still in large sheets. In commercial production the tape is taken through a long oven through which warm air is gently circulated. The length of the oven and the speed at which the tape travels through is set so that the tape is dry by the time it emerges. Since the pilot plant is much smaller the drying oven is also significantly smaller, and in order to achieve dry tape the hot air is made to impinge on the tape surface. The tape is then calendered to improve the surface. However, it is possible that the drying method still alters the final tape surface.

Thus some quality control is required for a pilot plant in order to avoid large differences in samples. This should include examination of the tape surface under the optical microscope and the examination of roughness, taking the readings from several points on the surface of the tape sample. The quality of the system of drying the tape

product should also be examined, as this is the one part of the pilot plant operation which does not parallel that of the commercial production.

4.6 The effects varying the level of head cleaning agent

Variations in the quality of pilot plant samples produced specifically for the project mean that the three main experiments which examined the effect of the HCA concentration must be treated separately. Within the batches however the samples were compared and trends obtained in this way.

The trends in performance with increasing HCA content were similar for all groups of samples. Head wear increased with increasing HCA content as would be expected. However, the signal degradation, did not vary significantly with HCA content. Thus, it would appear that observations made in the pilot experiment which indicated a direct correlation between wear and degradation are not strictly correct.

Thus it would appear that an increase in HCA content, although raising the wear rate, does not necessarily produce the desired decrease in signal degradation. A possible reason for the lack of improvement in signal degradation emerges from considering the difference in wear rate between iron oxide and chromium dioxide tape formulations, as in experiment IN2. Increasing the HCA content of the pilot plant samples increased the wear rate, although even in the case of the highest wear rate recorded for an iron oxide formulation in this project, the wear rate remained at least 50% lower than the wear rate of the chromium dioxide tape. Thus no feasible increase in the concentration of either Cr_2O_3 or Al_2O_3 HCAs would bring the abrasivity level of this particular formulation of iron oxide tape out of the low wear category. In addition, it would not be commercially practical to use an HCA level above approximately 8% due to the expense of the raw material. It is also possible that above a certain level the HCA would begin to reduce the

recording density of the tape, although no published work was found which examined any of the effects of adding an HCA to the magnetic coating.

In considering the change in wear rate with HCA content, it should be noted that the wear rate of the commercial iron oxide product was lower than the equivalent pilot plant produced sample containing 4% Cr_2O_3. If the HCA was increased in the commercial product the resulting wear rate would be correspondingly lower. The chromium dioxide sample tested was also a commercial product.

Examining the results as a whole, the most significant difference in performance was observed between the two different HCAs. Samples containing Al_2O_3 produced a series of consistently low degradation figures, whereas the samples containing Cr_2O_3 produced high signal degradation. Table 4.1 shows a summary of the average RF degradation and the average roughness values for the samples for experiments GC1 and GC2 (samples containing Cr_2O_3), and AL1 (samples containing Cr_2O_3) . The samples containing Al_2O_3 exhibited very low wear, no wear being recorded until 8% HCA content. Looking at the roughness values, the low wear exhibited by the Al_2O_3 samples may have been a product of the low roughness of these samples. For comparison, it should be noted that the roughness of the commercial iron oxide product is in the region of 11.7nm. The roughness of the two Cr_2O_3 sample batches are similar to each other but far higher than the commercial product or the Al_2O_3.

Thus it is possible that the difference in performance between the two HCAs is a function of production of the samples only, however, in the next section, differences in the behaviour of the two particles within the magnetic coating are discussed which would tend to refute this assumption. It would appear that the two particles produce different degrees of abrasive wear under the same conditions. One of the main differences between the wear surfaces produced by the use of the two HCAs is the damage to the gap. Examination of the damage to the gap for each sample series reveals that there is little correlation between the amount of damage and the HCA content. This observation is

consistent with the signal degradation figures in that the degradation does not vary with increase in HCA. Thus the correlation between signal degradation and gap damage is confirmed.

	GC1 0%-10%	GC2 8%-16%	AL1 2%-10%
RF degradation (dB)	3.32	1.60	0.41
Roughness (nm)	13.2	13.8	10.8

Table 4.1: Summary of average roughness and RF degradation for the three main experiments.

4.7 Head wear mechanisms

In the first part of this section the damage caused by the iron oxide particles alone will be discussed. Wear to the head caused by the magnetic pigment and binder system alone was examined by testing a sample which contained no HCA. Damage to the ferrite surface was observed on heads worn by all iron oxide samples in the project in the form of ploughed grooves. However, the appearance of the surface worn purely by the magnetic particles exhibited more severe abrasive damage than a sample containing an HCA. The wear rate for the sample containing no HCA was very low, to the extent that after twelve hours of testing, no wear was measured using indentation and no wear scar was observed. Thus the gross abrasive damage was caused under conditions of very low wear. In addition, damage to the gap is present in the form of chipping.

The iron oxide particles of the coating are, on average, 0.2μm by 0.02μm. Previous studies of abrasive grits embedded in resin suggest that particles of this size are not involved in abrasive wear and thus can not be responsible for the ploughing damage caused to the ferrite surface (64, 65, 123). Suh suggests that particles smaller than 1μm would not cause abrasive wear, whereas Rabinowicz (64) assumes that only microabrasion or polishing will occur for particles smaller than 5μm.

The polishing mechanism suggested by Rabinowicz (64) is characterized by the wear caused by small abrasive grains supported by an elastic backing, as found in magnetic tape. The mechanism is supposedly similar to abrasion but the total force on each particle is small. Thus, given the size of the particles involved, polishing would be the type of wear expected for head-tape interaction, and indeed was observed for two of the tape brands tested in the pilot project. The wear surface produced by the chromium dioxide formulation in both the pilot project and experiment IN1 suggests that the ferrite had undergone microabrasion or polishing by the magnetic particles of this tape formulation. This type of wear mechanism would appear to be the optimum for reproduction, continually providing a wear surface with a finish as good as or better than the original. However, as mentioned previously, the wear rate is too high with chromium dioxide tape for commercial duplicating. Above 1μm particle size the wear rate increases rapidly up to a critical particle diameter, above which the increase levels off (64,65). Buckley and Miyoshi (82) observed a change in both wear mechanism and wear rate with increasing grit size. Two sizes of silicon carbide grits were tested, and the extent of plastic deformation of the resulting wear surface was examined using electron diffraction. It was found that the smaller grit size (4μm) produced extensive plastic deformation to the surface, whereas with the 15μm grits the abrasive wear mechanism was one of brittle fracture.

The appearance of the wear surface produced by iron oxide particles alone shows definite signs of ploughing wear in the form of grooves (124). Examination of the size of

the grooves formed shows that, on average, the width is submicron and of the same order of magnitude as the width of the iron oxide particles. The observation that the width of the scratches is similar to the width of the iron oxide particles has been made previously in the literature (23), where the groove width was often quoted as 0.1μm and cited as evidence that the gross abrasive damage was caused by the magnetic particles. However, studies by Buckley and Miyoshi (82) of the sliding wear of Mn-Zn ferrite against various grit sizes of either Al_2O_3 or silicon carbide embedded in a resin matrix showed that only the tips of the grits were involved in abrasive action. For example, sub-micron grooves were produced on the surface of Mn-Zn ferrite by 14μm particles of Al_2O_3. The areas of the resin surface which had been involved in abrasive wear were determined by the position of the debris particles, which also indicated that very few abrasive grit particles had been involved in the abrasive wear. The theory that few asperities are required to form the type of abrasive damage observed to the video head was also postulated by Hahn (92). Hahn flattened the asperities of the surface of magnetic media using a cleaner blade, and found that the wear rate and the abrasion damage was greatly reduced. Thus, a few, large asperities may result in abrasive damage characterised by ploughed grooves of widths much smaller than the ploughing asperity, rather than general ploughing of the surface by all the magnetic particles.

The ploughing of the asperities of one surface through another is dependent on the shape, size and hardness of the abrasive particle (125,126). This will influence both the load required to achieve plastic contact and the size and geometry of the grooves formed. If the shape of surface asperities is assumed to be approximately conical, with a range of different slope angles (Ø), Halliday (127)proposed that plastic flow will occur if Ø satisfies the following conditions;

$$Ø = C\,(H/E)x(1-v^2) \qquad (4.1)$$

where C = constant. (C= 0.8, for the onset of plastic flow. C=2 for full plastic deformation).

ν = Poisson's ratio, E = Young's modulus, H = hardness.

In general, plastic deformation occurs for metals if $\emptyset \geq 1°$. Computer analysis of hard surfaces has shown that Tan $\emptyset_{ave}$ is approximately proportional to the square of the centre line average (c.l.a) roughness (μm) of the surface*(70). Thus for an angle of 1° the surface roughness required to cause plastic deformation of the surface can be approximated as follows;

$$\text{Tan } 1° \approx (\text{c.l.a})^2$$

$$\text{c.l.a} \approx 0.13\ \mu\text{m}\ \ (130\ \text{nm})$$

The average surface roughnesses of the three tape batches used for Experiments GC1, GC2, and AL1 are tabulated in Table 4.1(Earlier in this chapter), the roughness of the standard iron oxide product being 11.7nm. Thus none of the tapes tested in this project should be capable of causing plastic deformation of the surface of the video head. This confirms the theory that the gross abrasive damage observed is due to isolated asperities on the tape surface, and/or debris. It would appear that the plastic deformation of the ferrite is not always related to the gap damage, as can be seen in Figure 3.55. The plastically deformed grooves travel the length of the head, and as they traverse the gap chipping is not always observed, just the continuation of deformation on the other side of the gap. As abrasive damage may arise from two sources, this concurs with the observation that plastic deformation of the surface occurs without the chipping of the gap. It is possible that plastic deformation is caused by isolated tape asperities, whereas the chipping damage is caused by hard debris particles. The transition between the two mechanisms is dependent on the size, shape and hardness of the particle or asperity. Kragelskii (128) suggests a set of simple rules for the transition between plastic deformation and chipping, based on the shape of the abrasive particle and its penetration

* It should be noted that this relationship is only valid for metal surfaces, however, it is interesting to see how the relationship fits the interaction between the head and the tape.

into the surface. For an asperity of radius r penetrating a surface such that the groove width formed is R, the ratio of groove width to tip radius determines the mechanism of wear, as follows;

$R/r < 0.28$ Elastic deformation

$0.28 < R/r < 0.87$ Plastic deformation

$R/r > 0.87$ Chip formation

Thus the wear occurring to the head caused by the iron oxide particles is abrasive, but is less likely to be caused by single iron oxide particles than by relatively few large, random asperities on the tape surface. The likely origin of large asperities on the tape surface is from the poor dispersion of the iron oxide particles. Poor dispersion would result in agglomerates of magnetic particles which, if occurring near to or at the surface, would create surface asperities.

The agglomeration of particles within the coating may have two effects on the wear mechanisms occurring to the head: First, agglomeration may create particles on the tape surface large enough to cause plastic deformation of the ferrite: Second, it is possible that debris is also produced from the asperities which results in three body abrasive wear. The chipping of the gap may be caused by this mechanism due to debris being trapped by the gap. Two types of debris are likely to be formed; polymer rolls; and debris containing iron oxide or HCA particles. The rolls of polymer may have formed as a result of adhesive transfer. Subsequent sliding over the transferred film may cause the polymer to roll up and create a debris particle. However, films formed on the head are likely to be too thin to form debris in this way and it is more likely that rolls are formed directly from the tape surface in the manner described by Reznikovskii and Brodskii (129) on the roll formation of rubber. Figure 4.6 shows the development of a polymer roll under a hard, smooth surface. The asperity is deformed under the sliding surface and the real area of contact is increased (Figure 4.6 a and b), leading to an increase in the

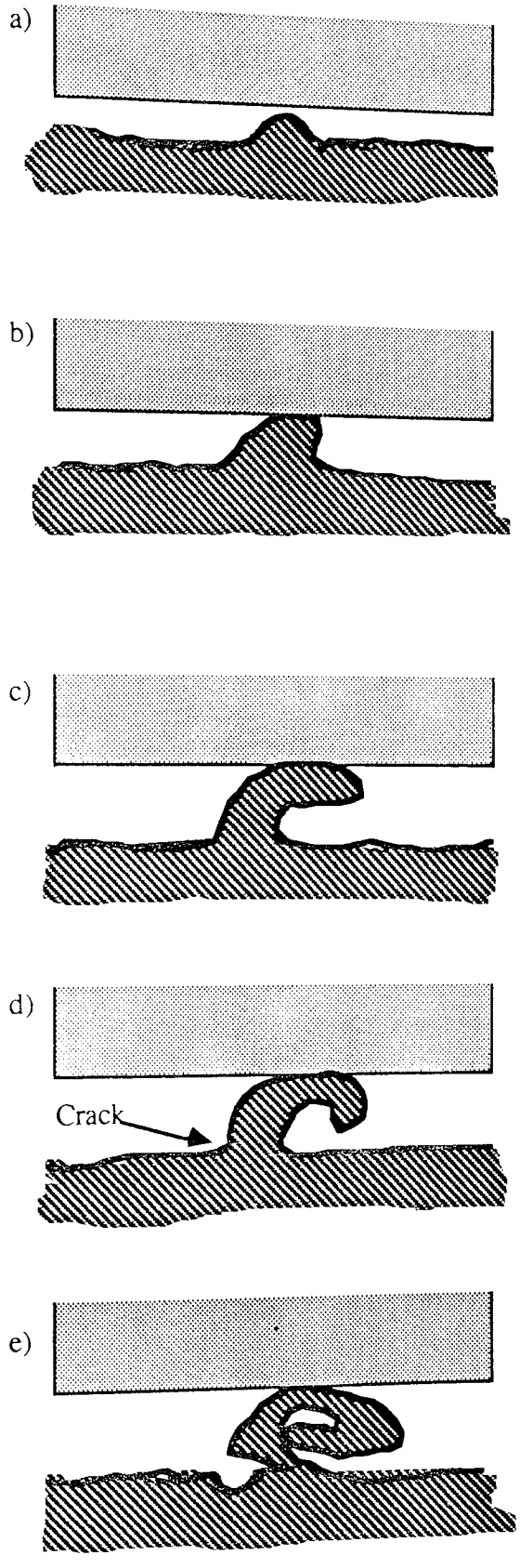

Figure 4.6: Formation of rolls of polymer debris

frictional force and stress on the asperity. The resulting stress causes the material to tear and further sliding will continue this rupture as the polymer rolls up (Figure 4.6 c and d). Further stress causes the material to break away from the bulk and form a wear particle (Figure 4.6 e). This type of debris was observed on many of the heads as shown in Figure 3.58. The rolls are not likely to cause abrasive wear but will roll between the sliding surfaces causing spacing loss. The second type of debris may originate from the formation of surface agglomerates. If the cohesion between the agglomerate and the binder system is poor the agglomerate could be pulled out from the surface, thereby forming a hard particle of debris capable of causing three body abrasive wear (130). Evidence of the formation of both types of debris is shown in Figures 3.56 to 3.58. Large rolls of polymer debris are shown in close up in Figures 3.58 a and b. The large debris particle shown in Figure 3.58c appears to be an accumulation of debris which has built up from successive wear of the tape and deposition outside the boundaries of the wear contour. Possible hard particles can be seen dotted over the head in amongst the polymer rolls, in Figures 3.56 and 3.57. These particles appear quite uniform in shape, suggesting that they are the same particle type, possibly the HCA.

Once formed, the particle may be trapped for a period of time before it is removed with subsequent sliding (130). The size of the debris particle may change, especially if it is composed of an agglomerate of particles. The location of chipping damage appears to be confined to the edges of the gap. This may be where the particle of debris was formed. If conditions are correct an asperity on the tape surface travelling towards the gap may plastically deform the ferrite as it slides. When the asperity reaches the gap it is likely that part of its surface will catch in the gap and tear out the asperity to form the debris particle. The removal of a debris particle in this way will depend on the shape of the particle and the cohesion between the particle agglomerate and the binder system. Micro-asperities on the surface of the asperity will also play a part in determining the future of the agglomerate. The removal of the agglomerate does not always take place as in some cases the groove simply continues the other side of the gap.

Another possibility is that the debris is formed elsewhere on the head but becomes trapped in the gap and thus causes fracture of the gap edges.

4.8 Effects of HCA concentration on head wear and damage

Comparing heads worn with the tape containing no HCA, with heads worn with a sample containing 4% Cr_2O_3 HCA. It would appear that an effect of adding an HCA to the magnetic coating is to remove or reduce some of the gross abrasive damage caused by the iron oxide particles. If the signal degradation for the sample containing no HCA is compared with that for the series of samples containing Cr_2O_3 it can be seen that the performance without HCA is approximately 1dB better than the performance with Cr_2O_3 HCA, despite the severe surface damage exhibited by the head worn with no HCA. The degradation may be explained by the damage caused to the gap during wear. In the case of samples containing Cr_2O_3, damage to the edges of the gap was particularly severe. Figure 3.17 shows the heads worn with 6% and 10% Cr_2O_3 samples. The head worn with 6% HCA shows a large percentage of gap damage. Figure 3.53 is an SEM photomicrograph of the gap of a head worn with a sample containing Cr_2O_3 which shows the removal of material from the edge of the gap in detail. The results indicate that ploughing of the ferrite surface does not necessarily result in damage to the gap. Thus damage to the gap appears to be the major contributor towards signal degradation.

An undamaged gap was a feature of the heads worn by samples containing AL_2O_3 HCA, which also exhibited good signal degradation. Considering the three types of samples tested in the main project, it would appear that the samples containing Al_2O_3 as the HCA produced the most satisfactory performance, whereas those containing Cr_2O_3 as the HCA produced the least satisfactory performance, with the samples containing no HCA performing somewhere between the two.

On addition of the HCA to the iron oxide formulation, the gross abrasive damage to the ferrite is reduced. However, depending on the HCA used two situations arise. The addition of Al_2O_3 results in an improvement in the condition of the ferrite surface and a reduction in damage to the gap, and thus a reduction in signal degradation. The addition of Cr_2O_3 to the formulation results in an improvement to the ferrite surface, but also results in further damage to the gap. The poor signal degradation observed for samples containing Cr_2O_3 suggests that it is dependant primarily on gap damage and only secondly on the damage to the ferrite. The effect of removing material from the gap is to lengthen the gap at that point. The length of the gap dictates the shortest recording wavelength and the highest frequency recorded. Hence, damage to the gap has the effect of reducing the high frequency response.

Examination of the HCA particles performed using the TEM showed that there was a tendency for the Cr_2O_3 particles to agglomerate, appearing as a group of particles of varying sizes. It appears that the particles do not disperse satisfactorily on processing. Problems with the dispersion of Cr_2O_3 HCA have been noticed in processing (3M Private com). When the Cr_2O_3 is added to the coating on mixing if the mixing process is stopped, such as, just before coating, after only a few seconds a green 'scum' of chromium particles comes to the surface of the magnetic slurry as the Cr_2O_3 separates out from the bulk. The agglomeration may be a product of the Van der Waals forces between the particles. Wetting agents are added to the coating in order to encourage dispersion of the iron oxide pigment. It would appear that the agent is not fully effective in the case of the Cr_2O_3, suggesting that the HCA requires an additional dispersive agent.

The HCA is not therefore operating in the optimum manner, and the tendency to agglomerate may be responsible for the damage to the gap observed with the use of Cr_2O_3. The effect of particle agglomeration is to produce an irregularly shaped and larger asperity on the surface of the tape, with results similar to the effect of agglomeration of ion oxide particles, that is, the production of hard debris and isolated asperities on the

tape surface. In general, damage to the gap was far worse with the addition of the Cr_2O_3 HCA to the coating, as shown in Experiments GC1 and GC2. It is possible that the Cr_2O_3 particles are more likely to be pulled out from the tape surface, creating hard debris particles which may then cause three body abrasive wear, resulting in chipping of the gap. Also the debris formed from Cr_2O_3 will not only be larger due to the relative size of the HCA particles, but also harder, the ratio of hardness of the Cr_2O_3 to the iron oxide particles is approximately 1: 0.65.

The agglomeration of the Cr_2O_3 also appears to effect the alignment of the iron oxide particles. Figure 3.45 shows a photomicrograph of an agglomerate of Cr_2O_3 particles. The iron oxide particles are forced to deviate from their parallel alignment in order to go round the lump of Cr_2O_3 particles. This may also affect the tape and signal reproduction.

The use of Al_2O_3 HCA particle was also examined. The shape of the Al_2O_3 particle was similar to the Cr_2O_3 particle as was the size distribution. The wear rates for the HCA particles were not very different, the wear rates for the Cr_2O_3 samples being slightly higher than for the Al_2O_3 samples. The relative hardnesses of these two particles are also very similar. Using the mineralogical scale (MOH) Al_2O_3 exhibits a slightly greater hardness of 9 compared with 8.5 for Cr_2O_3. Again the damage to the gap correlates with signal degradation, and the results may be due simply to the better dispersion of the Al_2O_3 within the magnetic coating. The Al_2O_3 particles were difficult to monitor under the TEM. Where a particle was found the tendency was towards a single particle, which are more difficult to locate than an agglomerate.

4.9 Progression of wear

In this section a model for the progression of wear over the head during the first few hours of wear is proposed. The curvature of the head is designed to encourage maximum head-tape contact at the gap. However, throughout the project no evidence was found to

suggest that this was occurring, even when good signal reproduction was observed. The results show that wear was confined mainly to the trailing pole piece, even in the case of high wear exhibited by Tapes B and D in the pilot experiment. The wear contours produced by these two samples were observed to be the largest, and in addition their centre was the closest to the gap of all samples tested. The wear was still biased towards the trailing pole piece. Tape B (chromium dioxide formulation) was also tested in the main project, using diamond indentation to study the wear to the head. The results revealed a wear profile similar to the iron oxide formulations. That is, the maximum wear was clearly situated on the trailing pole piece. Although the abrasivity of this sample is somewhat higher than the iron oxide formulations, and the resulting wear surfaces are quite different, it would appear that the profile of wear across the head is very similar. In the case of Tape C (iron oxide, plus 4% Cr_2O_3 HCA) of the pilot experiment, very low wear was observed in the form of a very small wear contour situated entirely on the trailing pole piece.

The position of the wear contour appears to be a function of the head design and its alignment on the video drum. Although the positioning of the head and its contoured shape are designed to encourage maximum head-tape spacing to occur at the gap, it would appear that this is not occurring. This conclusion was reached from the observation of contours produced by a variety of tape samples exhibiting a range of wear rates. All the contours were biased towards the trailing pole piece to varying degrees. The contour position was confirmed by the wear profile obtained using the indentation technique. Thus it is possible that no amount of alteration to the physical parameters of the tape would cause the maximum head-tape contact to occur at the gap. It may be that the head needs to be mounted at a slight angle to the drum. The movement of the head and tape relative to one another are such that in order to achieve central contact, the head would have to be mounted at an angle which would face the gap towards the incoming tape.

It appears that the wear is initiated on the trailing pole piece and later spreads to the second pole piece as the head wears away. Figure 4.7 shows the wear as it is occurring from its nucleus to its extent after six hours of wear, beginning at the point of highest normal pressure on the trailing pole piece (wear scar 1). As wear progresses the contoured head is flattened under the maximum area of tape contact, gradually creating a larger area over which the normal pressure is reduced (wear scar 2). The average normal pressure between head and tape therefore decreases slightly. The way that the head is contoured will encourage the wear to spread towards the gap and the second pole piece. The pressure is now more evenly distributed over the head surface (wear scars 3 and 4). However, the maximum pressure still occurs on the trailing pole piece. Thus the progression of wear proceeds from the trailing pole piece and then spreads to cover the gap. This model is supported by the shape of the RF degradation curves for all the ion oxide samples tested. Over the first few hours of wear of a new head the signal degradation falls steeply, which corresponds to the period of time during which the wear had not yet reached the gap. In the case of the head worn by Tape C of the pilot project, after 6 hours of wear the degradation curve was still falling (Figure 3.11), and the wear contour was still situated on the trailing pole piece. In the case of Tape D, which produced a large wear contour covering both pole pieces after the same wear period, the RF degradation was seen to fall within the first few minutes of wear and then recover very quickly after this (Figure 3.11).

The absence of wear at the gap during these first stages of wear may be a contributing to the high signal degradation.During this time little cleaning of the gap is occurring, and more damage to the ferrite surface and the gap is likely to occur under these conditions. The wear contour was monitored for all tape samples throughout the project. Debris was not found to occur inside the bounds of the wear contour. This was also true under the very low wear conditions exhibited by Tape C. Thus it would appear that the continual removal of material inside the region of maximum contact does not

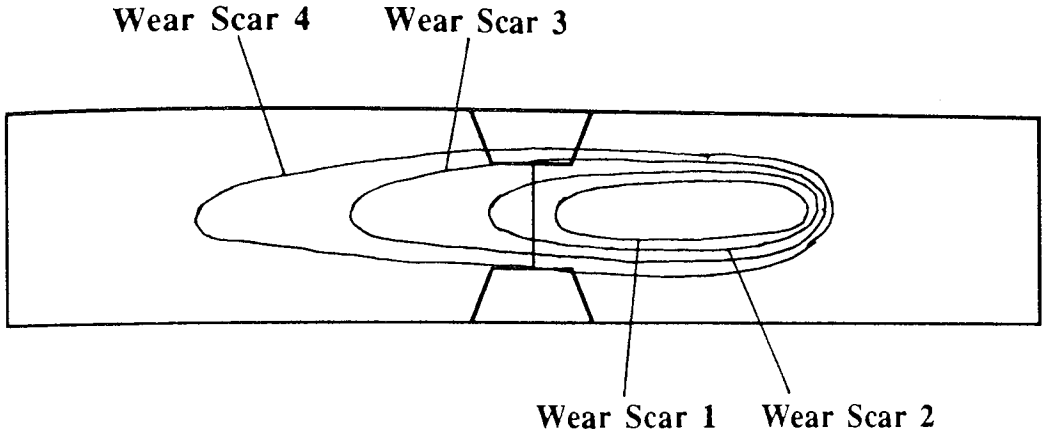

Figure 4.7: Progression of wear to the video head over the first few hours of use

allow the accumulation of debris even under low wear conditions. However, debris was seen to build up just outside the wear contour.

Figure 3.56 is a photomicrograph of the edge of a wear contour which shows that the edge of the scar is marked by the deposit of debris. It is possible that debris which is deposited outside the contour has contributed towards wear of the ferrite surface within the contour boundary by three body abrasion, before being deposited outside the area of greatest pressure. During the first minutes of head-tape contact the maximum contact takes place only on the trailing pole piece. Any debris produced will collect out side of this area and will therefore collect near to or even at the gap. This would occur up until the wear has spread over to the second pole piece, when the gap will be cleaned by the tape as intended. Thus it is possible that a majority of damage to the gap and gap area may be occurring within the first minutes of wear. The occurrence of debris in the gap area has two main consequences which may result in signal degradation; first, an increase in three body abrasion due to hard debris particles trapped between the two sliding surfaces; second, the presence of debris will cause head-tape separation and the corresponding signal loss. Thus it is possible that in the case of Tape D, the fall in wear over the first few minutes of wear was due to the production of debris collecting at the gap and possibly causing abrasive damage in that area. The wear rate for this tape was high enough to recover this situation in a matter of minutes and remove any abrasive damage, producing good signal reproduction.

In the case of Tape C (the iron oxide tape contained 4% Cr_2O_3) the wear was very low in comparison with other samples, and after six hours of wear the wear contour was still situated entirely on the trailing pole piece. Thus damage to the ferrite surface and the gap were still occurring due to debris collecting in the gap area and causing gross abrasive damage by the three body mechanism. Hence, the signal degradation for this sample was correspondingly bad.

The wear surface produced by Tape C gave an insight into the damage which results when the maximum head-tape contact does not spread to cover the gap and the second pole piece. This assumes that the wear is initiated on the trailing pole piece. Examination of the interferograms of the wear surface shows that the curvature of the head was distorted, presumably due to the preferential wearing of one pole piece. Additionally, from the cross-sectional plots it can be seen that the differential wear has resulted in a large increase in pole piece height difference. The effect of this difference on signal degradation was calculated in section 4.2.2. It appears that one of the main factors affecting the wear mechanism in this case was the low wear rate. After six hours of the test insufficient wear had occurred to spread the normal pressure over to the second pole piece, and more importantly, over the gap.

Debris is usually observed outside the boundary of the wear contour. Thus another factor contributing to the wear damage and resulting signal degradation is the trapping of debris in the gap area, which is likely to cause three body abrasion just outside the boundary of the wear contour, which in this case, is situated close to the gap. Although trapping of debris and three body abrasion of the gap area are likely to occur independently of the position of the wear contours, it is likely that the resting time of debris in this area will be greatly increased under these conditions, resulting in severe gap damage.

Thus it appears there are two main contributions towards the poor signal degradation observed when the wear is concentrated on one pole piece; first, the head-tape spacing created by the increase in pole piece height difference; and second, the damage to the gap and ferrite surface, aggravated by the fact the gap area is not cleaned naturally by the action of the tape.

Chapter 5:

Conclusions and Future Work

5.0 Conclusions

The following is a summary of the main conclusions which can be drawn from the work reported in this thesis.

Wear to the video head in sliding contact with iron oxide media is fundamentally an abrasive process, characterised by ploughing of the ferrite surface by relatively few random asperities on the tape surface, and the chipping of the sides of the gap. The damage to the gap appears to be critical in causing signal degradation.

The asperities on the tape surface are a product of poor dispersion of both the HCA and the magnetic pigment within the tape coating. Poor dispersion results in the formation of agglomerates, which if situated near to the surface will form isolated asperities. The asperities cause abrasive wear in two ways; first, by the ploughing of the asperity through the ferrite surface, causing plastic grooving of the surface; and second, by the production of hard particles of debris which cause chipping of the edges of the gap by the three body abrasive wear process.

Polymeric debris is also produced from the tape in the form of rolls. This debris is relatively soft and does not contribute to the abrasive damage of the surface, but may cause spacing loss. Lubricant and thin polymer films (which can only be removed by mechanical means) are transferred from the tape to the head surface. However, the build up of these components is low, and of secondary importance compared with the ferrite damage in contributing to signal degradation.

The rate of wear to the head in sliding contact with iron oxide media containing an HCA increases approximately linearly with increasing HCA content. The increase in wear was observed for two HCA types, Al_2O_3 and Cr_2O_3, over a range of HCA level from 2% to 16% for Cr_2O_3, and from 2% to 10% for Al_2O_3. However, the RF signal degradation was found not to vary significantly over the range of HCA levels. Thus the performance of the standard commercial iron oxide formulation would not be improved by increasing

the HCA content above its currently existing level. In addition the performance would not deteriorate if the HCA level was lowered.

Of the two types of HCA examined in this project, tapes containing Al_2O_3 HCA exhibit better wear characteristics, resulting in lower signal degradation than those containing Cr_2O_3. The improvement in signal degradation is a result of the better quality of dispersion exhibited by Al_2O_3 HCA. An even dispersion of HCA throughout the tape coating avoids the formation of surface asperities and subsequent production of hard debris particles responsible for gap damage. Poor dispersion of Cr_2O_3 HCA within the coating results in particle agglomerates and the formation of isolated asperities on the tape surface and hard debris particles.

Good dispersion of all particles of the tape coating are essential for even wear and continual good reproduction of the video head. Chromium dioxide magnetic pigment exhibits good dispersive qualities. The resulting media wears by microabrasion of the surface creating a wear surface as good, if not better than the original. Wear by microabrasion of the surface is optimum for signal reproduction. However, the hardness of chromium dioxide creates wear rates too high for commercial duplicating.

The knoop diamond indentation technique has proved to be an accurate and sensitive method of wear measurement, which succeeds in measuring wear occuring to the video head in situ. The use of the diamond indentation technique emphasised the need to study wear to the video head in situ, since the wear is a function not only of the abrasivity of the tape, but also of the curvature of the head and the way it changes with wear. The disadvantages of the technique include the time taken in accurately measuring the indentations and the removal of the drum in order to make the measurements.

Wear to the video head is initiated on the trailing pole piece and then spreads over to the gap and leading pole piece as the head is worn. The wear results in the appearance of a wear contour which is formed as the curvature of the head is flattened with wear. This

contour provides immediate information on the wear to the head caused by a particular tape sample.

5.1 Future work

The work performed in this project provides new evidence about wear to the head and has linked problematic wear features with the particles of the magnetic coating. Although a greater understanding of the effect of the HCA on wear has been established, there are other constituents of the tape coating, PVC base and back coat which can affect wear, and which therefore require further reasearch.

The advent of innovative technologies such as metal evaporated media, perpendicular media and CD might suggest that conventional particulate media will eventually be phased out. However, this is unlikely to be the case, partly because most of the recent technologies have yet to prove themselves to be competetive with particulate media, and partly because of the well established technology used to produce longitudinal magnetic media. In the following section future work is suggested which would further the understanding of the interaction between the video head and particulate tape media.

5.1.2 Wear measurement

The method of wear measurement revealed the importance of studying wear occuring in the actual tape drive. Important features of the wear, such as the appearence of the wear contour are informative under in-situ conditions, since wear is a function of the size and curvature of the head. Although successful, the technique was relatively time consuming for two main reasons; first, the removal and repositioning of the heads; and second, the need to measure each indentation six times in order to obtain an accurate mean measurement. If a technique could be devised which was similar to the indentation technique, but which allowed the measurements to be made with the heads in-situ, use of the technique could be improved dramatically. When the heads were removed from the

drive after 6 hours wear, they were also examined under the optical microscope for wear damage, debris and the appearance of a wear contour. Thus, an in-situ observation method would have to include these facitities in order to provide all the information obtained from the method used in this project.

The scanning electron microscope has recently been used by various authors to observe in situ wear (131, 132). Calabrese, Bhushan and Davis (133), have recently developed and build wear apparatus which fits into the vacuum chamber of a scanning electron microscope. The apparatus was designed specifically to observe sliding wear between magnetic tape and a ceramic head material. The head is in the form of a pin as opposed to an authentic head. The technique concentrates on the production and analysis of debris and the wear tracks formed on the tape due to the ploughing of the ceramic through the tape. It is acknowledged that the this does not simulate the wear occuring in a real tape drive.

Future work must examine the wear occuring in the actual tape drive in order to obtain definitive measurements of wear to the head and greater understanding of head-tape interaction.

5.1.3 Further research into the constituents of the tape

The results of this project reveal that damage to the gap produces the greatest contribution to signal degradation. This damage appears to be directly related to the dispersion of both magnetic and head cleaning particles within the coating. Hence, the performance of the tape may be improved by better dispersion techniques. This may involve a change in the formulation or level of the wetting agent used to disperse the particles. However, it is felt that even with an improvement in dispersion and consequent reduction in gap damage, the very low wear of the commercial iron oxide formulation may still prove problematic, and an increase in the abrasivity of this tape is desirable. After 6 hours the wear contour for the commercial formulation was very small and was also situated only on the trailing pole piece. This position of the contour was shown to be related to the wear rate and was also

shown to increase the signal degradation in several ways, and is therefore an undesirable situation. It was also. Ideally the abrasivity of this tape should be increased, so that after 6 hours the wear contour has spread to both pole pieces and covers the gap.

Two avenues of research should be pursued in order to obtain near optimum abrasivity. First, further examination of the HCA is required, which includes an examination of the effect of a variation in particle size, and possibly the use of more than one particle. Second, the binder system since it also plays a role in establishing the abrasivity of the tape and should be re-examined (134). The ratio of hard to soft binder segments can be varied to obtain a more or less abrasive medium. A combination of both a change in HCA type and a higher hard-soft binder ratio may be required to raise the abrasivity of the commercial iron oxide formulation.

Although the position of the wear contour appeared to be directly related to the wear rate, this does not fully explain the initiation of wear on the trailing pole piece. Thus further research is also required to examin the position of the wear contour and its relationship with the physical parameters of the tape. Research on head-tape contact has been reported by Suarnasern (122) who used a white light interferometer encorporating a transparent head to examine the distance of the head from the tape at different points along the head surface. This research produced a semi-empirical formula for the head-tape spacing (4.1) but this did not appear to observe or take account of the variation of head-tape spacing along the head. Therefore, further research is reqiured in order to examine this aspect of head wear and possibly to relate it to head-tape spacing.

5.1.4 The use of alumina as the HCA.

Use of Al_2O_3 as the HCA appears to provide lower signal degradation than that observed with the current Cr_2O_3 HCA. The main difference in wear appears to be the damage to the gap. The addition of Al_2O_3 to the coating appears to reduce such damage whereas the

use of Cr_2O_3 HCA may increase this damage. The results also suggest that the difference in severity of the wear is due to thefact that Al_2O_3 has a greater tendency to disperse than Cr_2O_3. Thus the substitution of Al_2O_3 as the HCA in the commercial iron oxide product should be considered. Since Al_2O_3 has been used previously as the HCA in this product it should not present any problems in production of the media. However, before this can be instigated, further research is required, for example to optimize the choice of level and particle size.

5.1.5 Surface analysis

The small size of the head and its complicated construction made analysis of the worn surface using SIMS and XPS difficult. Both techniques are relatively new and still under development. Since the beginning of this project improvements have been made to both techniques, for example, in the field of small area analysis. Although the problems created by the small size of the head were partly overcome in this project by the use of small spot XPS, difficulties were nonetheless encountered in focussing the primary beam on such a small specimen. Improvements in XPS, such as laser sighting may provide better analysis of the sample. The evidence of material transfer obtained by analysis of the surface using either of the techniques mentioned here would be enhanced by a more extensive examination using accurate small area analysis.

5.1.6 Progression of wear

A model for the progression of wear over the head was proposed in chapter 4. To confirm this model, further research which examines the wear contour at regular intervals of, for example, every half hour is required. Again this would be time consuming unless a method of monitoring in situ is developed.

References

(1) J F Robinson, "Video Tape Recording: Theory and Practise", Focal Press, London, 1975.

(2) F Jorgensen, "The complete handbook of Magnetic Recording", Tab Books Inc., Blue Ridge Summit, 1980.

(3) S J Begun, "Magnetic Recording", Murray-Hill Books, England, 1949.

(4) C.Denis Mee, C.D.Daniel, Eds., "Magnetic Recording, Vols I and II", Mc-Graw Hill Book Company, New York, 1987.

(5) W K Westmijze, "Studies on magnetic recording III: The Recording Process", Philips Res. Rep. no. 8, Aug. 1953, pp 245-269.

(6) P Spring, "Tape Recording; Performance analysis and service techniques", Focal Press, London, 1967.

(7) T D Lee, P A Papin, "Analysis of dropouts in video tapes", IEEE Trans. Magn., Vol. MAG-18, No. 6, Nov. 1982, pp 1092-1093.

(8) R L Wallace, Jr., "The Reproduction of Magnetically Recorded Signals", The Bell System Technical Journal, Oct, 1951, pp 1145-1173.

(9) W T Scott, "The physics of electricity and magnetism", 2nd Edition, John Wiley and Sons Inc., New York, USA, 1966.

(10) J Mallinson, "The Foundations of Magnetic Recording", Academic Press, Inc., London, 1987.

(11) F Granum, A Nishimura, "Modern developments in magnetic tape", IEEE Conf. on Video and Data Recording, Proc., no. 43, Southampton, 1979, pp 49-59.

(12) R E B Hickman, "Magnetic Recording Handbook", George Newnes Ltd., London, 1956.

(13) E D Daniel, D F Eldridge, "Magnetic Recording Media", Chapter 3 in " Magnetic Recording in Science and Industry", C B Pear, Ed., Reinhold Publishing Corp., New York, 1967.

(14) G Demazeau, P Maestro, T Plante, M Pouchard, P Hagenmuller, "New magnetic materials derived from chromium dioxide", IEEE Trans. Magn., Vol. MAG-16, No. 1, Jan. 1980, pp 9-10.

(15) R Bradshaw, B Bhushan, C Kalthoff, M Warne, "Chemical and mechanical performance of flexible magnetic tape containing chromium dioxide", IBM J. Res. Develop. Vol. 30, no.2, March 1986, pp 203-215.

(16) M Amemiya, M Kishimoto, F Hayama, "Formation and magnetic properties of γ-Fe_2O_3 particles surface modified with crystallized cobalt-ferrite", IEEE Trans. Magn., Vol. MAG-16, No. 1, Jan. 1980, pp 17-19.

(17) G Bate, "Recent developments in magnetic recording materials", J. App. Phys. Vol. 52 (3), 1981, pp 2447-2452.

(18) A R Corradi, "Progress in recording materials: a critical review", IEEE Trans. Magn., Vol. MAG-14, No. 5, 1978, pp 655-660.

(19) J Wade Van Valkenburg, "Video recording tape", Patent Proposal MTL X-4, Memory Technologies Group Laboratories, June, 1986

(20) R G Bayer, "A model for wear in an abrasive environment as applied to a magnetic sensor", Wear, Vol. 70, 1981, pp 93-117.

(21) "Scotch Magnetic Media Video Tracking", 3M Magnetic Media Div., 3M centre, St. Pauls, MN55144-1000, pp1-16.

(22) R L Bradshaw, B Bhushan, "Friction in Magnetic Tapes III: Role of Chemical Properties", ASLE Trans., Vol. 27, No.3, April 1983, pp 207-219.

(23) J Kelly, "Tape and head wear", Chpt. 2 of 'Magnetic Tape Recording for the Eighties', NASA Ref. Publ. 1075, F Khalil Ed., April, 1982, pp 7-22.

(24) Y Kimachi, F Yoshimura, M Hoshino, A Terada, "Uniformity quantification of lubricant layer on magnetic recording media", IEEE Trans. Magn., Vol. MAG-23, No. 5, Sept. 1987, pp 2392-2394.

(25) U Bagatta, A R Corradi, L Flabbi, L Salvioli, "Lubrication of tapes with fluorocarbon (Fomblin) oils", IEEE Trans. Magn., Vol. MAG-20, No. 1, Jan. 1984, pp 16-18.

(26) R E linder, P B Mee, "ESCA determination of fluorocarbon lugricant film thickness on magnetic disc media", IEEE Trans. Magn., Vol. MAG-18, No. 6, Nov. 1982, pp 1073-1076.

(27) S Tanabe, S Iwasaki, "Reproducing process of perpendicular magnetic recording", Electronics and Communications in Japan, Part 2, Vol. 70, No. 5, 1987, 1-7

(28) S Iwasaki, Y Nakamura, H Muraoka, "Wavelength response of perpendicular magnetic recording", IEEE Trans. Magn., Vol. MAG-17, No. 6, Nov, 1981, pp 2535-2537.

(29) J C Mallinson, H N Bertram, "A theoretical and experimental comparison of the longitudinal and vertical modes of magnetic recording", IEEE Trans. Magn., Vol. MAG-20, No. 3, May. 1984, pp 461-467.

(30) J C Mallinson, "The next decade in magnetic recording", IEEE Trans. Magn., Vol. MAG-21, No. 3, May 1985, pp1217-1220.

(31) T Kunieda, K Shinohara, A Tomago, "Metal Evaporated Video Tape", Proc. of the Conf. on Video and Data Recording, Southampton, April 1984, IERE, pp 37-43.

(32) K Shinohara, H Yoshida, M Odagiri, A Tomago, "Columnar Structure and Some Properties of Metal-Evaporated Tape", IEEE Trans. Magn., Vol. MAG-20, No. 5, Sept. 1984, pp 824-826.

(33) F Vom Wege, E Hornbogen, "Wear properties of metal-evaporated video tape", Wear, Vol. 128, no.3, 1988, pp 291-305.

(34) D E Speliotis, "Barium ferrite magnetic recording media", IEEE Trans. Magn., Vol. MAG-23, No. 1, Jan. 1987, pp 25-28.

(35) D E Speliotis, "Distinctive characteristics of barium ferrite media", IEEE Trans. Magn., Vol. MAG-23, No. 5, Sept. 1987, pp 3143-3145.

(36) M P Sharrock, "Magnetic remanence properties of particulate recording media: comparison of barium ferrite with acicular materials", IEEE Trans. Magn., Vol. MAG-24, No. 5, Nov. 1988, pp 2856-2858.

(37) O H Wyatt, D Dew-Hughes, "Metals, Ceramics and Polymers", Cambridge University Press, London, 1974.

(38) K Miyoshi, D H Buckley, "Friction and wear of single-crystal manganese-zinc ferrite", Wear, vol. 66, 1981, pp 157-173.

(39) R W Davidge, "Mechanical behaviour of ceramics", Cambridge University Press, Oxford, 1979.

(40) K Hirota, M Sugimura, E Hirota, "Hot-press ferrites for magnetic recording heads", Ind. Eng. Chem. Prod. Res. Dev., vol. 23, no.3, 1984, pp 323-330.

(41) K Kugimiya, E Hirota, "A hot pressed coprecipitated ferrite and its application to magnetic heads", IEEE Trans. Magn., Vol. MAG-13, No. 5, Sept. 1977, pp 1472-1474.

(42) K Miyoshi, D H Buckley, K Tanaka, "Effect of wear on structure-sensitive magnetic properties of ceramic ferrite in contact with magnetic tape", pp 112-118.

(43) A Broese Van Groenou, S E Kadijk, "Sliding experiments on various single crystals of MnZn ferrite", Wear, Vol. 131, 1989, pp353-364.

(44) F J Jeffers, R J McClure, W W French, N J Griffith, "Metal-in-gap record head", IEEE Trans. Magn., Vol. MAG-18, No. 6, Nov. 1982, pp 1146-1148.

(45) D Kirk, "Audio and Video Recording", Faber and Faber, London, 1975, pp 144-154.

(46) J F Carroll, R C Gotham, "The measurement of abrasiveness of magnetic tape", IEEE Trans. Magn., Vol. MAG-2, 1966, pp 6-13.

(47) R H Basotti, R N Hyland, "A method of applying results obtained with the media abrasion tester", IBM Tech. Rep. TR 44.0122, June 1970.

(48) W D Kehr, C B Meldrum, R F M Thornley, "The influence of grain size on the wear of nickel-zinc ferrite by flexible media", Wear, Vol. 31, 1975, pp 109-117.

(49) F W Hahn, "Material selection for digital recording heads", IEEE Trans. Magn., Vol. MAG-2, 1975.

(50) B Bhushan, "Assessment of accelerated head-wear test methods and wear mechanisms", in B Bhushan and N S Eiss (Eds.), "Tribology and mechanics of magnetic storage systems", Vol. 2, SP-19, American Society of Lubrication Engineers, 1985, pp 101-111.

(51) H M Lewis, G I Williams, "Review of methods for measuring abrasiveness of magnetic tapes", Proc. of the Fourth Int. Conf. on Video and Data Recording, IERE, Southampton, 1982.

(52) B Bhushan, "Magnetic Head-Media Interface Temperatures. Part 1-Analysis", Journal of Tribology, vol. 109, April 1987, pp 243-251.

(53) B Bhushan, "Magnetic head-media interface temperatures. Part 2-Application to Magnetic Tapes", Journal of Tribology, Vol. 109, April, 1987, pp 252-256.

(54) J F Archard, "The temperature of rubbing surfaces", Wear, Vol. 2, 1958, pp 438-455.

(55) A Levy, "Wear testing", chpt 3, Magnetic Tape Recording for the Eighties, NASA Publ. Ref. 1075, 1982, pp 23-34.

(56) F W Hahn Jr., "Thin film wear sensors", Wear, Vol. 74, 1981, pp 157-164.

(57) D A Cash, R Pagel, "Wear in recorder heads by magnetic tape", IERE Proc. Conf. Video and Data Recording, no.35, Birmingham, July 1976, pp 217-222.

(58) A Broese van Groenou, M I L Uijterschout, "A quick test on wear of head materials by recording tapes", IEEE Trans. Magn., Vol. MAG-19, No. 5, Sept. 1983, pp 1674-1676.

(59) R C F Schaake, H F Huisman, "Headwear regulations of CrO_2 video tape", IEEE Trans. Magn., Vol. MAG-23, No. 1, Jan. 1987.

(60) A Begelinger, A W J Degee, "Wear measurements using Knoop diamond indentations", Wear, Vol. 43, no.2, June 1977.

(61) J Lancaster, "Friction and Wear", Chapter 14 of "Polymer Science", A D Jenkins Ed., North-Holland Publishing Co., London, 1972.

(62) J F Archard, "Contact and rubbing of flat surfaces", Journal of Applied Physics, Vol.24, no.8, Aug., 1953, pp 981-988.

(63) J Halling Ed., "Principles of Tribology", The Macmillan Press Ltd., London, 1978.

(64) E Rabinowicz, "Friction and wear of materials", John Wiley and Sons, Inc., New York, 1965.

(65) N P Suh, "Polymer Composites", Chapter 6 in Tribophysics, Prentice-Hall, Inc., New Jersey, 1986.

(66) F P Bowden, D Tabor, "The friction and lubrication of solids: Part II", Clarendon Press, Oxford, 1964.

(67) D F Moore, "The friction and lubrication of elastomers", Pergamon Press, Oxford, 1972.

(68) L E Samuels, E D Boyle, D M Turley, "Sliding wear mechanisms", in D A Rigney (Ed.), "Fundamentals of Friction and Wear of Materials", American Society for Metals, Ohio, 1981.

(69) J M Galligan, P McCullough, "On the nature of static friction", Wear, Vol. 105, 1985, pp 337-340.

(70) J K Lancaster, "Basic mechanisms of friction and wear of polymers", Plastics and Polymers, Vol. 41, Dec., 1973.

(71) E Hornbogen, K Schafer, "Friction and wear of thermoplastic polymers", in D A Rigney (Ed.), "Fundamentals of Friction and Wear of Materials", American Society for Metals, Ohio, 1981.

(72) B Bhushan, R L Bradshaw, B S Sharma, "Friction in magnetic tapes II: Role of Physical Properties", ASLE Trans., Vol. 27, No.2, April, 1984, pp 89-100.

(73) B Bhushan, B S Sharma, R L Bradshaw, "Friction in Magnetic Tapes I: Assessament of Relevant Theory", ASLE Trans., Vol. 27, No.1, Jan 1984, pp 33-44.

(74) B J Briscoe and D Tabor, "Friction and wear of polymers", in Polymer Surfaces, John Wiley and Sons, Ltd, Chichester, 1978.

(75) B J Briscoe, "Fundamental aspects of the sliding wear of polymers", Selection and performance of dry bearings, National Centre of Tribology, Risley, 25th May 1983.

(76) H Czichos, "Introduction to friction and wear", Chapter 1 in Friction and wear of polymer composites, K Friedrich editor, Elsevier, Amsterdam, 1986.

(77) M A Moore, "Abrasive Wear", in D A Rigney (Ed.), "Fundamentals of Friction and Wear of Materials", American Society for Metals, Ohio, 1981.

(78) B J Briscoe, D Tabor, "The sliding wear of polymers: A brief review", Proc. Int. Conf. on the Fundamentals of Tribology, Cambridge, Massachusetts, June, 1978.

(79) M K Kar, S Bahadur, "Mechanism of film formation in polymer -metal sliding", Proc. Int. Conf. on the Fundamentals of Tribology, Massachsettes Inst. of Tech., Cambridge, Massachsettes, June 1978.

(80) K Tanaka, in "Wear of materials, 1979", Ed. by W A Glaeser, K C Ludema, S K Rhee, ASME, New York, 1977.

(81) S X Li, "Grain size effects on magnetic properties and core process of recording head ferrites", IEEE Trans. Magn., Vol. MAG-22, No. 1, Jan. 1986, pp 14-18.

(82) D H Buckley, K Miyoshi, "Friction and Wear of Ceramics", Wear, Vol. 100, 1984.

(83) S Chandrasekar, B Bhushan, "Friction and Wear of Ceramics for Magnetic Recording Applications-Part 1: A review", Journal of Tribology, vol. 112, Jan. 1990, pp 1-16.

(84) K Miyoshi, D H Buckley, B Bhushan, "Friction and morphology of magnetic tapes in sliding contact with nickel-zinc ferrite", Nasa Technical Paper no. 2267, Jan., 1984.

(85) J A L Potgiesser, J Koorneef, "Mechanical wear and degeneration of the magnetic properties of magnetic heads caused by the tape", The Radio and Electronic Engineer, Vol. 44, no.6, June 1974, pp 313-318.

(86) F W Hahn, Jr., "Wear of recording heads by magnetic tape", Tribology and Mechanics of Magnetic Storage Systems, ASLE Special Publication, SP-16, ASLE, Park Ridge, Illinois, 1984, pp 21304-21311.

(87) R W Polleys, "Work-hardening of ferrite head surfaces by wear with recording media", IBM J. Res. Dev., vol. 22, no. 6, 1978, pp 675-680.

(88) K Ozawa, H Wakasugi, K Tanaka, "Friction and wear of magnetic heads and amorphous metal sliding against magnetic tapes", IEEE Trans. Magn., Vol. MAG-20, No. 2, March 1984, pp 425-430.

(89) K Tanaka, O Miyazaki, "Wear of magnetic materials and audio heads sliding against magnetic tapes", Wear, Vol. 66, 1981, pp 289-306.

(90) J Larsen-Badse, "Influence of atmospheric humidity on abrasive wear-1: 3-body abrasion", Wear, Vol. 31, 1975, pp 373-379.

(91) R M Waghorne, H M Lewis, "The effect of tape integrity and tape cleaning on drop-out performance", Fifth International Conference on Video and Data Recording, Southampton, April, 1984, pp 63-65.

(92) F W Hahn, "Head wear as a function of isolated asperities on the surface of magnetic tape", IEEE Trans. Magn., Vol. MAG-20, No. 5, Sept. 1984, pp 918-920.

(93) T Sugita, A Hashikawa, "The roles of brittle microfracture and plastic flow in the wear of MgO single crystals", Wear, Vol.72, no.3, 1981, pp 295-303.

(94) E F Cuddihy, "Hygroscopic Properties of Magnetic Recording Tape", IEEE Trans. Magn., Vol. MAG-12, No. 2, March. 1976.

(95) Neal Bertram, E F Cuddihy, "Kinetics of the humid aging of magnetic recording tape", IEEE Trans. Magn., Vol. MAG-18, No. 5, Sept. 1982, pp 993-999.

(96) J P C Bernards, C P G Schrauwen, S B Luitjens, V Zieren, R W de Bie, "Material and recording properties of perpendicular CoCr media", IEEE Trans. Magn., Vol. MAG-23, No. 1, Jan. 1987, pp 125-127.

(97) J F Carroll, R C Gotham, "The measurement of abrasiveness of magnetic tape", IEEE Trans. Magn., Vol. MAG-2, 1966, pp 6-13.

(98) Larsen-Badse, S S Sokoloski, "Influence of atmospheric humidity on abrasive wear-II. 2-Body abrasion", Wear, Vol. 32, 1975, pp 9-14.

(99) Manual to the Zeiss Micro Hardness Tester, Carl Zeiss, Germany.

(100) N C Wallbridge, D Dowson, "Distribution of wear rate data and a statistical approach to sliding wear theory", Wear, Vol. 119, 1987, pp295-312.

(101) JVC Service manual for the model HR-D170E/EG/EK VHS cassette recorder.

(102) O C Wells, "Scanning Electron Microscopy", McGraw-Hill, USA, 1974.

(103) S Wischnitzer, "Introduction to Electron Microscopy", 3rd Edition, Pergamon Press, N.Y., USA, 1981.

(104) P J Godhew, F J Humphreys, "Electron Microscopy and Analysis", 2nd Edition, Taylor and Francis, London, 1988.

(105) A A Staals, M C van Houwelingen, H F Huisman, "Localization and characterization of sub-surface particles in magnetic tape", IEEE Trans. Magn., Vol. MAG-23, No. 1, Jan. 1987.

(106) G M Robinson, C D Englund, T J Szczech, R D Cambronne, "Relationship of surface roughness of video tape to its magnetic performance", To be published in IEEE Trans. Magn.

(107) "Mirau interference equipment: Operating instructions", D-7082, Carl Zeiss, West Germany, 1980.

(108) G M Robinson, G D Hanson, K E Palquist, "The analysis of interferometrically measured surface roughness data", Proc. of the Sixth Int. Conf. on Video, Audio, and Data Recording University of Sussex, Brighton, England, March, 1986.

(109) D M Perry, G M Robinson, "Measurement of surface topography of magnetic recording materials through computer analysed microscopic interferometry", IEEE Trans. Magn., Vol. MAG-19, No. 5, Sept. 1983, pp 1656-1658.

(110) D M Perry, P J Moran, G M Robinson, "Three-dimensional surface metrology of magnetic recording materials through direct-phase-detecting microscopic interferometry", Journal of IERE, Vol.55, No. 4, April 1985.

(111) A E Morgan, H W Werner, "Modern methods for solid surface and thin film analysis", Physica Scripta, Vol. 18, 1978, pp.401-408.

(112) W Reuter, "Techniques for the compositional and chemical state analysis of surfaces and thin films", Nuclear Instruments and Methods in Physics Research, 218, 1983, pp.391-399.

(113) A E Morgan, "A comparison of secondary ion mass spectrometry and auger electron spectroscopy as surface analytical techniques", Nuclear Instruments and Methods in Physics Research, 218, 1983, pp 401-408.

(114) P J Stephenson, "Surface chemistry and analytical methods", 3M Internal Report, Sept. 1984.

(115) P J Stephenson, P A Bishop, "Further FABMS Studies", 3M Internal Report, Jan. 1985.

(116) J L Sullivan, "Surface analysis techniques", Final year undergraduate lectures, University of Aston, Birmingham, England, 1987.

(117) S A Chambers, "Surface characterization of 3M VHS video tape via X-ray photoemission and scanning Auger microscopy", 3M Internal Report March 1984.

(118) J C Riviere, "Instrumentation", Chapter 2 in "Practical surface analysis by Auger and X-ray photoelectron spectrometry", D Briggs & M P Seah, Eds., John Wiley & sons, Chichester, 1983.

(119) D Briggs, J C Riviere, "Spectral interpretation", Chapter 3 in "Practical surface analysis by Auger and X-ray photoelectron spectrometry", D Briggs & M P Seah, Eds., John Wiley & sons, Chichester, 1983.

(120) D Briggs, "Applications of XPS in polymer technology", Chapter 9 in "Practical surface analysis by Auger and X-ray photoelectron spectrometry", D Briggs & M P Seah, Eds., John Wiley & sons, Chichester, 1983.

(121) P M Roderick, Private Communications.

(122) A M Berg, N J Suwarnasarn, "Head-tape contact of 3M and competitive 1/2 inch tapes", 3M Technical report no.002, 3M St. Pauls, USA, March, 1985.

(123) M A Moore, "Abrasive Wear", in "Fundamentals of Friction and Wear of Materials", D A Rigney, Ed., ASM publ., Pennsylvania, 1980.

(124) K H Zum Gahr, "Modelling of two-body abrasive wear", Wear, Vol.124, 1988, pp 87-103.

(125) J Larsen-Badse, "Influence of grit size on the groove formation during sliding abrasion", Wear, Vol.11, 1968, pp 213-222.

(126) E Rabinowicz, A Mutis, "Effect of abrasive particle size on wear", Wear, Vol.8, 1965, pp 381-390.

(127) Halliday, "Surface examination by reflection electron microscopy". Proc. Inst. Mech. Eng. Lond., Vol. 169, 1955, pp777-781.

(128) I V Kragelskii, "Friction and Wear", Butterworths, London, 1965.

(129) M M Reznikovski, G I Brodskii, "Features of the abrasion of highly abrasive materials", from 'Abrasion of rubber", D I James Ed. , McLaren & sons, 1967.

(130) M Godet, "The Third-Body approach: a mechanical view of wear", Wear, Vol. 100, 1984, pp 437-452.

(131) W A Glaeser, "Wear experiments in the scanning electron microscope", Wear, Vol. 73, 1981, pp 371-386.

(132) Y Tsuya, KSaito, R Takagi, J Akaoka, "In situ observation of wear process in a scanning electron microscope," ASME, Proc. Int. Conf. on Wear of Materials, Dearborn, MI, April, 1979, New York, pp 57-71.

(133) S J Calabrese, B Bhushan, R E Davis, "A study by scanning electron microscopy of magnetic head-tape interface sliding", Wear, Vol.131, no.1, 1989, pp123-133.

(134) P M Roderick, Private Communications.

The measurement of in-situ wear of video heads

. A. Reeves** and J. L. Sullivan*

BA2 7AY, UK

the wear characteristics to be examined, and an

0301-679X/90/040251-07